THE UNIVERSITY *of* EDINBURGH

The functions of receptor activator of NF-κB ligand (RANKL) and its receptors, RANK and OPG, are evolutionarily conserved.

Kate Sutton

A dissertation submitted for the degree of Doctor of Philosophy

University of Edinburgh

2014

Author's declaration

I declare that the work in this dissertation is original except where indicated by special reference in the text and no part of the dissertation has been submitted for any other degree

Signed…….

Date…….....

Abstract

The tumour necrosis factor (TNF) superfamily is a group of cytokines that orchestrate a variety of functions, both in the development of the architecture of immune organs and of the immune response. The mammalian TNF superfamily consists of 19 ligands and 29 receptors, whereas in the chicken only 10 ligands and 15 receptors are present. Chickens do not develop lymph nodes, possibly due to the absence of the lymphotoxin genes (TNF superfamily members) in their genome. New members of the chicken TNF superfamily have recently been identified in the genome, namely chicken receptor activator of NF-κB ligand (chRANKL), its signalling receptor, chRANK, and its decoy receptor, osteoprotegerin (chOPG). In mammals, RANKL and RANK are transmembrane proteins expressed on the surface of Th1 cells and mature dendritic cells (DC), respectively. OPG is expressed as a soluble protein from osteoblasts and DC, regulating the interaction between RANKL and RANK. To investigate the bioactivity of this triad of molecules, the extracellular soluble domains of chRANKL and chRANK and full-length chOPG were identified and cDNAs cloned. ChRANKL, chRANK and chOPG mRNA are ubiquitously expressed across non-lymphoid and lymphoid tissues and immune cells in the chicken. Similar to mammals, chRANK and chOPG mRNA expression levels are upregulated in mature bone marrow-derived DC (BMDC). ChRANKL transcription is regulated by Ca^{2+}-mobilisation and is further enhanced by the activation of the protein kinase C pathway, as seen in mammals.

The biological activities of chRANKL, chRANK and chOPG were investigated by the production of recombinant soluble fusion proteins. The extracellular, TNF-homology, domain of chRANKL (schRANKL) was sub-cloned into a modified pCI-neo vector expressing an in-frame isoleucine zipper to encourage trimer formation. FLAG-tagged schRANKL produced in COS-7 cells predominantly forms homotrimers and chOPG is expressed as homodimers, both signatures of their mammalian TNF superfamily orthologues. SchRANKL enhances the mRNA expression levels of pro-inflammatory cytokines in mature BMDC and BM-derived macrophages (BMDM). Pre-incubation with soluble chRANK-Fc or chOPG-Fc blocked the schRANKL-mediated increase in pro-inflammatory cytokine mRNA

expression levels in BMDC. Expression of surface markers on BMDC and BMDM were not affected by schRANKL treatment. SchRANKL enhances the survival rates of BMDC and BMDM and can drive osteoclast differentiation from monocyte/macrophage progenitor cells.

The chRANKL signalling receptor, chRANK, does not contain an intracellular catalytic domain but requires the binding of intracellular TNF receptor-associated factors (TRAF) to initiate signalling. TRAFs are a family of seven proteins (TRAF1-7) grouped due to their highly conserved RING domains, zinc finger domains, TRAF-N and TRAF-C domains. ChRANK possesses four of the five TRAF peptide-binding motifs found in mammalian RANK. The "missing" chRANK TRAF peptide-binding motif is TRAF6-specific, a vital protein for RANKL-mediated osteoclastogenesis. All seven members of the mammalian TRAF family are present in the chicken genome. To investigate the conservation of RANK-specific TRAF signalling proteins, chicken TRAF2 (chTRAF2), chTRAF5, chTRAF6 and a newly found member, chTRAF7, were identified and their cDNAs cloned. ChTRAF5, chTRAF6 and chTRAF7 had mRNA expression patterns, in non-lymphoid and lymphoid tissues and in a number of immune cells, similar to their orthologues in mammals. Interestingly, chTRAF2 has two variants, the full-length chTRAF2 and a novel isoform (chTRAF2S) lacking exon 4. ChTRAF2S lacks a portion of zinger finger one, all of zinc finger two and a portion of zinc finger three, producing a protein with a hybrid of zinc fingers 1 and 3 and intact zinc fingers 4 and 5. RT-PCR analyses indicated differential expression of both of the chTRAF2 isoforms in a number of non-lymphoid and lymphoid tissues, splenocyte subsets and in a kinetic study of ConA-stimulated splenocytes. ChTRAF2S is biologically active compared to chTRAF2, inducing higher levels of NF-κB activation. Co-transfections indicate that chTRAF2 may regulate chTRAF2S bioactivity as no synergistic effect was identified when cells were transfected with both isoforms.

Knowledge gained from this study will help work to further dissect the interactions between chRANKL-expressing T cells and chRANK-expressing DC to drive Th1 immune responses and to understand how the chicken mounts an effective

immune response while expressing a minimal essential repertoire of the TNF superfamily.

List of contents

Chapter 5 Cloning and molecular characterisation of chicken TRAF2 (chTRAF2), chTRAF5, chTRAF6 and chTRAF7

Chapter 6 Discussion

List of tables

Chapter 1

List of Figures

Chapter 1

Chapter 2

Chapter 3

Chapter 4

Chapter 5

Chapter 6

Acknowledgements

I would like to give a massive thank you to Professor Pete Kaiser for his support and advice during my PhD studies. Also I would like to thank my co-supervisor, Dr. Zhiguang Wu for her help and advice. Dr. Tuanjun Hu, Lisa Rothwell and Dr. Lonneke Vervelde deserve a special thank you for all their help, training and advice over the past few years.

A really special thank you goes to my parents, Margaret and Timmy, who have given great love and support over the years along with the rest of the Sutton gang! Daniel, George, Jarlath, Patricia, Johnathan, Grace and the Morrissey family Marguerite, Siofra, Cian and Philip.

A special thank you to Michael Murray whose love and support meant so much to me over the years! Also thank you to the Murray family for their support. To all my friends who never tired of me talking about the PhD, especially Dominika Borowska!

Abbreviations and acronyms

%	Percentage
°C	Degrees Celsius
µg	Microgram
µm	Micromolar
aa	Amino acid
AIRE	Autoimmune regulator
AP-1	Activator protein-1
APC	Antigen presenting cells
APRIL	A proliferating-inducing ligand
BAFF	B cell activating factor of the TNF family
BALT	Bronchus-associated lymphoid tissues
Bcl-6	B cell lymphoma-6
BCMA	B cell maturation antigen
BCR	B cell receptor
BMDC	Bone marrow-derived DC
BMDM	Bone marrow-derived macrophages
bp	Base pairs
Ca^{2+}	Calcium ions
CARD	Caspase recruitment domains
cDNA	Complementary DNA
CDR3	Complementary-determining region 3
CHIR	Chicken Ig-like receptors
CIA	Collagen-induced arthritis
CLP	Common lymphoid progenitor cells
CLR	C-type lectin receptors
CMV	Cytomegalovirus
ConA	Concanavalin A

CRD	Cysteine -rich domain
Ct	Cycle threshold
cTEC	Cortical thymic epithelial cells
CTLA-4	Cytotoxic T-lymphocyte antigen-4
D	Diversity
DC	Dendritic cells
DC-SIGN	DC-specific intercellular adhesion molecule-3-grabbing non-integrin
DD	Death domain
DETC	Dendritic epidermal T cells
DISC	Death-inducing signalling complex
DMEM	Dulbecco's modified Eagle's medium
DMSO	Dimethyl sulphoxide
dNTP	Deoxyribonucleotide
DP	Double positive
DR	Death receptor
dsRNA	Double-stranded RNA
DTT	Dithiothreitol
E. coli	*Escherichia coli*
EAE	Experimental autoimmune encephalomyelitis
EDTA	Ethylenediaminetetra-acetic acid
ERK	Extracellular signal regulated kinase 1
FAM	5-carboxyfluorescein
FChS	Foetal chicken serum
FCS	Foetal calf serum
FITC	Fluorescein isothiocyanate
FoxP3	Forkhead box P3
g	Relative centrifugal force
GATA3	GATA-binding protein 3

h	Hours
HRP	Horseradish peroxidise
HVEM	Herpes virus entry mediator
IFN	Interferon
Ig	Immunoglobulin
IL	Interleukin
ILF	Isolated lymphoid follicles
ILT	Intestinal lymphoid tissues
IPS-1	IFN-β promoter stimulator-1
IPTG	Isopropyl β-D-1-thiogalactopyranoside
IRAK	IL-1 receptor-associated kinase
ITAM	Tyrosine-based activation motif
iTregs	Inducible Treg cells
J	Joining
JNK	Jun-N terminal kinase
kDa	KiloDalton
KLR	Killer cell Ig-like receptors
LAG3	Lymphocyte activation gene-3
LGP2	Laboratory of genetics and physiology 2
LIGHT	Lt-like inhibits inducible expression and competes with HSV glycoprotein D for HVEM a receptor expressed by T lymphocytes
LMP1	Epstein-Barr virus latent membrane protein 1
LRR	Leucine-rich domain
LT	Lymphotoxin
LTi	LT-inducer cells
LTo	LT-organiser cells
M cell	Microfold cell
mAb	Monoclonal antibodies
MAdCAM-1	Mucosal vascular addressin cell adhesion molecule-1

MALT	Mucosal-associated lymphoid tissues
MAPK	Mitogen-activated protein kinases
MAVS	Mitochondrial anti-viral signalling
MCL-1	Myeloid cell leukemia-1
MCR	Multiple cloning region
MDA-5	Melanoma differentiation-associated gene-5
MHC	Major Histocompatibility Complex
Min	Minute
ml	Millilitre
mM	Millimolar
Mo-DC	Monocyte-derived DC
MR	Mannose receptor
MS	Multiple sclerosis
mTEC	Medullary TEC
MyD88	Myeloid differentiation primary response gene 88
NEMO	NF-κB essential modulator
NFATc1	Nuclear activator of T cells 1
NF-κB	Nuclear factor kappa-light-chain-enhancer of activated B cells
ng	Nanogram
NIK	NF-κB inducing kinase
NK	Natural killer cells
NLR	NOD-like receptors
NOD	Nucleotide-binding oligomerisation domain
OPD	o-phenylenediamine dihydrochloride
OPG	Osteoprotegerin
PAMP	Pathogen-associated molecular pattern
PBS	Phosphate-buffered saline
PCR	Polymerase chain reaction

pDC	Plasmacytoid DC
PHA	Phytohaemagluttinin
PMA	Phorbal myristate acetate
PRR	Pattern-recognition receptor
pTreg	Peripheral Treg cells
qRT-PCR	Quantitative real-time-PCR
RA	Rheumatoid arthritis
RAG	Recombination activating gene
RANK	Receptor activator of NF-κB
RANKL	Receptor activator of NF-κB ligand
RHR	Rel homology region
RIG-1	Retinoic acid-inducible gene-1
RING	Really interesting new gene
RIP-1/2	Receptor-interacting protein-1/2
RLR	RIG-1-like receptors
ROR	RAR-related orphan receptor
RPMI	Roswell Park Memorial Institute medium
RS	Recombination signals
RT-PCR	Reverse transcriptase-PCR
schRANKL	Soluble chRANKL
sec	Second
SMART	Simple molecular architecture research tool
SP	Single positive
ssRNA	Single-stranded RNA
STAT-6/4/3	Signal transducer and activator of transcription-6/4/3
TACI	Transmembrane activator and CAML interactor
TAK1	Transforming growth factor-β activated kinase 1
TAMRA	Tetramethylrhodamine

T-bet	T box expressed in T cells
TCR	T cell receptor
TFh	Follicular T helper
TGF-β	Transforming growth factor-beta
Th	T helper
TIR	Toll/IL-1R homology domains
TLR	Toll-like receptor
TMB-8	3, 4, 5-trimethoxybenzoic acid 8-(diethylamino)octyl ester
TNF	Tumour necrosis factor
TRAF	TNF receptor-associated factors
TRAIL	TNF-related apoptosis-inducing ligand
Treg	Regulatory T cells
TRIF	TIR-domain containing adaptor-inducing interferon-β
TSA	Tissue-specific antigens
TWEAK	TNF-like weak inducer of apoptosis
V	Variable
w/v	Weight to volume
X-gal	5-bromo-4-chloro-3-indolyl-β-D-galactopyranoside

Chapter 1

Introduction

1.1 Chicken health

The poultry industry is growing in size. In the EU, there are over 350 million laying hens producing 100 billion eggs, annually (Tarlton *et al.*, 2013). Chicken meat production has increased to around 91 million tonnes in 2012 and the average consumption of chicken meat has substantially increased from 11.1 kg in 2000 to 14.6 kg in 2012 (http://www.thepoultrysite.com/articles/2640/global-poultry-trends-2012). In order to raise as many birds, chickens are reared under intensive conditions. Chickens are selectively bred based on weight gain, feed conversion, muscle colour and egg production. For example, broilers selected to grow quickly can now reach 2 kg in body weight in only 35 days. This advancement in breeding has both positive and negative effects; poultry farmers can produce large quantities of eggs and chicken meat but the birds have decreased reproductive success and susceptible to a wide range of immune diseases (Harford *et al.*, 2014; reviewed in Hocking, 2014).

The development of bacterial antibiotic resistance led to the ban on the use of antibiotics in Europe, increasing the risk of outbreaks of bacterial and parasitic infections in poultry flocks. Newcastle disease virus (NDV), Marek's disease virus (MDV) and avian influenza virus are now recognised as major destructive diseases in the poultry industry. NDV has a wide host range, infecting over 236 species of birds (Kaleta & Baldauf, 1988). Low virulent NDV induces subclinical disease with low morbidity whereas high virulent NDV causes rapid onset of disease and mortality. Marek's disease is a highly contagious viral infection that causes major economic loss to the poultry industry (Biggs & Nair, 2012). It is not just poultry health that requires protection but also public health. Chickens are a source of zoonotic infection, with 60% of emerging human diseases from 1940 to 2004 being linked to a wildlife origin (Jones *et al*., 2008). The highly pathogenic avian influenza virus, H_5N_1, causes 100% mortality in infected birds and can also infect humans (Peiris *et al.*, 2007).

Vaccines have been successfully used for the last 30 years to prevent clinical disease and mortality. However, there is increasing evidence that vaccination is driving the evolution of viruses to overcome the immune response. It is evident that

the vaccination regime against MDV has increased the virulence of the virus with time (reviewed in Nair, 2005).

The increase in zoonotic infections poses a serious threat to human and animal health. Understanding emerging disease outbreaks is hindered by their unpredictability, absence of effective control measures and lack of essential knowledge of the immune responses induced by zoonotic infections (Bean *et al.*, 2013). Progress in characterising the avian equivalent of mammalian immune genes has been slow due to the evolutionary distance between birds and mammals. For example, birds lack lymph nodes, create antibody diversity with a mechanism different to mammals (Glick, 1991) and have a reduced number of genes in their MHC (Kaufman *et al.*, 1999). Amino acid identity can be as low as 25% between mammalian and avian immune proteins and therefore little or no cross-reactivity occurs with reagents and bioassays used for mammalian research (Kaiser, 2010). The greatest advance leading to the identification and cloning of avian immune genes was the release of the chicken genome sequence (Wallis *et al.*, 2004). This, along with the availability of other avian genomes, such as the turkey (Dalloul *et al*., 2010), zebra finch (Warren *et al*., 2010) and duck (Huang *et al.*, 2013), has provided a larger platform to identify chicken orthologues of mammalian immune genes and also avian-specific immune genes.

1.2 Overview of the mammalian immune system

The immune system encounters millions of different antigens daily which are constantly recognised by cells of the immune system. The immune system can be divided into two arms, innate and adaptive immunity. The innate immune system requires a number of cells, such as mast cells, dendritic cells (DC), macrophages, natural killer (NK) cells, basophils, eosinophils and γδ T cells, to recognize and kill invading pathogens. Cell receptors called pattern-recognition receptors (PRR) are required for the detection of components of bacteria, fungi and viruses and for the innate immune response to mould the adaptive immune response. The sites of lymphoid cell accumulations are termed primary and secondary lymphoid organs. Primary lymphoid organs (e.g. bone marrow, thymus and foetal liver) are the sites where naïve but functionally mature lymphocytes are generated in the absence of

antigen. Cells from the primary lymphoid organs seed the secondary lymphoid organs (e.g. spleen, lymph nodes, Peyer's patches and tonsils). During infection, specialised lymphoid organs appear in the lung, bronchus-associated lymphoid tissues (BALT), and in the intestine, intestinal lymphoid tissues (ILT) (Ruddle & Akirav, 2009). Lymph nodes are located at vascular junctions and have lymphatic vessels which allow the transport of antigens and cells from the blood into the lymph nodes. Another important lymphoid system is the mucosal-associated lymphoid tissues (MALT) which are a major producer of IgA and responsible for maintaining tolerance to commensal bacteria and food allergens. The MALT accounts for ~60% of the total body's immune system and produces over ~80% of the body's immunoglobulin per day (Brandtzaeg *et al.,* 1989). The MALT protects the host against pathogen invasion in the gastrointestinal tract, respiratory tract, nasal passages, uro-genital tract and mammary glands (Kudsk, 2002).

1.2.1 Pattern Recognition Receptors

The innate immune system was once thought to be non-specific. However, it is able to discriminate between "self" and a variety of pathogens. The innate immune system can recognise pathogens by germline-encoded PRR. These have the advantage of being independent of immunological memory and they recognise pathogen-associated molecular patterns (PAMP), small molecular molecules common within a class of microbes which are usually vital for the survival of the incoming pathogens and therefore rarely able to be mutated. PRR are constitutively expressed in the host and can recognise the pathogen at any stage of their cell cycle (Kaisho & Akira, 2006). Different PRR react with different PAMP, leading to the activation of specific downstream signalling pathways that drive distinct immune responses. The most studied PRRs are the Toll-like receptor (TLR) family. TLRs are evolutionarily conserved from *Caenorhabditis elegans* to mammals. Toll, the founding member of the family, was first identified in *Drosophila* and is vital for antifungal immunity (Lemaitre *et al.,* 1996). Humans express 10 TLRs (TLR1-10) while mice express 12 (TLR1-9, TLR11-13), each of which differs in their recognition of PAMPs, their subcellular location and the nature of their responses.

TLRs are type I transmembrane glycoproteins which are expressed on the cell membrane (TLR1, TLR2, TLR4, TLR5 and TLR6) or intracellularly, such as in endosomes (TLR3, TLR7, TLR8 and TLR9). Their extracellular domains are characterised by leucine-rich repeats (LRR), with 19-25 LRR motifs, each of which are 24-29 amino acids in length, responsible for pathogen recognition. This is followed by the transmembrane domain and the intracellular region containing Toll/interleukin (IL)-1R homology domains (TIR), that are responsible for recruiting adaptor proteins, such as myeloid differentiation primary response gene 88 (MyD88) and other adaptor proteins that activate signal transduction cascades. Surface TLRs engage a core signalling pathway, leading to the activation of nuclear factor kappa-light-chain-enhancer of activated B cells (NF-κB), activator protein-1 (AP-1) and other transcription factors involved in pro-inflammatory cytokine and chemokine expression (O'Neill & Bowie, 2007). TLRs are expressed on a number of lymphocytes and epithelial cells of mucosal surfaces (Muzio *et al.,* 2000; Zarember *et al.,* 2002) and are expressed in macrophages and subsets of DC (Kadowaki *et al.,* 2001).

The TLR family can be sub-divided into six families based on sequence homology; TLR1, TLR2, TLR4, TLR5, TLR7 and TLR11 sub-families. The TLR1 family is made up of TLR1, TLR6 and TLR10, each residing on the cell membrane. In mammals TLR1, TLR6 and TLR10 genes are tandemly arranged and seem to have arisen due to gene duplication events. Each recognises components of microbial cell walls, such as lipoproteins and peptidoglycans, with only the TLR10 agonist not yet fully identified (Guan *et al.,* 2010). All members of the TLR1 family can form heterodimers with TLR2 (Ozinsky *et al.,* 2000). Ben-Ali *et al.* (2011) carried out an extensive analysis of the extent of amino acid sequence-altering variation on the effects of TLR1, TLR2 and TLR6 functions and host genetics in disease susceptibly and progression in humans. Their work suggested that amino acid alterations are a constraint for TLR2 compared to TLR1 and TLR6. Evolutionary and functional data suggest that TLR2 fulfils an essential function in innate immune responses and its ability to form heterodimers with TLR1 and TLR6 broadens the ability of the host to recognise PAMPs (Farhat *et al.,* 2008). TLR4 and TLR5 are cell surface proteins that recognise bacterial LPS and flagella, respectively. TLR4, upon binding to LPS, is

trafficked to endosomal membranes where it can activate the production of type I interferon (IFN) (Husebye *et al.,* 2006).

TLR3, TLR7, TLR9 and TLR11 are intracellular TLRs found in endosomes and lysosomes, which are more suitable locations to detect viruses. All four require the protein UNC93B1 for transportation from the endoplasmic reticulum to the endolysosomal compartments where they are processed by proteases to become functional receptors (Brinkmann *et al.,* 2007; Kim *et al.,* 2008; Lee *et al.,* 2013). TLR3 recognises double-stranded RNA (dsRNA) to induce pro-inflammatory cytokines and IFNs production (Alexopoulou *et al.,* 2001). The TLR7 family is made up of TLR7, TLR8 and TLR9. Both TLR7 and TLR8 detect single-stranded RNA (ssRNA) while TLR9 detects unmethylated CpG DNA (Kreig & Vollmer, 2007). The TLR11 family consists of TLR11, TLR12 and TLR13 (Zhang *et al.,* 2004). TLR11 and TLR12 can form heterodimers which are vital for the detection of and immune responses against profilin from *Toxoplasma gondii* (Andrade *et al.,* 2013). TLR13 can detect bacterial 23S ribosomal RNA (Li & Chen, 2012). Humans do not possess orthologues of TLR11, TLR12 and TLR13. In fish and frogs the TLR11 family members are called TLR21-TLR23 (Roach *et al.,* 2005).

In addition to TLRs, the innate immune system in vertebrate animals consists of other PAMP receptors, including retinoic acid-inducible gene-1 (RIG-I)-like receptors (RLR), nucleotide-binding oligomerisation domain (NOD)-like receptors (NLR) and C-type lectin receptors (CLR). The type I IFN system is a powerful and vital strategy against viral infection (Samuel, 2001). RLR specifically detect viral RNA in the cytoplasm and there are three family members. RIG-I possesses a central DExD/H box RNA helicase domain involved in RNA binding and two caspase recruitment domains (CARD) at its NH_2-terminus required for the recruitment of downstream IFN-β promoter stimulator-1 (IPS-1) (Yoneyama *et al.,* 2004). Melanoma differentiation-associated gene-5 (MDA-5) is the second member of the RLR family and is similar to RIG-I, possessing two CARD (Kang *et al.,* 2002). RIG-I and MDA-5 recognize different types of RNA; RIG-I detects short dsRNA (<1 kb) or RNA in complex secondary structures whereas MDA-5 detects long dsRNA (>1 kb) (Loo *et al.,* 2008). The CARD regions of RLR interact with the CARD regions of

the mitochondrial antiviral-signalling protein (MAVS), which recruits multiple proteins to assemble a multiprotein complex anchored to the mitochondria where it coordinates signalling events initiated by RIG-I and MDA-5 (Belgnaoui *et al.*, 2011). The third member, called laboratory of genetics and physiology 2 (LGP2) (Kang *et al.*, 2002), does not possess CARD regions and negatively regulates RIG-I and MDA-5 signalling (Rothenfusser *et al*., 2005). However, LPG2 can detect dsRNA but its role in antiviral activity remains unclear. LPG2 overexpression does not activate IFN-α or IFN-β transcription and can block RIG-I-mediated IFN induction (Rothenfusser *et al.*, 2005) but is required for MDA-5 signalling (Pippig *et al.*, 2009). More studies are required to understand the role of mammalian LPG2 in antiviral immune responses.

The NLR family members work as cytosolic receptors that sense intracellular PAMPs. These proteins are characterised by the presence of a NACHT nucleotide-binding domain with a COOH-terminal domain containing multiple LRR motifs that sense their ligands (Ting *et al.,* 2010). There are at least 23 NLR members in humans and 34 members in mice (Liu *et al.*, 2013). NOD1 and NOD2 are the prototypical members of the NOD-like receptor family and sense various bacterial peptidoglycan fragments inducing pro-inflammatory cytokine expression and autophagy (Travassos *et al.*, 2010; Boyle *et al.*, 2013). The well-studied pathway of several NLR is the assembly of the multi-protein complex, the inflammasome, which includes caspase 1. Inflammasome complexes induce the proteolytic cleavage of pro-IL-1β and pro-IL-18 allowing release of the soluble pro-inflammatory cytokines IL-1β and IL-18 (Elinav *et al.*, 2011). These cytokines can initiate a number of biological processes, such as neutrophil influx and the activation of T helper (Th) cells, depending on the presence of other cytokines, such as IL-17, IL-4 or IL-12 and IFN-γ (reviewed by Keyel, 2014).

CLR are a large superfamily of proteins that possess one or more structurally related C-type lectin-like domains. Extracellular and transmembrane members are involved in antifungal immunity by binding to the fungus and mediating its uptake, subsequent killing and appropriate modulation of the immune response. The best characterised members of the CLR superfamily are the mannose receptor (MR),

dectin-1 and DC-specific intercellular adhesion molecule-3-grabbing non-integrin (DC-SIGN) (Willment & Brown, 2008). MR is a transmembrane protein with eight extracellular C-type lectin-like domains. MR can recognise both bacterial pathogens and fungi and induces a variety of cellular responses upon recognition of fungi, such as activation of the NF-κB pathway which induces pro-inflammatory cytokine expression (Zhang *et al.,* 2005). Dectin-1 has a single carbohydrate-recognition domain and an intracellular tyrosine-based activation motif-like domain (Brown, 2006). It can recognise a number of fungal species mediating their uptake and killing by inducing the expression of tumour necrosis factor (TNF)-α, IL-2, IL-10, IL-6 and IL-23 (LeibundGut-Landmann *et al.,* 2007). DC-SIGN is found primarily in microdomains of immature DC (Cambi *et al.,* 2003). Eight orthologues have been identified in mice, each one is differentially distributed and all are structurally different. DC-SIGN detects carbohydrates with high mannose structures in a calcium ion (Ca^{2+})-dependent fashion (Powlesland *et al.,* 2006).

1.2.2 Cells of the innate immune system

PRR are expressed on a number of innate immune cells, such as NK, DC and macrophages. NK cells are large granular lymphocytes that are involved in innate immunity against bacteria, viruses and parasites. These cells share many features with T cells. NK cells have two major effector functions: direct cytolysis and production of pro-inflammatory chemokines and cytokines (Martin-Fontecha *et al.,* 2004). The ability of cells to undergo cytotoxicity has been due to the development of a sophisticated and robust system to control cellular processes while not damaging healthy tissue. NK cells can detect the presence of both negative and positive signals which may cooperate or antagonise each other, called the dynamic equilibrium concept (Vivier *et al.,* 2004). NK cells use inhibitory receptors to gauge the absence of constitutively expressed self-molecules on target cells. NK cells express inhibitors for MHC class I molecules that include killer cell Ig-like receptors (KLR) in humans, Ly49 in mice and NKG2A conserved in both species. A conserved feature of these molecules is the presence of one or two intracytoplasmic domains called immunoreceptor tyrosine-based activation motifs (ITAM) (Anfossi *et al.,* 2006). These molecules interact with constitutively expressed MHC class I molecules on the

surface of healthy cells which may be lost when cells undergo stress or infection. NK cells lose their inhibitory characteristics when they come into contact with "missing self" cells and activate their effector functions.

B and T lymphocytes are mediators of adaptive immunity but their activation and effector functions are controlled by antigen-presenting cells (APC), such as DC and macrophages. DC are a heterogeneous cell population which have the capacity to present antigen to B and T lymphocytes (Steinman, 1991). DC capture antigen by three approaches: phagocytosis, macropinocytosis and receptor-mediated endocytosis (Sallusto *et al.,* 1995). During non-inflammatory conditions there are two types of DC, plasmacytoid DC (pDC) and conventional DC (cDC). pDC circulate through tissues and produce large amounts of type I IFN at sites of viral infection (Yang *et al.,* 2005). cDC consist of both lymph node-resident and migratory cells. Resident cDC are maintained in a steady state of immaturity in the lymph node tissues where they survey the surrounding environment and the blood for signs of infection (Wilson *et al.,* 2003). In the mouse, resident cDC can be subdivided by their surface receptors, such as the expression of the homodimeric protein $CD8\alpha\alpha^+$ cDC, $CD8\alpha\alpha^-$ cDC, $CD8\alpha\alpha^-CD4^+$ cDC or $CD8\alpha\alpha^-CD4^-$ cDC. Each cell type differs in their cytokine and chemokine production profiles upon antigenic exposure (Proietto *et al.,* 2004). Migratory cDC circulate in the peripheral tissues and upon detection and phagocytosis of the antigen they migrate to the draining lymph nodes where they present antigenic peptides in the context of MHC molecules to the T cell receptor (TCR) (Banchereau & Steinman, 1998). Again these cells can be further categorised by their surface antigens. $CD8^-CD103^-$ cDC are potent presenters of antigen by MHC class II molecules and are generally associated with inducing a Th2 immune response. $CD8^+CD103^+$ cDC are characterised by their ability to present antigenic peptides to $CD8^+$ T cells by MHC class I molecules and the initiation of a Th1 immune response (Proietto *et al.,* 2004).

Macrophages are found in all tissues where they display functional diversity and have roles in every aspect of an organism's biology, such as development, repair, homeostasis and immune response to pathogens (Wynn *et al.,* 2013). Macrophages are a heterogeneous family of phagocytic cells. In response to pathogens,

macrophages are polarised phenotypically. For example, when activated by IFN-γ or TLR interaction, macrophages undergo classical activation (M1), whereas alternatively activated macrophages (M2) are elicited by Th2-type cytokines, such as IL-4, IL-13 and IL-21, which are produced during helminth infection (Biswas & Mantovani, 2010). M1 cells produce large amounts of pro-inflammatory cytokines, such as IL-12, TNF-α and IL-23, express MHC class II molecules and produce reactive nitrogen intermediates. M2 cells are more potent phagocytes and express higher levels of mannose and galactose receptors, low expression of IL-12 and high expression of IL-10 and IL-1RN (Mantovani *et al.*, 2002).

The most important characteristic of APC is their ability to present antigen to the effector cells of adaptive immunity. Antigens phagocytosed by APC are processed by degradation to small peptides that dock with and are presented by MHC molecules. MCH class I and class II molecules are similar in function; they present peptides at the cell surface to $CD4^+$ and $CD8^+$ T cells, respectively. MHC class I molecules present peptides from intracellular sources whereas MHC class II molecules present exogenous peptides (reviewed in Vyas *et al.*, 2008). Intracellular antigens are degraded by cytosolic proteasomes and peptide fragments are then transported to the endoplasmic reticulum (ER) by the transporter-associated with antigen presentation (TAP) proteins where they encounter the MHC class I molecules. Within the ER, the MHC class I heterodimer is assembled with a polymorphic heavy chain and a light chain called β_2-microglobulin. This heterodimer complex is stabilised by the docking of the 8-9 amino acid antigen peptide fragment whereupon the MHC class I complex exits the ER to present the peptide at the cell surface (reviewed by Neefjes *et al.*, 2011). MHC class II molecules are assembled in the ER where the transmembrane α and β chains associate with the invariant chain. This complex is transported to the late endosomal compartment where the invariant chain is digested and the class II-associated invariant chain peptide (CLIP) resides in the peptide-binding groove of the MHC class II molecule. MHC class II molecules will dissociate CLIP to allow peptide fragments degraded in the endosomal compartments to bind and then travel to the plasma membrane for presentation to T cells (reviewed by Neefjes *et al.*, 2011). Although both MHC class I and II molecules are assembled in the ER, MHC class I molecules require the binding of a peptide to

exit the ER, whereas MHC class II molecules associate with the invariant chain allowing their transport from the ER.

1.2.3 B and T cell receptors

Adaptive immunity is required for the late phase of infection that is characterised by its exquisite specificity, clonal expansion of lymphocytes expressing antigen-specific receptors and generation of immunological memory. B and T cells have major roles in the development and organisation of adaptive immunity. In the adaptive immune response, antigen is recognised by two distinct sets of highly variable receptors, the B cell receptor (BCR) and the TCR. To protect against pathogens, the host needs to generate a diverse pool of BCR that will recognize a broad range of antigens. Human and mouse B cell development occur in the bone marrow where stromal cells induce the differentiation of common lymphoid progenitor cells (CLP) into multi-potential pre-B cells (Izon *et al.*, 2001). These B cell progenitors go through a process of assembling their BCR and signalling proteins, Igα and Igβ, giving rise to immature IgM^+ IgD^+ B cells. The basic subunits of a Y-shaped antibody molecule are a pair of identical heavy-chains and a pair of identical light-chains that are bound by non-covalent bonds and disulphide bridges. The NH_2-terminal region of an antibody molecule is called the variable region, as it has a unique amino acid sequence that is involved in binding with the antigen. The COOH-terminal region is known as the constant region and only comes in a few forms. The constant region provides the class and the function of the antibody. The variable regions of the heavy chain are assembled from germline-encoded variable (V), diversity (D) and joining (J) gene segments, whereas the light chain is assembled using V and J segments, by a process called V(D)J recombination (Tonegawa, 1983). While the light chain may be less diverse by not encoding D segments, its diversity is derived from the presence of two independent genes, κ and λ, either of which can be recombined to form light chains. Recombination occurs between two segments expressing recombination signals (RS). The RS are highly conserved heptamer and nonamer sequences separated by 12 bp and 23 bp spacer sequences (12/23 bp rule). Therefore rearrangement takes place between a RS with a 12 bp spacer and a 23 bp spacer allowing for the docking and activation of the

recombination activating gene-1 (RAG-1) and RAG-2, forming the RAG endonuclease complex which introduces single-strand nicks to form a hairpin structure (Oettinger *et al.*, 1990). The RS regions are joined together while the coding ends are modified by potential nucleotide loss or addition (Tonegawa, 1983).

The potential of variation within the variable region of the antibody can been seen in the mouse heavy chain locus that spans 3 Mb and consists of over 150 V_H genes, 4-5 D_H genes and 4 J_H genes. Somatic hypermutation also induces more diversity into the variable regions of immunoglobulins by introducing point mutations into the V exons and into the introns upstream of the J regions. This increases DNA sequence diversity but also allows for the selection of B cell clones with stronger affinity for the antigen (Di Noia *et al.*, 2007).

Antigen recognition by T cells requires the expression of TCR. TCR are heterodimeric proteins expressed on the membrane surface composed of two immunoglobulin domains. Vertebrates possess four TCR chains, α, β, γ and δ, which form αβ or γδ heterodimers connected by a disulphide chain. The variable region consists of a V-type Ig domain linked to a D and J segment (TCRβ and TCRδ) or a V domain linked to a J segment (TCRα and TCRγ). As with antibodies, TCR diversity occurs via the recombination of the heavy and light chains and within the area of the V(D)J joins, called the complementarity-determining region 3 (CDR3), various deletions/additions of nucleotides introduce additional variability. T cells migrate from the bone marrow to the thymus and are double-negative ($CD4^-$ $CD8^-CD45^{hi}CD25^+$) when they undergo β, γ or δ chain rearrangement (Burtrum *et al.*, 1996) expressing a single chain at their surface. When the β chain is expressed, cells lose the expression of CD25 and upregulate both CD4 and CD8 ($CD4^+CD8^+CD45^{hi}CD25^-$) becoming double-positive (DP) cells leading to the rearrangement of the α-chain. These DP cells undergo positive and negative selection to generate either $CD4^+$ or $CD8^+$ single-positive αβ T cells. $CD4^+$ αβ T cells recognise peptide complexed to MHC class II molecules and $CD8^+$ cells recognise peptide complexed to MHC class I molecules. The mature TCR has no catalytic function but signals through intracellular tyrosine-based ITAM motif-containing

TCR-associated molecules, CD3γε, CD3δε and CD3ζζ (Samelson, 2002), which ultimately activate the T lymphocytes after the initial recognition steps.

As for γδ T cells, after productive recombination and correct pairing, a subset of these cells leave the thymus and populate secondary lymphoid organs (Turchinovich & Pennington, 2011), as another subset of γδ T cells undergo further differentiation in the thymus to become IL-17A-producing γδ T cells, dendritic epithermal γδ T cells and NK γδ T cells (Haas *et al.*, 2009). γδ T cells can be further sub-categorised by the expression of different TCR segments. In the mouse, subpopulations of γδ T cells can be distinguished in the skin (Vδ5), spleen and intestine (Vδ1) (Haas *et al.*, 1993). γδ T cells have both activating and regulatory roles in controlling both the innate and adaptive immune system (He *et al.*, 2014).

1.2.4 T helper cells

A protective immune response often relies on the ability of conventional $CD4^+$ T cells to accumulate high numbers of effector cells to activate a strong reaction against the invading pathogen. The primary response of T cells takes place over 3-7 days. They can also differentiate into follicular T (TFh) cells to promote B cell immunity and antibody production, generally taking 5-15 days. During this period T cells have the opportunity to come into contact with both lymphoid (DC, B cells) and non-lymphoid (stromal, epithelial cells) cells and each surface receptor contact may direct, modulate or control the activity of the T cell. The existence of distinctive populations of differentiated $CD4^+$ T cells was first demonstrated by Mosmann & Coffmann in 1986 from *in vitro* murine T cell clones. Each cell type can be distinguished by their signature cytokine expression and pattern of cell surface markers (Mosmann & Coffmann, 1986; Killar *et al.*, 1986). These effector T helper cells were named Th1 and Th2 cells and investigations into their roles in immunity dominated the field of immunology for over 15 years.

The differentiation and activation of $CD4^+$ T cells is regulated by three signalling components: the TCR (Signal 1), costimulatory molecules (Signal 2) and the cytokine receptors (Signal 3) on the surface of cells (Nagashima *et al.*, 2014). Binding of the cytokine receptors serves an essential role in the lineage decision of

the Th subsets. However, it has been proposed that the antigen dosage, co-stimulators, genetic modifiers and non-cytokine factors can have a role in the lineage pathway (Murphy & Reiner, 2002). The presentation of antigen by MHC class II to naïve $CD4^+$ T cells leads to the upregulation of certain transcriptional machinery that activates the appropriate effector T cells. The T box expressed in T cells (T-bet) transcription factor has a central role in Th1 differentiation, required to control infection with intracellular pathogens. T-bet induces the transcription of the loci encoding IFN-γ and lymphotoxin and increases the cells responsiveness to IL-12 by inducing the expression of the IL-12βR (Szabo *et al.,* 2002).

Th2 differentiation is dependent on the expression of IL-4 which is controlled by c-MAF, a member of the basic leucine zipper family of proteins (Ho *et al.,* 1998). The activation and increase in signal transducer and activator of transcription (STAT)-6 expression is quickly followed by the expression of IL-4 and leads to GATA-binding protein 3 (GATA3) expression. GATA3 transactivates the IL-5 promoter and also drives the expression of IL-4, IL-13 and IL-25, producing Th2 cells (Zhang *et al.,* 1997; Ouyang *et al.,* 2000). These cytokines protect against extracellular pathogens by orchestrating a humoral response through the induction of immunoglobulin class switching of IgG and IgE. The cytokines produced by either Th subsets negatively regulate the other. For example, IL-12 signalling via STAT4 is required for the repression of GATA3 (Ouyang *et al,* 1998) whereas IL-4 represses the expression of IL-12 receptors on the surface of naïve T cells (Murphy *et al.,* 1997). Terminally differentiated T cells can be driven to induce their signature cytokines by the presence of other cytokines. For example, IL-12 and IL-18 synergise to drive Th1 cells to produce IFN-γ (Robinson *et al.,* 1997; Neighbors *et al.,* 2001).

Since the identification of the Th1 and Th2 paradigm, various other Th subsets have been identified in mammals (Figure 1.1). As mentioned previously, IL-12 is a signature cytokine of Th1 cells. This is a heterodimeric protein consisting of two chains, α (p35) and β (p40). p35 or p40 knockout mice differed in their ability to clear an infection (Brombacher *et al.,* 1999). Soon after, it was demonstrated that the p40 subunit can form heterodimers with a novel p19 subunit, a cytokine now called

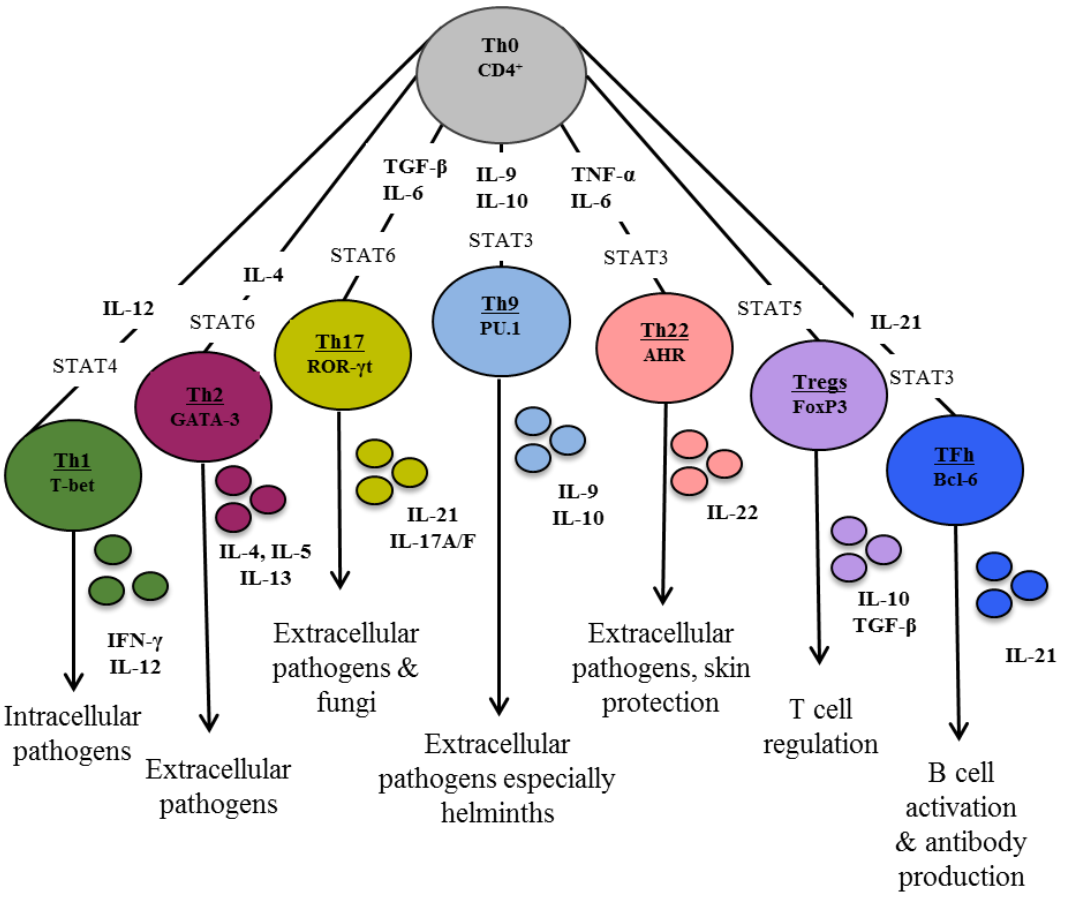

Figure 1.1 Overview of mammalian Th cells. *Naïve Th0 cells differentiate under various immunological conditions that produce their driving cytokines and activate the transcription factors required for their maintenance and the expression of their effector cytokines.*

IL-23 (Oppmann *et al.*, 2000). In 2003, IL-23 was identified as the cytokine responsible for joint autoimmune inflammation (Murphy *et al.*, 2003). IL-23$^{-/-}$ (p19) mice were immune to collagen-induced arthritis and lacked IL-17-producing T cells at the site of infection (Murphy *et al.*, 2003). The development of IL-17-producing CD4^{+} T cells was inhibited by the presence of IL-4 or IFN-γ, indicating a T cell lineage not associated with Th1 or Th2 (Harrington *et al.*, 2005). The newly identified IL-17A-, IL-17F-, IL-21- and IL-22-producing Th17 cells require the presence of IL-6 and TGF-β to activate STAT3 and induce the expression of transcription factors, RAR-related orphan receptor-γt (RORγt) and RORα (Ivanov *et*

al., 2007). IL-23 is required to sustain Th17 cells but not their differentiation (Ivanov *et al.,* 2007). Th17 cells are required for the control of a variety of bacterial and fungal infections in the mucosa (Liang *et al.,* 2006). Th1/Th17 pathogenesis has been linked to a number of autoimmune diseases, with IFN-γ and IL-17 expression associated with prolonged and uncontrolled inflammation. The pathogenesis of these cytokines contributes to disorders such as experimental autoimmune encephalomyelitis (EAE), a model for multiple sclerosis (MS), and collagen-induced arthritis (CIA), a model for rheumatoid arthritis (RA) in mice. These diseases arise from a break in tolerance of self-antigens and the development of auto-aggressive effector T cells infiltrating the target tissues (Leung *et al.,* 2010).

T cells can also differentiate into regulatory cells where they can have immunosuppressive functions to control against damaging self-reactivity. Self-reactive T and B cells are exposed to self-antigens during stages of their development and this is one of the major mechanisms of discriminating between self and non-self (self-tolerance). Activation and expansion of T cells that have escaped clonal deletion during the thymus selection process are actively suppressed in the periphery by naturally occurring $CD25^+$ (IL-2Rα) $CD4^+$ regulatory T (Treg) cells (Sakaguchi *et al.,* 2008). Treg cells are derived from a separate lineage to TCRαβ, TCRγδ, $CD4^+$ and $CD8^+$ T cells (Apostolou *et al.,* 2002). A number of diseases are attributed to the loss or malfunction of Treg cells, such as immune dysregulation, polyendocrinopathy enteropathy X-linked syndrome and scurfy. These autoimmune diseases are linked to uncontrolled expansion of $CD4^+$ T cells and further analysis identified a common mutation in one gene, a forkhead-winged helix transcription factor called Forkhead box P3 (FoxP3) (Hori *et al.,* 2003). The FoxP3 transcription factor is necessary for the development of $CD25^+$ $CD4^+$ Treg cells in the thymus (Fontenot *et al.,* 2003). Treg cells inhibit the activation and production of IL-2 by a contact-dependent mechanism and produce huge amounts of the anti-inflammatory cytokine, IL-10 (Dieckmann *et al.,* 2001). Recently, two further Treg cell populations have been identified in mammals, $FoxP^-$ Treg cells that are found in the periphery called pTreg and inducible Treg cells (iTregs) which are differentiated independent of the thymus in the presence of TGF-β (Chen *et al.,* 2003). Treg cells have also been implicated in targeting DC by expressing the cytotoxic T-lymphocyte antigen-4 (CTLA-4). Studies

suggest that CTLA-4-expressing Treg cells interact with CD80/CD86 on the surface of DC and inhibit effective T cell activation (Larsson *et al.,* 2009). Treg cells also express lymphocyte activation gene-3 (LAG-3), a CD4 homologue that can bind to MHC class II on DC and suppress their maturation (Bruniquel *et al*., 1998). Tr1 is another subfamily of regulatory T cell subsets that can suppress immune responses through a contact-independent approach by producing large amounts of IL-10. Tr1 cell differentiation is driven by IL-27 and TGF-β and they do not express the FoxP3 transcription factor (Awasthi *et al.,* 2007)

IL-9- (Th9) and IL-22- (Th22) producing Th cells have recently been added to the list of $CD4^+$ T cells. IL-4 inhibits TGF-β-mediated upregulation of FoxP3 expression. The stimulation of $CD4^+$ T cells with both IL-4 and TGF-β led to unexpected Th cells, expressing both IL-9 and IL-10, now called Th9 cells. Th9 cells have the ability to enhance proliferation of fellow Th cells but also have a role in autoimmune disease (Dardalhon *et al.,* 2008). Th22 cells produce IL-22 without IL-17 production and express the skin cell-homing chemokines, CCR4 and CCR10 (Duhen *et al.,* 2009). IL-6 and TNF-α synergise to enhance IL-22 production in these cells (Duhen *et al.,* 2009). TFh cells are an important Th cell subset involved in T-dependent B cell responses. These CXCR5-expressing cells are less dependent on cytokines and transcription factors for their differentiation (Nurieva *et al.,* 2008). TFh cell differentiation is driven by the transcriptional repressor B cell lymphoma-6 (Bcl-6) (Yu *et al.,* 2009) and they produce copious amounts of the plasma cell inducer cytokine, IL-21 (Zotos *et al.*, 2010).

1.3 Overview of the chicken's immune system

Like mammals, chickens have developed innate and adaptive immune responses to protect against a range of pathogens. Major differences have been identified between the mammalian immune system and that of chickens. Chickens lack lymph nodes and functional eosinophils, possess a unique organ for B cell development, perform BCR repertoire variation using a different mechanism to that seen in mammals and possess only three Ig isotypes. Although mammals and birds arose from a common ancestor over 300 million years ago, the chicken represents a

species with a more primitive immune system that carries out an immune response with much less architecture and sophistication than the mammalian immune system.

1.3.1 Chicken PRRs

Like mammals, the chicken innate immune system relies on the detection of PAMPs with germline-encoded PRR, such as TLR, RLR, NLR and CLR family members. The avian repertoire of TLR comprises mammalian orthologues and avian-specific members (Table 1.1). The mammalian TLR1 family (TLR1, TLR6 & TLR10) can form heterodimers with TLR2 to increase the capacity of the innate immune system to detect invading pathogens (Ozinsky *et al.,* 2000). In the chicken, the TLR1 family is represented by tandemly duplicated TLR1-like genes, chTLR1-like a (TLR1La), chTLR1Lb and two TLR2-like genes, chTLR2a and chTLR2b (Boyd *et al.,* 2001; Fukui *et al.,* 2001). These molecules, like mammalian TLR2, can form heterodimers to increase the capacity of the chicken's innate immune system to detect PAMPs (Higuchi *et al.,* 2008). ChTLR2a and chTLR2b vary in their capacities to respond to TLR2 antagonists. For example, the chTLR2a and chTLR1b heterodimer exclusively recognises peptidoglycan of mycobacterial origin and react more robustly to *Mycobacterium avium* exposure (Higuchi *et al.,* 2008). Chickens have orthologues of TLR3 (Schwarz *et al.,* 2007), TLR4 (Leveque *et al.,* 2003), TLR5 (Iqbal *et al.,* 2005) and TLR7 (Philbin *et al.,* 2005) which are encoded within genomic regions with conserved synteny (Roach *et al.,* 2005). ChTLR4 is linked to the early regulation of *Salmonella* infection (Leveque *et al.,* 2003) and chTLR5 can detect flagellated *Salmonella* (Iqbal *et al.,* 2005).

Both chTLR3 and chTLR7 are intracellular receptors that detect viral RNA (Schwarz *et al.,* 2005; Philbin *et al.,* 2005). However, certain members of the chicken TLR7 family are non-functional or missing. ChTLR8 is a pseudogene, fragmented and disrupted by a chicken repeat-1 (CR1) retrovirus-like element (Philbin *et al.,* 2005). The disruption of the avian TLR8 gene was found in galliform birds but not in non-galliform bird species, perhaps due to the differences in susceptibility of galliform bird species to highly pathogenic viral infections (Boyd *et al.,* 2007). TLR9 is absent from the chicken genome. However, chicken cells can respond to CpG

Human	Chicken	Antagonists	Pathogen
TLR1/6/10	TLR1La TLR1Lb	Lipoprotein	Mycobacteria
TLR2	TLR2a TLR2b	Peptidoglycan	$Gram^+$ bacteria
TLR3	Present	dsRNA	Viruses
TLR4	Present	LPS	$Gram^-$ bacteria
TLR5	Present	Flagella	$Gram^-$ bacteria
TLR7	Present	ssRNA	Viruses
TLR8	Pseudogene	ssRNA	Viruses
TLR9	TLR21	CpG	Bacteria and viruses
Absent	TLR15	LPS Lipoprotein CpG Lipoprotein	$Gram^{-/+}$ bacteria viruses mycobacteria Fungi Yeast

Table 1.1 TLR family members and their antagonists in humans and chickens.

motifs (Vleugels *et al.*, 2002; St Paul *et al.*, 2011), which are detected by chTLR21 (Brownlie *et al.*, 2009; Keestra *et al.*, 2010). ChTLR21 is an intracellular nucleotide receptor that shares many functional characteristics with mammalian TLR9 (Brownlie *et al.*, 2009; Keestra *et al.*, 2010; Chrząstek *et al.*, 2014). Orthologues of TLR21 have been identified in fish and reptile species (Gao *et al.*, 2013; Yeh *et al.*, 2013).

TLR15 is unique to avian species having been identified in the chicken (Higgs *et al.*, 2006), turkey (Ramasamy *et al.*, 2012) and goose genomes (Genbank Accession Number JQ014619.1). ChTLR15 may have been gained over evolutionary time to compensate for the loss of TLR members in the chicken genome (Table 1.1). ChTLR15 has the closest identity to chTLR2 and its mRNA expression levels were

increased in chicken fibroblast cells infected with heat-killed *Salmonella* Typhimurium and *Salmonella* Enteritidis, intestinal cells and heterophils (Higgs *et al.*, 2006; Shaughnessy *et al.*, 2009; Nerren *et al.*, 2010). In another study, the TLR9 agonist, CpG, the TLR1 agonist, PAM3CSK4 and the TLR4 and the TLR5 agonists, LPS and flagella, significantly upregulated chTLR15 mRNA expression levels in stimulated HD11 cells but levels were not affected by stimulation with poly I:C (TLR3), peptidoglycan (TLR2) or CL075 (TLR7) (Ciraci & Lamont, 2011). ChTLR15 can be activated by proteolytic cleavage of its receptor ectodomain and can sense virulence-associated fungal and bacterial proteases (De Zoete *et al.*, 2011). When HEK293-T cells were transfected with chTLR15, NF-κB levels were increased when cells were exposed to yeast-derived lysates (Boyd *et al.*, 2012). The NH_2-terminal portion of the haemagglutinin protein from *Mycoplasma synoviae* induced increased chTLR15 mRNA expression levels which mediated activation of NF-κB in chicken macrophages (Oven *et al.*, 2013). *Eimeria tenella* sporozoites stimulated heterophils and monocyte-derived macrophages increased chTLR15 mRNA expression levels (Zhou *et al.*, 2013). In MDV infected chickens, chTLR15 mRNA expression levels were increased in the spleen 4, 14 and 21 days post-infection (Jie *et al.*, 2013). It seems chTLR15 can detect a range of PAMPs.

A RIG-I orthologue has not been identified in the chicken genome (Karpala *et al.*, 2011) but it is present in both the duck and goose genomes (Barber *et al.*, 2010; Sun *et al.*, 2013). Waterfowl are the natural reservoir of avian influenza virus but do not normally succumb to severe disease. Ducks infected with the highly pathogenic H_5N_1 virus produce huge amounts of RIG-I in their lungs. DF-1 cells also produced IFN-β upon H_5N_1 infection (Barber *et al.*, 2010). Geese are also resistant to the highly pathogenic NDV and RIG-I expression has been demonstrated in infected birds (Sun *et al.*, 2013). The absence of RIG-I from the chicken genome may be the reason why chickens are highly susceptible to highly pathogenic influenza virus and NDV. An ortholog of MDA-5 has been identified and characterised in the chicken (Karpala *et al.*, 2011; Liniger *et al.*, 2012) and the duck (Wei *et al.*, 2014). LPG2 is also present in the chicken genome and its RNA silencing reduces H_5N_1-mediated type I IFN secretion (Childs *et al.*, 2007). The chicken genome contains NOD1 but does not possess a NOD2 gene. Recently an antibody was generated against the

chicken C type-lectin DEC-205 (Staines *et al.,* 2013) and mRNA transcripts of MR and DC-SIGN have been detected in BMDC treated with avian influenza-derived glycans (De Geus *et al.,* 2013).

1.3.2 Cells of the chicken innate immune system

Various cells of both the innate and adaptive immune responses have been described in chickens. Polymorphonuclear leukocytes are vital components of the innate immune system. They function to kill microbes by expressing Fcγ and complement receptors that mediate the opsonisation-dependent phagocytosis of invading pathogens. Heterophils are the chicken functional equivalent of mammalian neutrophils and are the most abundant granulocytes circulating in the chicken's blood. These cells are highly phagocytic. Phagocytosis is generally followed by degranulation and production of oxidative burst to kill pathogens (Kogut *et al.,* 1994). Heterophils, like mammalian neutrophils, have the capacity to release fibrous structures called heterophil extracellular traps (Chuammitri *et al.,* 2009). The one major difference between neutrophils and heterophils is the lack of myeloperoxidase in chickens, meaning that heterophils generate a relatively weak oxidative burst compared to their mammalian counterparts (Wells *et al.,* 1998). However, avian heterophils are quite effective at killing pathogens by phagocytosis and utilising anti-microbial proteins, such as lysosomes, β-defensins and peptides (reviewed by Genovese *et al.,* 2013). Heterophils are important mediators of the innate immune system, as highlighted by their ability to express a number of TLRs. Heterophils express chTLR1La, chTLR1Lb, chTLR2a, chTLR2b, chTLR3, chTLR4, chTLR5, chTLR7 and chTLR15 (Kogut *et al.,* 2005a; Kogut *et al.,* 2005b; Nerren *et al.,* 2009) and probably chTLR21, as they respond to CpG stimulation (He *et al.,* 2012). The engagement of heterophil receptors leads to their activation and expression of pro-inflammatory cytokines and chemokines (Kogut *et al.,* 2005a; He *et al.,* 2005).

NK cells have been identified in the chicken. To date, three subsets of chicken NK cells have been identified from the embryo, intestinal epithelial lymphocytes (IEL) and peripheral blood mononucleated cells (PBMC), distinguished by differential surface expression of antigens, such as CD8, CD25 and CD56 (reviewed by Straub *et al.,* 2013). The chicken leukocyte receptor complex has been

mapped to micro-chromosome 31 and so far only one multi-gene receptor family has been identified, called the chicken Ig-like receptors (CHIR) (Luan *et al.,* 2006). CHIR have similar structure to mammalian KIR and Ly46 and have both positive and negative signalling capacities required for NK cell regulation and activation (Viertlboeck & Göbel, 2011).

In 2010, the first non-mammalian bone marrow-derived DC (BMDC) were cultured from chicken bone marrow cells using recombinant chicken IL-4 (chIL-4) and GM-CSF (CSF-2) (Wu *et al.,* 2010). Avian BMDC have the capacity to upregulate mRNA expression levels of pro-inflammatory cytokines upon LPS and CD40L stimulation, express maturation markers on their cell surface, such as MHC class II, CD40, CD86 and the chemokine receptor, CCR7, and are potent stimulators of T cells (Wu *et al.,* 2010; Wu *et al.,* 2011). Chicken BMDC express a variety of TLRs, such as chTLR2, chTLR4, chTLR5 and chTLR21 (Liang *et al.,* 2013). Immature BMDC are highly phagocytic, like mammalian DC (Wu *et al.,* 2010) and play a role against avian influenza virus in the chicken lung (De Geus *et al.,* 2013). Recently, avian DC have been characterised from the chicken spleen (Quéré *et al.,* 2013). Chicken bone marrow-derived macrophages (BMDM) cultured with recombinant chicken CSF-1 (chCSF-1) to induce their differentiation have also been described; although functional studies were not as comprehensive as the BMDC study, the cells were capable of phagocytosis (Garceau *et al.,* 2010).

1.3.3 Chicken B and T cell receptors

In contrast to bone marrow models of B cell development in human and mouse, avian species differ both in the anatomical location and method of generation of BCR diversity. In 1954, Glick and colleagues identified the requirement of the bursa of Fabricius for antibody production against *Salmonella* type O-antigen, and so these antibody-producing cells became known as B (for bursa) cells. Primary antibody generation in the chicken occurs through somatic gene conversion rather than the V(D)J recombination process seen in human and mouse. The chicken light chain locus contains 25 V_L genes upstream from the functional V_L. All 25 V_L genes are pseudogenes (ψV_L) due to the lack of functional RS, out of frame deletions or truncations. The locus also expresses only one C_L and one J_L segment (Reynaud *et*

al., 1987). The chicken also lacks the κ light chain locus so it would seem that its antibody diversity is much more limited than mammals. However, chickens display considerable heterogeneity in their circulating light chains (Jalkanen *et al.,* 1984). The same applies for the chicken heavy chain locus, where single functional V_H and J_H genes are present with 15 functional D_H genes with similar sequence patterns (Reynaud *et al.,* 1991). Like the light chain locus, the heavy chain locus also contains V_H pseudogenes upstream from its functional V_H gene (Reynaud *et al.,* 1989). Interestingly, the heavy chain pseudogene sequences are homologous to V_H and D_H genes suggesting that these genes fused together and multiplied by gene duplication at some point in evolutionary time (Ota & Nei, 1995). Like mammals, gene rearrangement takes place using the RAG-1 and RAG-2 proteins with rearrangement of the chicken light chain being straightforward. The V_L and J_L are flanked by RS sequences and are joined together using the 12/23 rule, meaning all chicken B cells express the same IgL chain. However, diversity does occur within the light chain in the junctional sequence between the VJ segments in terms of length (McCormack *et al.,* 1989). The chicken does not process deoxyribonucleotidyl transferase gene meaning that non-template (N) nucleotides are not added to the coding ends before joining as would occur in mammals.

As for heavy chain rearrangement, the chicken possesses only three heavy chain isotypes-IgM, IgA and IgY. IgM and IgA are similar to their mammalian counterparts whereas chicken IgY, from a phylogenetic perspective, is similar to mammalian IgG and IgE. There appear to be no mammalian homologues of IgD or IgE or isotypes of IgG present in the chicken (Ratcliffe, 2006). Chicken heavy chain rearrangement is similar to mammalian V(D)J recombination events; the VDJ segments are joined together as in mammals but in the chicken D_H-D_H joining can occur. D_2J_H and D_3J_H segments have been identified in the chick embryo but not in hatched chickens making their biological functions uncertain (Reynaud *et al.,* 1991). Diversity is created within the chicken light chains by somatic gene conversion. As mentioned previously, the light gene locus contains 25 ψV_L genes upstream from their functional V_L gene. The light chain ψV_L genes have high diversity at sites of complementarity-determining regions (CDR) similar to V_L regions that correspond to the variable region of the antibody. A stretch of the IgV_L can be replaced by a

sequence derived from the ψV_L genes of varying size (10-300 amino acids) leading to an extensive repertoire of diversity at the site of antigen recognition (McCormack & Thompson, 1990).

With the chicken TCR, both αβ and γδ TCR-expressing T cells are conserved. Chicken γδ T cells can be sub-categorised by the expression of surface CD8α antigen: CD8α-negative ($CD8\alpha^-$), CD8α-diminished ($CD8\alpha^{Dim}$) and CD8α-high ($CD8\alpha^+$) cells. The $CD8\alpha^+$ cells can be further sub-divided on the expression of either the homodimeric CD8αα or heterodimer CD8αβ (Berndt *et al.*, 2006). Both these cell types produce Th1-associated cytokines upon *Salmonella* Typhimurium infection in chickens (Pieper *et al.*, 2011).

Unlike mammals, where three distinct CD3 proteins, CD3γ, CD3δ and CD3ε signal upon TCR engagement, the chicken possesses a CD3ε-like protein and one gene that has high homology to both mammalian CD3γ and CD3δ, called chCD3γ/δ (Bernot & Auffray, 1991). It is postulated that mammalian CD3γ and CD3δ arose from gene duplication over 230 million years ago after separation of the mammalian and avian lineages (Bernot & Auffray, 1991). Recently, NMR studies have determined the heterodimer composition of the chCD3ε-chCD3γ/δ complex and their unusual juxtapositioning that is not seen in the mammalian CD3 complex. Two copies of the chCD3ε-chCD3γ/δ interact with the αβ TCR and signalling is thought to be similar to the mammalian CD3 complex, due to conservation of ITAM motifs in the chicken CD3 proteins (Berry *et al.*, 2014).

1.3.4 Chicken T helper cells

The Th1 and Th2 arms of immunity are vital to control infection with intracellular and extracellular pathogens, respectively. The signature cytokines and transcription factors required in mammals for Th1 and Th2 responses have been identified in the chicken genome (Kaiser *et al.*, 2005) and some functional analysis, such as for IL-12 (Degen *et al.*, 2005), IFN-γ (Digby & Lowenthal, 1995) and the Th2 gene cluster (Avery *et al.*, 2004), has been carried out. In 2004, the ability of a non-mammalian species to mount a Th1 and Th2 immune response was demonstrated in the chicken through the quantification of signature cytokines during

intracellular and extracellular infection (Degen *et al.*, 2005; Avery *et al.*, 2005). However, during a chicken's Th2 immune response, IL-5 transcription is not activated (Powell *et al.*, 2009). This could be linked to chickens lacking functional eosinophils and basophils, as in mammals, IL-5 is required for the activation of these cells after IL-4 induces IgE production. In mammals, IgE is the first line of defence against parasites, such as helminths, and its inappropriate production is associated with allergic diseases (Gould & Sutton, 2008).

The existence of Th17 and Th9 cells in the chicken is still unresolved. However, Th17 effector cytokines, IL-17A (Min & Lillehoj, 2002), IL-17F (Kim *et al.*, 2012), IL-23 (Louise Welch, unpublished results) and IL-21 (Rothwell *et al.*, 2012) have been identified in the chicken genome. IL-17A mRNA expression levels are upregulated during *Eimeria tenella* infection and chickens treated with anti-IL-17A antibody have increased body weight and enhanced production of Th1 cytokines during infection (Zhang *et al.*, 2013; Min *et al.*, 2013). IL-9 and IL-10 have also been identified and cloned in the chicken (Rothwell *et al.*, 2004; Lisa Rothwell, unpublished results) and our laboratory is currently carrying out functional analyses to identify Th9 cells in chickens.

During an infection, the immune system concentrates effector cells to the site of inflammation. When the infection subsides, an influx of Treg cells occurs to deactivate immune cells to protect the host against excessive cytokine production and to maintain self-tolerance (Workman *et al.*, 2009). In the chicken, $CD25^+$ $CD4^+$ Treg cells have been identified through surface markers and their ability to express high levels of IL-10 and TGF-β4 mRNA. These cells do not express IL-2 (Shanmugasundaram & Selvara, 2011). Avian Treg cells are similar to mammalian Treg cells, they develop in the thymus and are stored in the bone marrow. Chicken Treg cells express a number of TLRs similar to mammalian Treg cells, such as chTLR2b and chTLR4 (Shanmugasundaram & Selvaraj, 2011). They also express CTLA-4 and LAP3, known to have a role in contact-dependent immunosuppressive functions against DC activation in mammals (Wing *et al.*, 2008; Shevach, 2009). One important piece of the puzzle missing for avian Treg cells is the lack of identification of an ortholog of FoxP3. *In silico* analysis and degenerate primers

designed to span various species, such as cows, human, mouse and fish FoxP3 cDNA, have all failed to identify FoxP3 in any avian species. However, two other members of the FoxP family, FoxP1 and FoxP2, are present in the chicken genome and appear during these searches indicating high sequence identities between these genes in the chicken (Selvaraj, 2013).

Although some important differences exist between mammals and chickens, such as the repertoire of cytokines, transcription factors, the process of BCR/TCR variability selection and the organs of immunity, the chicken can induce a robust immune response upon pathogen exposure.

1.4 Tumour necrosis factor superfamily

Members of the TNF superfamily are key regulators of the activities of a variety of pathways associated with the regulation and modulation of the immune system. The TNF superfamily is made up of TNF ligands and their respective receptors, the TNFR superfamily. The signals from TNFR superfamily members control survival versus death signals but they also have a role in regulatory events, such as controlling cytokine and chemokine expression. The activation of T cells requires ligation of costimulatory molecules and many members of the TNF superfamily play this role in T cell activation. Death-inducing TNFR family members are also expressed on T cells, such as FAS, TNF-related apoptosis-inducing ligand receptor 1 (TRAILR1), TRAILR2 and TNFR1, all of which negatively regulate T cell survival. TNF ligands are also expressed on the surface of T cells, such as CD40L, LT-β, CD27 and 4-1BBL, which interact and signal through their cognate receptors expressed on APC, neighbouring T cells or non-lymphoid cells. These signals are associated with the upregulation of costimulatory molecules and pro-inflammatory cytokine expression. TNF members can send both bidirectional and reverse signals, enhancing their own expression on the surface of cells.

1.4.1 Features of the TNF superfamily

The mammalian TNF superfamily orchestrates a variety of functions both in the architecture of immune organs and the development of immunity (Locksley *et al*., 2001). The receptor family are characteristically type I transmembrane proteins

that have low degrees of homology and are grouped due to the presence of conserved cysteine-rich domains (CRD) in their extracellular ligand-binding domain (Naismith & Sprang, 1998). These CRDs are typically defined by three intra-chain disulphide bridges generated by highly conserved cysteine residues that act as a scaffold to produce an elongated structure protruding from the cell (Smith *et al.,* 1994). They are believed to be involved with specific ligand-binding and generation of a pre-assembly site for the docking of the ligand. The TNFR superfamily can be further categorised into TRAF motif-expressing receptors or death domain (DD)-containing receptors. The DD receptors are characterised by the presence of ~80 amino acids of cytoplasmic sequence necessary for apoptosis (Nagata, 1997). In mammals, eight DD-expressing TNFR have been identified and are further categorised into four homologous groups or clades. The $p75^{NTR}$ clade consists of ectodysplasin A receptor (EDAR), death receptor 6 (DR6) and p75 neurotrophin (NTR), the TNFR1 clade consists of TNFR1 and DR3, the FAS clade and the TRAIL clade consisting of TRAILR1 and TRAILR2, respectively (Sessler *et al.,* 2013). Although their names may imply death-inducing molecules, many members of the DD-containing TNFR family have roles in development. For example, EDAR is required for hair follicle development (Monreal *et al.,* 1999) and DR6 is strongly expressed in the brain and upregulated during neuron injury and is involved in regulating inappropriate axonal branches (Nikolaev *et al.,* 2009).

TNF superfamily ligands are mostly type II transmembrane proteins with an extracellular site for proteolytic cleavage to release a soluble protein from the membrane. All TNF cytokines share a common structural core, a scaffold of ten hydrogen bonds that assume a jellyroll β-sandwich fold. Each member of the TNF superfamily has varying lengths and composition of residues on the surface of the loops connecting the β-strands (Naismith & Sprang, 1998). These molecules are predominantly expressed as non-covalent trimers and the core β-strands are intrinsic to these structures as monomers oligomerize around the axis of the strands (Lam *et al*., 2001).

1.4.2 Mammalian and chicken TNF superfamily members

Studies on the functions of members of the mammalian TNF superfamily are

exhaustive, with many studies identifying both negative and positive roles of each member in development, immunity and disease, and have been reviewed extensively (e.g Watts, 2005; Croft, 2014). Previous analysis of the chicken genome has identified the presence and absence of a number of the TNF superfamily members (Kaiser *et al.,* 2005) (Table 1.2). This phenomena is not only restricted to the TNF superfamily in the chicken but has been identified in the IFN, IL-1, IL-10, IL-12 and the chemokine CCL families (Table 1.3) (Kaiser, 2010; Kaiser, 2012). Table 1.2 identifies the members of the TNF superfamily that are "missing" from the chicken genome. When a ligand and its respective receptor are not present in the chicken, it is assumed that these members are really non-existent rather than not annotated in the chicken genome (Kaiser *et al.,* 2012). Out of the 19 ligand and 29 receptors TNF family members identified so far in mammals, the chicken genome only possesses 10 ligands and 15 receptors.

The TNF superfamily members are present as sub-families that are physically adjacent to one or two additional TNF superfamily genes on the same loci. In humans, eleven out of the nineteen TNF superfamily members are clustered with the MHC or paralogous regions of the MHC on chromosomes 1, 6, 9 and 19. These paralogous regions may have resulted from *en bloc* duplication over 500-800 million years ago in vertebrates (Abi-Rached *et al.*, 2002). The first sub-family missing from the chicken genome is that containing LT-α, TNF-α and LT-β. These TNF family members are tightly linked with the MHC on chromosome 6p21.3 in humans and chromosome 17qB1 in the mouse (Browning *et al.*, 1993; Lawton *et al.*, 1995). Bony fish also have this chromosomal organisation suggesting a gene duplication event occurred before the divergence of fish and amphibians (Glenney & Wiens, 2007). LT-α can form homotrimers and heterotimers with LT-β at the membrane surface in a 1:2 stoichiometric ratio (LT-α_1LT-β_2). LT-α_1LT-β_2 binds and signals through the LT-βR while TNF-α and LT-α_3 bind to two receptors, TNFR1 and TNFR2 (Browning *et al.*, 1993). LT-α_1LT-β_2 is expressed on a number of lymphoid cells, from T to B cells and innate lymphoid cells. The LT-βR is expressed on DC, macrophages and stromal cells (Upadhyay & Fu, 2014). In addition to binding to these two receptors, LT-α_3 also binds to herpes virus entry mediator (HVEM). A

Name	Human Chr	Chicken genome	Chicken Chr	TNFR in chickens	Receptors in chicken
LT-α	6	No		No	
TNF-α	6	No		Yes	TNFR1 TNFR2
LT-β	6	No		No	
OX40	1	Yes	21	Yes	OX40R
AITRL	1	Yes	21	Yes	AITR
FASL	1	Yes	21	Yes	FAS
CD27	19	No		No	
4-1BBL	19	No		Yes	4-1BB
LIGHT	19	No		No	
TWEAK	17	No		No	
APRIL	17	No		No	
VEGI	9	Yes	17	Yes	APO-3 DR6
CD30L	9	Yes	17	Yes	CD30
CD40L	X	Yes	4	Yes	CD40
TRAIL	3	Yes	9	Yes	TRAILR2
RANKL	13	Yes	1	Yes	RANK OPG
BAFF	13	Yes	1	Yes	BAFFR TACI
		TRAIL-Like	4	Unknown	

Table 1.2 The TNF superfamily members present in the human and the chicken genomes. *The chromosomal location and presence of TNF superfamily members in human are shown along with the chromosomal locations and presence of the chicken TNF family members and their receptors (adapted from Kaiser et al., 2012).*

recent study demonstrated that LT-α_3 and TNF-α bind with the same affinity to TNFR1 and induce similar downstream activities (Etemadi *et al.*, 2013). It is believed that the lack of the lymphotoxin genes in the chicken genome is linked to the lack of lymph nodes in chickens. For example, LT-$\alpha^{-/-}$ mice have defects in lymph node development and splenic architecture (Banks *et al.*, 1995). On the other hand, TNF-$\alpha^{-/-}$ mice develop normally but are highly susceptible to infectious agents

Name	Mammals	Chickens
Interferons	IFN-α, -β, -ω,-ζ IFN-γ IFN-λ 1-3	All except IFN-ζ IFN-γ IFN-λ1
Interleukins	IL-1: 11 members IL-10: 6 members IL-12: 4 members IL-17: 6 members	4 members 4 members 2 members 5 members
Transforming growth factors	TGF-β1-3	All present (TGF-β1 is called TGF-β4 in chickens)
Colony stimulating factors	3 members	All present
Chemokines	XCL: 2 members CCL: 28 members CXCL: 16 members CX3CL: 1 member	1 member 14 members 8 members Present

Table 1.3 Cytokine and chemokine family members present in mammalian and chicken genomes. *The number of cytokine and chemokine family members in mammals is shown along with the number of chicken family members present (adapted from Kaiser et al., 2012).*

(Pasparakis *et al.,* 1996). There is evidence of the presence of the two receptors for TNF-α, TNFR1 (Bridgham & Johnson, 2001) and TNFR2 (Abdalla *et al.,* 2004a), in the chicken genome. The second human sub-family missing in the chicken genome contains 4-1BBL, CD27 and lymphotoxin-like inhibits inducible expression and competes with HSV glycoprotein D for HVEM a receptor expressed by T lymphocytes (LIGHT), which all reside on chromosome 19 in humans and chromosome 17 in mice. When first identified, the receptor for 4-1BBL, 4-1BB, was thought to be a costimulatory molecule on T cells but its expression has since been identified on $CD8^+$ T cells, Treg cells, follicular DC, eosinophils, NK T cells and NK

cells (Wilcox *et al.,* 2002). 4-1BB is essential for the control of T cell proliferation, as 4-1BB$^{-/-}$ T cells are hyperproliferative (Lee *et al.,* 2005). 4-1BBL is expressed in CD40L-stimulated B cells, DC and LPS-stimulated macrophages driving pro-inflammatory cytokine production upon activation (Wang *et al.,* 2009). Genetically modified DC expressing high levels of 4-1BBL enhance cytotoxic T cells (CTL), making it a potential DC adjuvant against pathogens and tumours (Asai *et al.,* 2007).

CD27 is closely related to CD40L and is expressed in defined subsets of T and B cells (Camerini *et al.,* 1991). In mammals around 30% of blood- and tonsil-derived and all mutated IgV B cells express CD27 and it is therefore considered an important developmental B cell marker (Maurer *et al.,* 1990). However, CD27 is not a potent inducer of B cell proliferation or isotype switching like CD40L. CD27 has minimal proliferative effects and can only induce IgG_1 isotype switching (Agematsu *et al.,* 1998). The ligand for CD27, CD70, is expressed on CD45RO$^+$ T cells, medullary thymic epithelial cells (mTEC), DC and B cells (Bossen *et al.,* 2006). CD27-deficient mice have no developmental defects in T and B cells but activation of CD4$^+$ and CD8$^+$ T cells is hampered by the loss of CD27 upon influenza virus infection (Hendriks *et al.,* 2000).

LIGHT can bind to three receptors, HVEM, LT-βR and a decoy receptor, DcR3. HVEM can also bind to LT-α3, and two members of the Ig superfamily, CD160 and BTLA, which deliver coinhibitory signals (Zhai *et al.,* 1998; Cai & Freeman, 2009). The interaction of LIGHT and HVEM leads to survival- and growth-producing signals, whereas LIGHT and LT-βR signals induce apoptosis (Chuang *et al.,* 2007). LIGHT is expressed on T cells and its interaction with HVEM induces T cell proliferation and DC maturation, which can be enhanced by the presence of CD40L (Harrop *et al.,* 1998). LIGHT$^{-/-}$ mice have no defects in lymphoid organ development but have defects in CD8$^+$ T cell activity (Tamada *et al.,* 2002).

The third missing sub-family consists of TNF-like weak inducer of apoptosis (TWEAK) and a proliferation-inducing ligand (APRIL). The two genes reside on human chromosome 17 within 700 bp of one another. An intergenic splicing event can occur between exon 6 of TWEAK and exon 2 of APRIL leading to a hybrid gene, called TWE-PRIL, in both human and mice. The protein consists of the NH_2-

terminal and transmembrane domain of TWEAK fused to the COOH-terminal domain of APRIL. TWE-PRIL can signal through the APRIL receptor and can be detected at the mRNA level in activated T cells (Pradet-Balade *et al.,* 2002). TWEAK mRNA is expressed in a variety of tissues and cell types, such as the thymus, spleen and lymph nodes (Chicheportiche *et al.,* 1997), and binds to the receptor TWEAKR, also known as Fn14 (Wiley *et al.,* 2001). TWEAK signalling induces cell proliferation and has been implicated in monocyte-mediated cytotoxicity (Nakayama *et al.,* 2000).

APRIL shares receptors with the TNF superfamily member B-cell activating factor (BAFF). These receptors include transmembrane activator and CAML interactor (TACI), BAFFR and B-cell maturation antigen (BCMA), in a redundant and specific manner. TACI binds to both ligands whereas BAFFR binds specifically to BAFF and BCMA binds only to APRIL (Bossen & Schneider, 2006). APRIL-BCMA interactions enhance plasma cell survival while APRIL-TACI interactions induce IgG and IgE class switching (Schneider, 2005). Unlike BAFF, APRIL is cleaved in the Golgi and expressed as a soluble protein from the cell (Lopez-Fraga *et al.,* 2001). Recently, a transmembrane form of APRIL, APRIL-δ, mutated at the furin cleavage site, was identified and found to be highly expressed in leukaemia cell precursors (Maia *et al.,* 2011).

The absence of these TNF family members in the chicken indicates their possible redundancy in the mammalian immune system. The chicken TNF superfamily may represent the "minimal essential" TNF members needed to control and regulate lymphoid development and immunity.

Of the ten TNF ligands present in the chicken genome, the biological activity of five members has so far been characterised. Cloning and RT-PCR analyses of chicken CD30 (chCD30) and chicken TRAIL (chTRAIL) demonstrated that both cytokines were highly conserved with their mammalian orthologues and mRNA transcripts were present in a number of chicken tissues and cells (Abdalla *et al.,* 2004b). Burgess *et al.* (2004) identified the enhanced expression of chCD30 on MDV-induced lymphomas. Mammalian CD30 promotes neoplastic cell survival in both Hodgkin's and non-Hodgkin's lymphoma disease (Pera *et al.,* 1998). ChCD30

has four CRD domains while there are only three in mouse CD30 (Burgess *et al.*, 2004). ChCD30 also lacks an intracellular TRAF6-binding motif. However, TRAF6 does not directly bind to the intracellular domain of CD30 in mammals (Ishida *et al.*, 1996). Chicken BAFF (chBAFF) is highly expressed in chicken B cells (Schneider *et al.*, 2004). ChBAFF binds to its receptor, BAFFR, and enhances B cell survival (Schneider *et al.*, 2004). TACI and BAFFR are present and functional in the chicken whereas the gene for BCMA is disrupted, implying functional differences in B cell survival in chickens compared to mammals (Reddy *et al.*, 2008).

Chicken CD40L (chCD40L) bioactivity was determined using mouse anti-chicken CD40L monoclonal antibodies (mAb). The chCD40L receptor, chCD40, was detected in chicken B cells, monocytes and macrophages. ChCD40L had conserved biological activities with mammalian CD40L, inducing NO synthase in macrophages and enhancing the survival of B cells (Tregaskes *et al.*, 2005). Chicken vascular endothelial growth inhibitor (chVEGI) (also called TL1A) has 50% homology with human VEGI and is expressed in a number of chicken tissues. Levels of chVEGI expression were significantly increased in LPS-stimulated splenocytes and induced cell cytotoxicity in chicken fibroblast cells (Takimoto *et al.*, 2005). Overall, the functions of the TNF family members cloned in the chicken are evolutionarily conserved.

In 1997, three new members of the mammalian TNF superfamily were identified; receptor activator of NF-κB ligand (RANKL) and its two receptors, RANK and osteoprotegerin (OPG). These three genes are present in the chicken genome.

1.4.3 Mammalian RANKL, RANK and OPG

In 1997, four independent groups isolated a type II TNF-like transmembrane protein using different experimental systems and each gave it a different name, i.e. TNF-related activation-induced cytokine (TRANCE) (Wong *et al*., 1997), receptor activator of NF-κB ligand (RANKL) (Anderson *et al*., 1997), osteoprotegerin ligand (OPGL) (Lacey *et al*., 1998) and osteoclast differentiation factor (ODF) (Yasuda *et al*., 1998). In recent years, RANKL is normally used as the receptor has been named

RANK. Mammalian RANKL is a transmembrane protein of 316 amino acids containing a COOH-terminal receptor-binding domain, a 20 amino acid hydrophobic transmembrane domain and a relatively long extracellular domain that contains a TNF-homologous domain that is the active receptor-binding site (Anderson *et al*., 1997; Lam *et al.*, 2001) (Figure 1.2). Human RANKL has 87% homology with murine RANKL (Lacey *et al*., 1998). Mammalian RANKL expression in the immune system is limited to the thymus and lymph nodes, a restricted pattern of expression not usually seen for TNF superfamily members. For example, FASL and TRAIL expression can be detected in both lymphoid and non-lymphoid organs (Anderson *et al*., 1997; Wong *et al.*, 1997).

RANKL has two receptors, a signalling receptor, RANK, and a decoy receptor, OPG, which is a secreted TNF-related protein that inhibits RANKL-RANK interaction (Simonet *et al.*, 1997). RANK, also known as TRANCEL and TNFRSF11a, is a relatively recent member of the TNFR superfamily. The RANK gene encodes a type I transmembrane protein of 616 amino acids, with an extracellular region (residues 30-194) comprised of four CRD (Anderson *et al*, 1997) (Figure 1.2). It has a high degree of amino acid homology with the extracellular region of CD40 (40%) and has the longest extracellular domain (residues 234-616) of all TNFR members identified so far (Figure 1.2). It is the only known signalling receptor for RANKL (Anderson *et al*., 1997; Wong *et al.*, 1997). Originally identified in a bone marrow-derived myeloid DC cDNA library, RANK mRNA expression is widely detected in the lungs, spleen, skeletal muscle, brain, liver, kidney and surface protein expression is widely detected in cells of the myelomonocytic lineage ranging from osteoclast progenitor cells to DC (Anderson *et al*., 1997; Wong *et al*,. 1997).

OPG was identified the same year as RANKL through sequence homology with the TNF superfamily (Simonet *et al.*, 1997). OPG contains two COOH-terminal homologous death domains of TNFR1 that are not functional. OPG is a naturally secreted protein which can form disulphide-linked dimers of 110 kDa and is cleaved

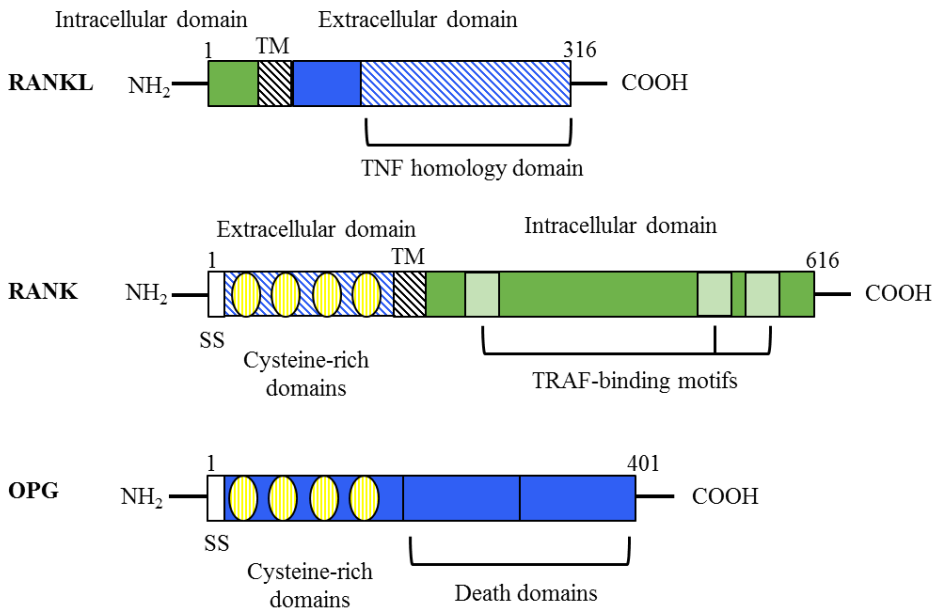

Figure 1.2 Schematic diagrams of the features of mammalian RANKL, RANK and OPG proteins. *Numbers indicate the amino acid length of the protein, SS signal sequence, TM transmembrane domain (adapted from Darnay et al., 1999).*

at position 22 to form a mature protein (Simonet *et al.*, 1997) (Figure 1.2). In mammals, OPG mRNA was detected in the liver, lung, kidney, intestines, skin and stomach. Transgenic mice overexpressing OPG suffer from osteopetrosis and osteoclastogenesis can be inhibited by the addition of OPG to cell cultures (Simonet *et al.*, 1997). Subsequently, the ligand for OPG was found to be RANKL and its affinity for RANKL is 1000-fold higher than that of RANK (Yasuda *et al.*, 1998; Schneeweis *et al.*, 2005). OPG binds to RANKL inhibiting its interaction with RANK. OPG also binds to and inhibits TRAIL-mediated apoptosis. TRAIL, a fellow TNF superfamily member, has four receptors; two DD-containing receptors, TRAILR1 and TRAILR2, and two membrane-bound decoy receptors, DcR1 and DcR2. OPG can bind and inhibit the interaction of TRAIL with its signalling receptors but its affinity is 10,000 times less than the OPG-RANKL interaction (Emery *et al.*, 1998; Vitovski *et al.*, 2007). TRAIL can detect tumour cells and induce apoptosis, therefore tumours expressing OPG may be an escape route from TRAIL-mediated cell death (Holen *et al.*, 2002).

RANKL, RANK and OPG arose during the ontogeny of bony fish reflecting the presence of reabsorbing and mineralisation activity in these vertebrates. This triad of genes post-date the formation of the primordial immune system that comprised a primitive thymus and lymphoid structures but preceded the development of LT-β-mediated development of lymph nodes in amphibians (Witten & Huysseune, 2009). Further insight into the biological roles of these novel cytokines led to the observation that $RANKL^{-/-}$ and $RANK^{-/-}$ deficient mice had entirely unexpected phenotypes: early defects in T and B cell development, complete absences of lymph nodes, severely reduced osteoclastogenesis and failure to develop mammary glands (Dougall *et al*., 1999; Kong *et al.*, 1999a).

1.4.4 The role of RANKL in lymphoid organ development

Lymph nodes are highly organised structures found in higher vertebrates that provide the optimal environment for APC, immune effector cells and antigens to come in close proximity to induce an optimal immune response. It is also the location in which antigen-specific T and B cells differentiate into effector cells. Arrested lymph node development in $RANKL^{-/-}$ mice is due to impaired colonisation of haematopoietic precursors cells in the lymph node anlage. Developing lymph nodes are colonised by $\alpha_4\beta_7CD45^+CD4^+CD3^-$ cells that also express LT-α_1-LT-β_2, RANKL, RANK, IL-7Rα and IL-2Rγc, also known as lymphotoxin-inducer cells (LTi) (Kim *et al.,* 2000). In $RANKL^{-/-}$ mice, the percentage of LTi cells and the expression of the mucosal vascular addressin cell adhesion molecule 1 (MAdCAM-1) (target for $\alpha_4\beta_7$) are reduced and endothelial cells are underdeveloped, in comparison to wild-type mice (Kim *et al.*, 2000). LTi cells induce the expression of RANKL on lymphotoxin-organiser cells (LTo) by interacting with LT-βR which also increases chemokine expression levels such as CXCL13, required for the influx of LTi cells to colonise and cluster with LTo cells to create the lymph node analage (Cupedo & Mebius, 2005).

1.4.5. Medullary thymic epithelial cells

The thymus provides an environment of non-haematopoietic stromal cells and cells of haematopoietic origin for the development of self-tolerant and Treg cells (Gill *et al.*, 2003). Thymic epithelial cells are central components of the thymic

microenvironment and are subdivided into two specialised cells associated with their location, cortical thymic epithelial cells (cTEC) and mTEC. Thymocytes develop and mature while migrating through the cortical and medullary compartments of the thymus. Positive selection is mainly carried out by cTEC and negative selection is carried out by mTEC through associated MHC and self-antigens (Guerder *et al.*, 2012). TEC development is very complex, requiring a number of cell to cell contacts with thymocytes, fibroblast and mesenchymal cells that provide important extrinsic signals for TEC differentiation. mTEC express a number of TNF receptors, such as RANK, CD40 and LT-βR (Akiyama *et al.*, 2012).

RANKL-RANK interactions are essential for mTEC formation and maturation. During development, RANKL is expressed on LTi cells and dendritic epidermal T cells (DETC) and engages with RANK on mTEC to develop from $CD80^{-}Aire^{-}$ mTEC to $CD80^{+}Aire^{+}$ mTEC (Rossi *et al.*, 2007). Furthermore, positively selected $CD4^{+}$ T cells in the thymus also provide RANKL signals. The importance of RANKL-RANK interaction in mTEC development is evident in $RANKL^{-/-}$ mice which have reduced mTEC numbers (Rossi *et al.*, 2007). OPG is also expressed by mTEC, indicating its regulatory role in RANKL-RANK interactions in mTEC development (Hikosaka *et al.*, 2008).

1.4.6 M cells

The intestine is distributed with various inductive sites that are required for the excretion of IgA and the generation of Treg cells to maintain haemostasis. Peyer's patches and isolated lymphoid follicles (ILF) are surrounded by follicle-associated epithelium that contain specialised epithelia called microfold cells (M cells) (Owen & Jones, 1974). M cells are phagocytic cells that differ from their neighbouring enterocytes. They lack the typical brush border but have variable microvilli and microfolds with large plasma membrane subdomains that are exposed to the lumen (Neutra *et al.*, 1996). M cells can uptake particulate antigen by actin-dependent phagocytosis, macropinocytosis and pinocytosis (Jones *et al.*, 1994). Antigens that are acquired by M cells are transported to intraepithelial pockets within the M cells where DC and lymphocytes can access from the sub-epithelial domains (Neutra *et al.*, 1996). Although described over 30 years ago, the mediators of M cell

differentiation and activation were only recently discovered to be RANKL and RANK. RANKL is expressed by stromal cells in the sub-epithelium and it was suggested that it may have a role in M cell development. $RANKL^{-/-}$ mice have smaller Peyers's patches and diminished numbers of M cells compared to wild-type mice (Knoop *et al.,* 2009). Levels of expression of RANK were determined in apical and basolateral aspects of epithelial cells. RANKL production is required for the continuous development and activation of M cells in the intestine, as anti-RANKL treated mice were depleted of M cells within 4 days (Knoop *et al.,* 2009). The data suggested that RANKL is secreted by the inner domes of the Payer's patches and expressed on the outer reticular cells where it instructs newly emerging epithelial cells to undertake the M cell fate. From this discovery, the ability to culture M cells was achieved using a 3-dimensional intestinal organoid culture system (mini-guts) and the transcription factor, SpiB, was identified as an essential requirement for M cell differentiation (de Lau *et al.,* 2012).

1.4.7 Bone metabolism

Osteoclasts originate from haematopoietic multinucleated cells that have the capacity to reabsorb bone whereas osteoblasts are derived from bone marrow mesenchymal stem cells and are responsible for new bone formation. In humans, around 10% of bone is renewed each year (Baud'huin *et al.,* 2007). Communication between osteoclasts and osteoblasts is mediated by soluble cytokines and growth factors that control the expression of genes and transcription factors. However, cell to cell contact is required for osteoclast differentiation and activation through membrane receptors (Yasuda *et al.,* 1998). It took over 30 years to identify RANKL-RANK and OPG as key players in osteoclast function (Simonet *et al.,* 1997, Yasuda *et al.,* 1997). RANKL is expressed on osteoblasts and interacts with RANK-expressing osteoclast progenitor cells. The interaction between RANKL and RANK is controlled by OPG which is expressed by osteoblasts and stromal cells. The progenitor cells of osteoclasts are chemotactically attracted to sites of bone resorption where they deposit in the mesenchyme surrounding the bone. Here, they proliferate and differentiate into mature osteoclasts. Mature osteoclasts are very large cells containing multiple nuclei and have abundant mitochondria, lysosomes and free

ribosomes (Li *et al.,* 2006). When these cells reach the site of bone resorption, a complete alteration of their cytoskeleton occurs. The cells become tightly attached to the bone leading to various changes in plasma membrane domains such as a ruffle border and sealing zone. This sealing zone divides the plasma membrane, thereby producing a closed compartment between the ruffle membrane and the bone matrix, the resorptive lacunae. This zone is distinct to osteoclasts (Li *et al.,* 2006). The balance between RANKL and OPG determines osteoclast activation, skeletal calcium levels and bone remodelling (Lacey *et al.,* 1998). Abnormalities in the RANKL-RANK-OPG system can lead various bone diseases, such as Paget's disease (Chung *et al.,* 2010) and crippling RA (Kong *et al.,* 1999b; Takayanagi, 2007).

1.5 RANKL, RANK, OPG and immunity

Before the discovery that RANKL, RANK and OPG were the key mediators of bone metabolism, research was aimed at identifying their roles in immunity. Mammalian RANK surface expression was shown to be restricted to the surface of DC while RANKL expression was found on T cells. Although $RANKL^{-/-}$ or $RANK^{-/-}$ mice expressed normal DC and macrophage numbers and functions (Darney *et al.,* 1999; Kong *et al.,* 1999a), these cytokines were shown to have a role in driving pro-inflammatory immune responses. In 1997, the novel TNF family member, RANKL, was shown to induce pro-inflammatory cytokine expression in mature DC (Anderson *et al.,* 1997; Wong *et al.,* 1997). Mammalian RANKL induces predominantly Th1 effector cytokines, such as IL-1β, IL-1Ra, IL-6, IL-12 and IL-15, and had no effect on expression levels of IL-2, IL-4, IL-5 or IL-10 (Josien *et al.,* 1999). In the same study, strong RANKL surface expression was predominantly found on activated murine Th1 clones compared to Th2 clones and its expression was inhibited by IL-4 treatment (Josien *et al.,* 1999). Interestingly, $RANKL^{-/-}$ T cells produce higher levels of IL-4 and IL-5 compared to wild-type cells (Kong *et al.,* 1999a). Schiano de Colella *et al.* (2008) demonstrated that RANKL had similar bioactivity on monocyte derived-DC (Mo-DC), where Th2 effector cytokine expression levels were unaltered by RANKL treatment. These studies strongly suggested that RANKL is a predominant Th1 surface marker. RANKL transcription is upregulated within 2 h of

TCR stimulation. Its expression on T cells is regulated by Ca^{2+} mobilisation and is enhanced by protein kinase C (PKC) activation (Wang *et al.*, 2002).

Further studies indicated the role of RANKL in CD40L-independent induction of IL-12. CD40L is expressed on activated T cells and interacts with CD40-expressing DC. Their interaction leads to the upregulation of a number of cytokines required for the activation of a Th1 response. $CD40L^{-/-}$ mice are capable of mounting a Th1 immune response upon infection albeit at a weaker level than wild-type mice, which led to the hypothesis that a fellow member of the TNF superfamily induces IL-12 expression independent of CD40L signalling. Padigel *et al.* (2003) generated double knockout, $CD40L^{-/-}RANKL^{-/-}$ mice and induced an immune response by infecting mice with *Leishmania major* and treating them with RANKL. The dual treated mice controlled the infection, compared to untreated mice, which did not (Padigel *et al.*, 2003). Blocking of RANKL with RANK-Fc inhibited the ability of DC to produce IL-12 and hindered Th1 polarisation. Bachmann *et al*. (1999) also demonstrated that an alternative pathway for IL-12 production in $CD40^{-/-}$ mice was due to RANKL-RANK interaction.

Various mucosal-derived DC express surface RANK and can interact with RANKL. However, RANKL does not activate similar downstream pathways in stimulated mucosal-derived DC. Peyer's patches treated with RANKL expressed enhanced levels of IL-10 and low levels of IL-12β expression in contrast to spleen-derived DC, where IL-12β was expressed at higher levels than IL-10 (Williamson *et al.*, 2002). More recently the bioactivity of RANKL was analysed in macrophages (Park *et al.*, 2005). BMDM treated with RANKL induced low levels of pro-inflammatory cytokine expression but cells co-stimulated with RANKL and LPS or IFN-γ were more potent inducers of pro-inflammatory cytokine expression (Park *et al.*, 2005), indicating that RANKL signals more efficiently on mature APC.

Various members of the TNF superfamily can upregulate the expression of costimulatory molecules on the surface of target cells. RANKL does not significantly increase the surface expression of MHC class II, CD80 and CD86 on DC but does upregulate the expression of a fellow TNF superfamily member, CD40 (Anderson *et al.*, 1997; Wong *et al.*, 1997). Mo-DC treated with RANKL induced partial

maturation of cells and enhanced the levels of CD83 and CD86 expression (Schiano de Colella *et al.,* 2008). Macrophages upregulate MHC class II and CD86 when stimulated with RANKL and can further increase surface expression by synergising with LPS and IFN-γ (Park *et al.,* 2005).

RANKL is a survival factor for APC. Treatment of DC and macrophages with RANKL encourages cell survival, upregulating the anti-apoptotic molecule Bcl-$X_{L,}$ a mitochondrial transmembrane protein involved in signal transduction (Wong *et al*., 1999; Park *et al.,* 2005). The decision between cell death and survival is fundamental to shaping the immune response. Immature interstitial tissue-derived DC express both RANKL and RANK but lose RANKL expression upon maturation. Using RANK-Fc, interstitial tissue-derived DC undergo spontaneous apoptosis due the blockade of RANKL-RANK signalling (Cremer *et al.,* 2002). The ability of RANKL to protect DC from spontaneous apoptosis is a potential avenue to improve the efficacy of vaccines and DC-based immunotherapy. DC that migrate to the draining lymph nodes upon infection to activate antigen-specific T cells have a very limited life span (Pugh *et al*., 1983). RANKL-treated, PPD-pulsed DC can enhance the levels of IFN-γ expression compared to non-treated PPD-pulsed cells and were found for up to five days in the draining lymph nodes of injected mice (Josien *et al.,* 2000).

Polymorphonuclear neutrophils express surface and intracellular RANK in vesicles and specific granules enhanced by Ca^{2+} mobilisation (Riegel *et al.,* 2012). Monocytes expressing RANK are chemoattracted to RANKL-expressing cells, which leads to the activation of Src kinases, a family of proteins implicated in a number of signalling pathways associated with cellular migration, growth and survival (Mosheimer *et al.*, 2004). Monocyte-derived multipotential cells, expressing CD14, CD34 and CD45, are circulating cells that have the potential to spontaneously induce the expression of RANKL upon clustering. These cells were capable of differentiating into osteoclasts without endogenous osteoclastogenic factors which may contribute to pathological conditions, such as RA (Seta *et al.,* 2008).

OPG not only regulates the interaction between RANKL and RANK in bone metabolism, but also has a regulatory role in RANKL-RANK signalling in immunity.

DC from OPG$^{-/-}$ mice produce enhanced levels of pro-inflammatory cytokine expression compared to DC from wild-type mice and had significantly increased survival rates (Chino *et al.*, 2009). OPG is expressed by mature DC and its expression is dependent on NF-κB activation (Schoppet *et al.*, 2007). Therefore, OPG also provides a molecular brake between RANKL-RANK signalling in immunity.

1.5.2 RANKL, RANK, OPG in non-mammalian species

Bone metabolism increases due to movement in a site-specific manner (Rubin *et al.*, 2001). Teleost fish are a good model to understand the cell to cell interactions required for the activation of osteoclastogenesis (Yoshikubo *et al.*, 2005; Sanuki *et al.*, 2007). Teleost fish, which include zebrafish, goldfish and Japanese rice fish, have scales with calcified tissues, such as osteoblasts and osteoclasts and bone matrix proteins (Yano *et al.*, 2013). When scales were removed and underwent static or dynamic centrifugation, expression levels of RANKL were significantly decreased after 3 and 6 h, whereas OPG expression levels were increased at 12 and 18 h in dynamic movement experiments, indicating inhibition of bone metabolism (Kitamura *et al.*, 2013). Goldfish RANKL had increased mRNA expression levels during scale regeneration. However, this study could not differentiate between osteoblasts or pro-inflammatory cells expressing RANKL at the site of scale damage (Thamamongood *et al.*, 2012).

1.6 RANKL-RANK signalling

The selectivity of RANKL binding to RANK is due to 46 buried polar interactions upon trimer formation, the highest number of polar interactions found in any TNF ligand and receptor pair (Lam *et al.*, 2001). It is accepted that TNFR binding is carried out by an elongated receptor molecule, along each of the three clefts of the neighbouring monomers of the homotrimer (Hymowitz *et al.*, 1999). This interaction induces the intracellular domain of RANK to recruit a number of TNF receptor-associated factors (TRAF) (Darnay *et al.*, 1998; Wong *et al.*, 1998; Kim *et al.*, 1999). The TNFR superfamily members do not possess catalytic domains and rely on the recruitment of adaptor proteins to signal and activate downstream

protein kinase cascades. The activation of the extracellular domain of RANK recruits five members of the mammalian TRAF family, TRAF1, TRAF2, TRAF3, TRAF5 and TRAF6, to the intracellular domain, triggering downstream signalling events, such as activation of the NF-κB, Jun-N terminal kinase (JNK), extracellular signal regulated kinase 1 (ERK1) and p38 signalling pathways (Wong *et al*., 1998).

TRAFs are a group of homologous intracellular molecules originally characterised in mammals but recently extensive research has been carried out in fish (Qiu *et al.*, 2009; Kim *et al*., 2011; Huang *et al.*, 2012; Li *et al*., 2014), insects, slime moulds and nematodes (Regnier *et al*., 1995). This group of adaptor proteins emerged as the key downstream signal transducers for the TNFR and TLR/IL-1R superfamilies. The hallmark feature of TRAF proteins is their COOH-terminal TRAF domain of approximately 230 amino acids (Figure 1.3). The COOH-terminal domain can be subdivided into more divergent NH_2-proximal (TRAF-N) and highly conserved COOH-proximal (TRAF-C) sub-domains. TRAF-N contains a coiled-coil domain, responsible for homo- and hetero-dimerisation of the TRAF proteins, as well as for indirect and direct interactions with cognate surface receptors (Park *et al.*, 1999). TRAF7 does not conform to the canonical TRAF-C domain but instead expresses seven WD40-repeat domains (Bouwmeester *et al.*, 2004). All TRAF family members, except TRAF1, possess an NH_2-terminal really interesting new gene (RING) domain which is highly conserved throughout TRAF2-TRAF7 at the amino acid level. Deletion of the RING domain in mammalian TRAF2, TRAF5 and TRAF6 led to the generation of dominant-negative (DN) TRAF mutants, suggesting that the RING domain is critical for downstream signalling (Hsu, 1996). The RING domain is followed by five to seven zinc finger motifs, depending on the TRAF (Figure 1.3).

Previous biochemical and structural analyses have identified two sequence motifs for TRAF binding: a major, (P/S/A/T)X(Q/E)E, and a minor, PXQXXD (X representing any amino acid). TRAF signalling predominantly leads to the activation of the canonical NF-κB (NF-κB) or non-canonical (NF-κB2) pathways which can activate a number of genes involved in pro-inflammatory responses, proliferation and

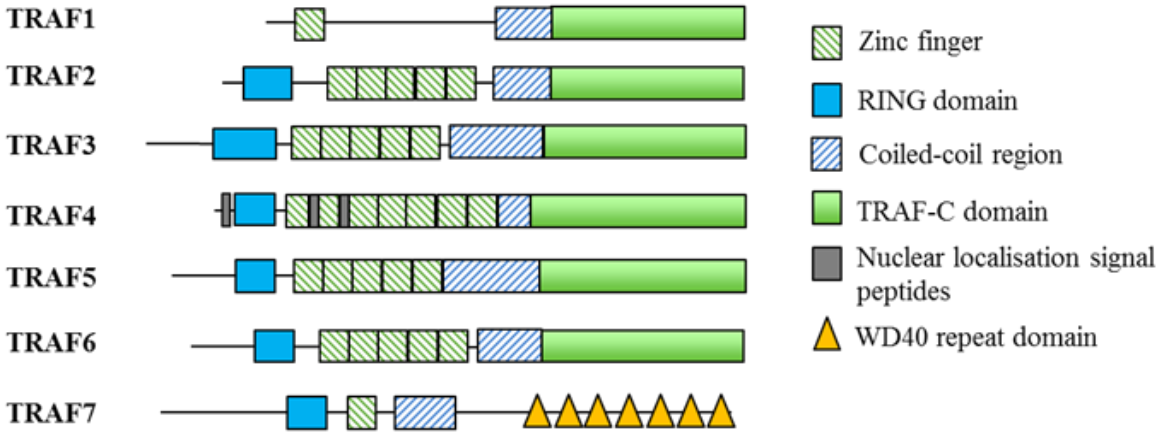

Figure 1.3 Schematic diagrams of mammalian TRAF family members *(adapted from Xie, 2013).*

differentiation, but also involved in the activation of mitogen-activated protein kinases (MAPK), such as JNK, p38, ERK1 and ERK2 (Arch *et al.*, 1998).

The NF-κB family of proteins are evolutionarily conserved master regulators of the immune system. They were first described as transcription factors in B cells that bound to the enhancer elements that control expression of the immunoglobulin kappa light chain (Sen & Baltimore, 1986). NF-κB regulates a number of mediators of immunity, such as cytokines, growth factors and effector enzymes. A large number of unstimulated cell types express NF-κB which correlates with a huge number of genes having promoter/enhancer sites for NF-κB binding. The mammalian NF-κB family consists of five members: p65 (RelA), RelB, c-Rel, p50/p105 (NF-κB1) and p52/p100 (NF-κB2). Both p50 and p52 are synthesized as precursor proteins (p100/p105) which are processed *in vivo* to release the active forms (Bours *et al.*, 1990). All members have a characteristic ~300 amino acid NH_2-terminal DNA-binding domain called the Rel homology region (RHR) (Baldwin, 1996). This RHR domain binds to the consensus sequence 5'-GGGPuNNPyPyCC-3' present in the regulatory elements of NF-κB target genes and is required for homo- and heterodimerisation and interaction with their regulatory proteins. NF-κB is kept inactive in the cytoplasm through association with its inhibitor IκBα. NF-κB is activated by the phosphorylation and degradation of IκBα by IKK, which is a

regulatory subunit of NF-κB essential modulator (NEMO) (Silverman & Maniatis, 2001).

Genome-wide analysis of the mRNA transcripts induced by osteoclast progenitor cells incubated with or without RANKL previously cultured with CSF-1 found that RANKL treatment led to the upregulation of nuclear activator of T cells 1 (NFATc1) transcription that was dependent upon c-Fos and TRAF6. The increase expression of NFATc1 was followed by an increase in Ca^{2+} oscillations, indicating the vital role of this transcription factor in osteoclast differentiation (Takayanagi *et al.,* 2002). RANKL-RANK signalling also activates phospholipase C, which enhances the release of intracellular stores of Ca^{2+} (Komarova *et al.,* 2003). TRAF6 is vital for RANKL-mediated osteoclastogenesis, as $TRAF6^{-/-}$ mice suffering from severe osteoporosis (Lomaga *et al.,* 1999; Naito *et al*., 1999).

1.6.2 The mammalian TRAF family

TRAF1

TRAF1 was one of the first TRAF family members to be identified by its ability to bind to the intracellular domain of TNFR2 (Rothe *et al.,* 1994). In contrast to the other TRAF members, TRAF1 does not possess a RING domain or E3 ligase activity and only has one zinc finger motif (Wajant *et al.,* 2003). Its expression is restricted to the testis and the spleen (Rothe *et al.,* 1994). TRAF1 can bind to a number of TNFR family members, such as OX40 (Kawamata *et al.,* 1998), CD30 (Tsitsikov *et al.,* 1997), RANK (Wang *et al.,* 1998) and CD27 (Yamamoto *et al.,* 1998). TRAF1 both positively and negatively regulates NF-κB depending on the nature of the ligand. For example, TNF-α and IL-1-mediated NF-κB activation is repressed in TRAF1 overexpression studies (Carpentier & Beyaert, 1999). $TRAF1^{-/-}$ mice have dysregulated T cell functions (Tsitsikov *et al.,* 2001) and it is required for 4-1BBL-mediated NF-κB activation (McPhearson *et al.,* 2012). TRAF1 can form heterodimers with TRAF2 at the expense of TRAF2 homodimers and may be a regulatory mechanism, as the recruitment of TRAF1/TRAF2 complex to CD40 reduces NF-κB activation (Zheng *et al.,* 2010).

In the hydroid, *Hydractinia echinata*, a homologue of TRAF1 has been identified that does not contain a coiled-coil region (Mali & Frank, 2004). A TRAF1 splice isoform missing the zinc finger was also identified. mRNA expression of this splice isoform was only detected in the larva and early metamorphosis stages, suggesting different functions for the two TRAF1 proteins in *Hydractinia echinata* development which have yet to be characterised. The existence of TRAF molecules in *Hydractinia echinata* again suggests ancient functions for the TNFR/Toll-IL-1R pathways in development and immunity.

TRAF2

TRAF2 is one of the best studied TRAF family members, first identified with TRAF1 by Rothe *et al.* (1994). Mammalian TRAF2 is ubiquitously expressed in all tissues (Rothe *et al.*, 1994). $TRAF2^{-/-}$ mice have a lethal phenotype complicating the use of this model to delineate its functions (Yeh *et al.*, 1997). Using the dominant negative form of TRAF2 (TRAF2DN), this adaptor protein was shown to be required for both TNF-α- and CD40-mediated JNK and NF-κB activation (Lee *et al.*, 1997). TRAF2 can interact with a number of intracellular adaptor proteins that both negatively and positively regulate NF-κB activity, such as A20, TRAF-interacting protein (TRIP) and NF-κB-inducing kinase (NIK) (Takeuchi *et al.,* 1996; Hsu *et al.,* 1997). TRAF2 is vital for both CD40- and BAFF-regulated B cell proliferation (Grech *et al.,* 2004). TRAF2KO MEF display enhanced cell death upon TNF-α treatment and TRAF2 inhibits apoptosis by targeting caspase-8 ubiquitination (Gonzalvez *et al.*, 2012).

A novel isoform of murine TRAF2, TRAF2A, contains an additional seven amino acids located within the RING domain and is incapable of mediating NF-κB activation (Brink & Lodish, 1998) but could activate JNK (Dadgostar & Cheng, 1998). Both isoform transcripts are expressed across a range of murine tissues, with TRAF2A expressed at much lower levels than TRAF2 (Brink & Lodish, 1998). TRAF2A may work to regulate TRAF2-mediated activation of downstream signalling pathways by competitively binding to TRAF2-binding motifs.

The rock bream TRAF2 (rbTRAF2) homologue was cloned and characterised by Kim *et al.* (2011). The full-length protein has 56% identity with both mouse and human TRAF2. Its biological activity was analysed in cells harbouring an NF-κB reporter gene. Upon TNF-α exposure, cells expressing rbTRAF2 induced higher levels of NF-κB activation compared to control cells.

TRAF3

TRAF3 was first identified in 1994 as binding to CD40 (Hu *et al.,* 1994). TRAF3 can bind to almost all TNFR superfamily members that do not express DD and is ubiquitously expressed. TRAF3 is a negative regulator of CD40-mediated NF-κB activation but a positive regulator of Epstein-Barr virus latent membrane protein 1 (LMP1)-mediated NF-κB activation in B cells (Xie *et al.,* 2004). This is due to TRAF3 binding to the different TRAF-motifs within these receptors (Graham *et al.,* 2009). $TRAF3^{-/-}$ mice die prematurely at around day 10 with no gross morphology of immune organs. The spleens of $TRAF3^{-/-}$ mice are structurally intact, but cellularity is around 1% compared to the cellularity of wild-type spleens. The percentages of B lineage precursors in the bone marrow were significantly reduced in $TRAF3^{-/-}$ mice indicating that TRAF3 may have a role in B cell development (Xu *et al.,* 1996). Using a conditional gene targeting approach, TRAF3 was disrupted in murine B cells and these had increased survival rates independent of BAFF and CD40 signalling (Xie *et al.,* 2007). Prolonged survival rates were linked to the upregulation of the non-canonical NF-κB2 (p52/RelB) pathway which is required for BAFF-R downstream pro-survival signalling. The NF-κB2 pathway is tightly regulated and its dysregulation is linked to many haematological malignancies (Courtois & Gilmore, 2006). Loss of function mutations in TRAF3 have been observed in different sub-types of B cell lymphomas and Waldenström's macroglobulinaemia, defined by lymphoplasmacytic infiltrates in the bone marrow and IgM paraprotein production, and are linked to the upregulation of NF-κB2 activation (Braggio *et al.,* 2009). There is evidence that TRAF3 regulates NIK but the relationship between TRAF3 and the negative regulation of B cell survival is still very complex (Lin *et al.,* 2013).

Several isoforms of mammalian TRAF3 have been described in which all or some of the zinc finger motifs are missing due to polyadenylation and exon-skipping

events (van Eyndhoven *et al.,* 1998; 1999). All isoforms, except for TRAF3Δ5-10 (numbers represent missing exons), were capable of activating NF-κB in a reporter gene assay and augmented its activation when co-transfected with full-length TRAF3 (van Eyndhoven *et al.,* 1999). In T cells, two isoforms of TRAF3 were expressed, the full-length gene and an isoform lacking exon 8, representing a zinc finger motif (TRAF3Δ8), previously described by van Eyndhoven *et al.* (1999). Levels of TRAF3Δ8 protein expression increased in PMA-stimulated T cells and were linked to the upregulation of NF-κB2 activation in a time-dependent manner (Michel *et al.,* 2014). T cell activity is known to be controlled by splice-dependent mechanisms as seen with CD45 splicing events (Lynch, 2004). It is proposed that splicing events are required for the response of immune cells to challenging environments (Heyd & Lynch, 2010).

TRAF4

Mammalian TRAF4 was first identified by differential screening of a cDNA library of metastatic lymph nodes derived from breast cancer cells (Régnier *et al.,* 1995). Its transcripts were not detected in a number of healthy tissues but were identified in four carcinoma cell lines and appeared to be mainly expressed in the cell nucleus (Régnier *et al.,* 1995). However, similar studies identified a low basal level of TRAF4 expression in a number of lymphoid tissues, such as the spleen and thymus (Cherfils-Vicini *et al.,* 2008). TRAF4 has a number of unique characteristics that differ from the other TRAF family members. It contains multiple nuclear localisation signal peptides (Régnier *et al.,* 1995). Pull-down assays and yeast two-hybrid systems have failed to identify a TNFR superfamily member that binds TRAF4 (Régnier *et al.,* 2002). Murine TRAF4 is highly expressed during the development of the central and peripheral nervous systems and is required for the development of the axial skeleton, trachea and neurons (Régnier *et al.,* 2002). There are limited studies identifying the role of TRAF4 in immune cells.

TRAF4$^{-/-}$ mice develop normally but only on a mixed genetic background (129/SvJ x C57Bl/6). However, these mice are still born with a constricted upper trachea at the site of the tracheal junction with the larynx (Shiels *et al.,* 2000). TRAF4$^{-/-}$ mice had no defects in lymphoid organ development, T cell, B cell or DC

numbers (Cherfils-Vicini *et al.*, 2008). However, DC migration was affected by the loss of TRAF4 expression, not due to the loss of CCR7 expression but possibly due to defects in actin polymerisation (Cherfils-Vicini *et al.*, 2008). TRAF4 also complexes with TRAF6, IL-1 receptor-associated kinase 1 (IRAK1) and TIR-domain containing adaptor-inducing interferon-β (TRIF), and negatively regulates the capacity of this signalling complex to activate NF-κB (Takeshita *et al.*, 2005). In a more recent study, TRAF4 overexpression attenuated IL-17-mediated phosphorylation of ERK1/2 and JNK (Zepp *et al.*, 2012).

TRAF5

The fifth member of the TRAF family, TRAF5, was identified by coimmunoprecipitation studies using CD40 or LT-βR as bait (Ishida *et al.*, 1996; Nakano *et al.*, 1996). TRAF5 can associate with other TNFR family members, such as CD27 (Akiba *et al.*, 1998), CD30 (Aizawa *et al.*, 1997), LMP-1 (HVEM) (Marsters *et al.*, 1997), OX40 (Kawamata *et al.*, 1998) and RANK (Darnay *et al.*, 1999). TRAF5 mRNA was detected in the thymus, spleen and kidney with low levels detected in the brain and liver, but not in the skeletal muscle, heart, testis or small intestine by Northern blot analysis (Ishida *et al.*, 1996). Although structurally more similar to TRAF3 (Ishida *et al.*, 1996), TRAF5 shares many biological functions, and binding motifs in a number of receptors, with TRAF2 (Aizawa *et al.*, 1997; Darnay *et al.*, 1999). Targeted disruption of the murine TRAF5 RING domain does not lead to abnormal development or defects in lymph nodes or lymphocyte numbers. However, CD40-mediated upregulation of CD23, CD54 and costimulatory molecules, CD80 and CD86, along with IgM and IgG_1 production were substantially reduced in $TRAF5^{-/-}$ B cells (Nakano *et al.*, 1999). LMP-1, a fellow member of the TNFR superfamily, is a functional mimic of CD40 (Fennewald *et al.*, 1984) and requires TRAFs for downstream signaling. Although both CD40 and LMP-1 bind to the same TRAFs, they induce different responses (Xie *et al.*, 2004). LMP-1 requires TRAF5 more than CD40 for B cell biology as it is vital for LMP-1-mediated IL-6 expression (Kraus *et al.*, 2009).

The requirement of TRAF5 for TLR signalling was recently described in $TRAF5^{-/-}$ B cells and APC (Buchta & Bishop, 2014). TLR-stimulated $TRAF5^{-/-}$

BMDC have enhanced IL-6 production whereas this was only seen in TLR7-stimulated TRAF5$^{-/-}$ BMDM. When TRAF5$^{-/-}$ B cells were stimulated with agonists for TLR4, TLR7 or TLR9, mRNA expression levels of IL-6, IL-10, TNF-α and IL-12p40, were enhanced compared to levels in wild-type cells. TRAF5 negatively regulates TLR signalling in B cells by interacting with and inhibiting the adaptor proteins, MyD88 and TAB2, known positive regulators of TLR downstream signalling cascades and NF-κB activators (Buchta & Bishop, 2014). TAB2 links TRAF6 to the transforming growth factor-β activated kinase 1 (TAK1), facilitating the downstream activation of MAPKs (Takaesu *et al.,* 2000).

TRAF5 also functions as a limiting step in the differentiation of the Th2 response. TRAF5$^{-/-}$ T cells induced higher levels of IL-4 and IL-5 after CD3/28 and OX40 costimulation. OX40 signalling promotes both Th1 and Th2 immune responses and the knockout of TRAF5 in mice induced a more robust Th2 response *in vitro* and *in vivo* to experimental OVA-induced allergic-inflammation (So *et al.,* 2004). It is hypothesized that, like TRAF2, TRAF5 interacts with and inhibits the NFAT-interacting protein, NIP45, which is required for the transcription of IL-4 (Lieberson *et al.,* 2001). More recently, TRAF5 was identified as a negative regulator of IL-6-mediated induction of Th17 cells by binding to gp130 (Nagashima *et al.,* 2014).

TRAF6

TRAF6 is considered one of the oldest members of the TRAF family and has the most divergent TRAF-C domain which binds to a number of cytoplasmic tails of receptors and upstream molecules. The TRAF-C domain of TRAF6 does not interact with the peptide motifs used by TRAF1, TRAF2, TRAF3 and TRAF5 (Park *et al.,* 1999). The *Drosophila* ortholog of TRAF6, DTRAF2, has a major role in gene expression and control of the NF-κB pathway and is required for antimicrobial activity (Grech *et al.,* 2000). TRAF6 is the only member of the TRAF family to signal for the Toll/IL-1R superfamily. However, it does not directly bind to their intracellular domains but instead binds to signalling complexes mediated by MyD88 which recruits two serine/threonine kinases, IRAK1 and IRAK4, or TRIF, which recruits TRAF6 with receptor-interacting protein-1 (RIP-1) and tyrosine-based

activation motif ITAM expressing proteins (Li *et al*., 2002). TRAF6 has ubiquitin ligase activity; it can synthesise non-degradative K63-chains onto target proteins required for the phosphorylation of IκBα (Deng *et al.,* 2000). TRAF6$^{-/-}$ mice suffer from severe osteopetrosis and this was linked to RANKL-RANK interactions requiring TRAF6 for downstream signalling (Lomaga *et al.,* 1999; Naito *et al*., 1999).

TRAF6$^{-/-}$ T cells are hypersensitive to IL-2 treatment due to TRAF6 binding to and negatively regulating the IL-2Rβ-chain (Motegi *et al.,* 2011) and they become resistant to Treg cells (King *et al.,* 2006). TRAF6$^{-/-}$ Tregs cells lose FoxP3 expression and are skewed towards Th2-like cells (Muto *et al.,* 2013). TRAF6 is essential for IL-17-mediated activation of NF-κB and MAPK as IL-17 cannot signal through IL-17RA in TRAF6$^{-/-}$ MEF (Schwandner *et al.,* 2000). The IL-17R is similar to the Toll/IL-1R superfamily but does not possess TIR domains or a TRAF6-binding domain, so adaptor proteins are required for IL17RA-TRAF6 signalling (Novatchkova *et al.,* 2003; Chang & Dong, 2011).

TRAF6 homologues have been identified in a number of fish species, such as the Zhikong scallop (Qiu *et al.*, 2009), common carp (Kongchum *et al.*, 2011), grass carp (Zhao *et al.*, 2013), *Epinephelus coioides* (Li *et al.*, 2014) and *Epinephelus tauvina* (Wei *et al.*, 2014). Fish species rely heavily on the innate immune system as their fundamental defence against pathogens. All fish TRAF6 proteins are highly conserved (65-98%) and tissue expression is highest in the stomach, blood and intestine (Li *et al.*, 2014; Wei *et al.*, 2014). The liver is one of the most important innate lymphoid organs of the fish. Various bacterial and viral antigens were used to infect fish and liver cells which were then analysed for the levels of TRAF6 expression. *Vibrio alginolyticus*-challenged fish had increased levels of TRAF6 mRNA expression, significantly higher than levels induced by other antigens (Wei *et al.*, 2014).

TRAF7

TRAF7 is the most recently identified member of the TRAF protein family and was only discovered in a screening for protein-protein interactions around the

known components of the TNF-α/NF-κB pathway (Bouwmeester *et al.,* 2004). TRAF7 differs from other TRAF members in that it does not possess a TRAF-C domain but instead has seven WD40-repeat domains. However, TRAF7 does express a RING domain and one zinc-finger motif (Xu *et al.,* 2004). TRAF7 mRNA was detected in the skeletal muscle, heart, brain, lung, thymus, spleen, colon, small intestine and peripheral blood leukocytes. TRAF7 requires its WD40-repeat domains to interact with and activate MEKK3 (Xu *et al.,* 2004) and inhibits the transactivation of c-Myb by activating its sumoylation (Morita *et al.,* 2005). TRAF7 also negatively regulates TNF-α-mediated activation of NF-κB by binding to NEMO and NF-κB sub-unit p65 and targeting each for K29 polyubiquitination (Zotti *et al.,* 2011). It also degrades the anti-apoptotic protein c-FLIP (Scudiero *et al.,* 2012) which appears to be a function of its RING domain since deletion of this domain no longer confers cell death (Zotti *et al.,* 2011).

TRAF7 E3 ubiquitin ligase activity has also been linked to stabilizing p53, a key tumour repressor and master regulator of several signalling pathways. TRAF7 protein expression was downregulated in breast cancer samples with no dysfunctional p53 gene (Wang *et al.,* 2013). In similar studies examining 300 cases of primary brain tumors, TRAF7 was mutated in its WD40-repeat domains in nearly a fourth of all samples examined (Clark *et al.,* 2013; Reuss *et al.,* 2013). Currently no $TRAF7^{-/-}$ mice, which could provide more insight into its role in cancer and NF-κB signaling, have been generated.

Acting alone or in combination, TRAFs are versatile regulators of cellular responses, including survival, cytokine production, differentiation and activation.

1.7 Aims and hypothesis of this study

Mammalian RANKL, RANK and OPG have vital roles in lymph node and thymocyte development, bone metabolism and APC biology. The chicken appears to have the "minimal essential" TNF superfamily, with fewer members than the same family in mammals. Those missing from the chicken genome have vital roles in mammalian T and B cell proliferation, activation and lymphoid organ development and it is therefore necessary to investigate the biological roles of the members that

are present in the chicken genome. Like mammals, chickens mediate a Th1/Th2 immune response upon infection with intracellular and extracellular pathogens, respectively, and possess DC and macrophages. Members of the TNF superfamily require a number of TRAF adaptor proteins to activate downstream signalling pathways, such as NF-κB. Our hypotheses are that chicken RANKL, RANK and OPG have evolutionarily conserved functions in driving pro-inflammatory cytokine expression, cell survival and other functions in DC and macrophages, similar to mammalian RANKL, RANK and OPG, and that the signalling molecules required for mammalian RANK signalling are conserved, along with their expression patterns, in chicken immune organs and cells.

The aim of this project was therefore to clone and characterise the roles of chicken RANKL, RANK and OPG in avian APC biology and to determine the presence and degree of conservation of the RANK adaptor proteins, TRAF2, TRAF5, TRAF6 and TRAF7.

Chapter 2

Materials and Methods

2.1 *In silico* materials

2.1.1 BLAST

Sequence similarly searches were used for all genes cloned. The BLAST program was used to analyse the similarity of nucleotide and amino acid sequences with the chicken and mammalian genomes and their genomic locations were identified.

2.1.2 Signal P4

Signal P4.1 (Center for Biological Sequence Analysis, Technical University of Denmark DTU (http://www.cbs.dtu.dk/services/SignalP/)) is an online server that allows the prediction of the presence and cleavage site of signal peptides present in an amino acid sequence from different organisms (Bendtsen *et al*., 2004).

2.1.3 CLUSTALX2

This software creates alignments of multiple amino acid and nucleotide sequences, allowing the identification of homologous genes between different species and variants of genes from the same species. It identifies residues within a gene of high conservation by colour coding (the darker the shading the higher the conservation of residues between species and variants) and has been used for all amino acid alignments in this study.

2.1.4 SMART

Simple molecular architecture research tool (SMART) is online software that allows the rapid identification of signalling domains and structure of proteins and genomes (Ponting *et al*., 1999). SMART version 7 was released in 2011 and contains 1009 manually curated models of protein domains. The database also has genome sequence data of 1133 different species therefore allowing the identification of species-specific proteins (Letunic *et al*., 2012).

2.2 Vectors

2.2.1 pGEM-T Easy

pGEM-T Easy is a 3.015 kb vector used for cloning complementary DNA (cDNA) (Figure 2.1). It is a linearised plasmid with a single 3' deoxythymidine overhang at both ends. The thymidine prevents the recirculation of the plasmid and improves ligation of cDNA clones produced by *Taq* polymerases, which add adenosines to the ends of the PCR product, complimenting the T base, thus allowing for efficient ligation. The advantage of using pGEM-T Easy for cloning the cDNA of interest is its blue/white screening selection after transformation of the vector into appropriate bacteria. The vector is a high-number copy plasmid with T7 and Sp6 RNA polymerase promoters flanking the multiple coding region (MCR). The MCR is located within a *lacZ* gene which encodes the α-peptide coding domain from the enzyme β-galactosidase. The β-galactosidase enzyme metabolises sugar producing a blue colour. When a product is inserted it shifts the reading frame, thereby inactivating the α-peptide protein and producing a non-functional β-galactosidase enzyme which will produce white colonies. However, when no insert in present blue colonies are formed as the α-peptide is produced and activated when exposed to isopropyl β-D-1-thiogalactopyranoside (IPTG) and 5-bromo-4-chloro-3-indolyl-β-D-galactopyranoside (X-gal). This colour screening allows for the identification of positive colonies. The plasmid also contains an ampicillin resistance gene permitting the selection of positive colonies. Colony screening was also carried out to ensure no false positives were selected for further analysis.

2.2.2 pCI-neo

pCI-neo is a mammalian expression vector of 5.47 kb used for protein expression in mammalian cells (Figure 2.2). It can be used for both transient and stable transfection of cells and contains a number of features to accommodate these routes of expression. The vector contains the cytomegalovirus (CMV) immediate early enhancer/promoter region that is vital for expression of the protein of interest in mammalian cell lines.

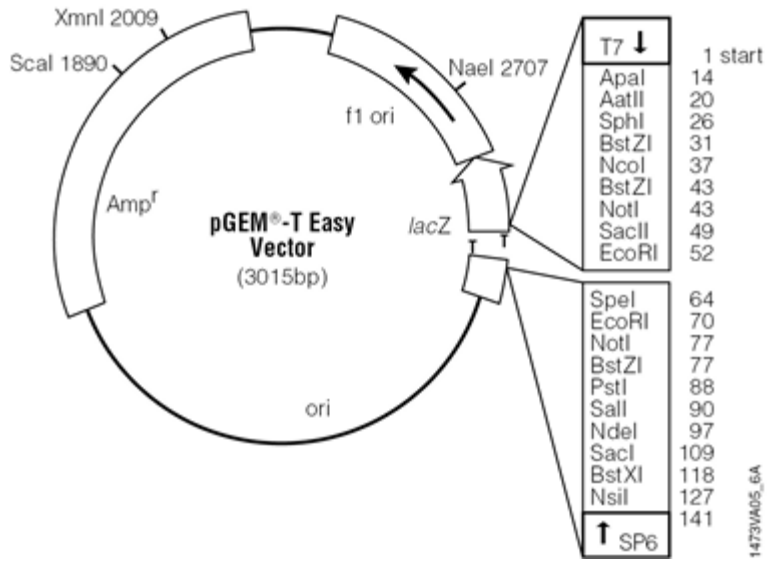

Figure 2.1 Map of pGEM-T EASY vector

2.2.3 pV20 and pV22

Two plasmids were designed for the expression of type II transmembrane proteins using the pCI-neo backbone (Tuan Jun Hu and John Young, IAH, UK, unpublished). The extracellular domains of type II transmembrane proteins are located at the COOH-terminal and interact with their cognate receptor. Therefore the plasmids were designed for the expression of an NH_2-terminal FLAG-tag protein (Figure 2.3A). To generate soluble proteins the mouse CD8 signal peptide was intregated upstream of the gene sequence. Upstream from the FLAG sequence, an isoleucine zipper sequence was integrated to encourage formation of homotrimers. This plasmid was named pV20. The second plasmid, named pV22, was designed with a cysteine residue between the FLAG-tagged sequence and the gene sequence to encourage stabilisation of the protein structure (Figure 2.3B).

2.2.4 Signal pKW06 and pKW06

Signal pKW06 and pKW06 are modified pCI-neo vectors (Staines *et al*., 2013). Both plasmids were designed to express recombinant proteins in mammalian cells with a COOH-terminal human IgG Fc-tag. Signal pKW06-Ig differs in that it contains the mouse CD8 signal peptide upstream of the target gene to facilitate

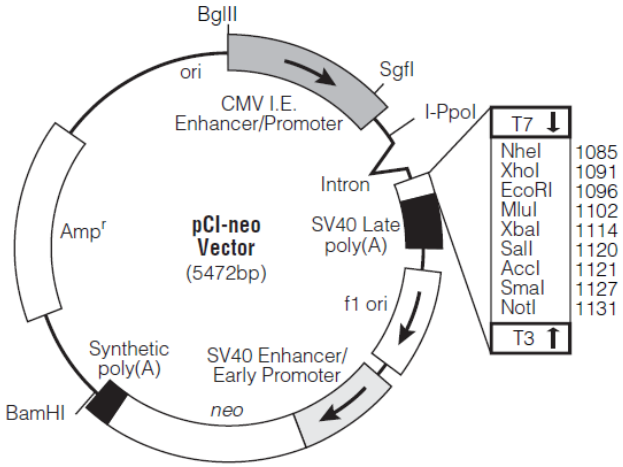

Figure 2.2 Map of pCI-neo

soluble protein production. The pKW06-Ig allows the use of the natural signal peptide of the target gene or for the production of intracellular proteins. The MCR contains two restriction sites: a *Nhe*I site lies after the signal peptide sequence and a *Bgl*II site lies between the gene of interest and the human IgFc domain (Figures 2.4A and B).

2.2.5 pcDNA3-HA

pcDNA3-human influenza haemagglutinin (HA) is a modified version of pcDNA3 (Invitrogen) (Figure 2.5). HA is a surface glycoprotein and the HA tag corresponds to amino acids 98-106. pcDNA3 is a 6.5 kb plasmid containing the CMV promoter for mammalian protein expression. The MCR was modified to express the HA tag between the *Hin*dIII and *Eco*RI restriction enzyme sites (kind gift from James Pease, Imperial College London) (de Mendonca *et al*., 2005).

2.2.6 pGL4.32-[*luc2 P*/NF-κB-RE/Hygro]

The pGL4 series of vectors were designed for genetic reporter systems to study gene expression (Promega) (Figure 2.6). The reporter gene system used is NF-κB and upon activation leads to the production of *Firefly* luciferase. pGL4.32-[*luc2P*/NF-κB-RE/Hygro] contains five copies of the NF-κB response elements that

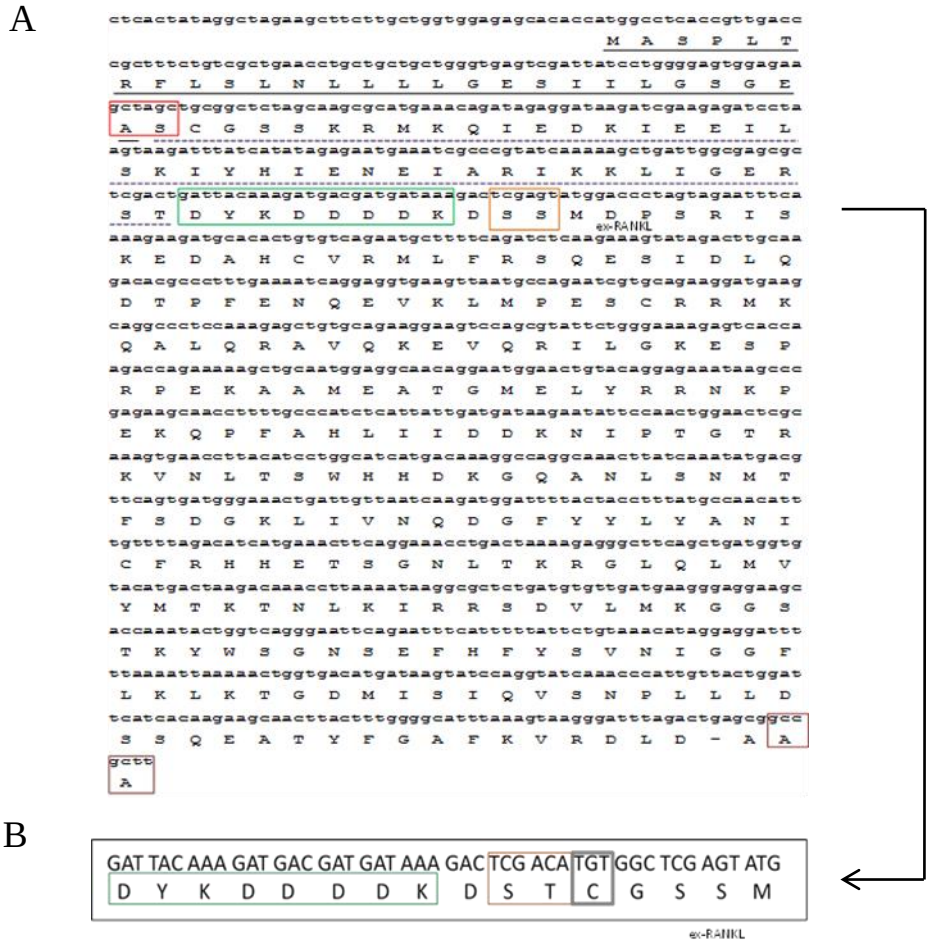

Figure 2.3 Map of pV20- and pV22-schRANKL vectors. A) *pV20-schRANKL: the black underlined sequence indicates the mouse CD8 signal peptide, the dotted purple underline the isoleucine zipper sequence, the red box the* Nhe*I restriction site, the green box the Flag-tag sequence, the orange box the* Xho*I restriction site and the maroon box* Not*I restriction site.* **B)** *pV22-schRANKL: the boxed area indicates the sequence between the FLAG-tag and extracellular schRANKL domain, the green box the FLAG-tag and the grey box the extra cysteine residue.*

drive the transcription of the luciferase reporter gene *luc2 P* from the *Photinus pyralis* firefly. A hydromycin resistant gene is also expressed to allow for stable transfection of mammalian cells.

A

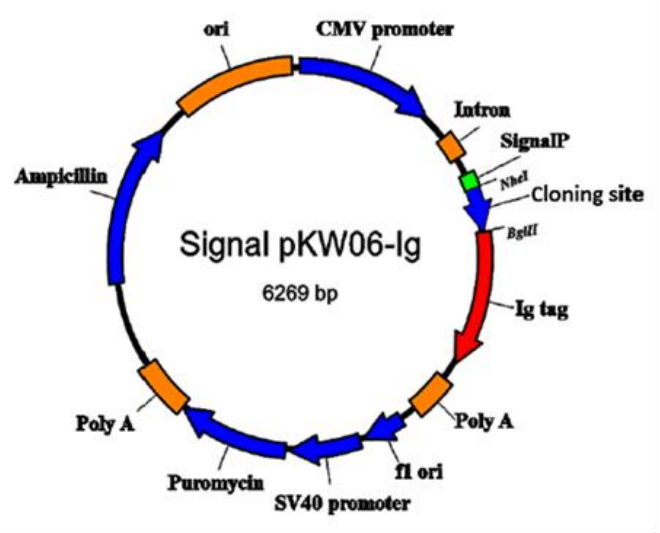

B

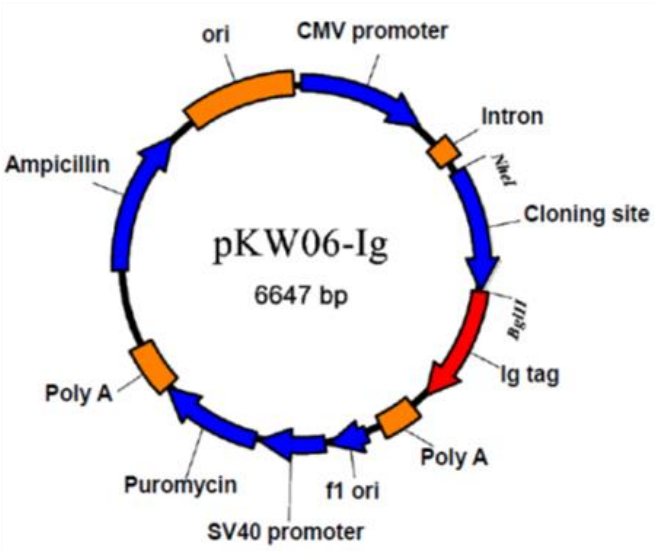

Figure 2.4 Map of pKW06 vector series A) *Signal pKW06 expressing the mouse CD8 signal peptide for production of soluble proteins,* **B)** *pKW06 for expressing intracellular proteins or soluble proteins with natural signal peptides. These are mammalian expression vectors with COOH-terminal human IgG Fc tag. cDNA are cloned into the* Nhe*I and* Bgl*II restriction sites for expression of recombinant fusion proteins (plasmid maps courtesy of Tuan Jun Hu).*

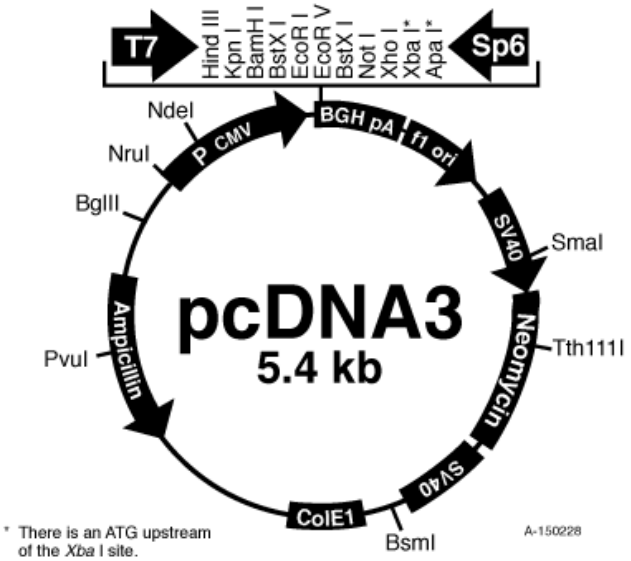

Figure 2.5 Map of the pcDNA3 plasmid

2.2.7 pEF1a-IRES-Neo

The pEF1a-IRES-neo plasmid is 5.6 kb in size and contains the human elongation factor-1 alpha sequence (Figure 2.7). The plasmid was designed for the ectopic expression of the 36 kDa *Renilla Firefly* protein. This plasmid was used as an internal control with the reporter assay system to investigate avian TRAF2 bioactivity in mammalian cells (Section 2.13.2). There is a chimeric intron located adjacent to the MCR which augments the expression of the DNA insert. A simian virus 40 (SV40) enhancer/promoter region is present to allow the plasmid to be expressed in cell types containing the SV40 large T-antigen, e.g. COS-7 cells and HEK-293T cells. The MCR is flanked by T7 and T3 RNA polymerase promoters that allow for easy sequencing of the insert. Inserts for pCI-neo require directional insertion using restriction sites available in the MCR. It contains two antibiotic resistance genes for selection of positively transfected cells, ampicillin (β-lactamase) and G-418 (neomycin phosphotransferase), more commonly used for stable transfection protocols.

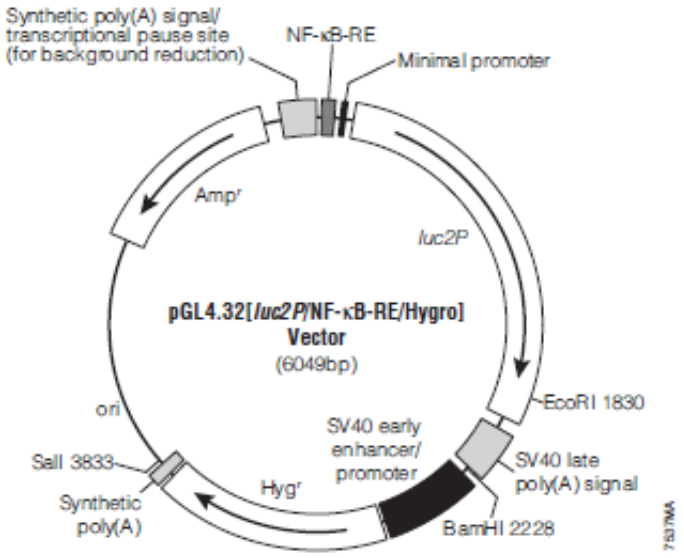

Figure 2.6 Map of pGL4.32-[*luc2 P*/NF-κB-RE/Hygro]

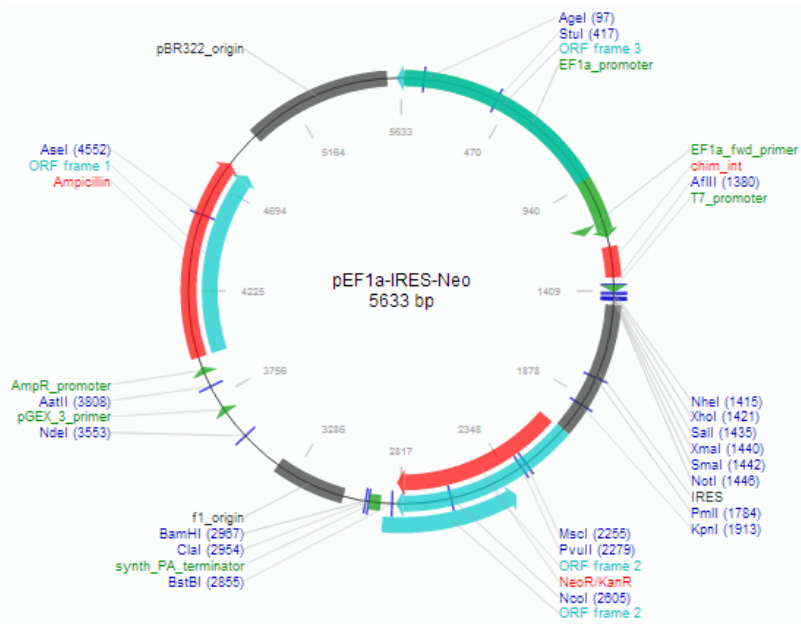

Figure 2.7 Map of pEF1a-IRES-Neo

2.2.8 Bacterial Strains

Escherichia coli JM109 competent cells (Promega) were used in plasmid transformations.

2.3 Cell lines

2.3.1 Resurrection of COS-7 and HEK-293T cells.

COS-7 or HEK-293T cells were removed from liquid nitrogen storage and quickly defrosted by placing in a pre-warmed 37°C water-bath. Cells were removed and resuspended in complete Dulbecco's Modified Eagle's medium (DMEM) (Invitrogen, Paisley, UK) supplemented with 10% foetal calf serum (FCS), 200 mM L-glutamine, 100X non-essential amino acids, 1 U/ml of penicillin and 1 µg/ml of streptomycin. Cells were then washed and pelleted at 1200 *g* for 5 min. The supernatant was discarded, the cells resuspended in 15 ml of complete DMEM placed in a 75 cm^2 culture flask (Niclon) and incubated at 37°C, 5% CO_2. The cells take up to 3 days to become 70-80% confluent and ready for passage.

To passage, the cell layer was washed twice with pre-warmed PBS. The cells were then washed with 5 ml of 10% (w/w) trypsin/versene solution. Another 5 ml of trypsin/versene solution was then added to the cells for 5 min at 37°C, 5% CO_2. The flask was tapped three times to dislodge any cells attached to the surface. Complete DMEM was then added to the flask to quench the trypsin enzymatic activity. Cells were then transferred to a 20 ml Universal and pelleted at 1200 *g* for 5 min. The supernatant was then removed and cells resuspended in 10 ml of complete DMEM. The total number of cells were counted using a haemocytometer and seeded at 7.5 X 10^5 cells/ml in 75 cm^2 flasks.

2.3.2 Cell culture reagents

All cell culture reagents were sourced from Sigma-Aldrich Ltd (Dorset, UK). Reagent details are provided in Appendix 1.

2.4 Transfecting cells with plasmid DNA

2.4.1 DEAE-dextran transient transfection method for COS-7 cells

Negatively charged plasmid DNA binds to the positively charged DEAE-dextran polymer creating a complex with an overall net positive charge, thus allowing for the uptake of this complex by the negatively charged cell membrane by endocytosis. Chloroquine is also added with the mixture to prevent the DNA being acidified and degraded in the endosomes upon endocytosis.

Twenty-four hours prior to transfection, COS-7 cells were passaged and seeded at 6 X 10^6/75 cm^2 flask with complete DMEM. Medium was removed from the cells and replaced with serum-free media containing the following for one 25 cm^2 flask; chloroquine (0.1 μm), plasmid DNA (37.5 μg), DEAE-dextran (600 μg/ml). Cells were then incubated for 3–3.5 h at 37°C, 5% CO_2 after which the cells were given a further shock to uptake the plasmid DNA with dimethyl sulphoxide (DMSO) (10% in PBS) for 2 min. Cells were allowed to recover for 24 h in complete DMEM at 37°C, 5% CO_2. To collect recombinant protein, serum-containing media was replaced with serum-free media and supernatant was harvested 72 h later. The supernatants were centrifuged at 1200 *g* to remove cell debris and stored at 4°C until use.

2.4.2 Calcium phosphate transient transfection method for HEK-293T cells

This approach to introduce plasmid DNA into mammalian cells is based on the formation of calcium-DNA precipitates that bind to the cell membrane leading to endocytosis. Calcium phosphate transfection was carried out according to the manufacturer's instructions. Twenty-four hours prior to transfection, HEK-293T cells were seeded at 1.5 X 10^4/ml in 96-flat well-plates in complete DMEM. Three h prior to transfection, the cell supernatant was removed and replaced with fresh complete DMEM. The kit components were defrosted at room temperature; calcium chloride ($CaCl_2$) (2 M), 2X HEPES buffer and tissue culture water. The following were added to tube A: 18 μl of $CaCl_2$, plasmid DNA (4-8 μg) and dH_2O to a volume of 150 μl. This mixture was added drop-wise to tube B containing 150 μl of 2X HEPES, while bubbling air through the mixture to ensure the formation of a fine

$CaCl_2$-DNA precipitate and allowed to incubate at room temperature for 30 min. The $CaCl_2$-DNA precipitate was added to each well of a 96-well plate. Supernatants and cell lysates were harvested 48 h later and stored at 4°C or -20°C.

2.4.3 Production of recombinant chIL-4, chCSF-2 and chCSF-1

ChIL-4 and chCSF-2 induce the differentiation of chicken bone marrow-derived cells into DC (Wu *et al.*, 2010). Plasmids expressing both chIL-4 and chCSF-2 were available as glycerol stocks. ChCSF-1 differentiates chicken bone marrow cells into macrophages (Garceau *et al.*, 2010) and a plasmid expressing chCSF-1 was also available as a glycerol stock. Each glycerol was streaked on LB agar plates with 100 µg/ml ampicillin (LB_{Amp100}) overnight at 37°C. Single colonies were picked from each plate and inoculated in 5 ml of LB_{Amp100} broth overnight at 37°C with shaking at 200 rpm. Two and half ml of the inoculum were removed, placed in 250 ml of LB-Amp_{100} broth and cultured for 18 h at 37°C with shaking at 200 rpm. The bacteria were pelleted at 3000 *g* for 30 min and stored at -20°C. DNA for transfections were later isolated using Maxi prep kits (QIAGEN) (Section 2.9.2).

2.5. Analysis of tagged recombinant proteins

2.5.1 Dot blot

Recombinant tagged proteins were initially tested by the dot blot approach allowing for quick detection of the expression of the protein of interest. All the proteins generated were indirectly detected by antibodies against the tag protein (Appendix 4, Table 5). Twenty-five to 50 µl aliquots of proteins were dotted onto nitrocellulose membrane along with positive (known protein with the relevant tag) and negative controls (PBS or dH_2O). The membrane was washed with PBS-Tween20 (PBST) and blocked for 1 h with 0.2% casein (PBS) (blocking buffer) on a rotating platform at room temperature. The membrane was then probed with the appropriate dilution of the primary antibody in blocking buffer for 1 h on a rotating platform. The membranes were washed once with PBST for 15 min, followed by two washes for 5 min. A secondary conjugated antibody (horseradish peroxidise (HRP))

was added to detect the primary antibody for 1 h on a rotating platform and washed 3 times for 5 min. To detect the proteins, ECL™ Western Blotting Detection Reagents were used (GE Healthcare Life Sciences, Little Chalfont, UK). The membrane was covered with equal volumes of detection reagent solutions 1 and 2 and incubated for 1 min. The membrane was covered in clingfilm and visualised using a G-Box.

2.5.2 SDS-PAGE

SDS-PAGE analysis of exCOS-7 or exHEK-293T supernatants was carried out using the MINI PROTEAN®-Tetra system (Bio-Rad). Samples were prepared by mixing 20 µl of sample protein with an equal volume of 2X reducing or non-reducing sample buffer (Appendix 1) and denaturation at 95°C for 5 min before being placed on ice. Samples were loaded into a precast Tris-HCI Mini PROTEAN® TGX™ 4-20% gel (Bio-Rad), which was clamped into the electrophoresis cell. Running buffer, containing Tris, glycine and SDS (Bio-Rad), was added to the chambers at 1X concentration. Samples were electrophoresed alongside the Precision Plus Protein Standards dual colour ladder (Bio-Rad) at 100 V for 1.5 h. Proteins were either analysed by western blotting or stained with Coomassie Blue stain (National Diagnostics, Hessle, UK), which was added to the gels for 2 h on a rotating platform. Digital images were taken of the gel using a scanner (EPSON Perfection V700).

2.5.3 Western blot

Following electrophoresis, proteins were electro-blotted onto nitrocellulose membrane (GE Healthcare Life Sciences, UK) using a Transblot Turbo-Transfer system (Bio-Rad). The gel was removed from the cassette and washed with dH_2O. Four 3MM filter papers (Bio-Rad) were pre-soaked in transfer buffer along with the nitrocellulose membrane. Two pieces of filter paper were placed on the bottom of the cassette holder and the nitrocellulose membrane was placed on top. To this the SDS-PAGE gel was added and sandwiched with two more pieces of filter paper before 5 ml of transfer buffer were added to the cassette which was then placed into the Transblot Turbo system. The protein was electrophoresed at 100 V for 40 min at 1.5 A. The nitrocellulose membrane was removed from the cassette and washed with PBST and then blocked with 0.2% casein at room temperature for 1 h on a rotating

platform. The appropriate primary antibody was diluted in 0.2% casein and added to the membrane for 1 h at room temperature on a rotating platform, followed by a 15 min wash with PBST and a further two 5 min washes. The secondary antibody was diluted in PBST and incubated with the membrane for 1 h, followed by three 10 min washes. Proteins were detected by enhanced chemiluminescence using ECL™ Western Blotting Detection Reagents. The membrane was covered with equal volumes of detection reagent solutions 1 and 2 and incubated for 1 min. The membrane was covered in clingfilm and visualised using a G-Box. For weak staining, membranes were visualised using an AEC substrate kit (BD Pharmingen, UK). The AEC substrate solution was made up by diluting 1 drop of AEC chromogen, 2 drops of acetate buffer and 1 drop of 3% hydrogen peroxide in 4 ml of H_2O. The membrane was incubated with the solution at room temperature for 1 h on a rotating platform. Digital images were taken using a scanner (EPSON Perfection V700).

2.5.4 Capture ELISA

To detect the expression of the recombinant proteins tagged with the human IgFc, capture ELISAs were carried out. A 96-well flat bottom plate (Falcon) was coated with mouse anti-human IgG antibody diluted in coating buffer for 24 h at 4°C. Each well was washed twice with PBS-T and 50 µl of blocking buffer (0.2% casein-PBS) were added to each well for 1 h at room temperature. Recombinant protein supernatants were added to the wells serially diluted from neat to 10^{-9} in PBS. A standard control was added to quantify the protein concentration; this was purified bovine IL-2 IgFc protein (kind gift from Dr. Zhiguang Wu). The proteins were incubated for 1 h at room temperature. The wells were washed 5 times with PBS-T and goat anti-human IgG-HRP-conjugated secondary antibody was added to the wells at a 1:1000 dilution in PBS-T. The plate was incubated for 1 h and washed 5 times with PBS-T. To detect the HRP enzyme, o-phenylenediamine dihydrochloride (OPD) (Sigma) was used. It utilises the HRP conjugates to produce a soluble brown-orange product that can be measured by spectrometry at 450 nm. The detection buffer containing OPD was added to each well and the reaction was allowed to stand for 1-2 min. The reaction was stopped by the addition of 50 µl of 2 N H_2SO_4 to each

well and readings were taken on a Spectra Max Plus (Molecular Devices, Berkshire, UK).

2.6 Primary Cells

All the animals used in the work reported in this thesis were handled and killed in accordance with the Animals (Scientific Procedure) Act 1986. The chickens used in the following experiments were Brown Leghorn J line which were housed in the Poultry Unit, The Roslin Institute.

2.6.1 Generation of bone marrow-derived dendritic cells (BMDC)

Femurs and tibias from 4-6 weeks old birds were removed ascetically and submerged in PBS on ice till use. Both ends of the bones were cut with a bone-cutter and flushed with 10 ml of PBS with a 0.8 x 40 mm diameter needle (21 G x 1.5 Terumo). To remove debris and large cells, the cell suspensions were poured through 70 μm nylon mesh cell strainers (Fisher Scientific) into 50 ml Falcon tubes. Cells were pelleted by centrifugation at 400 *g* for 5 min at 4°C. The supernatants were discarded and cells were resuspended in 10 ml of PBS and overlaid on Histopaque-1.077 (Sigma) at room temperature. To separate the cells, the Histopaque overlay was centrifuged at 1200 *g* for 20 min at room temperature with brakes and acceleration switched off. The cells residing on the interface were carefully removed using a Pasteur pipette and placed in a 20 ml Universal. Cells were then washed with complete Roswell Park Memorial Institute (RPMI) medium supplemented with 10% foetal chicken serum (FChS), 200 mM L-glutamine, 100X non-essential amino acids, 1 U/ml of penicillin and 1 μg/ml of streptomycin) at 400 *g* for 5 min. The supernatants were removed and cells were washed in 10 ml of complete RPMI at 400 *g* for 5 min. Cell numbers and viability were assessed by haemocytometer and trypan blue staining (Sigma-Aldrich) and adjusted to 1 X 10^6 cells/ml with pre-warmed complete RPMI media containing the appropriate dilutions of chIL-4 and chCSF-2 (exCOS-7). Cells were cultured on 6-well plates (Thermo Scientific) with 3 ml per well and incubated at 41°C, 5% CO_2. On day two and four of culture, 75% of the

media were removed and replaced with 2 ml of fresh complete RPMI containing the appropriate dilutions of chIL-4 and chCSF-2.

2.6.2 Generation of bone marrow-derived macrophages (BMDM)

Macrophage progenitor cells were isolated from bone marrow using a similar procedure as that for BMDC in section 2.6.1. Cells were adjusted to 1 X 10^6 cells/ml with pre-warmed complete macrophage RPMI (2% FChS, 3% FCS, 200 mM L-glutamine, 100X non-essential amino acids, 1 U/ml of penicillin and 1 µg/ml of streptomycin). Cells were cultured in 25-well chamber plates (Thermo Scientific) with appropriate dilutions of chCSF-1 (exCOS-7) and incubated at 41°C, 5% CO_2. Cells were differentiated for 6 days without replacing media or cytokines.

2.6.3 Pilot Study: Generation of chicken osteoclasts

Macrophage cells were routinely grown as outlined in section 2.6.2. On day 2 of culture, cells were removed from the plate by gentle pipetting and pelleted at 300 *g* for 5 min at 4°C. Cells were counted by haemocytometer and trypan blue staining and adjusted to 5 X 10^4 cells/ml in complete macrophage RPMI. Cells were incubated on 6-well plates (Thermo Scientific) with or without various dilutions of schRANKL at 41°C, 5% CO_2 for up to 8 days.

2.6.4 Tissues and primary cells

Tissues were removed from three 6-week old birds using sterile scissors and forceps and were immediately stabilised in RNA*later* (Sigma). Lymphoid tissues taken were the bursa of Fabricius, bone marrow, spleen, thymus, caecal tonsils, crop, gizzard, Meckel's diverticulum, Harderian gland, caecum, mid- and upper-gut. Non-lymphoid tissues taken were brain, muscle, heart, lung, liver, skin and kidney. Tissues were stored at 4°C or -20°C for long term storage.

Further tissues were taken from three 6-week old birds. Spleen, thymus and bursa of Fabricius were removed aseptically and placed in PBS on ice till use. Cells were purified as follows; each tissue was torn apart using forceps and pressed through a 40 µm nylon mesh (Fisher Scientific) with chilled RPMI. Spleen cells were overlaid on Histopaque-1.077 and centrifuged at 500 *g* for 20 min with brakes and

acceleration switched off. Cells residing at the interface were removed using a Pasteur pipette and placed in a 20 ml Universal and washed twice in complete RPMI at 400 *g* for 5 min. Thymocytes and bursal cells were allowed to stand in PBS for 20 min, allowing the cells to segregate to the bottom of a 50 ml Falcon tube. Supernatants were carefully removed and cells were washed twice in complete RPMI. Cell numbers and viability were assessed by haemocytometer and trypan blue staining (Sigma-Aldrich), adjusted to 5 X 10^6 cells/ml with pre-warmed complete RPMI and cultured in 25 mm^2 flasks for 2, 4, 18 and 24 h either unstimulated or stimulated as follows: splenocytes with 1 μg/ml Concanavalin A (ConA), bursal cells with 500 ng/ml phorbal myristate acetate (PMA) and ionomycin (1 μg/ml) and thymocytes with 25 μg/ml phytohaemagluttinin (PHA). Cells were pelleted after the specified time-point and lysed using RNeasy RLT lysis buffer (QIAGEN) and stored at -20°C until use.

2.6.5 Purification of chicken splenocyte subsets

Three whole spleens were removed from 6-week old birds and purified as outlined above. To separate the population of cells of interest, positive selection was carried out. After cells had been counted and cell numbers adjusted as appropriate, 500 μl of primary mouse anti-chicken antibody (Appendix 4, Table 6) were added for 30 min on ice in 15 ml Falcon tubes. Cells were washed twice in AutoMac Pro™ Rinsing Solution (wash buffer) at 300 *g* for 10 min. After removal of the supernatant, cells were resuspended in 80 μl of wash buffer and 20 μl of mouse anti-IgG labelled magnetic beads for 30 min on ice. Cells were washed twice with 1 ml of wash buffer at 300 *g* for 10 min and resuspended in 500 μl of wash buffer and placed into a 15 tube chilled rack for positive selection separation using the AutoMac Pro™ Cell Separator (Miltenyi, Biotech). Twenty microliters of cells were retained prior to separation to compare sorted and unsorted cells by FACS and stored in a 96-well U-bottomed plate on ice.

During cell separation, the AutoMac Separator places the cells over a magnetic column which is placed within a magnetic field. Here, magnetic IgG-positive cells are captured. The column is washed multiple times to remove non-specific bound cells and the negative cells are released. The column is then removed

from the magnetic field to release positive cells and undergoes multiple washes to elute 500 µl of the positive cell population. 50 µl aliquot of each population was retained for FACS analyses. Cells numbers were counted (Appendix 4, Table 6) and adjusted to 5 X 10^5 cells/ml. Cells retained for FACS analysis are pelleted at 300 *g* for 2 min and were stained with 50 µl of goat anti-mouse secondary conjugated antibody for 20 min on ice. Cells were washed twice and resuspended with 300 µl of FACS buffer and analysed using the FACS Calibur machine (BD Biosciences) (Appendix 4, Figure 2)

2.6.6 Control of RANKL transcription in chicken spleenocytes

Whole spleens were aseptically removed from three 6-week old birds and purified as previously described in section 2.6.1. Cells numbers were adjusted to 5 X 10^6 and stimulated as follows: medium alone, ionomycin (3 µg/ml), ionomycin (3 µg/ml) and PMA (500 ng/ml) or ionomycin (3 µg/ml) with 50, 20 or 10 µM of the calcium ion (Ca^{2+}) inhibitor 3, 4, 5-trimethoxybenzoic acid 8-(diethylamino)octyl ester (TMB-8) (Sigma) for 18 h at 41°C in 96-well U-bottomed plates. Cells were harvested by gentle pipetting and pelleted with centrifugation at 500 g for 5 min. Cell pellets were resuspended in lysis buffer, RLT, and stored at -20°C until use.

2.7 Purification of nuclei acids

2.7.1 Purifying total RNA from chicken tissues

Total RNA was purified from chicken tissues using the RNeasy mini kit (QIAGEN) following the manufacturer's instructions. Tissues stored at -20°C in RNA*later* were removed and allowed to thaw. Using sterile forceps and scissors, 30 mg of each tissue were placed into a lysing matrix tube containing 1.4 mm ceramic spheres (MD Biomedicals). To this, 600 µl of RLT buffer containing β-mercaptoethanol were added to protect the RNA from RNases. Tubes were placed into a homogenizer (FAST-PREP, Thermo Savant) and agitated vigorously for 20 sec at 20 Hz to release cellular RNA and shear genomic DNA. The lysates were removed and placed in a clean 1.5 ml tube to which 600 µl of 70% ethanol were

added. This mixture was then placed over an RNeasy silica membrane (spin columns) and centrifuged for 15 sec at 1300 *g*. The flow through was discarded and the column was washed once with RW1 buffer and twice with ethanol-containing RPE buffer for 15 sec at 1300 *g* to remove contaminants. A final 2 min RPE wash was carried out followed by a 1 min centrifugation to remove residual ethanol. The spin columns were placed into clean 1.5 ml tubes and RNA was eluted from the silica membrane by the addition of 50 µl of RNase-free H_2O.

2.7.2 Purifying total RNA from chicken cells and cell lines

Total RNA was purified from chicken cells (BMDC, BMDM, splenocytes, thymocytes and bursal cells) and cell lines (COS-7 and HEK-293T) using RNeasy mini kits following the manufacturer's protocol as in section 2.7.1.

2.8 DNA and RNA amplification

2.8.1 Oligonucleotide primer design

All oligonucleotides for cDNA amplification were designed using the predicted cDNA templates from the Ensembl (www.ensembl.org) or NCBI (http://www.ncbi.nlm.nih.gov/gene/) databases using Primer3 software and are given in Appendix 2, Table 2.

2.8.2 Two-step RT-PCR

cDNA for cloning and reverse transcription-polymerase chain reaction (RT-PCR) analysis were generated from various mRNA sources using Superscript III (Invitrogen) following the manufacturer's instructions. The reverse transcription is carried out in two steps. First the oligo(dT) primer or gene-specific reverse primer is annealed to the mRNA by adding oligo$(dT)_{20}$ (500 ng), mRNA sample (100 ng), dNTP (10 µM) and dH_2O to a total volume of 13 µl and heating the mixture to 65°C for 5 min. In the second reaction, 4 µl of 4X first-strand buffer containing $MgCl_2$, 1 µl of dithiothreitol (DTT) reducing agent, 1 µl of RNaseOUT (Promega) and 1 µl of Superscript III reverse transcriptase (RT) were added and incubated at 50°C, or 55°C

for gene-specific primers, for 55 min. Finally, the RT enzyme is inactivated by heating to 70°C for 15 min. All samples were stored at -20°C until use.

2.8.3 DNA amplification by PCR

Double-stranded DNA was amplified by PCR in standard 20 or 50 µl reactions. Each reaction consisted of 50-100 ng of cDNA template, 0.1 µm dNTPs, 0.75 mM $MgCl_2$, 1X PCR buffer, 0.1 µm of primers and 1.25 U of *Taq* polymerase (Invitrogen). PCR were performed on either the G-storm or MJ machine thermal cycler.

Thermal cycling conditions:

95°C for 5 min

95°C for 40 sec

*X°C/ for 40 sec

**72°C for 1 to 1.5 min

95°C for 40 sec

*X°C/ for 40 sec

**72°C for 1 to 1.5 min

*Annealing temperatures were dependent on the T_m of the each set of primers and ranged from 50-70°C.

**The length of the elongation steps was dependent on the size of the product. For every kb, 1 min was added.

2.8.4 Quantitative Real-time RT-PCR (TaqMan)

Quantitative real-time RT-PCR (qRT-PCR) was used to quantitatively measure cytokine mRNA expression levels in a range of chicken tissues and cells. To account for variation and to normalise the data, the housekeeping gene, 28S, was also measured for each sample. The 28S ribosomal RNA gene encodes for the large

subunit of ribosomes and is abundantly expressed in eukaryotic cells making it an appropriate gene to normalise the expression levels of the target gene.

For each gene analysed, a pair of primers and a probe were designed against the template for the target gene using the Primer Express software package (Applied Biosystems). All primers were acquired from Sigma and probes from Eurogentec (Belgium). The probes were labelled at the 5' end with the fluorophore 5-carboxyfluorescein (FAM) and the 3' end with the quencher dye tetramethylrhodamine (TAMRA). Primers and probes for chRANKL, chRANK and chOPG were designed under seven strict conditions. The melting temperature of the primers was between 58°C and 60°C, with the probes being 10°C higher. Both the primers and probes were designed to be no longer than 30 nucleotides and have a GC content in the range of 30-80%. To reduce non-specific priming, the five last nucleotides at the 3' end of the primers did not contain G or C residues and amplicons were ideally between 50-150 bp. To design an optimal probe, there were no G or C residues at the 5' end as this could quench the FAM fluorophore and, to prevent its mis-priming, probes were designed to have less than four identical nucleotides in a row. Finally, all primer and probe sets were designed so that at least one component overlapped an intron/exon boundary so that no genomic DNA was amplified producing “false positives”.

Detection of a specific product is based on the fluorescence released due to hydrolysis of the target-specific probes by the 5' exonuclease activity of the DNA polymerase. The close proximity of the 5' reporter fluorophore allows the 3' quencher to inhibit the fluorescence of the reporter dye. During the PCR stage of RT-PCR, the primers anneal to the template and the probe anneals at a position between the forward and reverse primer. When the primers are extended during PCR the DNA polymerase moves along the template. However, when the polymerase encounters the bound probe, its 5'-3' exonuclease activity degrades the probe releasing the reporter from the inhibition of the quencher. This leads to an increase in the fluorescence intensity which can be measured. The greater the fluorescence intensity, the greater the abundance of the target gene in each sample. The results are presented

as the cycle threshold (Ct) value, the number of cycles at which the fluorescence emission of the reporter minus the background passes the threshold of detection.

The optimal concentration of each primer set needs to be determined before examining the expression of the target gene. For IL-1β, IL-6, IL-10, IL-12α and 28S, primer optimisations were previously determined (Wu *et al*., 2010; 2011). For chRANKL, chRANK and chOPG, optimal primer concentrations were determined as follows; COS-7 cells were transfected with the pV22-exRANKL, pKW06-RANK or pKW07-OPG constructs by the DEAE-dextran approach as in section 2.4.1. RNA was extracted using an RNeasy mini kit according to the manufacturer's instructions (Section 2.7.1). These RNA samples were used as positive standard controls. The RNA samples were diluted in DNase-free H_2O from 10^{-1}-10^{-6} and primers were used at concentrations between 0.25-2.5 μM to determine the optimal concentration. For chRANKL, chRANK and chOPG, 0.4 μM primer concentrations were optimal for detection of each cytokine and was used for all analyses.

All RT-PCR reactions were performed using the TaqMan FAST Universal PCR Master Mix and the One-step RT-PCR Multiscribe enzyme (Applied Biosystems). Samples were analysed in a 10 μl reaction volume consisting of 5 μl of 2X FAST Master mix, 0.5 μl of primer mix, 0.25 μl (125 nM) of probe, 0.25 μl 40X Multiscribe enzyme, 1.5 μl of DEPC-H_2O and 2.5 μl of diluted RNA. For 28S analysis, RNA samples were diluted 1:500 and RNA test samples used for detection of target gene were diluted at 1:5. All assays were done in triplicate wells. For positive standard RNA for 28S detection, RNA from HD11 cells stimulated with LPS (200 ng/ml) for 6 h was used. Amplification and detection of products was carried out using the 7500FAST TaqMan machine (Applied Biosystems).The thermal cycling conditions were as follows. RT steps: 48°C for 30 min, 95°C for 20 sec followed by PCR steps: 95°C for 3 sec, 60°C for 30 sec repeated for 40 cycles. Primers and probe sequences and concentrations for all target genes tested are given in Appendix 2, Table 4.

To calculate the corrected 40-C*t* values for all target genes, the following formulas were used: standard curves were created using the C*t* values of the serially diluted standard RNA of the specific gene. The slope of the line (y=mx+c) allows for

the examination of the efficacy of the reaction using the following formula E= (10(-1/slope))-1 (E=efficacy). To calculate the corrected 40-Ct values the following equation was used: normalised C*t*= C*t*+(N'*t*-C'*t*)*(S/S') where N'*t* is the mean C*t* value for 28S RNA among all samples, C'*t* is the mean value for 28S RNA in the sample and the S and S' are the slopes of regression of the standard plots for the cytokine mRNA and the 28S RNA, respectively. Corrected 40-C*t* is calculated by 40- normalised C*t*.

2.8.5 Agarose gel electrolysis

All DNA was visualised using agarose gels. DNA agarose gels were prepared by adding agarose at a (w/v)% dependent on the size of the expected PCR product in TAE. TAE is made up of Tris-buffer, acetic acid and EDTA which works to sequester divalent cations. Although TAE is not a stable as TBE, linear, double-stranded DNA runs faster through agar dissolved in TAE buffer. The mixture was heated until agarose powder was fully dissolved and allowed to cool to 50°C. The DNA intercalating dye, SYBR Safe® (Invitrogen) was added to the mixture and poured into a plastic mould to set with appropriate comb sizes inserted.

2.8.6 PCR purification

When a single band was visualized on a DNA agarose gel, the remaining PCR product was cleaned up using the QIAquick PCR Clean-up kit (QIAGEN) according to the manufacturer's instructions, as follows. PB binding buffer was added at 5 times the volume of the PCR mix and placed in spin column with a 2 ml collection tube. The DNA was bound to the silica membrane by centrifugation at 1300 *g* for 1 min. The flow through was discarded and the column washed twice with ethanol-containing PE buffer. To ensure all ethanol was removed before elution, the column was given a dry spin at 1300 *g* for 1 min. The DNA was eluted in 30 µl of H_20, allowed to stand for 1 min for optimal absorption and spun at 1300 *g* for a further 1 min to elute the DNA. Samples were stored at -20°C or used immediately for ligation into the appropriate vector.

2.8.7 Gel extraction

PCR reactions that contained multiple bands were purified using a QIAquick Gel Elution kit (QIAGEN) according to the manufacturer's instructions, as follows. The bands of interest were excised using a disposal scalpel blade from the gel under a UV transilluminator. QG dissolving buffer was added at 5 times the volume of the excised gel portion. This was allowed to dissolve for 15 min at 56°C on a heating block after which it was vortexed repeatedly. The QG buffer also contains a pH colour and salt indicator which, when orange, indicates the pH is <7.5 and salt concentration is high for optimal DNA absorption to the silica membrane of the spin column. Sodium acetate (pH 5.0) was added to samples that needed adjusting for optimal absorption. The dissolved gel was mixed 1:1 with isopropanol, applied to a spin column and centrifuged for 1 min at 1300 *g*. The flow-through was discarded and the column was washed using PE buffer at 1300 *g* for 1 min. The column was washed for an additional min to ensure any residue of ethanol was removed. The column was transferred to a clean 1.5 ml microcentrifuge tube and the DNA was eluted using 30 µl of autoclaved H_20, allowed to stand for 1 min for optimal absorption and spun at 1300 *g* for a further 1 min. Samples were stored at -20°C or used immediately for ligation into the appropriate vector.

2.8.8 Ligation

Ligation is a method which allows the covalent bonds at the ends of DNA fragments to be joined together. This process requires three components: DNA fragments that have compatible or sticky ends, buffer containing ATP which is a vital co-factor for the bioactivity of the last component and T4 ligase. The T4 ligase is from the bacteriophage T4 and works to fix nicks in the phophodiester backbone of DNA. T4 ligase works across a broad range of temperatures with 16°C being the most optimal. However, 4°C overnight incubation works efficiently. All sub-cloning procedures were carried out using T4 ligase buffer (Promega).

2.8.9 Directional sticky-end cloning into expression vectors

To directionally ligate DNA into expression vectors, primers were designed to integrate the appropriate restriction sites at the 5' and 3' end of the cDNA. The

empty expression vectors were cut using the same restriction enzymes as the sites incorporated into the cDNA sequence. The restriction enzymes create overhanging ends on the vector and cDNA that complement one another, allowing T4 ligase to join them together creating a closed circular plasmid.

2.8.10 Restriction digestion

Restriction digestion was carried out using the restriction enzymes and their appropriate buffers (Appendix 1) to release the DNA inserts from pGEM-T Easy or to cut the cDNA after gel or PCR purification. The same restriction enzymes used to cut the cDNA were used to linearize the empty expression vectors (pKW06, pcDNA3-HA, etc.). All digestions were carried out in 10 µl reactions containing 1 µl of DNA, 1 µl of 10X reaction buffer and 1 µl of restriction enzyme. Reactions were incubated at 37°C overnight. For double digestions, the initial digest was incubated overnight at 37°C, after which the mixture was cleaned up to remove the original restriction enzyme and buffer using a PCR clean-up kit (QIAGEN), as described in section 2.8.6, and the second restriction enzyme added for a further 8 h incubation at 37°C.

2.8.11 Transformation

Escherichia coli JM109 competent cells were removed from -80°C storage and defrosted on ice for 5 min. A 45 µl aliquot of the cells was added to a chilled 1.5 ml eppendorf tube containing 2 µl of ligation reaction and gently flicked before incubating on ice for 20 min. The mixture was then placed in a water-bath heated to 42°C for 50 sec. This heat-shock approach creates small holes in the wall of the bacteria allowing the uptake of the DNA/plasmid. The cells were then returned to ice for a further 2 min. A 950 µl aliquot of room temperature SOB media was added to the cells and incubated at 37°C with shaking (2000 rpm) for 90 min. The cells were gently pelleted at 200 *g* for 3 min and supernatants discarded. The cell pellets were resuspended in 200 µl SOC of which 100 µl was plated on each of two LB agar plates.

2.8.12 Screening bacterial colonies by colony PCR

Bacterial colonies were screened for gene inserts by PCR using either gene-specific primers, those used to clone the gene, or plasmid-specific primers, designed to overlap the MCR of the plasmid. Using a pipette tip, colonies were individually picked and streaked in a small numbered area of a Luria broth (LB) agar plate supplemented with 100 mg of ampicillin (LB_{amp100}). The same tip was then incubated in 50 µl of dH_2O for 1 min. These samples were then boiled for 5 min at 95°C and 10 µl were used as template in PCR. The LB_{amp100} agar plates were incubated at 37°C for 24 h. Positive colonies were identified by PCR and picked from overnight agar plate into 5 ml of LB_{amp100} broth for plasmid purification.

2.9 Plasmid DNA purification

2.9.1 Small-scale plasmid purification

For sequencing, plasmid DNA from *E. coli* cells was purified using a Mini Prep kit from QIAGEN following the manufacturer's instructions as follows. A single colony was grown overnight in 5 ml LB_{amp100} broth at 37°C with shaking at 200 rpm. Cells were pelleted for 15 min at 3000 *g* and supernatants were discarded. Cells were resuspended in 250 µl of buffer P1 containing Lysis Blue (colour indicator to ensure optimal buffer mixing) and placed in a 1.5 ml tube. Next, 250 µl of lysis buffer P2 were added and the tube was inverted 4-6 times. A 350 µl aliquot of neutralising N3 buffer was added to the mixture and inverted 4-6 times to degrade the cell components, leaving the DNA in the supernatant. To compact the cell debris, the mixture was centrifuged at 1300 *g* for 10 min. The supernatant was applied to a spin column and centrifuged at 1300 *g* for 1 min to capture the DNA in the silica membrane. To remove endonucleases and ensure no degradation of the DNA, the membrane was washed with 500 µl of PB buffer. The flow through was discarded and the column washed twice with ethanol-containing wash buffer with a further dry spin to remove residual ethanol. The spin column was placed in a new 1.5 ml tube and the DNA eluted using 50 µl of dH_2O and centrifugation at 1300 *g* for 1 min. The concentration of the plasmid DNA was analysed using a Nanodrop.

2.9.2 Large-scale endotoxin-free plasmid purification

To acquire a high yield of plasmid DNA for transfection and protein production, an endotoxin-free Maxi prep kit (QIAGEN) was used according to the manufacturer's instructions as follows. Single colonies previously sequenced verified were grown in 5 ml of LB_{amp100} broth at 37°C with shaking at 200 rpm for 8-12 h. A 2.5 ml aliquot was added to 250 ml of LB_{amp100} broth and incubated at 37°C with shaking at 200 rpm. Cells were pelleted at 3000 *g* for 30 min. The cell pellets were either stored at -20°C until use or immediately resuspended with 10 ml of P1 buffer containing Lysis Blue. The cells were lysed by addition of 10 ml of buffer P2, mixed by inversion and incubated at room temperature for 5 min. Chilled P3 buffer was added to the mixture to precipitate cell debris, genomic DNA and proteins. To compact the cell debris the mixture was centrifuged for 15 min at 4000 *g*. The lysates were removed and placed in a clean 50 ml Falcon tube to which 5 ml of ER buffer were added to remove endotoxins and incubated on ice for 30 min. A 30 ml QIAGEN-100 column was equilibrated with 10 ml of QBT buffer; to this the lysate mixture was added and allowed to flow through. The column was washed twice with 30 ml of QC buffer and DNA was eluted with elution buffer QF into a clean 50 ml Flacon tube. To precipitate the DNA, 10.5 ml of isopropanol were added and mixed by vigorous inversion. The DNA was pelleted by centrifugation at 4000 *g* for 1 h at 4°C. The supernatant was removed and the DNA was washed once with 5 ml of 70% ethanol at 4000 *g* for 1 h at 4°C. The ethanol was removed and the DNA pellet was air-dried for 15-20 min at room temperature. The DNA pellet was resuspended in 500 µl of dH_2O and stored at -20°C until use.

2.9.3 Sequencing plasmid DNA

Sequencing of all genes for verification was carried out using a Big Dye Sequencing Kit (Applied Biosystems) and analysed using the Applied Biosystems 3730 DNA Analyser (Ark Genomics, The Roslin Institute or DNA Sequencing & Services Dundee).

2.10 Optimising bioassay conditions

2.10.1 Optimising LPS concentration for stimulating BMDC and BMDM

Preliminary assays were carried out to determine the concentration of lipopolysaccharide (LPS) to induce sub-optimal maturation of antigen-presenting cells (APCs). BMDC and BMDM were differentiated from bone marrow cells as described in section 2.6.1. Cells were stimulated on day 6 of culture with various amounts of LPS (*E. coli* serotype 055:B5, Sigma) (1-200 ng/ml) for 3, 6 and 9 h, after which the cells were removed from wells by gentle pipetting and pelleted at 500 *g* for 5 min. The cells were then lysed using RLT lysis buffer from the RNeasy mini kit (QIAGEN) and stored at -20°C until use. RNA was purified for each sample following the manufacturer's protocol as described in section 2.7.1. For cell surface expression of activation markers on BMDC and BMDM, various amounts of LPS (1-200 ng/ml) and exCOS-7 IFN-γ dilutions were tested to identify the optimal concentration to induce maturation in APCs, as determined by flow cytometry using a FACs Calibur (BD Biosciences) as described in section 2.11.1. For BMDC, 2 ng/ml, and for BMDM, 1 ng/ml of LPS were sufficient to induce expression of cell surface molecules after 24 h. For BMDM, the more potent activator IFN-γ was optimal at a 1:100 dilution of exCOS-7 cell supernatant.

2.10.2 Optimising schRANKL concentrations for stimulating BMDC and BMDM

Two similar plasmids differ in the location of cysteine residues were designed to express of type II transmembrane proteins (Section 2.2.4). To determine which recombinant chRANKL was expressed from both vectors for further studies and bioassays, BMDC were differentiated from bone marrow cells as described in section 2.6.1. Cells were stimulated on day 6 of culture with LPS (2 ng/ml) with or without various dilutions of pV20- or pV22-schRANKL for 3, 6, 24 and 48 h. To determine the bioactivity of each protein, RNA was extracted from each sample and pro-inflammatory cytokine mRNA expression levels were determined by qRT-PCR.

2.11 Flow cytometry

2.11.1 Cell surface analysis of proteins expressed by chicken APC

Flow cytometry allows analysis of the expression of specific proteins on the surface of cells or intracellularly. Due to the relatively small number of chicken APC- specific mAb available, single staining of BMDC and BMDM was carried out for this study. Cells were harvested after the specified time-point by addition of EDTA (0.5 mM) for 2 min at room temperature. Cells were removed by gentle pipetting using a Pasteur pipette and placed in a 20 ml Universal tube. Cells were pelleted at 350 *g* for 5 min and resuspended in the appropriate amount of FACS buffer (PBS, 0.005% bovine serum albumin and 0.001% azide). All antibodies were diluted in FACS buffer with dilutions and further information is given in Appendix 4, Table 7. In a 96-well U-bottomed plate, 50 µl of cells were added to each well. Cell were washed with 150 µl of FACS buffer and centrifuged at 350 *g* for 3 min at 4°C. The plate was quickly inverted to release the supernatant and the cell pellet dispersed using a plate shaker. The cells were resuspended in 50 µl of the appropriate primary mAb on ice for 20 min. Cells were washed twice with FACS buffer and shaken to disperse the cell pellet. The appropriate secondary conjugated antibody was added to the cells for a further 20 min after which the cells were washed twice and resuspended in 400 µl of FACS buffer. To distinguish between live and dead cells, the 7-AAD viability dye (Biolegend) was added to cells prior to analyses on the FACS Calibur (BD Biosciences).

2.11.2 Flow cytometry-based survival assay

During the different stages of apoptosis, the cell membrane undergoes a number of changes such as expression of thrombospondin-binding sites and exposure of phosphatidylserine (PS). PS is usually found on the inner membrane of the cell and upon apoptosis-inducing signals, this negatively charged phospholipid flips to the outer membrane (Fadok *et al*., 1992). This occurs at the early stages of apoptosis and is not linked to membrane leakage, unlike the necrosis form of cell death. Annexin-V is part of large family of calcium-dependent proteins that recognise and bind to a wide variety of phospholipids. However, Annexin-V only binds to PS

which makes it appropriate for staining early apoptotic cells. To differentiate between early and late stages of apoptosis and necrosis, propidium iodine (PI) is used to stain DNA which becomes exposed during cell death by cell membrane leakage.

To analyse cells undergoing early or late apoptosis, BMDC and BMDM were treated on day 6 of culture with media alone or with various dilutions of ex-COS-7 exRANKL for 24 and 48 h. Cells were harvested from the plates by gently pipetting as EDTA inhibits the calcium-dependent annexin-V binding. Cells were pelleted at 350 *g* for 5 min and washed twice with annexin-V binding buffer (eBioscience-Affymetrix). Cells were resuspended in 190 µl of binding buffer to which 10 µl of recombinant annexin-V-biotin were added at room temperature for 20 min. Cells were washed twice with binding buffer at 350 *g* for 3 min. Streptavidin-Alexa-647 was added to the cells for 30 min at room temperature in the dark. Cells were washed twice with binding buffer and resuspended in 350 µl of buffer. Prior to FACS analysis, 20 µg of PI were added to the appropriate wells and FACs analysis was performed on a FACS Calibur (BD Biosciences).

2.11.3 Phagocytosis assay

Immature DC and macrophages can engulf solid particles to form internal phagosomes. As the cells mature they lose the ability to endocytose particles. On day 6 of BMDC culture, the media were removed and replaced with fresh media or a 1:50 dilution of schRANKL for 24 h, after which 100 particles/well of Zymosan A BioParticles labelled with fluorescein isothiocyanate (FITC) (Molecular Probes), except in control wells, were added for 1 h. Experiments were carried out in duplicate with one plate incubated at 41°C, 5% CO_2, and a control plate at 4°C to inhibit phagocytosis. Phagocytosis was stopped by the addition of 550 µl of ice-cold PBS followed by 4 washes with cold PBS. The cells were fixed with 4% PFA for 20 min at room temperature, followed by two washes with PBS containing 2% FBS, and analysed under the Zeiss Axiovert fluoresence microscope with attached camera or by FACs by detecting FITC-positive cells.

2.12 Dual-Luciferase Reporter system

Dual-Luciferase Reporter system (Promega) are widely used for the study of eukaryotic gene expression and allows a number of biological processes to be analysed, e.g. transcription factors, intracellular signalling, RNA processing and protein folding. The dual reporter approach allows for the simultaneous expression and detection of two individual reporter enzymes. The *Firefly* luciferase-containing vector, pGL4.32-[*luc2 P*/NF-κB-RE/Hygro] (section 2.2.7), is a reporter plasmid that is affected by specific experimental conditions while the co-transfected control *Renilla* luciferase plasmid, pEF1a-IRES-Neo (section 2.2.8), serves to provide a baseline response. *Firefly* and *Renilla* luciferase have distinct evolutionary origins, different enzyme structure and have different substrate requirements, giving them utility in these assays.

The pGL4.32-[*luc2 P*/NF-κB-RE/Hygro] vector contains NF-κB response elements that drive the transcription of the luciferase reporter gene *luc2 P* from the *Photinus pyralis Firefly* when the NF-κB pathway is activated. The *Firefly* luciferase is a 61 kDa monomeric protein that can be oxidised through a luciferyl-AMP intermediate that requires ATP, Mg^{2+} and O_2 upon which it releases a "flash" of light that can be detected by a luminometer (Figure 2.6). *Renilla* luciferase on the other hand is a 36 kDa monomeric protein from *Renilla reniforms.* The luminescent reaction is catalysed by the coelenterate-luciferin and O_2 (Figure 2.6). To distinguish between the luminescent of the two luciferases, the Dual-Luciferase reporter system provides two substrate kits; a Luciferase Assay Reagent II kit to activate the *Firefly* luciferase and a Stop & Glo® Reagent kit which inhibits the *Firefly* luciferase and activates the *Renilla* luciferase.

HEK-293T cells were grown and passaged as described in section 2.3.2. Cells were seeded at 1.5 X 10^4 cells/ml and grown on 96-well flat bottomed plates at 37°C, 5% CO_2 for 48 h to allow cells to become 80% confluent. Cells were then co-transfected using the calcium-phosphate method (section 2.3.4). To each well, 40 ng/ml of pGL4.32-[*luc2 P*/NF-κB-RE/Hygro] vector were added along with 10 ng/ml of pEF1a-IRES-Neo vector, with or without chTRAF2 or chTRAF2S or both

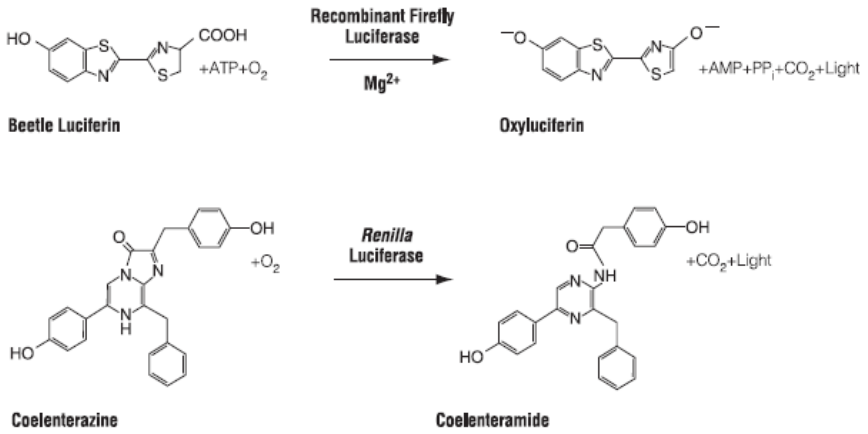

Figure 2.6 Bioluminescent reactions catalysed by *Firefly* and *Renilla* luciferases.

plasmids at 75 or 150 ng/ml. Cells were grown for 48 h and media were removed and replaced with 30 µl of 1X Passive Lysis buffer (Promega) for 10 min at room temperature on a rotating platform to release intracellular protein. To detect luciferase activity of the firefly luciferase, 50 µl of Luciferase Assay Reagent II were added to each well and luminescence was detected immediately using the GloMax® 96 luminometer (Promega). To quench the firefly luminescence and activate the *Renilla* luciferase, 50 µl of Stop & Glo® Reagent was added to each well and a second reading of luminescence detected using the GloMax® 96 luminometer (Promega). To normalise the data, the luminescence of the *Firefly* luciferase was divided by the *Renilla* luciferase data and expressed as relative luciferase activity.

2.13 Statistical analysis

All data were checked for normality and statistical analyses were carried out using either Mann Whitney-U test or Student's *t*-test as indicated in Minitab 16.1.0 (State College, USA). Statistical significance was determined as $p<0.05$ (significant) or $p<0.01$ (highly significant).

Chapter 3

Cloning and expression of chicken receptor activator of NF-κB ligand (RANKL), and its receptors, chRANK and chOPG

3.1 Introduction

The mammalian TNF receptors and their ligands orchestrate a variety of functions in the architecture of immune organs, development, inflammation, invasion, proliferation and angiogenesis (Locksley *et al*., 2001; Aggarwal, 2003). The receptor family are characteristically type I transmembrane proteins that have low degrees of homology and are grouped due to the presence of conserved CRD in their extracellular ligand-binding domain (Naismith & Sprang, 1998). The ligand family has 19 members which interact with their cognate receptor(s). This family of cytokines are typically type II transmembrane proteins with highly conserved COOH-terminal TNF homology domains. Members of the TNF superfamily usually share 20-30% sequence identity within this domain. The hallmark of ligand:receptor interactions is their three-fold symmetry. The ligands self-assemble into non-covalent trimers, whose individual chains form a β-sheet "jelly-roll" fold (Jones *et al*., 1990).

To date, 19 ligands and 29 receptors have been identified in mammalian species. However, only 10 ligands and 15 receptors have been identified in the avian genome. One of the most recent members of the mammalian TNF superfamily to be identified was RANKL along with its signalling receptor, RANK (Anderson *et al.,* 1997; Wong *et al.,* 1997). RANKL is a transmembrane protein of 316 amino acids containing a COOH-terminal receptor-binding domain, a 20 amino acid hydrophobic transmembrane domain and a relatively long extracellular region that contains a TNF homologous domain (Anderson *et al*., 1997; Lam *et al*., 2001). RANKL predominantly exists as a membrane-bound form but soluble protein can be generated by enzymatic cleavage and alternative splicing (Ikeda *et al.,* 2001; Walsh *et al.,* 2013). At the cell surface, RANKL aggregates into trimers through conserved residues in the extracellular domain and this three-fold symmetry is required for the activation of its cognate receptor, RANK. RANKL interacts with RANK on the surface of DC, enhancing pro-inflammatory cytokine expression and survival of cells (Anderson *et al.,* 1997; Wong *et al*., 1997). Around the same time as RANKL was cloned and identified, various other groups identified the inhibitory effects of osteoprotegerin (OPG) on osteoclast cells (Simonet *et al*., 1997). Using OPG as bait, two independent groups identified its ability to interact with RANKL and inhibit its

bioactivity (Simonet *et al*., 1997; Yasuda *et al.,* 1998). OPG functions to limit the interaction between RANKL and RANK, working as a decoy receptor. Further insight into the biological roles of these novel cytokines led to the observation that $RANK^{-/-}$ and $RANKL^{-/-}$ deficient mice had entirely unexpected phenotypes: early defects in T and B cell development, complete absence of lymph nodes, severely reduced osteoclastogenesis and failure to develop mammary glands (Dougall *et al*., 1999; Kong *et al*., 1999a; Perlot & Penninger, 2012). RANKL-RANK interaction is critical for a number of important biological activities required for development, immunity and bone metabolism. Their role in T cell and DC communication was at the forefront of research until the discovery that these cytokines drive interactions between the immune system and bone turnover, leading to an interdisciplinary research field, coined osteoimmunology by Arron & Choi (2000).

With the TNF superfamily playing vital roles in immunity it is important to understand the bioactivity of the family members present in the chicken genome. To date, of the 11 TNF ligands identified in the avian genome, research has been carried out on 5; CD30L and TRAIL (Abdalla *et al*., 2004b), BAFF (Schneider *et al.,* 2004), CD40L (Tregaskes *et al.,* 2005) and VEGI (T1A) (Takimoto *et al*., 2005). These studies identified the conserved bioactivity of each gene in the chicken. To begin examining the bioactivity of chicken RANKL, RANK and OPG, their sequences were examined for conservation with their mammalian orthologues. In this Chapter, the molecular cloning of the full-length and extracellular domains of chRANKL, chRANK and full-length chOPG is described. The ability of chRANKL to form trimers, along with the ability of chOPG to form dimers, was analysed with recombinant protein expressed in COS-7 cells.

3.2. Methods

3.2.1 *In silico* analysis

Mammalian RANKL and RANK are type II and type I transmembrane proteins, respectively. To identify the various domains within the chicken proteins, the SMART prediction program was used to compare them to the known human and mouse sequences. Signal peptide sequences, N-glycosylation sites and domain structures were analysed using SignalP4, NetNGly, TMHMM and PSIPRED programs Amino acid conservation between mammalian and chicken genes were analysed using CLUSTALX V2 (Chapter 2, section 2.1).

3.2.2 *In vitro* methods

The full-length and extracellular domains of chRANKL and chRANK were cloned, along with the full-length sequence of chOPG, using RNA from ConA-stimulated splenocytes or bone marrow cells as template by RT-PCR. Each gene was sub-cloned into their respective expression vectors to produce recombinant proteins (Chapter 2, section 2.2). To express chRANKL, two plasmids were specifically designed to induce the correct folding of the protein, called pV20-schRANKL and pV22-schRANKL (Chapter 2, section 2.2). Recombinant fusion proteins were generated from COS-7 cells transfected with the respective expression vectors by a DEAE-dextran-based approach (Chapter 2, section 2.4). The TNF family form dimeric or trimeric proteins and to investigate the ability of the chicken TNF superfamily members to fold correctly, protein structures were analysed by western blot. Preliminary experiments were carried out to investigate the bioactivity of the pV20- and pV22-schRANKL. BMDC were generated and stimulated with LPS or chCD40L, with or without pV20- and pV22-schRANKL, and pro-inflammatory cytokine mRNA expression levels were analysed by qRT-PCR.

3.3 Results

3.3.1 Identification of the genes for RANKL, RANK and OPG in the chicken genome

To characterise the biological roles of chRANKL, chRANK and chOPG, the cDNA for all three were cloned and sequence verified. All three genes are present in the chicken genome with chRANK (NP_001076830.1) being the only sequence that is currently predicted. Using the chicken genome sequence v4.0, the location of each gene was identified. The chRANKL gene is located on chromosome 1 and has conserved synteny with both the human (chromosome 13) and mouse (chromosome 14) genes (Kaiser *et al.*, 2005). ChRANK and chOPG both lie on chromosome 2 and also have conserved synteny with both the human (chromosomes 18 and 8 respectively) and mouse genes (chromosomes 1 and 15, respectively) (Kaiser *et al.*, 2005). Wang *et al.* (2008a) characterised the ability of chRANKL to activate osteoclasts from chicken bone marrow preparations. However, that study does not indicate whether the full-length or extracellular domain of the protein was used. It refers to another paper (Wang *et al.*, 2008), stating that the protocol to clone chRANKL is in this other paper. However, this other paper does not exist in any searchable database.

To verify the sequence identified was chRANKL, the human RANKL protein sequence (NP_003692.1) was blasted against the chicken genome. Human RANKL has 61% identity to chRANKL (NP_001076830.1) and therefore this chicken sequence was used for further analyses. In the chicken genome, the chRANK cDNA sequence was predicted and was verified by blasting the human protein RANK sequence against the chicken genome sequence. Human RANK has the highest similarity to the predicted chRANK protein (~44%). In 2003, a group identifying the expression of TNF decoy receptors during follicle development and atresia in chickens cloned a partial sequence of chOPG. This partial sequence contained the CRD but not the COOH-terminal domain (Bridgham & Johnson, 2003). Several years later an independent group cloned the full-length sequence of chOPG (Hou *et al.*, 2011). Their sequence was added to the NCBI database in 2012

(NM_001033641.1) and was used for the design of forward and reverse primers to clone chOPG cDNA.

3.3.2 Signal peptide analysis of chRANKL, chRANK and chOPG

To verify the position, presence and cleavage sites of signal peptides in chRANKL, chRANK and chOPG, their predicted amino acid sequences were analysed with SignalP4 (Figure 3.1). Mammalian RANKL is a type II transmembrane protein; therefore its COOH-terminal is exposed to the extracellular space. Type II transmembrane proteins do not contain signal peptides but possess long hydrophobic residues that have the dual function of targeting and harbouring the protein within the endoplasmic reticulum. The chRANKL predicted protein sequence was analysed for the presence of a signal peptide using SignalP4 (Figure 3.1). The signal peptide analysis was negative, strongly suggesting a type II protein structure.

RANK is a type I transmembrane protein and therefore contains a signal peptide at its NH_2-terminal region. The predicted signal peptide for chRANK is from position 1 to 19 (Figure 3.1). The first 20 bases in chRANK contain a high percentage of G/C residues making it difficult to design appropriate primer pairs. It was therefore decided to design primers omitting the signal peptide as the designated protein expression plasmid vector contained a signal peptide.

OPG is produced as a soluble protein and therefore contains a signal peptide to ensure the protein is processed for transport to the cell membrane, where upon appropriate signals it will be exported outside the cell. The predicted amino acid sequence of chOPG has a signal peptide of 19 amino acids (Figure 3.1) which was included in the primer design.

3.3.3 Identification of the extracellular domains of chRANKL and chRANK

To express chRANKL as a soluble recombinant protein, its extracellular domain was identified using the known human and mouse sequences. The extracellular portions of the TNF superfamily contain conserved canonical 'TNF homology domains' required for trimerisation and are responsible for receptor interaction (Lam *et al*., 2001). Using the SMART prediction program, the various

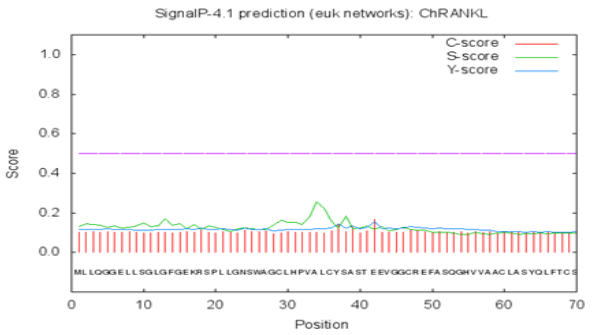

Measure	Position
Max C	42
Max Y	42
Max S	34

RANKL

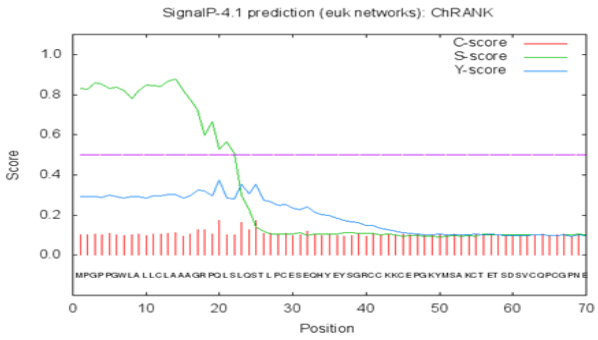

Measure	Position
Max C	24
Max Y	20
Max S	14

RANK

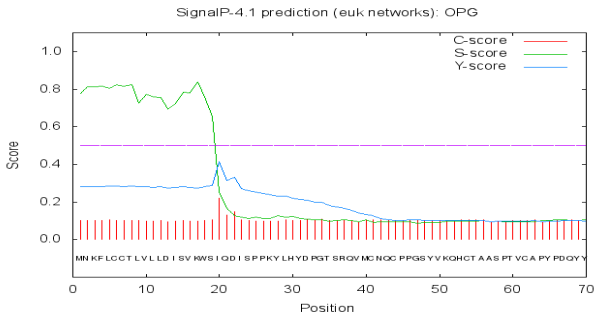

Measure	Position
Max C	20
Max Y	20
Max S	17

OPG

Figure 3.1 SignalP4 predictions for the presence of signal peptides in chRANKL, chRANK and chOPG. *The predicted chRANKL protein was analysed for signal peptide sequence, chRANK predicted signal peptide sequence and cleavage site, and chOPG predicted signal peptide sequence and cleavage site. Max C values represent the C-score, which identifies the position of the first amino acid of the mature protein. Max S values represent the S-score of the positions within the signal peptide from those in the mature protein. The Max Y values are the combinations of the slope of the Max S and the Max C-score to predict a more precise signal peptide cleavage site.*

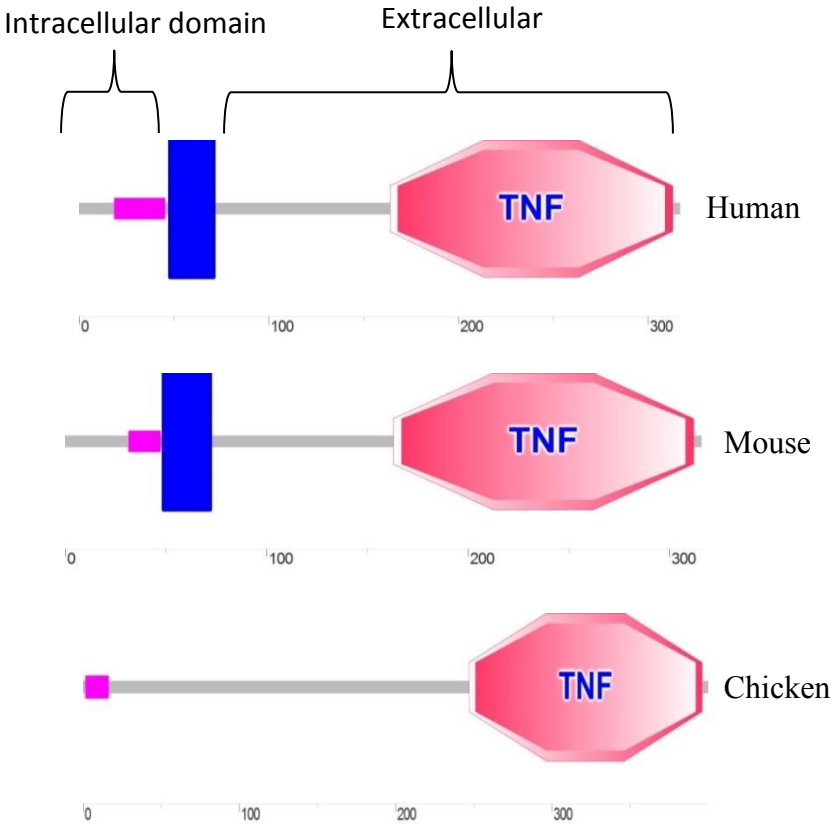

Figure 3.2 SMART predictions of the structure of human, mouse and chicken RANKL proteins. *The pink boxes show low complexity regions with unknown functions, blue boxes the transmembrane domains and pink diamonds the TNF homology domains. The locations of each domain within the protein are indicated by the amino acid scale below each protein.*

domains of proteins can be identified. In Figure 3.2, SMART prediction using the human and mouse RANKL sequences identified the location and presence of the transmembrane domain and TNF homology domain. Interestingly, when the chRANKL SMART prediction was analysed, there was no predicted transmembrane domain. The TMHMM transmembrane prediction model was also used to identify this region in chRANKL, and, like the SMART prediction, this model did not predict a transmembrane domain (data not shown).

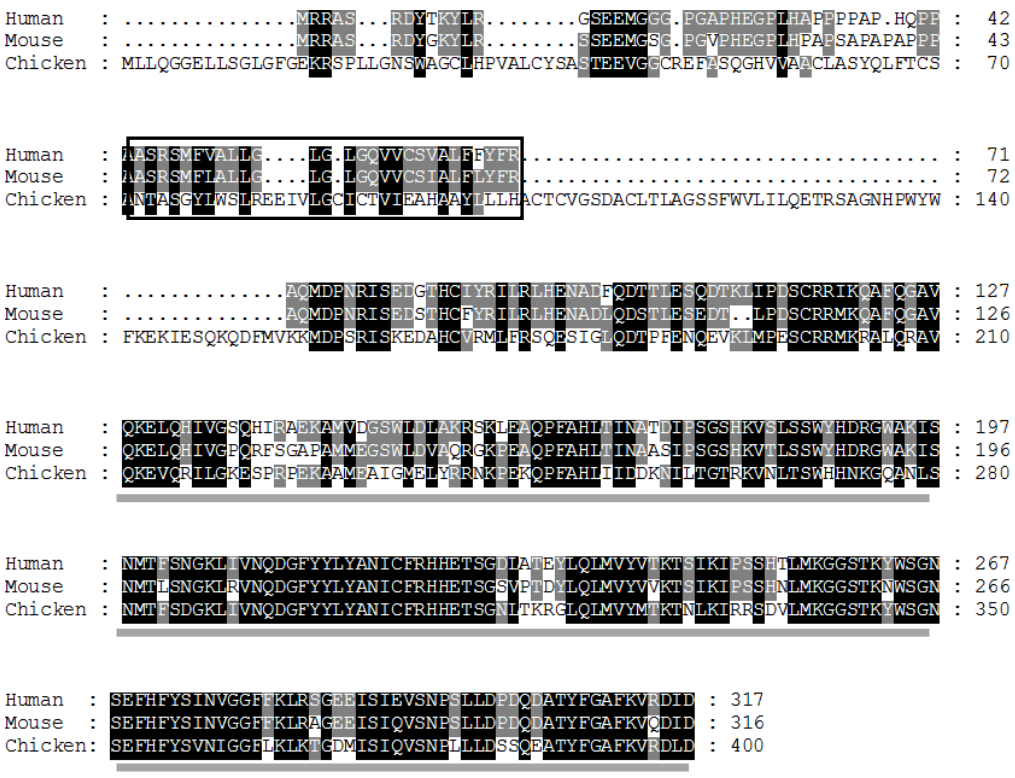

Figure 3.3 Amino acid alignment of human, mouse and predicted chicken RANKL. *Shaded areas represent conservation of amino acid – the darker the shading, the more conserved the residue across species: black shading indicates conservation between all species, dark grey with white lettering indicates conservation between 2 species. Dots indicate gaps in the alignment. The black box indicates the mammalian transmembrane domains and the grey underlined sequence represents the TNF homology domains.*

To further validate the extracellular domain of chRANKL, the amino acid sequences of human and mouse RANKL were aligned with the predicted chRANKL sequence to analyse conservation between the species within the TNF homology domain (Figure 3.3). The NH_2-terminal of chRANKL was longer in comparison to human and mouse proteins. There is low conservation of residues within this region compared to the mammalian counterparts. When the mammalian RANKL transmembrane domains were identified in the comparison, it became obvious that this region of the chRANKL gene was not predicted correctly. The domain with the

most conservation and similarity was the extracellular, TNF homology, domain. The correct chRANKL sequence was obtained by blasting the human RANKL protein against the chicken genome V4. Analysis indicated that the first two exons of the predicted chRANKL were incorrect and that the correct sequence was present in various EST. The full-length sequence of chRANKL was retrieved and further analysed using the SMART prediction model (Figure 3.4). The annotated chRANKL sequence was incorrect as the new sequence contained a predicted transmembrane domain (Figure 3.4). It is clear that this is the correct chRANKL sequence and was added to the Ensembl database (Accession Number: LM999949). The full-length cDNA sequence was cloned and, to produce soluble recombinant proteins, the extracellular domain of chRANKL was cloned and expressed as a FLAG-tagged protein to examine its bioactivity in chickens (Chapter 4). The extracellular domain of RANKL is bioactive in human, mouse (Anderson *et al*., 1997; Wong *et al.,* 1997; Simonet *et al*., 1997; Park *et al*., 2005) and pig (Böcker *et al*., 2012).

The TNFR superfamily members are characteristically type I transmembrane proteins, with their NH_2-terminal domains exposed to the extracellular space. Using the SMART prediction program, the various domains of the human and mouse RANK proteins were identified and used to locate these domains in the predicted chRANK gene (Figure 3.5). SMART prediction was also carried out on the predicted chRANK sequence to analyse whether these domains were conserved. It is clear that the chRANK contains a signal peptide, transmembrane and TNFR domains, also known as CRD (Figure 3.5).

3.3.4 Amplification and molecular cloning of chRANKL, chRANK and chOPG

Primers were designed against the full-length and extracellular domains of both chRANKL and chRANK and full-length chOPG, using the sequences deposited in the NCBI database. To clone the full-length and extracellular domains of chRANKL and chRANK, cDNA was amplified by RT-PCR using RNA from ConA-stimulated splenocytes as template. The resulting products were a ~954 bp cDNA fragment corresponding to 318 amino acids for full-length chRANKL and a 735 bp cDNA fragment, corresponding to 244 amino acids ($chRANKL^{75\text{-}318}$) for the extracellular domain of chRANKL (Figure 3.6A).

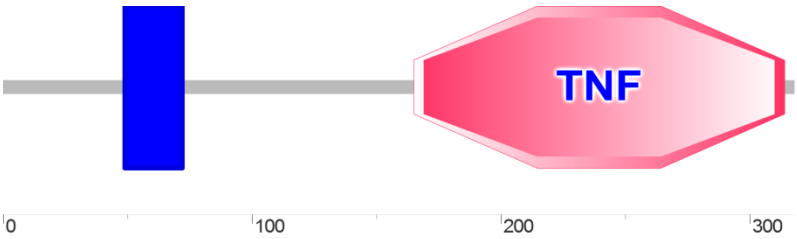

Figure 3.4 SMART prediction of the structure of the corrected predicted chicken RANKL protein. *The blue box indicates the transmembrane domain and the pink diamond the TNF homology domain.*

For the extracellular domain of chRANK, a 498 bp cDNA fragment, which corresponded to 166 amino acids (chRANK$^{24\text{-}195}$) (Figure 3.6B), was cloned. Primers were also designed to amplify the cDNA of the full-length sequence of chRANK, without the signal peptide. Various primer combinations were used to try and clone the full-length sequence, without success. However, primers designed to clone the intracellular and transmembrane domains generated a ~1.5 kb product, corresponding to 465 amino acids (chRANKL$^{190\text{-}655}$), using cDNA from ConA-stimulated splenocytes as template. There was an 18 base-pair cDNA overlap between the cloned extracellular and transmembrane domains, allowing the full-length cDNA sequence of chRANK to be verified. Full-length chOPG cDNA was generated from RNA derived from bone marrow cells. The expected band of 1.2 kb was identified after agarose gel electrophoresis (Figure 3.6C). All three cDNAs were ligated into the pGEM-T Easy vector and sequences were verified for three individual clones.

For protein expression, all genes were sub-cloned into their appropriate expression vectors. To sub-clone the genes directionally, primers were designed to integrate restriction enzyme sites at the 5' and 3' ends of the cDNAs. For chRANKL, primers were designed to place *Xho*I and *Not*I sites at either end of the cDNA. For chRANK and chOPG, *Nhe*I and *Bgl*II sites were included (primer sequences are given in Appendix 2, Table 2). PCR reactions contained a 1:100 dilution of the respective cDNA in pGEM-T Easy as template DNA. Each restriction product was

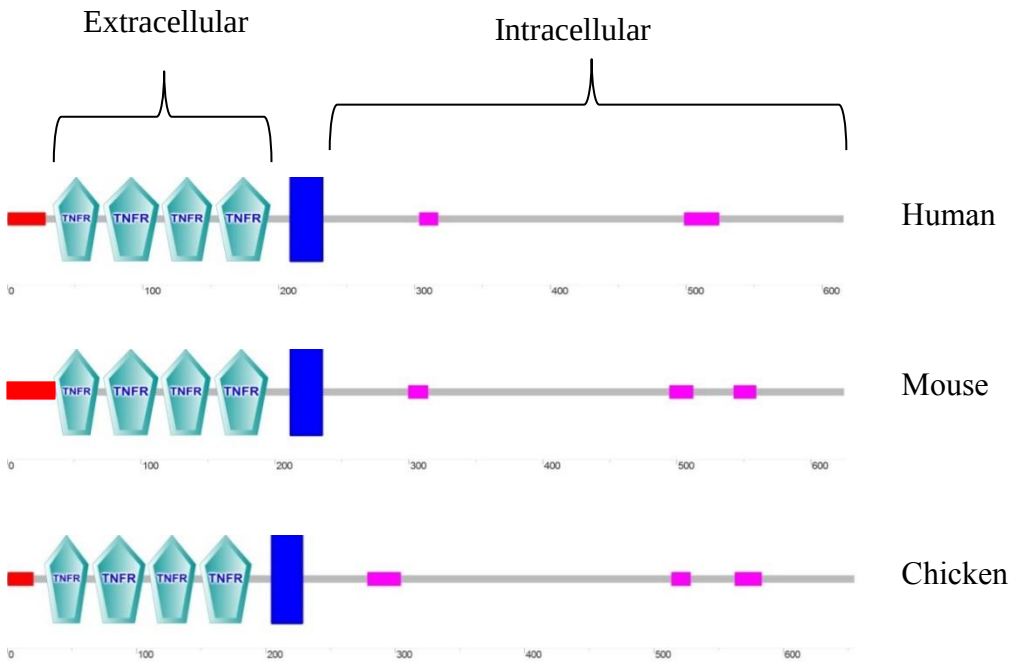

Figure 3.5 SMART predictions of the structure of human, mouse and predicted chicken RANK proteins. *The red boxes indicate the predicted signal peptide sequences, the triangles the TNFR domains (CRD), the blue boxes the transmembrane domains and the pink boxes regions of highly conserved, unknown structure.*

gel purified and restriction digestion was carried out with appropriate restriction enzymes before ligation into linearized expression plasmids. All sub-cloning was verified by sequencing.

3.3.5 *In silico* analysis of chRANKL

The full-length corrected cDNA of chRANKL was cloned and its predicted amino acid sequence was aligned with human and mouse RANKL (Figure 3.7). The correct chRANKL sequence shares 61-64% amino acid identity with mammalian RANKL, is similar in size and possesses a transmembrane domain (Figure 3.7). The core TNF homology domain (residues 160-388) is required for receptor interaction and trimerisation. Mammalian RANKL are composed of β-strands and loops connected in a "jelly-roll" fold, characteristic of the TNF family members (Lam *et*

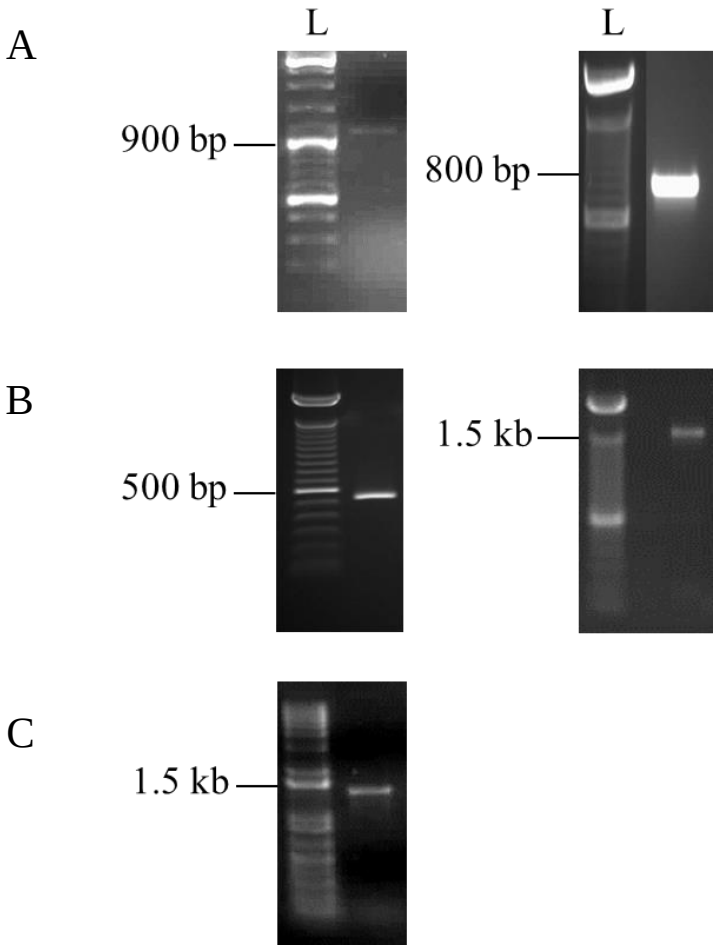

Figure 3.6 Gel electrophoresis of chRANKL, chRANK and chOPG. A) *RT-PCR generated a ~954 bp product corresponding to the full-length cDNA of chRANKL and an 800 bp product corresponding to the extracellular domain of chRANKL from ConA-stimulated splenocytes;* **B)** *RT-PCR generated a ~500 bp product corresponding to the extracellular domain of chRANK and a 1.5 kb product for the transmembrane and intracellular domains, both from ConA-stimulated splenocytes;* **C)** *RT-PCR generated a 1.2 kb product for the full-length sequence of chOPG from bone marrow cDNA. L = 1 kb DNA ladder (Invitrogen).*

al., 2001). To investigate the conservation of these β-strands in chRANKL, each β-strand was identified in the human and mouse proteins (Lam *et al.*, 2001; Cheng *et al*., 2009) and PSIPRED was used to predict the secondary structure of chRANKL. ChRANKL has conserved residues at the positions of the β-strands and loops found

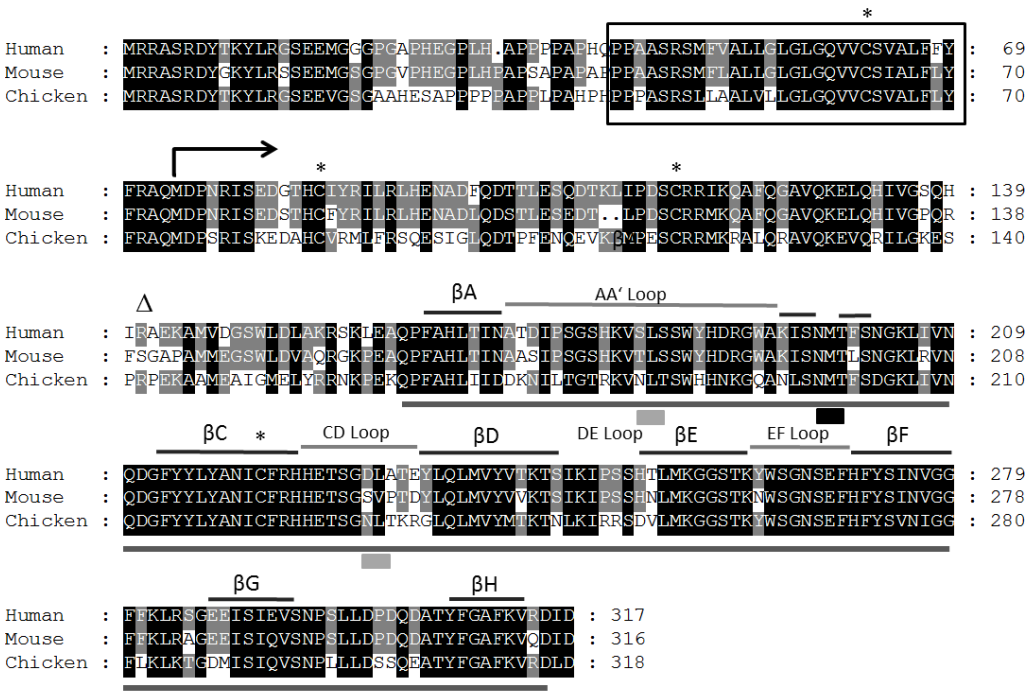

Figure 3.7 Amino acid alignment of the human, mouse and chicken RANKL. *Shaded areas represent conservation of amino acid – the darker the shading, the more conserved the residue across species: black shading indicates conservation between all species, dark grey with white lettering indicates conservation between 2 species. Dots indicate gaps in the alignment. The box indicates the transmembrane domains, the arrow the start of the extracellular domains, the dark grey underline the TNF homology domains, asterisks the conserved cysteine residues, the light grey boxes the chicken RANKL predicted N-linked glycosylation sites and the black box the N-linked glycosylation site conserved across all species. The open triangle indicates the murine TACE cleavage site, and the black lines above the sequence the location of the 10 highly conserved β-strands involved in the "β-jelly" roll structure. The surface loops are shown as grey lines between the β-strands, labelled AA', CD, DE and EF.*

in its mammalian counterparts, suggesting it folds in the "jelly-roll" conformation. Mouse RANKL is cleaved from the membrane surface by TACE converting enzyme at position 140 (Lum *et al.*, 1999). The cleavage site is not conserved in chRANKL.

3.3.6 *In silico* analysis of chRANK

ChRANK was cloned in two parts; the extracellular domain and the transmembrane domain with the intracellular domain. The whole sequence was combined and aligned with the known human and mouse RANK proteins using CLUSTALX2 software (Figure 3.8). ChRANK shows relatively high amino acid identity with the mammalian orthologues, with 40-42% sequence identity with human and mouse. ChRANK is larger than both the mammalian proteins by 39-48 amino acids. The predicted signal peptide is slightly larger in the chicken and there is an 11 amino acid insert in the intracellular domain between residues 450-461. Members of the TNFR superfamily are grouped due to the presence of conserved CRD in their extracellular ligand-binding domain (Naismith & Sprang, 1998). These CRDs are typically defined by three intra-chain disulphide bridges generated by highly conserved cysteine residues that act as a scaffold to produce an elongated structure protruding from the cell (Smith *et al.*, 1994). They are believed to be involved with specific ligand binding and generation of a pre-assembly site for the docking of the ligand (Chan *et al*., 2000). All four CRD are present in chRANK (labelled I-IV) and the cysteine residues are conserved between all species (Figure 3.8).

The extracellular domains of RANK are highly conserved across all species which could indicate conserved bioactivity. RANK has one of the largest intracellular domains of all TNFR family members yet identified. The TNFR family do not possess catalytic domains and require adaptor proteins for downstream signalling called TNF receptor-associated factors (TRAFs). This family of adaptor proteins are made up of seven members (TRAF1-7). Previous biochemical and structural analysis have identified two amino acid sequence motifs for TRAF1, TRAF2, TRAF3, and TRAF5 binding: a major one, (P/S/A/T)X(Q/E)E and the minor one, PXQXXD (X being any amino acid) (Ishida *et al*., 1996). TRAF6 has a specific binding motif, PXXGXX. Numerous studies have identified the specific TRAF-binding domains required for RANK activity (Wong *et al*., 1998; Galibert *et*

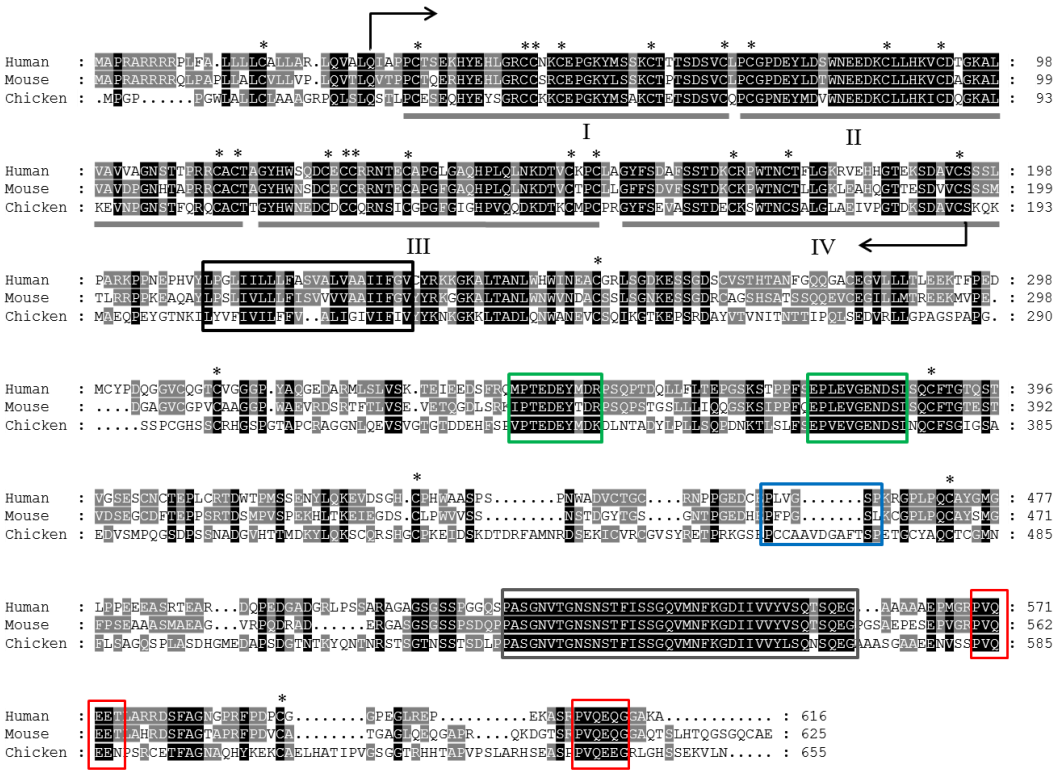
Human : MAPRARRRRPLFA.LLLLCALLAR.LQVALQLAPPCTSEKHYEHLGRCCNKCEPGKYMSKCTTTSDSVCLPCGPDEYLDSWNEEDKCLLHKVCDTGKAL : 98
Mouse : MAPRARRRRQLPA.PLLALCVLLVP.LQVTLQVTPPCTQERHYEHLGRCCSRCEPGKYLSSKCTPTSDSVCLPCGPDEYLDTWNEEDKCLLHKVCDAGKAL : 99
Chicken : .MPGP.....PGWLALLCLAAAGRPQLSLQSLLPCESEQHYEYSGRCCKKCEPGKYMSAKCTETSDSVCQPCGPNEYMDVWNEEDKCLLHKICDQGKAL : 93
I
II
Human : VAVVAGNSTTPRRCACTAGYHWSQDCECCRRNTECAPGLGAQHPLQLNKDTVCKPCLAGYFSDAFSSTDKCRPWTNCTFLGKRVEHHGTEKSDAVCSSSL : 198
Mouse : VAVDPGNHTAPRRCACTAGYHWNSDCECCRRNTECAPGFGAQHPLQLNKDTVCTPCLLGFFSDVFSSTDKCKPWTNCTLLGKRLEAQGTTESDVVCSSSM : 199
Chicken : KEVNPGNSTFQRQCACTTGYHWNEDCDCCQRNSICGPGFGIGHPVQQDKDTKQMPCPRGYFSEVASSTDECKSWTNCSALGLAQIVPGTDKSDAVCSKQK : 193
III
IV
Human : PARKPENEPHVNLPGRILILLFASVALVAAIIFGVGYRKLKGKALTANLKHWTNEACGRLSGDKESSGDSCVSTHTANFGQQGAGEGVLLLTLEEKTPEED : 298
Mouse : TLRRPPKEAQAYLPSHIVLLFISVVVAAIIFGVGYRKLGGKALTANLNWWNDACSSLSGNKESSGDRQAGSHSATSSQQEVCEGILLMTREEKMVPE. : 298
Chicken : MAEQPEYGTNKILPYVFIVILPFV..ALIGIVIFIVGYKNKGKKLTADLQNWANEVCSQIKGTKEPSRDAYVTVNITNTTIPQLSEDVRLLGPAGSPAEG. : 290
Human : MCYPLQGVCQGLCVGGGE.VACGEDARMLSLVSK.TEIEEDSFRQMPTEDEYMDRPSQPTDQLLFLTEPGSKSTPPFSEPLEVGENDSISQCFTGTQST : 396
Mouse : ....DGAGVCGPVCAAGGE.VAEVRDSRTFTLVSE.VETQGDLSRLIPTEDEYTDRPSQPSTGSLLLIQQGSKSTPPFCEPLEVGENDSISQCFTGTEST : 392
Chicken : .....SSPCGHSSCRHGSEGTAPCRAGGNLQEVSVGTGIDDEHESEVPTEDEYMDKDLNTADYLPLLSQLDNKTISLESEPVEVGENDSINQCFSGIGSA : 385
Human : VGSESCNCTEPLCRLLWTPMSSENYLQKEVDSGH.CCHHAASPS.....PNWADVCTGC....RNPPGEECLPLVG.....SFKRGPLPQCAYGMG : 477
Mouse : VDSEGCDFTEPPSRTLSMPVSPEEHLTKEIEGDS.CLPAVVSS.....NSTDGYLGS....GNTPGEDHLPFPG.....SLKGGPLPQCAYSMG : 471
Chicken : ELVSMPQGSPESSNAEGVHTEMDKYLQKSCQRSHGCEKEIDSKDTDRFAMNRDSEKICVRGGVSYRETERKGSHECCAAVDGAFTSEGTGCYAQCTCGMN : 485
Human : LEPEEEASRTEAR...DQPEDCADGRLPSSARAGAGSGSSEGGQSPASGNVTGNSNSTFISSGQVMNFKGDIIVVYVSQTSQEG...AAAAAEPMGRPVQ : 571
Mouse : FPSEAASMAEAG...VRPQRADGGG

al., 1999). Using the published data available for TRAF-binding motifs found in human and mouse RANK (Galibert *et al.*, 1998; Darnay *et al*., 1999; Wong *et al.*, 1998), four out of five TRAF-binding motifs were identified in chRANK (Figure 3.7). Surprisingly the "missing" TRAF-binding domain is a TRAF6-specific binding motif (residues 452-463). RANK also requires a region of its intracellular domain to signal in osteoclastogenesis. This domain is called the highly conserved region (HCR) and within this region there is an IVVY motif required for osteoclastogenesis (Xu *et al*., 2006). Both the HCR and IVVY motifs are conserved in chRANK suggesting conserved bioactivity for osteoclastogenesis in the chicken.

3.3.7 *In silico* analysis of ChOPG

The full-length cDNA sequence of chOPG was cloned and the predicted amino acid sequence was aligned with human and mouse OPG (Figure 3.9). ChOPG has 64-69% amino acid identity with mammalian OPG. ChOPG possesses four CRD domains (labelled I-IV) with 17 out of 18 cysteine residues in them conserved (Figure 3.9). Using NetNGly software to predict N-linked glycosylation sites in all species, chOPG has two potential sites whereas there are five in human and four in the mouse. OPG contains two DD with no known function and these domains are conserved between all species. ChOPG contains a cysteine residue at position 401 which is conserved in human and mouse. This cysteine is vital for dimer formation in mammalian OPG.

3.3.8 Protein expression and analysis of FLAG-chRANKL

To produce soluble fusion proteins of chRANKL, the extracellular domain was sub-cloned into expression vectors as described in section 2.2.3 and transfected into COS-7 cells using the well-described DEAE-dextran approach (Rothwell *et al.*, 2004). The cell supernatants were collected after 72 h of incubation in serum-free DMEM. To analyse the composition of chRANKL, protein produced in COS-7 cells was subjected to SDS-PAGE under both reducing and non-reducing conditions and analysed by western blot using antibodies against the FLAG-tag (Figure 3.10). In reducing conditions, prominent bands are evident at ~37 kDa and ~75 kDa; the predicted molecular masses of the FLAG-tagged chRANKL monomer and dimer

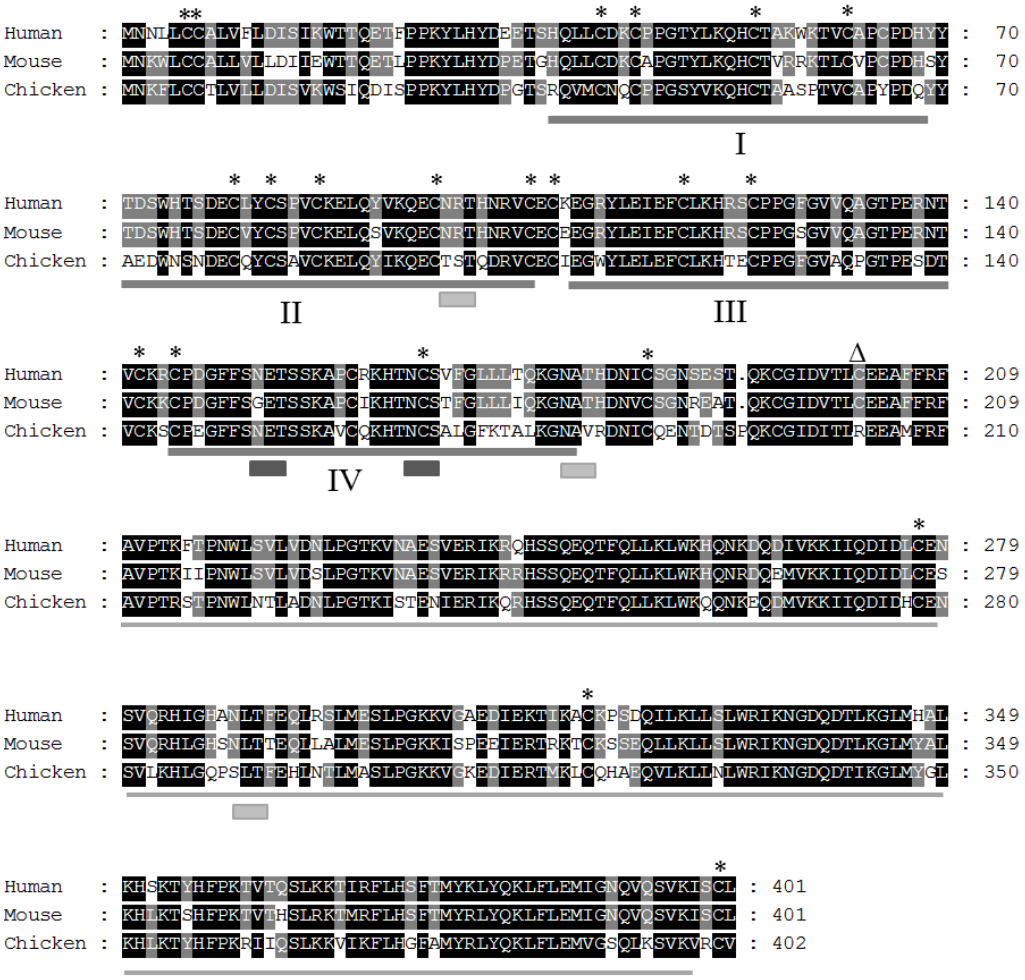

Figure 3.9 Amino acid alignment of human, mouse and the predicted chicken OPG. *Shaded areas represent conservation of amino acid – the darker the shading, the more conserved the residue across species: black shading indicates conservation between all species, dark grey with white lettering indicates conservation between 2 species. Dots indicate gaps in the alignment. The CRD domains are numbered I-IV (grey underline), asterisks indicate the conserved cysteine residues, the open triangle the conserved cysteine residue in mammals absent in the chicken, the light grey underline DD regions, the light grey boxes chOPG predicted N-linked glycosylation sites and the dark boxes mammalian N-linked glycosylation sites.*

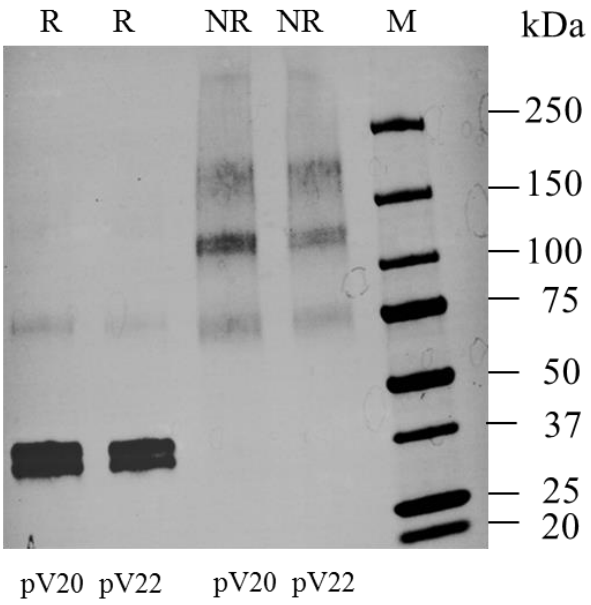

Figure 3.10 Western blot analysis of pV20- and pV22-schRANKL. *COS-7 cells were transfected with pV20- or pV22-chRANK using the DEAE-dextran approach and cell supernatants were collected 72 h later. The expression of the FLAG-chRANK was analysed under both reducing (R) and non-reducing (NR) conditions and the FLAG-tag was detected using mouse anti-Flag (M2) antibody. M = Precision plus protein standard (BioRad).*

respectively. Protein analysis under non-reducing conditions, in which higher order structures of proteins are not disturbed, showed three predominant bands; dimers at ~75 kDa, trimers at ~120 kDa and tetramers/hexamers at ~185 kDa (Figure 3.10).

3.3.9 Protein expression and analysis of recombinant chRANK-Fc

Plasmids expressing the extracellular domain of chRANK were transfected into COS-7 cells using the DEAE-dextran-based approach. The resulting cell supernatants were analysed by western blot to investigate the expression of chRANK protein, using antibodies against the IgFc tag. The extracellular domain of chRANK consists of 4 CRD which each consist of five irregular β-strands that are linked by three inter-strand disulphide bonds (Naismith & Sprang, 1998). Although bioactivity of the TNFR superfamily requires trimerisation to form heterohexamers with their

ligands, RANK dimers can partially induce osteoclast activation (Iwamoto *et al.,* 2004). ChRANK protein was analysed under both reducing and non-reducing conditions (Figure 3.11). In non-reducing conditions, using AEC staining to analyse structures with weak staining, three bands were present for chRANK (Figure 3.11). As an IgFc-tagged monomer, the predicted molecular mass of chRANK is ~43 kDa. The extracellular domain of chRANK has two potential N-glycosylation sites. Glycosylation at target asparagines contributes to the molecular mass of the protein. In non-reducing conditions, bands corresponding to ~100, ~160 and ~200 kDa were present. These bands could represent dimeric, trimeric and tetrameric structures. In reducing conditions, no intense band was evident which may be due to weak staining of the monomeric proteins.

3.3.10 Protein expression and analysis of recombinant chOPG-Fc

The full-length sequence of chOPG was sub-cloned into pKW06-Ig and transfected into COS-7 cells to produce an IgFc fusion protein. To detect the expression of recombinant proteins, the COS-7 cell supernatants were treated with reducing or non-reducing buffer and analysed by western blot using antibodies against the Fc tag (Figure 3.12). The chOPG-Fc monomer has a predicted molecular mass of ~72 kDa. In reducing conditions, a ~75 kDa band was evident whereas in non-reducing conditions there was a strong band at ~150 kDa, suggesting the formation of homodimers.

3.3.11 Assessment of BMDC and BMDM functions

The main aim of the study was to characterise the role of chRANKL, chRANK and chOPG in the biology of chicken APC. DC play key roles in host defence by recognizing, engulfing and presenting microbial peptides to effector T cells.

BMDM were stimulated and pro-inflammatory cytokine mRNA expression levels and cell surface markers were analysed. Chicken BMDC were the first non-mammalian DC to be differentiated using recombinant chIL-4 and chCSF-2 and characterised (Wu *et al.,* 2010). Since then, studies using these cells have measured the production of a number of chicken cytokines and chemokines (Wu *et al*., 2010;

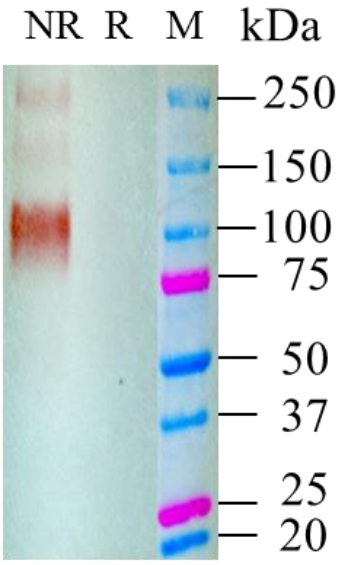

Figure 3.11 Western blot analysis of chRANK-Fc. *COS-7 cells were transfected with pKW06-chRANK using the DEAE-dextran approach and cell supernatants were collected 72 h later. The expression of chRANK-Fc was analysed under both reducing (R) and non-reducing (NR) conditions and detected using a goat-anti mouse Ig Fc-HRP antibody. M = Precision plus protein standard (BioRad).*

Rothwell *et al.*, 2012). They have also paved the way to understanding how chicken BMDC react upon pathogen exposure (De Geus *et al.*, 2013; Quéré *et al.*, 2013; Liang *et al.*, 2013; Vervelde *et al.*, 2013). However, in comparison to mammals, there are limited cell surface markers available to differentiate between BMDC and BMDM in the chicken.

In Wu *et al*. (2010), the optimal concentration of LPS required to induce maturation of BMDC after 24 h culture was 200 ng/ml. In initial experiments in this study, this amount of LPS was too strong a stimulant and masked any potential effect of chRANKL on pro-inflammatory cytokine mRNA expression levels but also induced cell death within 9-10 h of treatment. Therefore, LPS was titrated to identify the optimal concentration to induce sub-optimal activation of BMDC, i.e. activation but not a strong pro-inflammatory cytokine response. Various amounts of LPS were added to BMDC for 3 and 6 h. RNA was extracted and IL-12α expression was

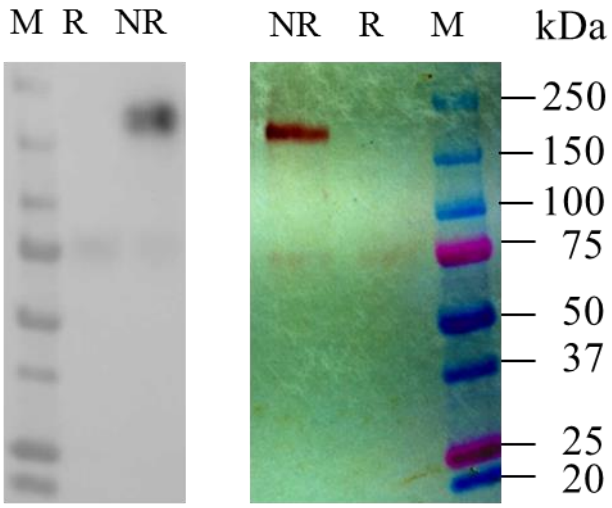

Figure 3.12 Western blot analysis of chOPG-Fc. *COS-7 cells were transfected with pKW06-chOPG using the DEAE-dextran approach and cell supernatants were collected 72 h later. The expression of chOPG-Fc was analysed under both reducing (R) and non-reducing (NR) conditions and detected using a goat-anti mouse IgFc-HRP antibody. Western blots were visualised using an ECL detection system (left) and AEC staining (right). M = Precision plus protein standard (BioRad).*

analysed by qRT-PCR (Figure 3.13). IL-12α mRNA expression was not detected in non-stimulated BMDC and therefore its expression is a good indicator of BMDC activation. A concentration of LPS of 2 ng/ml led to an increase in IL-12α mRNA expression levels at both time-points, whereas at 1 ng/ml, IL-12α expression was not detectable (Figure 3.13).

To determine if this concentration of LPS could alter the expression of cell surface markers on BMDC, cells were stimulated with LPS (2 ng/ml) for 24 h. Cells were removed from the culture plates and stained with mouse anti-chicken mAb against cell surface markers associated with cell activation: MHC class II, CD40 and the mononuclear phagocyte marker, KUL01 (Mast *et al.*, 1998), and analysed by FACs (Figure 3.14). As the chRANKL fusion protein was not purified but exCOS-7 cell supernatant, cells were also treated with supernatant from COS-7 cells transfected with an empty pCI-neo plasmid (mock) to ensure COS-7 supernatant

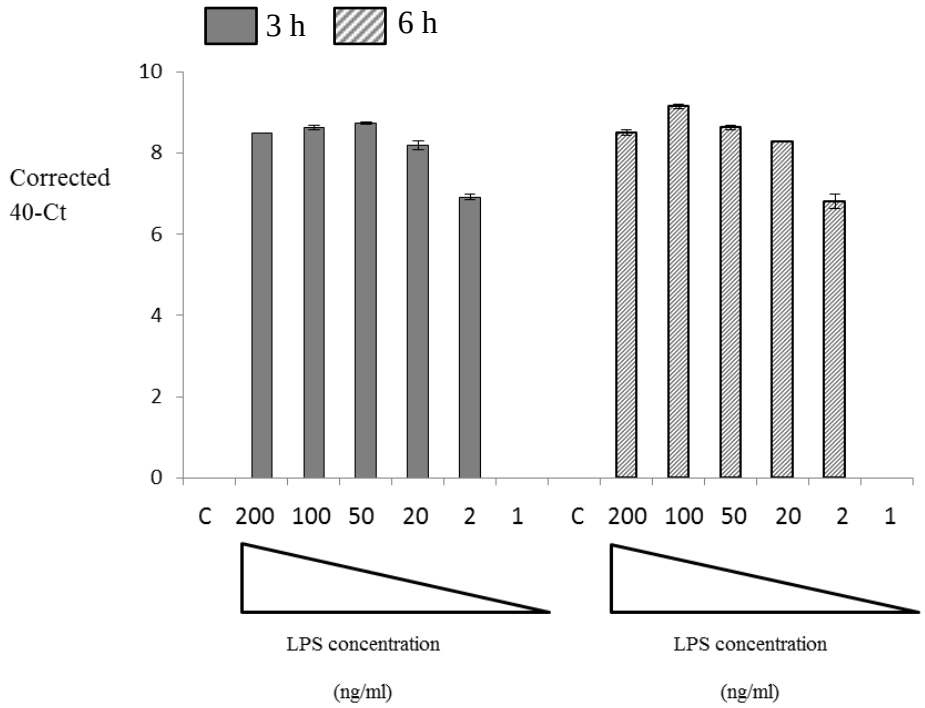

Figure 3.13 IL-12α mRNA expression levels in BMDC as measured by qRT-PCR. *BMDC were unstimulated (C) or stimulated with LPS at 200, 100, 50, 20, 2 and 1 ng/ml for 3 and 6 h. Data are presented as corrected 40-Ct ± SEM of triplicate wells.*

itself did not activate the cells. The upregulation of CD40 on the surface of BMDC is an indication of cell activation. In unstimulated and mock-treated cells, the surface expression of CD40 was negative. When the cells were treated with LPS for 24 h, the cell surface expression levels of CD40 increased in comparison to controls. KUL01 expression decreases as BMDC mature (Wu *et al*., 2010; De Geus *et al*., 2013). Unstimulated and mock-treated cells expressed KUL01. However, in LPS-stimulated cells there was a mixed population, with a portion of cells expressing KUL01 on their surface and a portion which were not (Figure 3.14). This could suggest that 2 ng/ml of LPS induces partial cell activation. For MHC class II expression, there was very little change in expression between control and LPS-stimulated cells. This could mean that the cells do not upregulate the expression of MHC class II after stimulation. However, chicken BMDC constitutively express MHC class II on their cell surface (Wu *et al.*, 2009). The ability of LPS to activate BMDM was

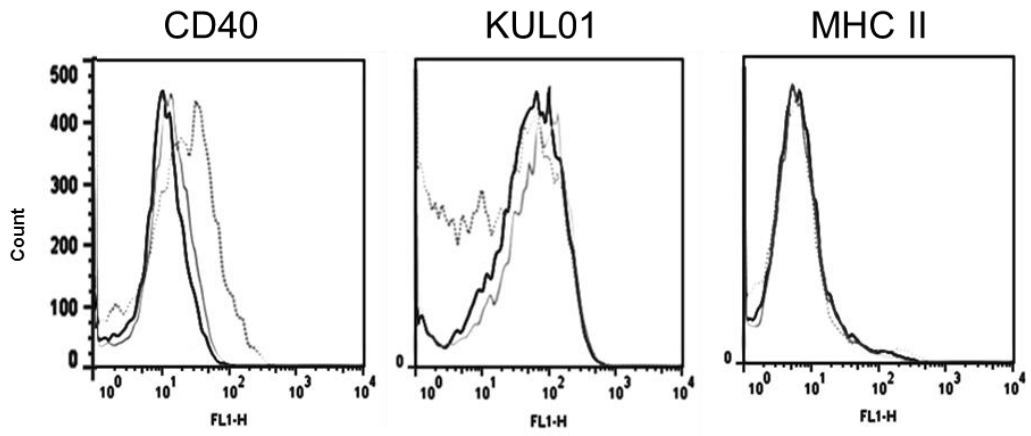

Figure 3.14 FACS analysis of cell surface markers on BMDC stimulated with LPS (2 ng/ml). *BMDC were unstimulated (black lines), treated with mock supernatant (pCI-neo empty vector exCOS-7) (grey lines) and LPS (2 ng/ml) (dotted grey lines) for 24 h. Cell surface expression of CD40, KUL01 and MHC class II was analysed by FACs. Analyses are shown as histograms with cell count versus FL1-staining and data represents one of three experiments with similar results.*

investigated next. Previous data available for BMDM were minimal. ChCSF-1 drives the differentiation of bone marrow cells to BMDM (Garceau *et al*., 2010). However, this study differentiated the cells at 37°C for 10 days rather than at the physiological temperature of chicken cells of 41°C. The initial studies for BMDM were to identify the sub-optimal concentration of LPS that could induce pro-inflammatory cytokine mRNA expression. The optimal concentration of LPS and IFN-γ needed to upregulate cell surface markers on BMDM grown at the appropriate temperature, 41°C, was also determined.

To identify the concentration of LPS to induce sub-optimal activation of BMDM, cells were grown with recombinant chCSF-1 (exCOS-7) for 6 days and then stimulated with various amounts of LPS for 3 and 6 h. RNA was purified and qRT-PCR was carried out to detect IL-12α mRNA expression levels. IL-12α was not detectable in any samples tested (data not shown), therefore IL-6 mRNA expression levels were analysed (Figure 3.15). At 3 h, there was very little difference in the expression of IL-6 in LPS-stimulated cells compared to control unstimulated cells

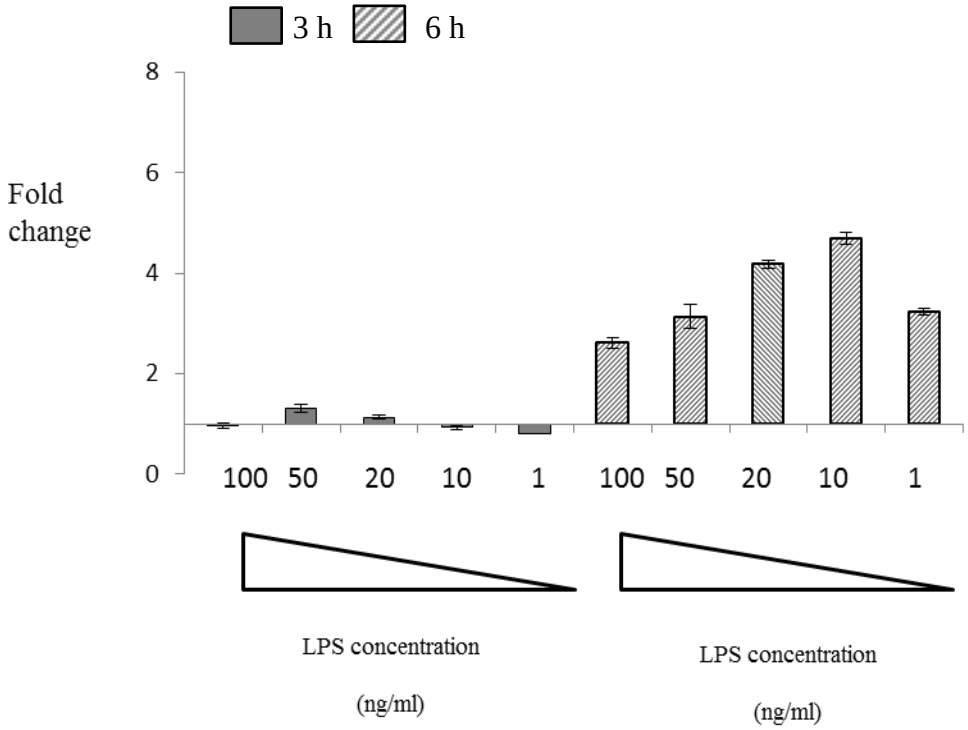

Figure 3.15 IL-6 mRNA expression levels in stimulated BMDM as measured by qRT-PCR. *BMDM were unstimulated or stimulated with LPS at 100, 50, 20, 10 and 1 ng/ml for 3 and 6 h. RNA was purified and IL-6 mRNA expression levels were detected by qRT-PCR. Data are shown as fold change between levels in unstimulated cells ± SEM of three replicate wells.*

However, a further 3 h stimulation led to an increase in IL-6 mRNA expression levels by ~4-5-fold. Interestingly, 10 ng/ml of LPS induced maximal expression of IL-6. From these initial studies, 1 ng/ml of LPS was chosen to induce sub-optimal maturation of BMDM. The expression of cell surface markers were also assessed in BMDC stimulated with 1 ng/ml LPS to investigate the ability of sub-optimal activation of cells to increase surface protein expression in BMDM. Cells were stimulated with LPS for 24 h and cell surface expression of MHC class II, KUL01 and CD40 were analysed by FACs (Figure 3.16). LPS-stimulated BMDM for 24 h, increased surface expression of CD40 compared to unstimulated cells and mock-treated cells. The expression of KUL01 was slightly decreased in LPS-stimulated cells. MHC class II expression levels were not altered by the addition of

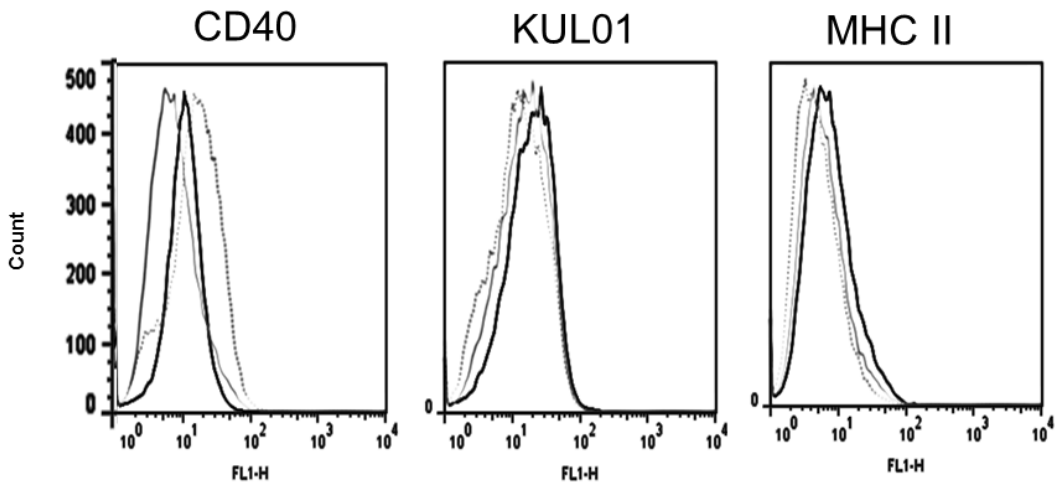

Figure 3.16 FACS analysis of cell surface markers of BMDM stimulated with LPS (1 ng/ml) for 24 h. *BMDM were unstimulated (black lines), treated with mock supernatant (1:5 pCI-neo exCOS-7) (grey lines) or LPS (1 ng/ml) (dotted grey lines) for 24 h. Cell surface expression of CD40, KUL01 and MHC class II were analysed by FACs. Analyses are shown as histograms with cell count versus FL1-staining and represent data from one of three independent experiments with similar results.*

LPS at 1 ng/ml for 24 h. This could be due to the sub-optimal concentration of LPS used to induce BMDM maturation.

3.3.12 Pilot Study: Bioactivity of pV20- and pV22-schRANKL

As described in section 3.3.9, two plasmids were designed to express soluble chRANKL. Western blot analyses indicated that both pV20- and pV22- schRANKL can form trimers, required for the interaction of RANKL with RANK in mammals. To verify the bioactivity of each protein, BMDC were stimulated with LPS (2 ng/ml) or CD40L (3 μg/ml) alone or in combination with a 1:50 dilution of exCOS-7 supernatant of pV20- or pV22-schRANKL protein for 3, 6, 24 or 48 h. Pro-inflammatory cytokine mRNA expression levels were analysed by qRT-PCR (Figures 3.17 and 3.18). This pilot study was carried out as a single experiment to determine which protein was more bioactive for the following experiments in Chapter 4, and therefore no statistical analysis was carried out.

As stated previously, IL-12α mRNA was not detected in immature BMDC and therefore the data are presented as corrected 40-Ct. At 3 h, LPS and LPS/V20 schRANKL-stimulated cells had similar levels of IL-12α mRNA expression (Figure 3.17). However, LPS/pV22-schRANKL-stimulated cells expressed higher levels of IL-12α mRNA in comparison to LPS or LPS/pV20-schRANKL stimulated cells (Figure 3.17). At 6 h, IL-12α mRNA expression was not detected in either LPS or LPS/pV20-schRANKL-stimulated cells. Cells stimulated with LPS/pV22-schRANKL had increased mRNA expression levels of IL-12α. This could suggest that pV22-schRANKL is more bioactive than pV20-schRANKL. At 24 and 48 h, IL-12α mRNA expression was not detectable in any sample (data not shown).

ChCD40L-stimulated BMDC had increased mRNA expression levels of pro-inflammatory cytokines (Wu *et al*., 2010). To analyse the bioactivity of schRANKL with this stimulant, cells were stimulated with CD40L alone or with either pV20- or pV22-schRANKL and were analysed for IL-12α mRNA expression levels at 3 and 6 h (Figure 3.17). At 3 h, the levels of IL-12α mRNA expression were similar between the CD40L/pV20- and CD40L/pV22-schRANKL-stimulated cells. CD40L-stimulated cells did not induce IL-12α mRNA expression levels at 3 h but did, however, at 6 h. At 6 h, IL-12α mRNA expression was not detectable in CD40L/pV20-schRANKL-stimulated cells. However, CD40L/pV22-schRANKL-stimulated cells have increased levels of IL-12α mRNA expression but not to the level of CD40L-stimulated cells. These data suggest that pV22-schRANKL is more bioactive than pV20-schRANKL.

The mRNA expression levels of IL-1β and IL-6 were analysed in the above samples to investigate the effect of schRANKL on other pro-inflammatory cytokines (Figure 3.18). As both IL-1β and IL-6 mRNA were detectable in unstimulated cells, data are presented as fold change between the levels in control and stimulated cells. For IL-1β mRNA expression levels, LPS-stimulated cells increased expression by ~5-fold at 3 h which was increased to ~6 fold in LPS/pV22-schRANKL-stimulated cells. At 3 h, LPS/pV20-schRANKL-stimulated cells only increased IL-1β mRNA

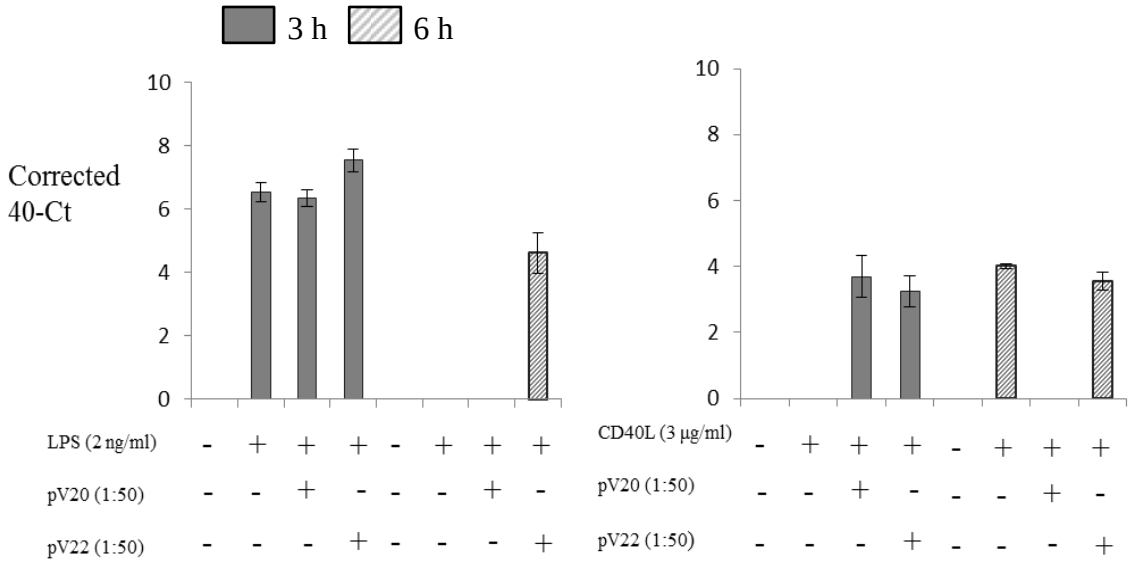

Figure 3.17 IL-12α mRNA expression levels in BMDC, as measured by qRT-PCR. *BMDC were unstimulated or stimulated with LPS (2 ng/ml) or LPS with either pV20- or pV22-schRANKL (1:50 ex-COS) for 3 and 6 h. RNA was purified and IL-12α mRNA expression levels were detected by qRT-PCR. Data are shown as corrected 40-Ct ± SEM of three replicate wells.*

expression levels by ~3-fold. At 6 h, the mRNA expression levels of IL-1β were decreased across all the stimulated cells. At 24 and 48 h, IL-1β mRNA expression levels were quiet low with no difference between LPS, LPS/pV20- or LPS/pV22-schRANKL-stimulated cells (Figure 3.18). For CD40L-stimulated cells, CD40L/pV22-schRANKL treatment enhanced IL-1β mRNA expression levels at 3, 6 and 24 h compared to CD40L- and CD40L/pV20-stimulated cells (Figure 3.18).

For IL-6 mRNA expression levels, LPS-stimulated cells increased expression by ~100-fold after 3 h. Neither LPS/pV20-schRANKL nor LPS/pV22-schRANKL-stimulated cells enhanced IL-6 expression levels above levels in LPS-stimulated cells (Figure 3.18). At 6 h, LPS/pV20-schRANKL-stimulated cells had a ~50 fold increase in IL-6 mRNA expression levels whereas LPS- and LPS/pV22-schRANKL-stimualated cells had low mRNA expression levels. At 24 and 48 h, IL-6 mRNA expression levels were similar between all stimulated cells. Similar to the IL-1β data,

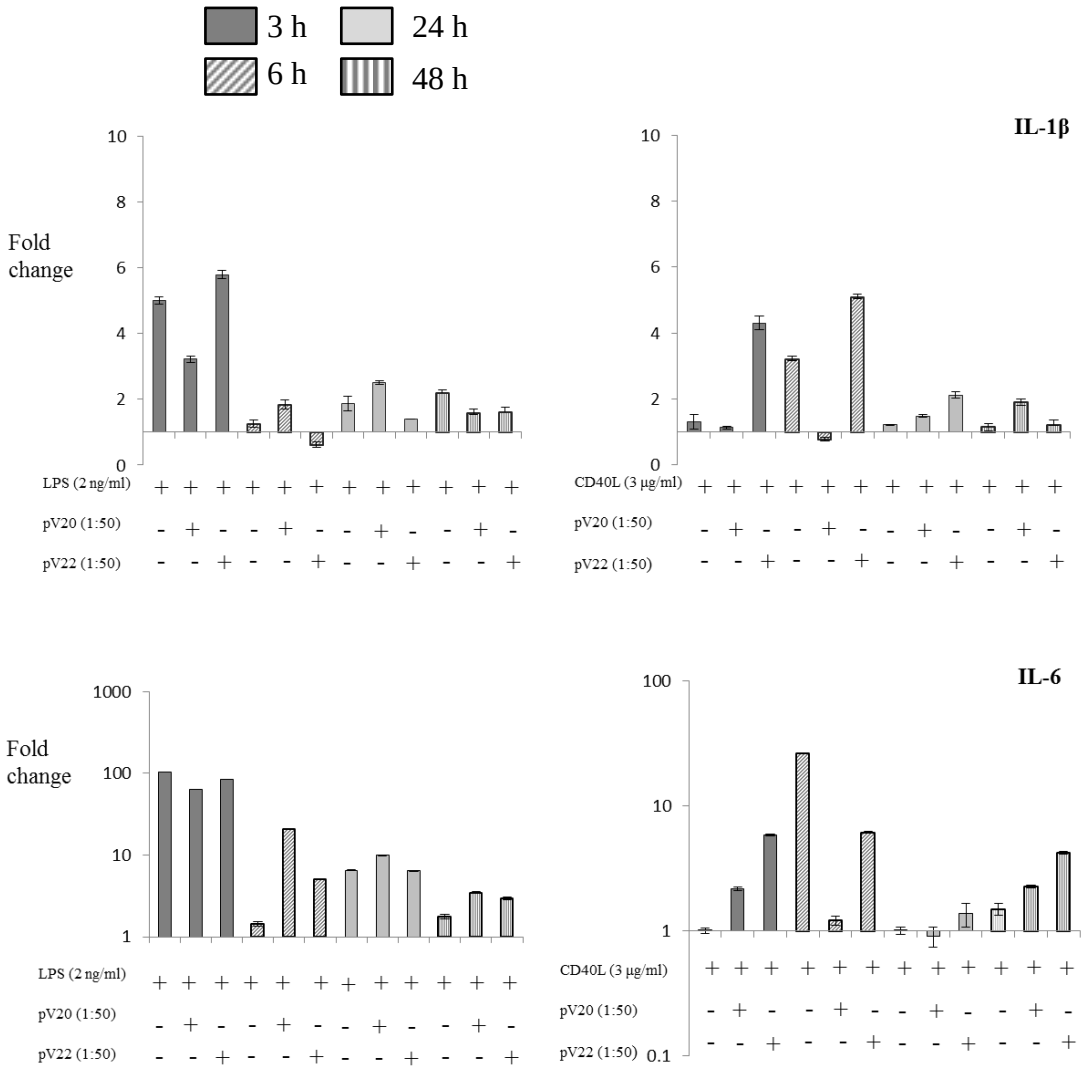

Figure 3.18 IL-1β and IL-6 mRNA expression levels in BMDC, as measured by qRT-PCR. *RNA was purified and IL-1β and IL-6 mRNA expression levels were analysed by qRT-PCR. Data are shown as fold change between levels in unstimulated and stimulated cells at specific time-points ± SEM of three replicate wells.*

CD40L/pV22-schRANKL enhanced the levels of IL-6 mRNA expression at 3 and 48 h. At 6 h, CD40L-stimulated cells had increased IL-6 mRNA expression levels above those of the other treatments. CD40L/pV22-schRANKL-stimulated cells induce higher levels of IL-6 mRNA expression compared to CD40L/pV20-schRANKL but

not to the levels of CD40L-stimulated cells. Overall these data suggest that pV22-schRANKL may be more bioactive than pV20-schRANKL. It was therefore decided that pV22-schRANKL (named schRANKL) would be used to further study the bioactivity of chicken RANKL in DC and macrophage biology.

3.4 Discussion

The repertoire of TNF superfamily members is different between chicken and mammals. To date, 19 ligands have been identified in the mammalian genome whereas only 11 have been identified in the chicken genome. Those that are absent in the chicken genome, exist as small sub-families in multigene loci on the same chromosomes in the human and mouse genomes (Kaiser *et al.*, 2005). The absence of the lymphotoxin genes, LT-α and LT-β, has been attributed to the lack of lymph nodes in the chicken. However, the absence of TNF superfamily members such as 4-IBBL, CD27L, HVEM, TWEAK and APRIL have not yet been linked to any abnormal development or differences in the chickens ability to mount an immune response, although knock-out mice have defective T and B cell responses (Locksley *et al*., 2001). One of the most recent TNF superfamily members to be identified was RANKL and since its discovery it has been implicated in a number of biological systems, e.g. osteoclastogenesis and DC-T cell interactions (Simonet *et al.*, 1997; Anderson *et al.*, 1997). RANKL has two receptors, a signalling receptor, RANK and a decoy receptor, OPG. In the chicken genome, all three genes are present and homologues for each have been found from human to fish (O'Brien, 2010).

Sequence analysis of chRANKL indicates that the NH_2-terminal is incorrectly annotated in the genome. SMART and TMHMM prediction programs identified the lack of a transmembrane domain in the predicted chRANKL sequence. Although mammalian RANKL can exist in various forms, such as membrane-bound or soluble (Ikeda *et al.*, 2001; Walsh *et al*., 2013), when aligned with the human and mouse genes, the extracellular domain was highly conserved across all species. Chicken immune proteins are usually similar in size to their mammalian counterparts. However, for chRANKL the annotated intracellular domain is large, having 96 more amino acids than the human RANKL protein. To identify the correct chRANKL sequence, the human RANKL sequence was blasted against the chicken genome to mine for the correct sequence. The results indicated that the first two exons of the predicted chRANKL sequence were incorrect and the correct sequence was extracted and primers were designed to clone the full-length correct cDNA. The extracellular domains of the TNF superfamily across species usually have between 20-30% homology, which would have helped the correct annotation of the extracellular

domain. Various studies have shown the ability of the extracellular domains of the TNF superfamily to retain their bioactivity. For example, the extracellular domain of CD40L retains its ability to stimulate B cell proliferation and drive immunoglobulin isotype switching (Armitage *et al*., 1992) although CD40L is rarely found as a soluble protein *in vivo* (Aggarwal *et al*., 2012). Mammalian RANKL can function either as membrane-bound or secreted form (Ikeda *et al.*, 2001; Walsh *et al*., 2013) and there is no functional difference between these two forms of RANKL (Nakashima *et al.*, 2000). The extracellular domain of chRANKL was cloned and called schRANKL. An amino acid alignment of chRANKL with human and mouse RANKL showed high conservation across all species. Internal hydrophobic residues within the extracellular domains of the TNF superfamily members are required for monomer folding and trimer assembly. The RANKL monomer consists of two anti-parallel β-sheets. The two β-sheets are formed by various β-strands (Lam *et al.*, 2001). The PSIPRED prediction program was used to verify the location of the residues involved in β-sheet formation in chRANKL. SchRANKL contains 10 β-strands and the 4 loops required for the assembly of a trimer (Figure 3.7). The extracellular domains of the TNF superfamily contain TNF homology domains and this region is conserved between mammals and birds. Mutations within the TNF homology domain have been linked to the genetically rare bone disorder, autosomal recessive osteoporosis (ARO) in mammals. For example, a mutation at residue V^{277} leads to a frameshift which introduces a stop codon forming a non-functional truncated RANKL protein (Frattini *et al*., 2007; Sobacchi *et al.*, 2007). Mutational analysis of the TNF homology domain shows its requirement for RANK signalling but not RANK interaction (Cheng *et al*., 2009). In particular, a RANKL mutant protein expressing only residues 248 to 316 can block RANKL induction of osteoclast activation by binding to RANK but not activating downstream signalling pathways (Cheng *et al*., 2009). SchRANKL was sub-cloned downstream of the mouse CD8 signal peptide to facilitate secretion of the protein from COS-7 cells. The plasmid also contained two more elements: an isoleucine zipper to encourage the formation of trimer proteins and a FLAG-tag for recombinant protein detection.

RANKL is one of the few TNF superfamily members with two receptors, one for downstream signalling, RANK, and the second working as a decoy receptor,

called OPG (Anderson *et al*., 1997; Simonet *et al*., 1997). Both receptors are present in the chicken genome with both residing on chromosome 2. RANK is a type I transmembrane protein with highly conserved CRD domains characteristic of members of the TNFR superfamily. The chRANK sequence was predicted and therefore the location and prediction of various domains were analysed using SignalP4 and SMART prediction models. The predicted chRANK contains an NH_2-terminal signal peptide, four CRDs, a transmembrane and a large intracellular domain, similar to mammals (Figure 3.5) (Anderson *et al.*, 1997). Using this sequence, primers were designed to clone the full-length sequence of the cDNA. To express chRANK as a soluble recombinant protein, primers were also designed to clone the extracellular domain. Attempts to clone the full-length sequence of chRANK in a single PCR were not successful. However, various primer pairs designed to clone partial pieces of the gene were successful. The extracellular domain was cloned with a second product containing the transmembrane and intracellular domains. Although chRANK was not cloned in one piece, the 18 base overlap allowed the full-length predicted protein sequence to be analysed. Conservation of RANK in non-mammalian species is relatively high with 40-42% sequence similarity with human and mouse RANK (Figure 3.8).

Members of the TNFR superfamily do not possess intrinsic catalytic domains and therefore require adaptor proteins for downstream signalling. The TNFR superfamily can be further categorised as either containing intracellular TRAF-binding motifs or DD. TRAFs are a family of adaptor proteins made up of seven members (TRAF1-7). Most signalling by the TNF receptors through TRAFs leads to activation of NF-κB and JNK pathways, that are in turn associated with the activation of immune genes linked to pro-inflammatory cytokine expression, cell survival and differentiation (Lee & Lee, 2002). Signalling though DD (TNFR1, FAS, DR3, DR4, DR5 and DR6) leads to cell death by activating apoptosis. Distinct TRAF-binding motifs have been identified in a number of TNFR members, such as CD40 (Rothe *et al.*, 1995; Ishida *et al*,. 1996a and Ishida *et al*,. 1996b), HVEM (Hsu *et al*., 1997), RANK (Darnay *et al*., 1998; Galibert *et al*., 1998; Kim *et al.*, 1999), CD30 (Gedrich *et al*., 1996; Aizawa *et al*., 1997) and LMP-1 (Devergne *et al.*, 1996). Using site-directed mutagenesis, various domains within these receptors were shown

to be required for specific TRAF binding. Two TRAF1, TRAF2, TRAF3 and TRAF5 binding motifs have been identified; a major one, (P/S/A/T)X(Q/E)E and a minor one, PXQXXD (X being any amino acid) (Devergne *et al*., 1996). The binding sites for TRAF6, however, differ from the motifs described above. TRAF6 is the only member of the TRAF family that participates in signalling for both the TNFR and the Toll/IL-1R superfamilies. The TRAF6-specific binding motif is the peptide PXEXX (X being aromatic/acidic residue), which is present in CD40, RANK and three IRAK adaptor proteins involved in Toll/IL-1R signalling (Ye *et al*., 2002).

Two independent groups first identified the location of TRAF-binding motifs in mammalian RANK (Darney *et al.,* 1998; Gilbert *et al.,* 1998). Deletion constructs of the intracellular domain of RANK at potential TRAF binding motifs allowed for the identification of TRAF1, TRAF2, TRAF3, TRAF5 and TRAF6 binding to RANK and which of these were required for downstream NF-κB activation (Darney *et al.,* 1998; Galibert *et al*., 1998; Wong *et al.,* 1999). Two membrane-distal TRAF binding motifs and three membrane-proximal TRAF6-specific motifs were identified in mammalian RANK. To verify the presence of these binding motifs in chRANK, the TRAF binding motifs in human and mouse were identified in an amino acid alignment. Interestingly, of the 5 mammalian TRAF-binding motifs, chRANK only contained four. The "missing" motif is one of the TRAF6-specific binding sites (Figure 3.8). $TRAF6^{-/-}$ mice suffer from severe osteoporosis, a similar phenotype to that of $RANKL^{-/-}$ and $RANK^{-/-}$ mice (Lomaga *et al.,* 1999; Naito *et al*., 1999).

In mammalian studies, the requirement for three TRAF6-binding motifs in RANK was analysed by expressing a chimeric protein consisting of the ectodomain of human CD40 with the transmembrane and intracellular domains of mouse RANK (hCD40/mRK) with or without mutations in one, two or three of the TRAF6-binding sites (Gohda *et al.,* 2005). These chimeric and mutational studies identified the requirement for at least one functional TRAF6-binding site in RANK for osteoclast cell activation, although a similar study identified the need for two sites for osteoclastogenesis (Kadono *et al.,* 2005). Interestingly, the TRAF6-binding motif in the membrane-proximal domain was more efficient than the other two sites (Gohda *et al*., 2005). CD40, a fellow member of the TNFR superfamily, is the only other

receptor within this family with a TRAF6-binding motif (Tsukamoto *et al*., 1999; Walsh & Choi, 2003). Although RANK and CD40 activate the NF-κB, MAPK and JNK pathways, CD40 cannot differentiate or activate osteoclasts (Gohda *et al*., 2005). To understand which different signalling pathways were being activated by RANK and not CD40 to drive osteoclastogenesis, various signalling pathways were analysed in bone marrow cells expressing the chimeric hCD40/mRANK protein or hCD40 stimulated with anti-CD40. The intracellular domain of RANK could activate the nuclear activator of T cells 1 (NFATc1) transcription factor and Ca^{2+} oscillation (Gohda *et al.,* 2005). NFATc1 is the master regulator for the differentiation and activation of osteoclasts (Ishida *et al*., 2002) and was first identified as a transcription factor required for the production of IL-2 upon T cell activation (Rao *et al*., 1997; Serfling *at al.,* 2000). Studies carried out by both Kadono *et al*. (2005) and Gohda *et al*. (2005) showed that overexpression of CD40 in bone marrow cells, or the addition of more TRAF6-binding motifs within the intracellular domain of CD40, could lead to the activation of osteoclastogenesis. It is therefore assumed that RANK, having three TRAF6-binding sites, leads to a quantitative recruitment of TRAF6 proteins, activating p38 and NFATc1 phosphorylation (Kadono *et al.,* 2005). Currently there is little knowledge surrounding avian TRAFs and it was therefore decided to identify and clone those involved in RANK signalling to investigate whether they were conserved in the chicken (Chapter 5).

To further understand the ability of RANK and not CD40 to activate osteoclastogenesis, even though both have TRAF6-binding motifs, Taguchi *et al*., (2009) set out to identify if there was another domain within the cytoplasmic region of RANK required for osteoclastogenesis. To identify regions within the RANK cytoplasmic tail with high conservation, an amino acid alignment of mouse, rat, chicken, dog and chimpanzee RANK was analysed by CLUSTALX. The analyses identified a region between Pro^{508} and Gly^{546} that was highly conserved between all species, which was named the highly conserved region (HCR) (Taguchi *et al.*, 2009). To understand the molecular requirement of this region for RANK signalling, mutational analyses were carried out omitting this domain. As mentioned earlier, RANK can activate Ca^{2+} oscillation leading to the activation of NFATc1 (Gohda *et al*., 2005). Ca^{2+} oscillation requires the phospholipase Cγ2 (PCγ2), which is activated

by immune receptors of tyrosine activation motifs (ITAM) harbouring adaptors, DNAX-activating protein (DAP) 12 and the γ-chain of the Fc receptor (FcRγ) (Mao *et al.*, 2006). Depletion of either of these in mice leads to profound osteopetrosis (Koga *et al.*, 2004). BMDM were transfected with WT and mutant RANK and stimulated with RANKL. PCγ2 was activated along with NF-κB and MAPK at the early stages of osteoclastogenesis (20 min). However, after 6 h of stimulation, NFATc1 was barely detectable in HCR-mutant cells. It was suggested that the HCR is required for the late stages of osteoclastogenesis by maintaining the expression of PCγ2. To further investigate the necessity of this domain for RANK signalling during osteoclastogenesis the HCR was integrated into the cytoplasmic tail of CD40. HCR containing CD40 could induce osteoclastogenesis (Gohda *et al*., 2005). The role, if any, of HCR in RANK's ability to induce pro-inflammatory cytokine expression and survival in APC has not been studied in mammalian species. To investigate the ability of soluble chRANK to block chRANKL bioactivity, the extracellular domain was sub-cloned into Signal pKW06-Ig to generate COOH-Fc-tagged protein in COS-7 cells.

Mammalian OPG cDNA encodes a 401 amino acid protein that is further processed to form a 380 amino acid mature protein after cleavage of the signal peptide. OPG is synthesised as a glycosylated 55 kDa protein which self-associates to form disulphide-linked dimers prior to secretion from cells. ChOPG had been previously cloned by Hou *et al.* (2007). However, no sequence alignment or analysis was carried out to investigate the conservation of the CRD, DD and penultimate cysteine residue required for chOPG dimer assembly. Using SignalP4, the presence and cleavage site of the chOPG signal peptide was identified (Figure 3.1) allowing prediction of the size of the mature chOPG protein. Amino acid alignment of chOPG with the human and mouse proteins identified the high conservation of the gene across species, with 64-65% amino acid identity (Figure 3.9). This percentage of conservation is relatively high for a chicken immune gene as usually conservation between mammalian and chicken cytokines is between 25-30% (Kaiser, 2011). Like RANK, OPG is composed of NH_2-terminal CRDs. These are followed by two modules homologous to DD, a heparin-binding domain and a penultimate cysteine residue required for dimer formation (Yasuda *et al.*, 1998). OPG can bind to heparin

and although it was once suggested that this domain contributes to dimer formation it does not appear to have much biological importance (Schneeweis *et al.*, 2005). However, rats treated with heparin had a decrease in bone density (Muir *et al*., 1996) and this was due to heparin inhibiting the interaction of OPG with RANKL (Irie *et al*., 2007). OPG contains 4 CRD domains similar to RANK but does not possess a transmembrane domain. Instead, OPG contains two DD with no known function. All DD containing receptors are expressed intracellualarly, driving cell death through the accumulation of caspase activation. OPG is the only death-domain containing receptor which is soluble. The CRDs behave as an independent structural unit with the second and third CRD interacting with RANKL (Luan *et al.*, 2012). This interaction is diminished by a mutation in OPG at position 117, where Phe was substituted to Leu. A subset of families with juvenile Paget's disease have the OPG^{F117L} mutation which causes long bone deformities, fractures, skull enlargement and deafness associated with accelerated bone resorption (Chong *et al.*, 2003). The cysteine residue at position 400 is required for dimer formation in mammals (Luan *et al*., 2012). It is believed that the OPG dimer is a Y-shaped structure with the CRD forming the arms and the death domains forming a stalk. The "arms" occupy two grooves in the RANKL trimer, blocking the site for RANK binding (Luan *et al*., 2012) (Figure 3.19). ChOPG was sub-cloned into pKW06 to generate a soluble Fc-tagged protein in COS-7 cells.

Having cloned the extracellular domains of chRANKL and chRANK along with the full-length sequence of chOPG, each was sub-cloned into expression vectors for recombinant fusion protein production in COS-7 cells and protein structures were analysed by western blot. Interaction and signalling between TNF and TNFR superfamily members is dependent on the obligatory 3-fold symmetry. In mammals, the crystal structure of TNF ligands alone or in complex with their receptors has provided insight into the regions of the ligand required for interaction. The first crystal structure of TNF-α was identified in 1990 and provided the first detailed identification of the ability of TNF superfamily members to form trimers (Jones *et al*., 1990). TNF monomers fold into a β-sandwich consisting of two anti-parallel β-

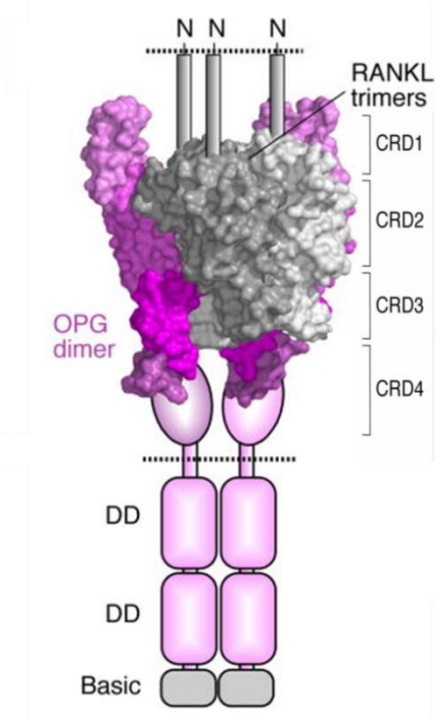

Figure 3.19 Schematic diagram of OPG and RANKL interaction. *OPG is a Y-shaped structure where the CRD form the arms and the DD the stalk of the protein. RANKL (grey) naturally forms trimers at the surface of the cell membrane. The "arms" of OPG accupy two groves inhibiting the docking of RANK. Picture adapted from Nelson et al. (2012).*

sheets. The β-sheets of three individual β-sandwiches lie parallel to the three-fold axis. The interaction between these sheets creates an edge-to-face stacking producing a tight association between the subunits (Figure 3.20A) (Jones *et al.*, 1990). The interface between these subunits is formed by mainly aromatic residues (Karpusas *et al*., 1995; Lam *et al*., 2001). TNFR superfamily members express CRD in their extracellular ligand-binding domains. These four-cysteine-repeat motifs produce very elongated structures from the cell surface (Smith *et al*., 1994). The six cysteine residues of each CRD form three intra-domain disulphide bridges which are shaped like the rungs of a ladder that are evenly spaced and do not come into contact with one another (Banner *et al.*, 1993). Recognition between the TNF ligand and their receptor(s) is highly specific with a dissociation constant in the nanomolar range

(Lam *et al*., 2001). The TNF ligand trimer structure allows the loops at the edge of the opposing monomers to from a cleft, the shape of which forms the specificity of the interacting receptor (Figure 3.20A). The conventional model of TNF receptor signalling proposes that the trimeric ligand recruits three separate chains of the receptor, bringing them within close proximity to form homotrimers themselves (Smith *et al*., 1994). The trimeric ligand inter-digitates between the receptor chains thus preventing their interaction with each other (Figure 3.20B) (Lam *et al*., 2001).

RANK is more elongated than OPG but both share 34% amino acid identity in their CRD. RANK and OPG share similar structural frameworks but RANKL adopts a different conformation when in complex with either of them. OPG has higher affinity for RANKL than RANK (Nelson *et al*., 2012). To verify the protein structures of schRANKL, chRANK and chOPG, exCOS-7 supernatants containing FLAG-schRANKL, chRANK-Fc or chOPG-Fc were analysed by western blot.

Two expression plasmids were designed for the expression of type II transmembrane proteins. Each plasmid contained the mouse CD8 signal peptide to drive soluble protein expression, a FLAG-tag for detection and an isoleucine zipper to facilitate trimerisation of schRANKL. The first initial study to identify the importance of TNF trimerisation was carried out by Morris *et al*. (1999), who identified enhancement of the biological activity of soluble CD40L expressed with an isoleucine zipper. It was suggested that the addition of the isoleucine zipper enhanced trimerisation and stability of the complex (Morris *et al*., 1999). More recently, studies of the bioactivity of TRAIL showed that although the extracellular domain could be produced as a soluble protein using the secretion signal from human fibrillin-1 protein, it was not bioactive (Kim *et al.*, 2004). TRAIL requires trimerisation to induce apoptosis, as the trimer acquires a zinc ion essential for bioactivity. This zinc ion cannot be attracted by a TRAIL monomer (Hymowitz *et al.*, 1999). To drive TRAIL trimerisation, the isoleucine zipper from the leucine trimerisation domain (Harbury *et al*., 1994) was integrated into pCR3 (Kim *et al*., 2004). Two plasmids were designed to express the isoleucine zipper with a cleavable or non-cleavable signal peptide and proteins were produced in HEK-293T cells. Both plasmids produced soluble trimeric protein and each retained their ability to induce

A

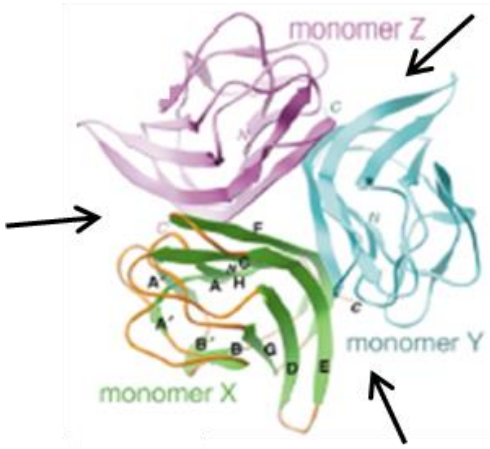

B

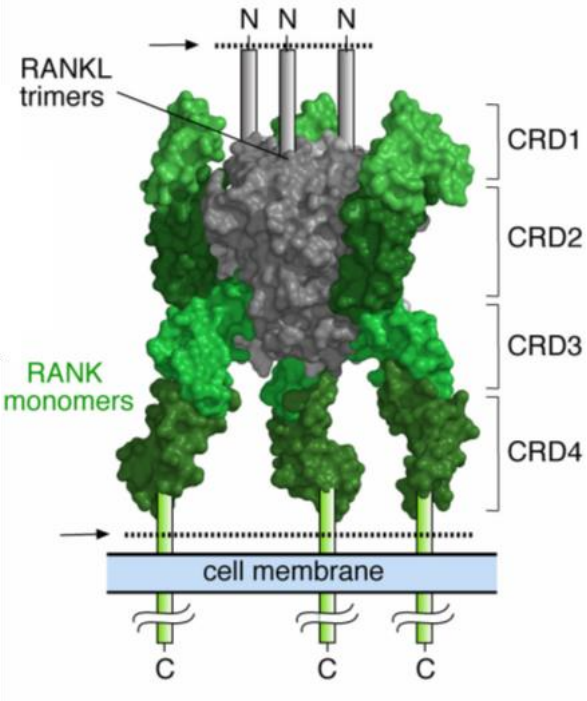

Figure 3.20 Schematic diagrams of A) RANKL trimer, B) RANKL and RANK interaction. A) *Ribbon diagram of the RANKL trimer shown down the axis of the three-fold symmetry. The three monomers are identified as monomers Z, Y and X, the β-strands and loops involved in trimerisation are lettered and the RANK binding clefts are shown with black arrows.* **B)** *Schematic diagram of RANKL trimers interacting with RANK monomers at the cell surface. Figures are adapted from Luan et al., (2012) and Nelson et al., (2012).*

cell death in HeLa cells (Kim *et al.,* 2004). To ensure schRANKL was predominantly produced as a trimeric protein, the isoleucine zipper was integrated into a modified pCI-neo vector called pV20-schRANKL. As cysteine residues are crucial for stabilisation of higher order protein structures, a second plasmid was designed with a cysteine residue at a different location. This cysteine was placed between the FLAG sequence and the schRANKL sequence and the vector was called pV22-schRANKL. The cysteine residue in pV20-schRANKL was placed between the isoleucine zipper and the FLAG-tag sequence. Each plasmid was transfected into COS-7 cells and structures of the expressed recombinant proteins were analysed by western blot. In reducing conditions, schRANKL appears as predominantly a monomeric protein at ~37 kDa with a weak band of ~75 kDa which is possibly a dimeric protein (Figure 3.10). Proteins analysed under non-reducing conditions produced bands at ~75, ~150 and ~180 kDa, suggesting the formation of dimeric trimeric and possibly a tetrameric protein structures (Figure 3.10). The data suggest the formation of trimeric protein for both pV20- and pV22-schRANKL.

ChRANK was expressed in COS-7 cells to produce a COOH-terminal Fc-tagged protein. Under non-reducing conditions a strong band was apparent at ~100 kDa (Figure 3.11). The predicted chRANK-Fc monomer is ~52 kDa, and this larger band could represent glycosylated monomers. Mammalian RANK self-association requires the cytoplasmic domain but not the extracellular domain (Kanazawa & Kudo, 2005). Hakozaki *et al.* (2010) transfected murine RANK into COS-7 cells and examined the expression of RANK in both the cell lysates and supernatants. In the cell lysates ~85 and ~200 kDa bands were present, representing the trimeric and monomeric proteins, respectively. However, in the cell supernatant containing soluble cleaved RANK, the trimeric protein was not present, suggesting the cytoplasmic tail is required for RANK self-association (Hakozaki *et al*., 2010). Although the conventional view is that TNFR only trimerises upon ligand interaction, one study identified the ability of TRAILR1 and CD40 to preassembled oligomers at the cell surface serving as a pre-ligand binding assembly domain (PLAD) (Chan *et al.,* 2000). It would be interesting to investigate the ability of the full-length chRANK protein to form a PLAD at the cell surface. ChOPG was expressed as Fc-tagged protein and shown to self-associate to form homodimers in

COS-7 cell supernatants, similarly to mammalian OPG (Yasuda *et al.,* 1998) (Figure 3.12).

The ability of chicken TNF members to fold correctly after expression in mammalian COS-7 cells is important for the study of their bioactivity and interactions. Both pV20- and pV22-schRANKL can self-associate to form homotrimers, which in mammals is vital for RANK trimerisation and downstream signalling (Cheng *et al*., 2009). To begin identifying the role of chRANKL in avian DC and macrophage biology, the activity of chRANKL on the phenotypes of each cell type were investigated. In the current model of DC and macrophage differentiation, each subset is derived from haematopoietic stem cells with a restricted myeloid differentiation potential (Geissmann *et al*., 2010). Within the bone marrow, there are macrophage/DC progenitor cells (MDP) which are constantly proliferating. MDP have a similar phenotype to granulocyte-macrophage progenitor cells, and are $CD34^{+}CD16^{+}$, $Lin^{-}Sca1^{-}IL\text{-}7R\alpha^{-}$ cells but specifically express the cytokine receptor, colony stimulating factor-1 receptor (CSF-1R), and the chemokine receptor, CX3CR1. These cells differentiate into monocytes and common DC precursor cells (CDP). Monocytes leave the bone marrow through the blood and under inflammatory conditions enter tissues and differentiate into macrophages or inflammatory DC (Auffray *et al*., 2009). CDP, on the other hand, can differentiate into plasmacytoid DC (pDC) or pre-classical DC which travel to the lymph nodes where they acquire a mature DC phenotype and morphology (Greissmann *et al*., 2010). Certain cytokines and transcription factors have been identified as crucial for macrophage and DC differentiation. CSF-1 is crucial for the development of monocytes, as $CSF1^{-/-}$ or $CSF\text{-}1R^{-/-}$ mice suffer osteopetrosis, have a reduced number of monocytes and have reproductive defects (Dai *et al*., 2003). Primary immature macrophage and DC can be generated from bone marrow cells using specific cytokines to drive their differentiation. For BMDC, IL-4 and CSF-2 drive their differentiation (Inaba *et al.,* 1992; Sallusto *et al.,* 1994) whereas BMDM differentiate in the presence of CSF-1 (Bonifer & Hume, 2008). The same pattern applies to the chicken where BMDC differentiate with recombinant chIL-4 and chCSF-2 (Wu *et al*., 2010) and BMDM with recombinant chCSF-1 (Garceau *et al*., 2010).

To induce sub-optimal maturation of APC, BMDC and BMDM were stimulated with various concentrations of LPS for 3 and 6 h. The mRNA expression levels of IL-12α were minimal in BMDC stimulated with LPS at 2 ng/ml (Figure 3.13). This concentration was sufficient to upregulate the cell surface expression of CD40 and decrease the expression of the phagocytic marker, KUL01. However, MHC class II expression was not enhanced by LPS stimulation (Figure 3.14). In Wu *et al*. (2010), BMDC constitutively expressed MHC class II on their cell surface and neither LPS nor CD40L stimulation led to a significant increase in expression. BMDM were sub-optimally matured with LPS at 1 ng/ml for 3 and 6 h which increased IL-6 mRNA expression levels (Figure 3.15). This concentration was also sufficient to induce the cell surface expression of CD40, decreased KUL01 expression but caused no change in MHC class II expression (Figure 3.16). Macrophages have two ways of being activated, by antigen exposure or by cytokines produced by activated Th cells (Th1 and $CD8^+$ cytotoxic T cells) and natural killer cells. Macrophage stimulated with IFN-γ undergo "classical activation" leading to pro-inflammatory cytokine expression, NO_2 release and MHC class II expression (Gordon, 2002). Chicken IFN-γ-treated BMDM upregulated the expression of CD40 and MHC class II suggesting the cells were activated. The qRT-PCR and FACs analyses indicated that bone marrow cells grown with chIL-4 and chCSF-2 were phenotypically BMDC, while chCSF-1 differentiated bone marrow cells into BMDM.

To investigate the bioactivity of chRANKL on avian APC, two plasmids were designed to encourage the formation of trimeric chRANKL proteins. Each protein was tested for their ability to enhance pro-inflammatory cytokine mRNA expression levels in BMDC. The pilot study indicated that both proteins could enhance pro-inflammatory cytokine mRNA expression levels, with pV22-schRANKL protein having slightly more bioactivity than pV20-schRANKL protein. Therefore pV22-schRANKL, referred to as schRANKL, was used for further analysis of chRANKL bioactivity.

Chapter 4

Characterisation of chRANKL, chRANK and chOPG

4.1 Introduction

In 1997, four independent groups isolated a type II TNF-like transmembrane protein using different experimental systems and provided various names for the novel protein, i.e. TNF-related activation-induced cytokine (TRANCE) (Wong *et al.*, 1997), RANKL (Anderson *et al*., 1997), osteoprotegerin ligand (OPGL) (Lacey *et al.*, 1998) and osteoclast differentiation factor (ODF) (Yasuda *et al.*, 1998). Both TRANCE and RANKL were isolated from immunology-based laboratories while OPGL and ODF were isolated from a myelomonocytic cell line and a bone marrow stromal cell line, respectively. In this thesis, this protein is called RANKL. Mammalian RANKL mRNA expression in the immune system is limited to the thymus and lymph nodes, a restricted pattern also demonstrated by LT-α which is expressed solely in the spleen, differing to the pattern of expression seen for other members of the TNF superfamily (Anderson *et al.*, 1997; Wong *et al.*, 1997). Mammalian RANKL surface expression is predominantly on Th1 cells, and is inhibited by IL-4, not surprisingly as IL-4 is a Th2 cytokine that inhibits IFN-γ production by Th1 cells. Stimulation of the TCR leads to the early onset of RANKL expression and its induction is believed to be regulated by calcium mobilisation and PKC activation (Wang *et al.*, 2002; Fionda *et al.*, 2007).

RANKL is known to bind to two receptors: RANK and OPG, a secreted TNF-related protein that inhibits RANKL and RANK interaction (Simonet *et al.*, 1997; Yasuda *et al.*, 1997). RANK was originally identified in a bone marrow-derived myeloid DC cDNA library. RANK mRNA expression is widely detected in the lungs, spleen, skeletal muscle, brain, liver, kidney and skin, while its surface expression is limited to mature DC and osteoclast progenitor cells (Anderson *et al*., 1997; Wong *et al,*. 1997). Mammalian OPG mRNA is expressed in a number of tissues, such as the lung, kidney, heart, intestine and bone (Simonet *et al.*, 1997; Yasuda *et al.*, 1998). RANKL enhances the expression of pro-inflammatory cytokines in DC due to activation of the NF-κB pathway. Initial analyses demonstrated that RANKL does not alter the expression of costimulatory molecules, such as CD80, CD86 and the adhesion molecule, I-CAM, on the surface of murine DC (Anderson *et al.*, 1997; Wong *et al.*, 1997). However, human Mo-DC, treated with RANKL, increased the surface expression of CD83 and CD86 at low levels,

suggesting that RANKL induces partial maturation of DC (Schiano de Colella *et al.,* 2008). Currently, there is only one study analysing the bioactivity of RANKL on murine macrophages (Park *et al.,* 2005). RANKL treatment induced low levels of pro-inflammatory cytokine expression but costimulating cells with LPS or IFN-γ induced more potent macrophage activity, such as pro-inflammatory cytokine expression, cell surface marker expression (MHC class II and CD86) and phagocytosis (Park *et al*., 2005).

Mammalian RANKL is a survival factor for both DC and macrophages (Anderson *et al.,* 1997, Cremer *et al*., 1999; Park *et al.,* 2005). The ability to enhance the survival of DC is linked to the up-regulation of the anti-apoptotic molecule, Bcl-X_L (Wong *et al.,* 1999). The ability of RANKL to protect DC from spontaneous apoptosis is a potential avenue to improve the efficacy of vaccines and DC-based immunotherapy. DC that migrate to the draining lymph nodes upon infection to activate antigen-specific T cells have a very limited life-span and it is difficult to identify DC in the efferent lymph two days after infection (Pugh *et al*., 1983). To investigate the ability of RANKL to enhance the adjuvant effects of DC, cells were antigen-pulsed with purified protein derivative (PPD) from *Mycobacterium*, a classical antigen for T cell-mediated immunity (Inaba *et al*., 1992). DC were pulsed with PPD to induce maturation and then treated with RANKL and injected into mice (Josien *et al.,* 2000). Immunization with RANKL-treated, PPD-pulsed DCs increased the production of IFN-γ compared to PPD-pulsed DC untreated with RANKL. Importantly, RANKL-treated PPD-pulsed DC were capable of inducing delayed type hypersensitivity (DTH) up to nine weeks after treatment. Therefore, RANKL-treated DC could induce both primary and secondary immune responses (Josien *et al.,* 2000). These DC were also found up to five days post-injection in the draining lymph node, with a 5-10-fold increase in the number of cells than in those not treated with RANKL prior to injection. The ability of RANKL to enhance and improve the survival and capabilities of DC upon infection is an important aspect of the adjuvant properties of RANKL. If DC can survive for longer in the draining lymph nodes, they can therefore enhance T cell-DC interactions.

The main aim of this study was to characterise the biological effect of schRANKL on avian APCs, but since its discovery in mammals, the role of RANKL in bone metabolism has been at the forefront of research. Bone is a dynamic tissue that is constantly being remodelled by bone forming cells (osteoblasts), and bone reabsorbing cells (osteoclasts) (Katagiri & Takahashi, 2002). The skeletal and immune systems are closely related sharing several regulatory molecules, including cytokines, chemokines and transcription factors (Horowitz *et al.*, 1984; Dewhirst *et al.*, 1985). The evidence that the pathology of one system affects the other has led to the term osteoimmunology to cover these overlapping scientific fields (Arron & Choi, 2000). The most typical example of these systems interacting is the prolonged activation of the immune system, leading to bone erosion due to osteoclast activation causing RA (Sato & Takayanagi, 2006). RANKL is necessary for osteoclast differentiation and activation (Kong *et al.*, 1999a) by binding to RANK on osteoclast progenitor cells leading to the activation of TRAF6, NF-κB, p38 and JNK MAPKs (Lomaga *et al.*, 1999; Naito *et al.*, 1999).

This Chapter describes the expression of chRANKL, chRANK and chOPG mRNA in a number of lymphoid and non-lymphoid tissues and primary immune cells, and examines the kinetics of their expression in splenocytes, bursal cells and thymocytes following stimulation with mitogens associated with proliferation and activation. The bioactivity of schRANKL is studied in more detail in both BMDC and BMDM, by analysing mRNA expression levels of pro-inflammatory cytokines and the phenotype of cells untreated or treated with schRANKL. The conservation of the role of RANKL as a survival factor in chickens was also investigated in BMDC and BMDM. Preliminary data are also presented on the ability of schRANKL to induce osteoclast cell differentiation from bone marrow cells.

4.2 Methods

4.2.1 Tissues and primary immune cells

Primers and probes were designed to amplify small regions of chRANKL, chRANK and chOPG that lie across an intron-exon boundary to prevent false positives for qRT-PCR analysis. The kinetics of mRNA expression levels of chRANKL, chRANK and chOPG were analysed in purified splenocytes, bursal cells and thymocytes, either unstimulated or stimulated with various mitogens, such as ConA for splenocytes, PMA/ionomycin for bursal cells and PHA for thymocytes (Chapter 2, section 2.6). Splenocyte subsets were purified using mouse anti-chicken mAb against CD4, CD8β, TCRγδ and TCRαβ1/αβ2 using an AutoMACs pro separator (Chapter 2, section 2.6). To investigate the transcriptional control of chRANKL, splenocytes were purified and unstimulated or stimulated with ionomycin or ionomycin and PMA for 2, 4 and 18 h. To determine if chRANKL expression was due to Ca^{2+} mobilisation, splenocytes were further treated with ionomycin with or without a Ca^{2+} channel blocker, TMB-8, for 18 h (Chapter 2, section 2.6).

4.2.2 BMDC and BMDM primary cells

To determine the effects of schRANKL on BMDC and BMDM, bone marrow cells were extracted from the tibias and femurs of 4-6-week-old birds. Bone marrow cells were cultured in the presence of chIL-4 and chCSF-2 for BMDC, and chCSF-1 for BMDM, for 6 days (Chapter 2, section 2.6). Three separate experiments were carried out. 1) BMDC were stimulated with or without various concentrations of LPS for 3, 6 or 9 h. RNA was purified and mRNA expression levels of the chRANKL receptors, chRANK and chOPG, were analysed to understand the kinetics of their expression in avian DC. 2) To further validate the bioactivity of schRANKL, cells were either unstimulated or stimulated with LPS, CD40L, schRANKL or combinations thereof for 3, 6 or 24 h. To verify the bioactivity of schRANKL, chRANK-Fc and chOPG-Fc were pre-incubated with schRANKL for 3 h prior to stimulating cells with LPS. Pro-inflammatory cytokine mRNA expression levels were measured by qRT-PCR. 3) Pro-inflammatory cytokine mRNA expression levels

were also assessed in BMDM, either unstimulated or stimulated with LPS, schRANKL or both, for 3 and 6 h.

4.2.3 Flow cytometric analysis

Using the same conditions as described in section 4.2.2, the effect of schRANKL treatment on the phenotype of BMDC and BMDM was assessed by flow cytometry. Cells were stained with mouse anti-chicken MHC class II, CD40 and KUL01 mAb or isotype control mAb and analysed by FACs. FACs analysis was also used to measure the uptake of FITC-labelled zymosan-A particles by BMDC in the presence or absence of schRANKL. The survival of BMDC and BMDM was analysed using flow cytometry. BMDC and BMDM were untreated or treated with various dilutions of schRANKL for 24 and 48 h and cells were stained with recombinant annexin-V and PI to distinguish between dead, apoptotic and viable cells, by flow cytometry (Chapter 2, section 2.11).

4.2.4 Osteoclasts differentiation

To analyse the ability of schRANKL to drive osteoclast cell differentiation, bone marrow cells were purified from 6-week-old birds. Cells were cultured in the presence of chCSF-1 for 2 days, followed by 8 days of incubation with schRANKL. To verify the generation of osteoclasts, the presence of multinuclear cells was detected by Hoescht-33258 staining and analysed by UV illumination (Chapter 2, section 2.6).

4.3 Results

4.3.1 Tissue distribution of chRANKL, chRANK and chOPG mRNAs

The mRNA expression profiles of chRANKL, chRANK and chOPG were determined in a broad range of non-lymphoid and lymphoid tissues by qRT-PCR. Primers and probes for chRANKL and chRANK were designed against their extracellular domains. In both non-lymphoid and lymphoid tissues, mRNA transcripts for each gene were detected, suggesting each is ubiquitously expressed in chicken tissues (Figure 4.1). In non-lymphoid organs, chRANKL and chRANK mRNA expression levels are highest in muscle tissue taken from the breast. Interestingly, the lowest level of chOPG mRNA expression was in the muscle tissue (Figure 4.1A). The lowest levels of chRANKL and chRANK mRNA expression were in the heart. Levels of mRNA expression of all three cytokine were consistent in the liver, kidney and lung and slightly lower in the skin and brain (Figure 4.1A).

In chicken lymphoid tissues, the highest levels of mRNA expression for all three cytokines were in the thymus, followed by the bone marrow and the upper-gut (Figure 4.1B). Overall, mRNA expression levels of all three molecules were similar within a tissue. In the crop, chRANKL mRNA expression levels were higher (~16-fold) than those of chRANK and chOPG. In the Harderian gland, chRANKL was more highly expressed than chRANK. In the majority of tissues tested, the levels of chRANKL mRNA expression were higher than those of its receptors.

4.3.2 Kinetics of expression of chRANKL, chRANK and chOPG mRNAs in primary chicken cells

To understand the kinetics of expression of all three molecules in primary lymphoid cells, the spleen, thymus and bursa of Fabricius were removed from three individual J-line birds and cells were purified as described in section 2.6.4. Cells were seeded at 5 X 10^6 per ml and either unstimulated or stimulated with various mitogens. Splenocytes were stimulated with ConA at 1 μg/ml for 2, 4, 18 and 24 h. The mRNA expression levels of chRANKL, chRANK and chOPG were quantified using qRT-PCR (Figure 4.2). ChRANKL mRNA expression levels were

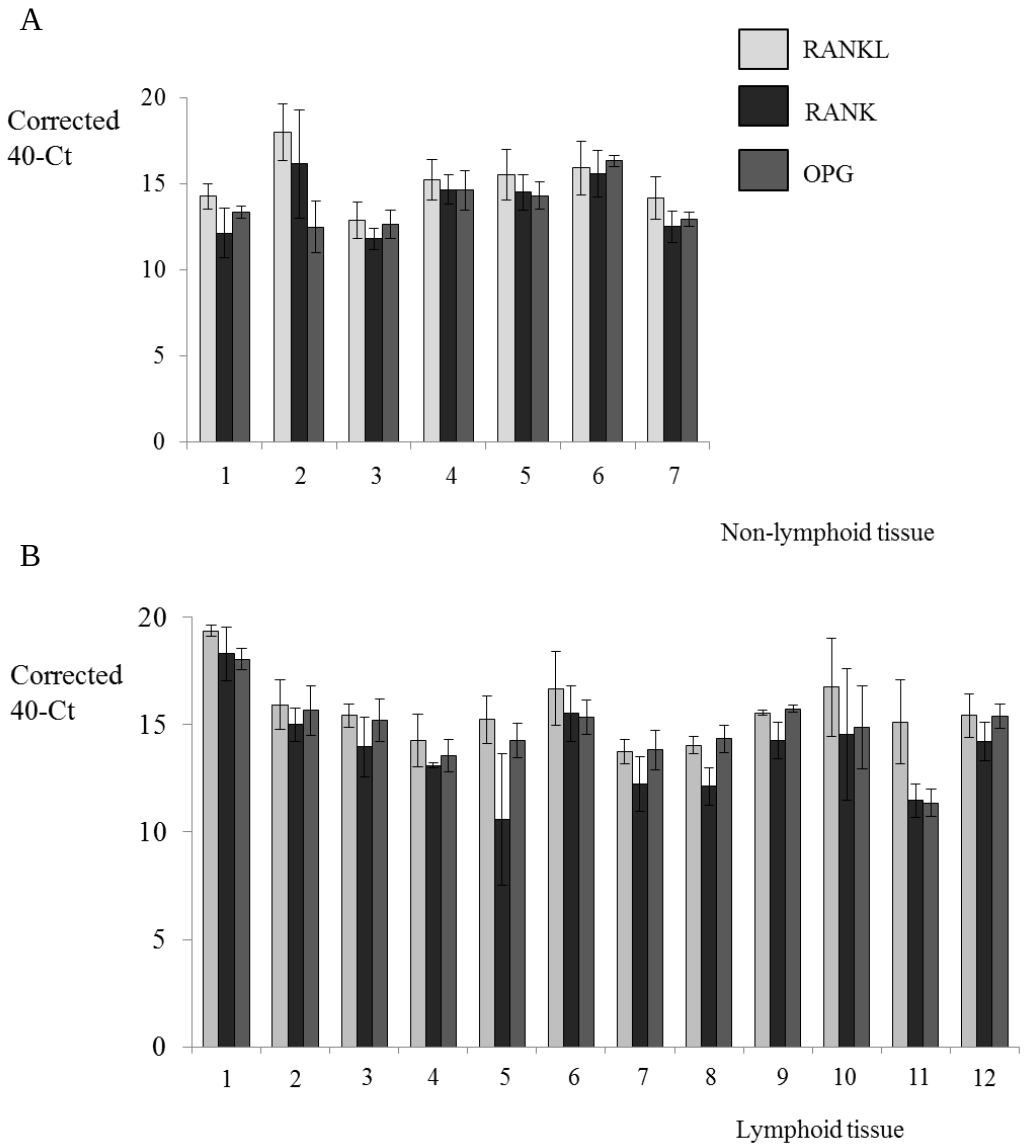

Figure 4.1 Expression profiles of chRANKL, chRANK and chOPG mRNA in A) non-lymphoid and B) lymphoid tissues, as measured by qRT-PCR. *ChRANKL, chRANK and chOPG mRNA expression levels in* **A)** *non-lymphoid tissues: 1) brain, 2) muscle, 3) heart, 4) liver, 5) kidney, 6) lung, 7) skin and* **B)** *lymphoid tissues: 1) thymus, 2) spleen, 3) bursa of Fabricius, 4) caecal tonsils, 5) Harderian gland, 6) bone marrow, 7) Meckel's diverticulum, 8) caeca, 9) mid-gut, 10) upper-gut, 11) crop, 12) gizzard. Data are presented as the average corrected 40-Ct values of three individual birds ± SEM.*

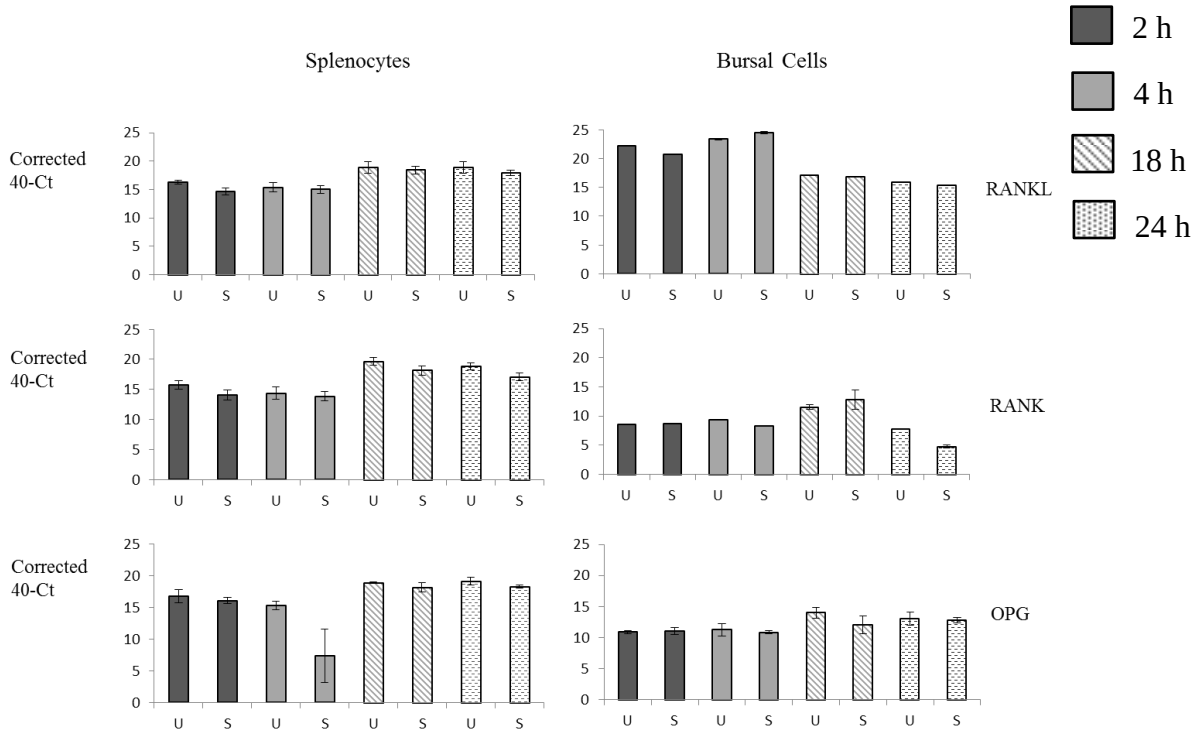

Figure 4.2 Kinetics of chRANKL, chRANK and chOPG mRNA expression levels in primary immune cells, as measured by qRT-PCR. *ChRANKL, chRANK and chOPG mRNA expression levels were analysed in unstimulated (U) or stimulated (S) primary immune cells at 2, 4, 18 and 24 h. Splenocytes were stimulated with ConA (1 µg/ml) and bursal cells were stimulated with ionomycin (3 µg/ml) and PMA (500 ng/ml). Data are presented as the average corrected 40-Ct values of three individual birds ± SEM.*

slightly down-regulated in ConA-stimulated cells compared to levels in unstimulated cells. ChRANKL mRNA expression levels were not statistically significantly different between unstimulated and ConA-stimulated splenocytes at any time-point (Figure 4.2). ChRANK and chOPG mRNA expression levels were slightly downregulated after ConA stimulation compared to levels in unstimulated cells but again mRNA expression levels were not statistically significantly different between levels in unstimulated and stimulated cells at any time-point. Overall mRNA expression levels of all three molecules were not significantly different after ConA stimulation of splenocytes.

The bursa of Fabricius is a specialised organ for the generation of the avian B cell receptor repertoire. Bursal cells were purified and co-stimulated with ionomycin and PMA for 2, 4, 18 or 24 h and examined for chRANKL, chRANK and chOPG mRNA expression levels by qRT-PCR (Figure 4.2). ChRANKL mRNA expression levels were high in unstimulated bursal cells at 2 and 4 h. When cells were stimulated with ionomycin and PMA, chRANKL mRNA expression levels were decreased at 2 h and increased at 4 h compared to levels in unstimulated cells. ChRANKL mRNA expression levels in stimulated bursal cells were not statistically significantly different between levels in unstimulated cells at any time-point examined. ChRANK and chOPG mRNA expression levels were lower compared to chRANKL mRNA expression levels in bursal cells. There was no statistically significant difference in the levels of chRANK and chOPG mRNA expression between unstimulated and stimulated bursal cells.

Thymocytes were also examined for chRANKL, chRANK and chOPG mRNA expression levels in either unstimulated or PHA-stimulated cells for 2, 4, 18 and 24 h (Figure 4.3). Similar to the previous data, PHA-stimulation did not significantly alter the levels of mRNA expression of any of the cytokines at all time-points examined (Figure 4.3). Overall, there was no statistical difference in the levels of chRANKL, chRANK or chOPG mRNA expression between unstimulated or stimulated splenocytes, bursal cells or thymocytes over the four time-points examined.

4.3.3 Expression of chRANKL, chRANK and chOPG mRNAs in chicken splenocyte subsets

The data from section 4.3.2 suggest that stimulation of splenocytes with ConA had no effect on the levels of chRANKL, chRANK or chOPG mRNA expression levels. Further analysis was carried out to determine if expression varied in different splenocyte subsets. Spleens were removed from three individual birds and splenocytes were purified over Histopaque-1077 and sorted using AutoMacs technology. The purity of cell populations were analysed by FACs (Appendix 4, Figure 2) and the percentage of purity for all cell subsets was between ~89-99%. The cell subsets analysed were $CD4^+$, $CD8\beta^+$, $TCR\gamma\delta^+$ and $TCR\alpha\beta1/\alpha\beta2^+$. mRNA

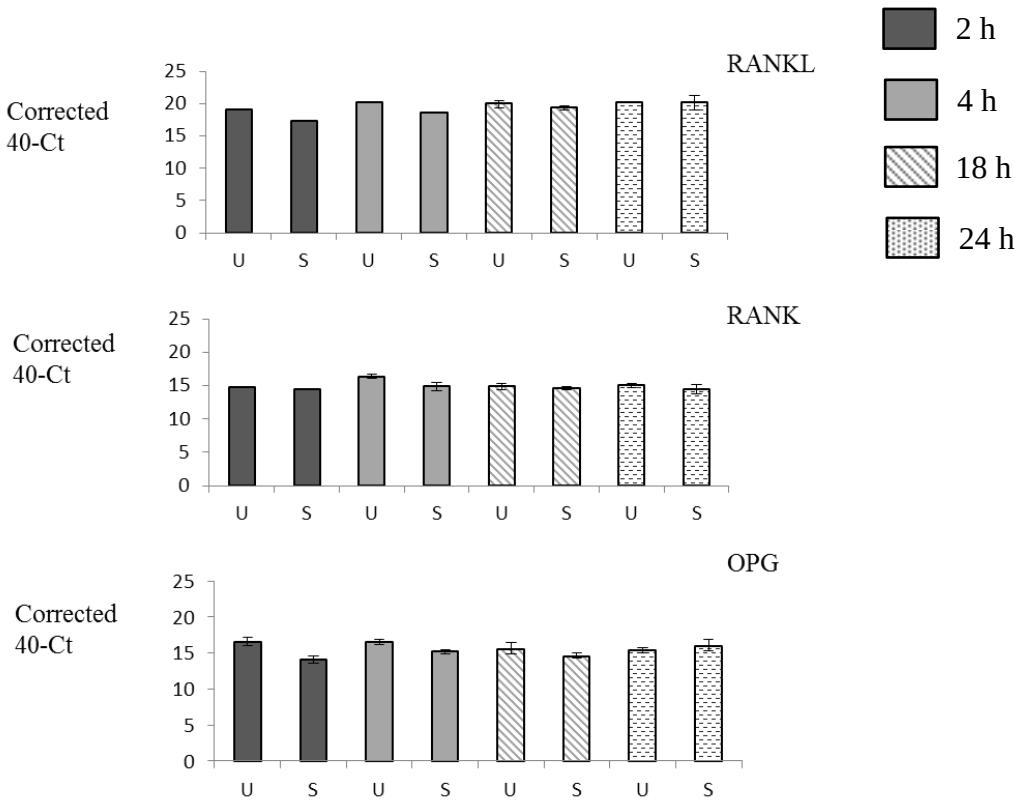

Figure 4.3 Kinetics of chRANKL, chRANK and chOPG mRNA expression levels in primary thymocytes, as measured by qRT-PCR. *ChRANKL, chRANK and chOPG mRNA expression levels were analysed in unstimulated (U) or PHA (25 µg/ml)-stimulated (S) thymocytes at 2, 4, 18 and 24 h. Data are presented as the average corrected 40-Ct values of three individual birds ± SEM.*

expression levels of all three molecules was detected in all four cell subsets (Figure 4.4). ChRANKL mRNA expression levels were generally higher across all subsets in comparison to those of its receptors, although there was no statistically significant difference in mRNA expression levels for any molecule across the subsets.

4.3.4 ChRANK and chOPG mRNA expression levels in mature BMDC

In mammals, RANK surface expression is predominantly found on mature DC and osteoclasts (Anderson *et al.*, 1997; Wang *et al.*, 1997) while OPG expression is found on osteoblast cells (Yasuda *et al.*, 1998), suggesting a role for the latter in regulating the interaction between RANKL-RANK in bone metabolism. A more

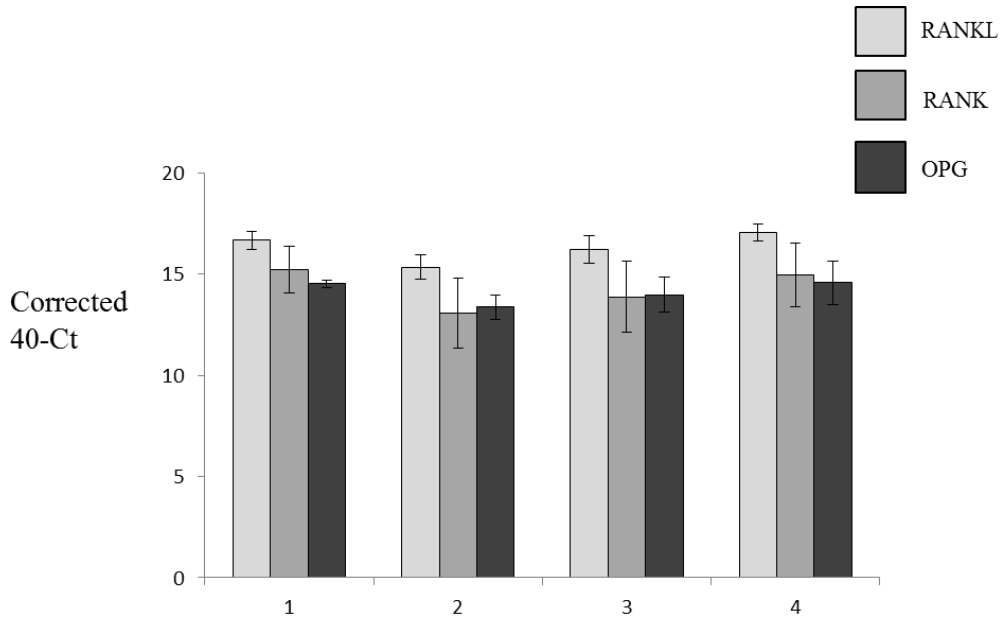

Figure 4.4 ChRANKL, chRANK and chOPG mRNA expression levels in purified splenocyte subsets as measured by qRT-PCR. *Splenocyte subsets were purified by AutoMacs separation and mRNA expression levels of chRANKL, chRANK and chOPG were analysed by qRT-PCR. 1) $CD4^+$, 2) $CD8\beta^+$, 3) $TCR\gamma\delta^+$, 4) $TCR\alpha\beta1/TCR\alpha\beta2^+$. Data are presented as the average corrected 40-Ct values of three individual birds ± SEM.*

recent study identified a similar role for OPG in human Mo-DC, where OPG expression levels increased as DC matured (Schoppet *et al.*, 2007). This suggests that OPG is also a molecular brake for RANKL-RANK interactions in the immune system. Before examining the bioactivity of schRANKL, the mRNA expression levels of both of its receptors were analysed in mature BMDC. BMDC were unstimulated or stimulated with various concentrations of LPS for 3 to 9 h and the mRNA expression levels of the receptors analysed by qRT-PCR (Figure 4.5). At 3 h, LPS-stimulated (200 ng/ml) cells had a ~2-fold increase in chRANK mRNA expression levels which dropped to ~1.6-fold at the lower amounts of LPS used, compared to levels in unstimulated cells. In contrast, chOPG mRNA expression levels were increased by ~1.3-fold in LPS-stimulated cells (200 ng/ml). At 6 h post-

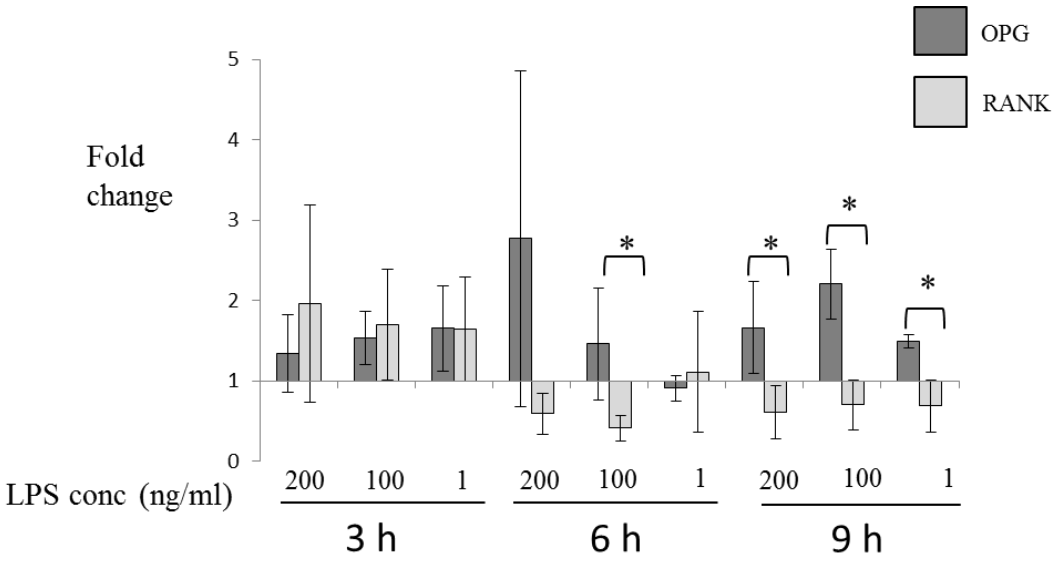

Figure 4.5 ChRANK and chOPG mRNA expression levels in mature BMDC, as measured by qRT-PCR. *BMDC were unstimulated or stimulated with various amounts of LPS (200, 100 and 1 ng/ml) for 3, 6 and 9 h. ChRANK and chOPG mRNA expression levels were analysed by qRT-PCR. Data are presented as fold change between unstimulated cells and stimulated cells at indicated time-points and represent the average results of three independent experiments ± SEM.*
**p<0.05(Mann-Whitney U test).*

stimulation, chOPG mRNA expression levels were increased by nearly 3-fold while levels of chRANK mRNA expression were only increased by ~0.4-fold (200 ng/ml). At lower concentrations of LPS, chRANK mRNA expression levels decreased to basal unstimulated levels or lower (Figure 4.6). However, cells stimulated with 100 ng/ml or 1ng/ml of LPS increased chOPG mRNA expression levels statistically significantly compared to chRANK mRNA expression levels ($p<0.05$). At 9 h, chOPG mRNA expression levels were statistically significantly higher than those of chRANK in all LPS-stimulated cells ($p<0.05$). There was no statistically significantly difference in chRANK or chOPG mRNA expression levels compared to those in unstimulated cells.

4.3.5 Transcriptional control of chRANKL mRNA expression in avian splenocytes

In mammals, RANKL is a regulator of the interactions between T cells and DC (Anderson *et al*., 1997; Wang *et al.,* 1997a). The expression of RANKL by mammalian T cells is induced by their activation and is dependent on Ca^{2+} mobilisation (Wang *et al*., 2002). Our previous data have shown that ConA stimulation has no effect on chRANKL mRNA expression levels in chicken splenocytes (section 4.3.2). Therefore to further understand the regulation of chRANKL transcription, splenocytes were activated with the Ca^{2+}-mobiliser/inducer, ionomycin, or ionomycin and the PKC activator, PMA, to mimic the signals initiated by TCR activation for 2, 4 and 18 h. Levels of chRANKL mRNA expression were analysed by qRT-PCR (Figure 4.6A).

At 2 h, in ionomycin-stimulated splenocytes, chRANKL mRNA expression levels did not increase compared to those in unstimulated cells whereas costimulated cells had a ~2-3-fold increase in chRANKL mRNA expression levels (Figure 4.6A). At 4 h, ionomycin-stimulated cells statistically significantly increased chRANKL mRNA expression levels by ~5-fold compared to levels in unstimulated cells ($p<0.05$). Costimulated cells also significantly increased chRANKL mRNA expression levels at 4 h ($p<0.05$). At 18 h, chRANKL mRNA expression levels in ionomycin-stimulated cells decreased compared to expression levels at 4 h. This could suggest that ionomycin-mediated Ca^{2+}-mobilisation declines over time and no longer induces chRANKL mRNA expression. ChRANKL mRNA expression levels were statistically significantly increased in costimulated cells compared to unstimulated cells ($p<0.05$), indicating that the concomitant activation of Ca^{2+} mobilisation and the PKC pathway are necessary to drive the transcription of chRANKL in chicken splenocytes.

To verify that the transcriptional regulation of chRANKL was linked to the activation and mobilisation of Ca^{2+}, splenocytes were stimulated with ionomycin or ionomycin with various concentrations of the Ca^{2+} channel and PKC inhibitor, TMB-8. The levels of chRANKL mRNA expression were analysed in these cells after 18 h of treatment by qRT-PCR (Figure 4.6B). ChRANKL mRNA expression levels were increased in ionomycin-stimulated cells in comparison to those in unstimulated cells.

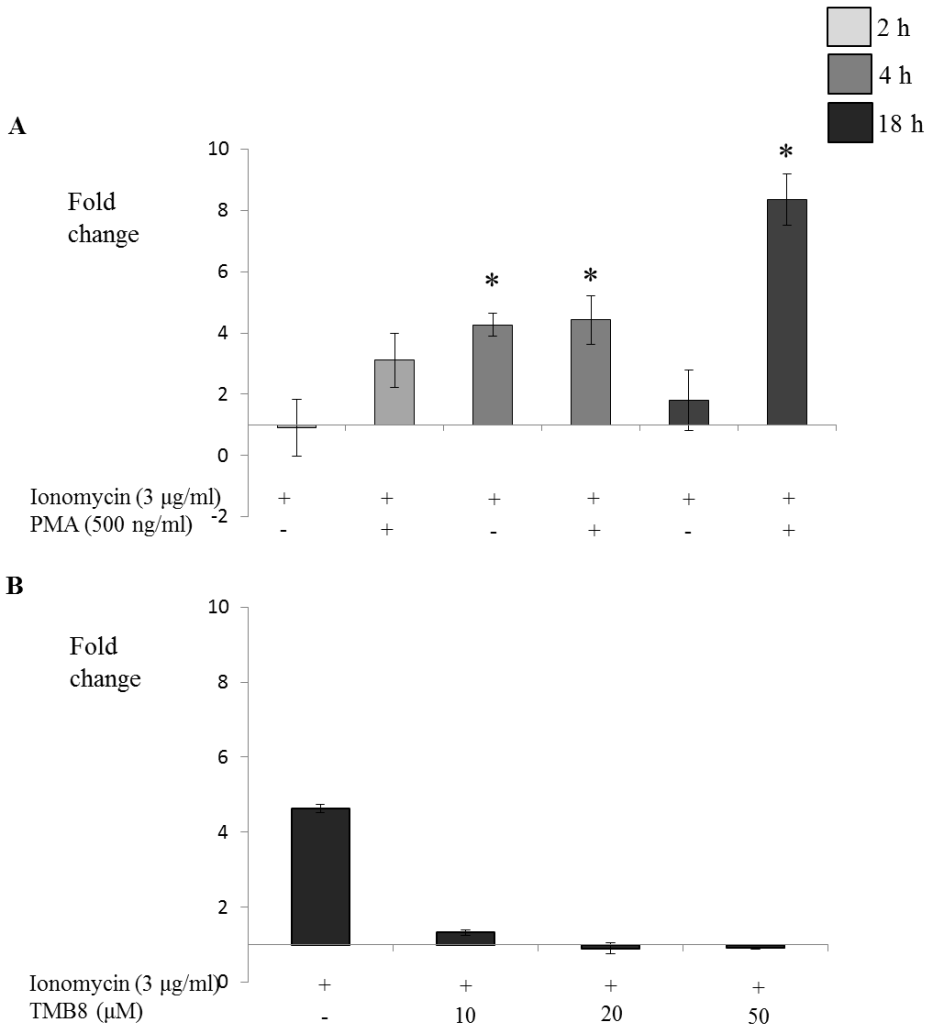

Figure 4.6 Transcriptional control of chRANKL expression in chicken splenocytes, as measured by qRT-PCR. A) *Splenocytes were unstimulated or stimulated with ionomycin (3 µg/ml) or ionomycin and PMA (500 ng/ml) for 2, 4 and 18 h. Levels of chRANKL mRNA expression levels were analysed by qRT-PCR.* **B)** *Splenocytes were unstimulated or stimulated with ionomycin or ionomycin with various concentrations of TMB-8 (10-50 µM) for 18 h and levels of chRANKL mRNA expression were analysed. Data are presented as the average of the fold change between unstimulated and stimulated cells of three individual birds ± SEM. Asterisks represent data that are statistically significantly different compared to levels in unstimulated cells (Mann-Whitney U test).*

In the presence of TMB-8, chRANKL mRNA expression levels were reduced to those in unstimulated cells (Figure 4.6B). These data suggest that the pharmacological inhibitor of Ca^{2+} mobilisation and PKC activation, TMB-8, can block the transcription of chRANKL in chicken splenocytes and that the transcriptional control of chRANKL is regulated by these two biological pathways.

4.3.6 The effects of chRANKL on pro-inflammatory cytokine mRNA expression levels in BMDC

To examine the bioactivity of schRANKL, recombinant protein was produced in COS-7 cells and its effect on pro-inflammatory cytokine mRNA expression levels in BMDC was explored. On day 6 of culture, BMDC were unstimulated or stimulated with LPS, schRANKL or both, for 3 and 6 h. mRNA expression levels of the pro-inflammatory cytokines, IL-1β, IL-6 and IL-12α, were analysed by qRT-PCR. At both time-points, LPS-stimulated cells had significantly upregulated IL-12α mRNA expression levels compared to levels in unstimulated cells ($p<0.05$). Costimulation with schRANKL had no effect at 3 h but did highly statistically significantly increase IL-12α mRNA expression levels compared to those in unstimulated cells at 6 h ($p<0.01$). However, in costimulated cells IL-12α mRNA expression levels were not statistically significantly altered compared to levels in LPS-stimulated cells at 6 h. Treatment of cells with schRANKL alone did not affect IL-12α mRNA expression levels (Figure 4.7).

At 3 h, IL-1β mRNA expression levels were significantly increased (26-fold) in LPS-stimulated cells compared to those in unstimulated cells ($p<0.05$). Costimulated cells also had a significant increase in IL-1β mRNA expression levels compared to those in unstimulated cells ($p<0.05$) but not statistically significantly different to those in LPS-stimulated cells ($p<0.07$) (Figure 4.7), indicating that the addition of schRANKL did not enhanced IL-1β mRNA expression levels. At 6 h, LPS stimulation led to a significant (~52-fold) increase in IL-1β mRNA expression levels which were further statistically significantly enhanced to ~79-fold in co-stimulated cells compared to levels in unstimulated cells ($p<0.05$) and statistically significantly compared to levels in LPS-stimulated cells ($p<0.05$) (Figure 4.7). SchRANKL-treated cells increased the levels of IL-1β mRNA expression at 6 h but

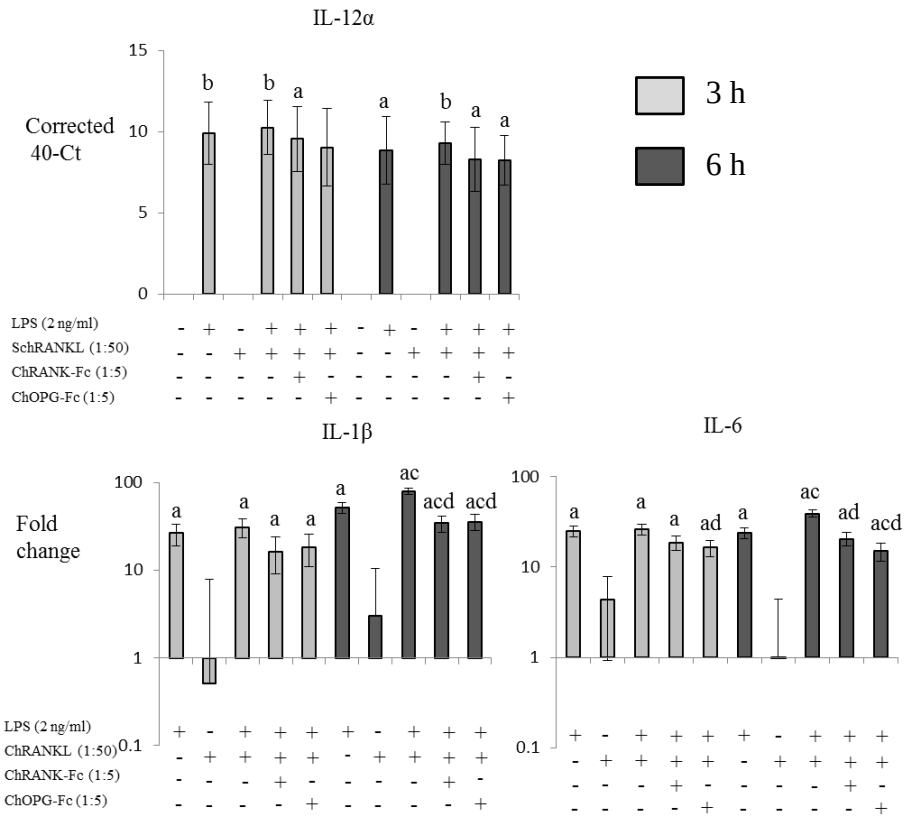

Figure 4.7 Pro-inflammatory cytokine mRNA expression levels in BMDC stimulated with LPS, schRANKL or both for 3 and 6 h, as measured by qRT-PCR. *BMDC were unstimulated or stimulated with LPS (2 ng/ml), schRANKL (1:50 ex-COS), or costimulated with both for 3 and 6 h. SchRANKL bioactivity was verified by pre-incubating with either chRANK-Fc (1:5 ex-COS) or chOPG-Fc (1:5 ex-COS) 3 h prior to stimulation of BMDC. Pro-inflammatory cytokine mRNA expression levels (IL-1β, IL-6 and IL-12α) were analysed by qRT-PCR. IL-12α mRNA expression was not detectable in unstimulated cells and data are therefore presented as the average corrected 40-Ct values. IL-1β and IL-6 data are presented as average fold change between unstimulated cells and stimulated cells of six independent experiments ± SEM. a represents data that are statistically significant ($p<0.05$) compared to unstimulated cells, b represents data that are highly significant ($p<0.01$) compared to unstimulated cells, c represents data that are significant ($p<0.05$) compared to LPS-stimulated cells, d represents data that are significant ($p<0.05$) compared to LPS and chRANKL-stimulated cells (Mann-Whitney U test).*

this was not statistically significant compared to levels in unstimulated cells. At 3 and 6 h, IL-6 mRNA expression levels were statistically significantly increased in LPS-stimulated cells. Co-stimulated cells statistically significantly increased IL-6 mRNA expression levels compared to unstimulated cells at 3 and 6 h ($p<0.05$) (Figure 4.7). IL-6 mRNA expression levels in co-stimulated cells were statistically significantly increased compared to those in LPS-stimulated cells at 6 h ($p<0.05$), suggesting that schRANKL enhances IL-6 mRNA expression in mature BMDC. Cells treated with schRANKL alone had a non-significant increase (~5-fold) in IL-6 mRNA expression levels at 3 h but there was no increase at 6 h (Figure 4.7).

The antagonistic effects of soluble chRANK-Fc and chOPG-Fc were determined by their ability to inhibit the schRANKL-mediated upregulation of pro-inflammatory cytokines in BMDC. SchRANKL was pre-incubated with chRANK-Fc or chOPG-Fc 3 h prior to stimulation of cells and IL-1β, IL-6 and IL-12α mRNA expression levels were analysed by qRT-PCR (Figure 4.7). Incubation of schRANKL with either chRANK-Fc or chOPG-Fc inhibited the enhanced pro-inflammatory cytokine mRNA expression levels induced by schRANKL and LPS (Figure 4.7). IL-12α mRNA expression levels were statistically significantly increased in cells co-stimulated with LPS, schRANKL and chRANK-Fc or chOPG-Fc, to those in unstimulated cells at 3 and 6 h ($p<0.05$). The expression levels were not as high as LPS and schRANKL co-stimulated cells. At 6 h, IL-1β mRNA expression levels were significantly increased in LPS, RANKL and chRANK-Fc or chOPG-Fc stimulated cells to those in unstimulated cells ($p<0.05$) and to LPS- or LPS and schRANKL co-stimulated cells ($p<0.05$). For IL-6 mRNA expression, cells stimulated with LPS, schRANKL and chRANK-Fc or chOPG-Fc, had significantly increased levels compared to those in unstimulated cells ($p<0.05$) at both 3 and 6 h and had significantly increased levels compared to those in LPS or costimulated cells ($p<0.05$). Overall, the pro-inflammatory mRNA expression levels mediated by schRANKL in costimulated cells were inhibited by the addition of chRANK-Fc and chOPG-Fc. These data suggest that the soluble receptors of chRANKL can interact with their ligand and block its activity.

SchRANKL-treated cells did not significantly alter pro-inflammatory cytokine mRNA expression levels in BMDC (Figure 4.7). To investigate the possibility that the mRNA expression levels of the anti-inflammatory cytokine, IL-10, were altered by schRANKL treatment, levels were analysed in stimulated BMDC. IL-10 mRNA expression levels was not statistically significantly altered in schRANKL-, LPS- and co-stimulated cells compared to those in unstimulated cells at either 3 or 6 h (Figure 4.8). This ruled out IL-10 for inhibiting of the ability of schRANKL to ehance pro-inflammatory cytokine mRNA expression levels. Next, the mRNA expression levels of chRANKL's receptors, chRANK and chOPG, were analysed by qRT-PCR (Figure 4.8). At 3 h, chOPG mRNA expression levels were increased by ~8-fold in schRANKL-treated cells but were not statistically significantly different compared to levels in unstimulated cells. ChRANK mRNA expression levels were decreased in schRANKL-treated cells levels were not statistically significantly different to levels in unstimulated cells. The data suggest that chRANKL enhances pro-inflammatory cytokine mRNA expression levels in mature rather than immature BMDC.

4.3.7 The effects of chRANKL on pro-inflammatory cytokine mRNA expression levels in BMDM

The bioactivity of schRANKL on BMDM was analysed by examining pro-inflammatory cytokine mRNA expression levels. Cells were unstimulated or simulated with LPS, schRANKL or both, for 3 and 6 h, similarly as previously described for BMDC. IL-12α mRNA expression was not detected in any sample, which may be due to the low concentration of LPS (1 ng/ml) used for this study (data not shown). At 3 h, LPS-stimulated cells increased IL-1β mRNA expression levels significantly by ~50-fold compared to those in unstimulated cells ($p<0.05$) (Figure 4.9). Co-stimulation with LPS and schRANKL increased IL-1β mRNA levels statistically significantly compared to levels in unstimulated cells ($p<0.05$) but not those in LPS-stimulated cells. At 6 h, IL-1β mRNA expression levels were lower in LPS-stimulated cells. Co-stimulated cells had increased IL-1β mRNA expression levels but levels were not statistically significantly different compared to those in unstimulated or LPS-stimulated cells. IL-6 mRNA expression levels were increased in LPS and co-stimulated cells at both 3 and 6 h but levels of expression were not

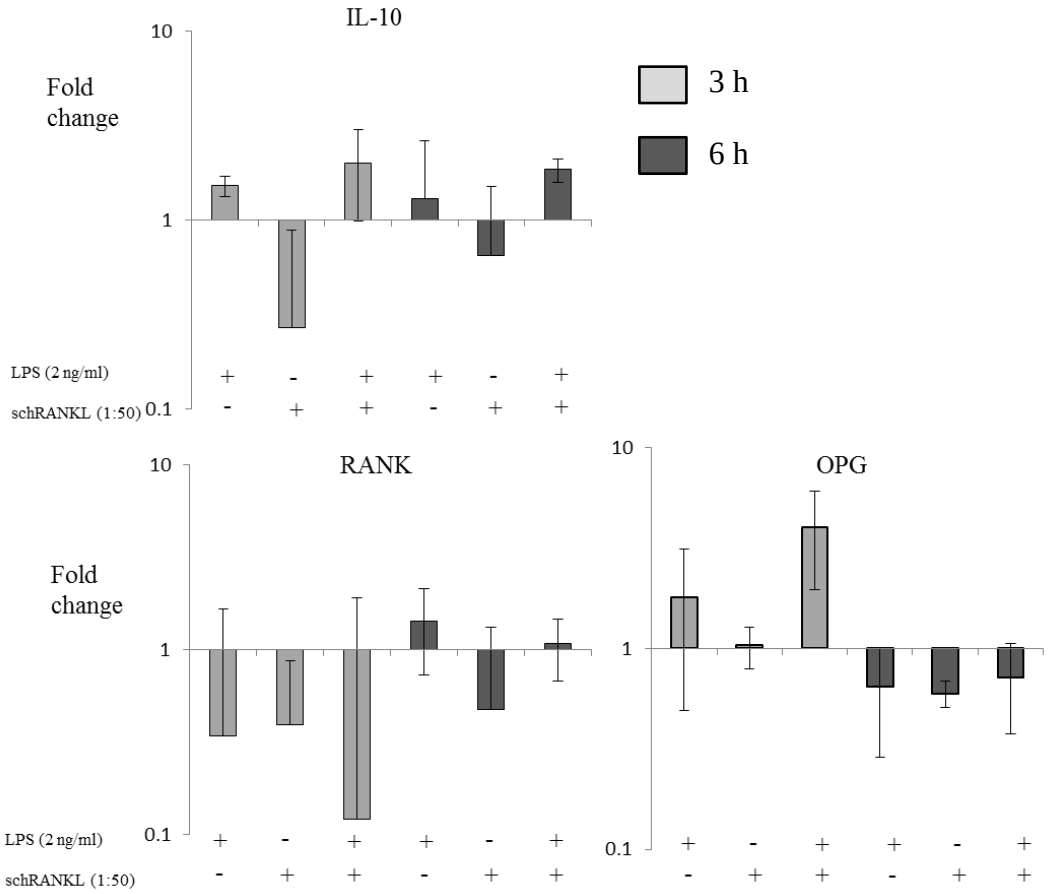

Figure 4.8 IL-10, chRANK and chOPG mRNA expression levels in BMDC stimulated with LPS, schRANKL or both, for 3 and 6 h, as measured by qRT-PCR. *BMDC were stimulated with LPS (2 ng/ml), schRANKL (1:50 ex-COS), or co-stimulated with both, for 3 and 6 h. mRNA expression levels of the anti-inflammatory cytokine, IL-10 and the chRANKL receptors, chRANK and chOPG, were analysed by qRT-PCR. Data are presented as average fold change between unstimulated and stimulated cells of three independent experiments ± SEM.*

statistically significantly different compared to those in unstimulated cells. Similar to BMDC, stimulation of immature BMDM with schRANKL had no effect on the levels of pro-inflammatory cytokine mRNA expression (Figure 4.9).

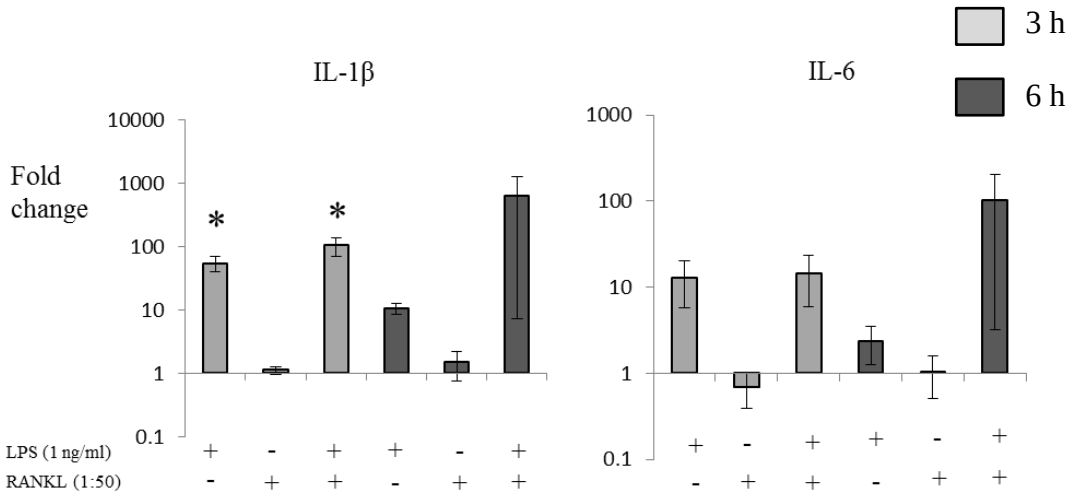

Figure 4.9 Pro-inflammatory cytokine mRNA expression levels in BMDM stimulated with LPS, schRANKL or both, for 3 and 6 h, as measured by qRT-PCR. *BMDM were unstimulated or stimulated with LPS (1 ng/ml), schRANKL (1:50 ex-COS) or both for 3 and 6 h. Pro-inflammatory cytokines (IL-1β and IL-6) were analysed by qRT-PCR. Data are presented as the average fold change between unstimulated and stimulated cells of three individual experiments ± SEM. * represents data that are statistically significant ($p<0.05$) compared to unstimulated cells at 3 h (Mann-Whitney U test).*

4.3.8 ChCD40L and schRANKL do not have synergistic effects on pro-inflammatory cytokine mRNA expression levels in BMDC

CD40L-CD40 interactions have similar characteristics as RANKL-RANK interactions, such as inducing pro-inflammatory cytokine expression in DC. To examine whether stimulating BMDC with two members of the chicken TNF ligand family, chCD40L and schRANKL, could have synergistic effects on pro-inflammatory cytokine mRNA expression levels, BMDC were unstimulated or stimulated with chCD40L or chCD40L and schRANKL for 3, 6 and 24 h (Figure 4.10). Previous data indicated that schRANKL has no effect on pro-inflammatory cytokine mRNA expression levels in immature BMDC; therefore data are not shown. IL-12α mRNA expression was not detected in any sample (data not shown). ChCD40L upregulated IL-1β mRNA expression levels around 2-fold at all

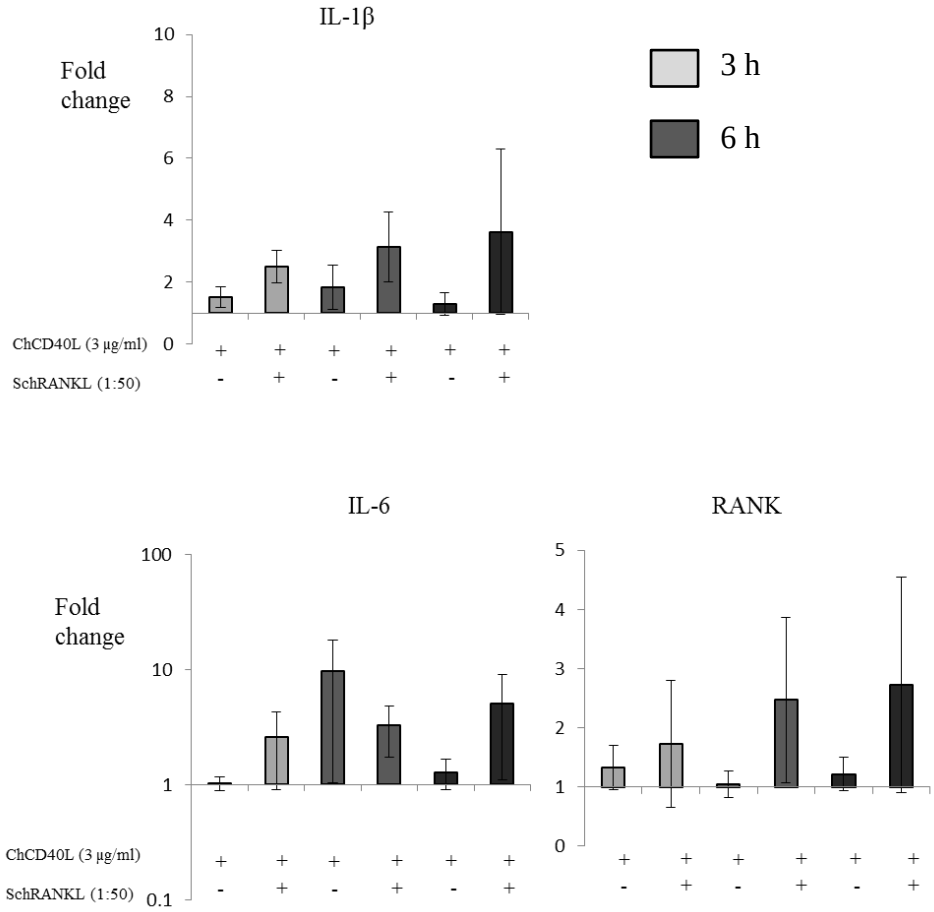

Figure 4.10 Lack of synergistic effects on pro-inflammatory cytokine mRNA expression levels in BMDC stimulated with chCD40L and schRANKL, as measured by qRT-PCR. *BMDC were unstimulated or stimulated with chCD40L (3 µg/ml) or chCD40L and schRANKL (1:50 ex-COS) for 3, 6 and 24 h. IL-1β, IL-6 and chRANK mRNA expression levels were analysed by qRT-PCR. Data are presented as the average of the fold changes between unstimulated cells and stimulated cells of three independent experiments ± SEM.*

time-points (Figure 4.10). Co-stimulated cells had increased IL-1β mRNA expression levels (~3-fold) but these were not statistically significantly different to levels in unstimulated cells or chCD40L-stimulated cells (Figure 4.10). IL-6 mRNA expression levels were increased in co-stimulated cells but were not statistically significantly different to levels in unstimulated cells. ChRANK mRNA expression

levels were not significantly altered by chCD40L stimulation or co-stimulation at any time-point (Figure 4.10).

4.3.9 Phenotype of BMDC treated with schRANKL

To investigate the ability of schRANKL to alter the expression of cell surface markers on BMDC, cells were treated with LPS (2 ng/ml), schRANKL (1:5 exCOS-7) or both, for 24 h (Figure 4.11). Cells were removed from culture plates and stained for the following chicken APC activation markers; MHC class II, CD40 and the chicken mononuclear phagocyte marker, KUL01 (Mast *et al*., 1997). Cells were stained with a viability dye, 7-AAD, prior to FACs to exclude dead cells from the data analysis (Appendix 4, figure 3). The histograms compare antigen staining with isotype controls (Figure 4.11A) while barcharts indicate the average geometric mean fluorescence intensity of four individual experiments (Figure 4.11B). Although a previous study demonstrated that MHC class II was constitutively expressed on chicken BMDC, either unstimulated or stimulated with LPS (200 ng/ml) (Wu *et al.*, 2010), the expression of MHC class II was not altered by the sub-optimal maturation of BMDC with the LPS concentration (1 ng/ml) used in this study (Figure 4.11). Co-stimulation of cells with LPS and schRANKL or with schRANKL alone did not increase the surface expression levels of MHC class II. CD40 expression levels were increased in LPS-stimulated cells and were slightly enhanced by the addition of schRANKL but not to a statsically significant level (p=0.4) (Figure 4.11). The expression of KUL01 decreases as BMDC mature (Wu *et al.*, 2010) and this was evident in the LPS-stimulated cells where a portion of the cell population lost the expression of KUL01. Co-stimulated cells had similar levels of KUL01 expression as the LPS-stimulated cells, indicating that schRANKL may not contribute to enhancing the maturity of BMDC. Overall there no statistically significant alternation in the phenotype of BMDC treated with schRANKL.

4.3.10 Phenotype of BMDM treated with schRANKL

BMDM were stimulated with LPS (1 ng/ml), schRANKL (1:5 exCOS-7) or both, for 24 h and analysed by FACS (Figure 4.12). Similar to BMDC, MHC class II expression levels were not significantly increased by the sub-optimal maturation of

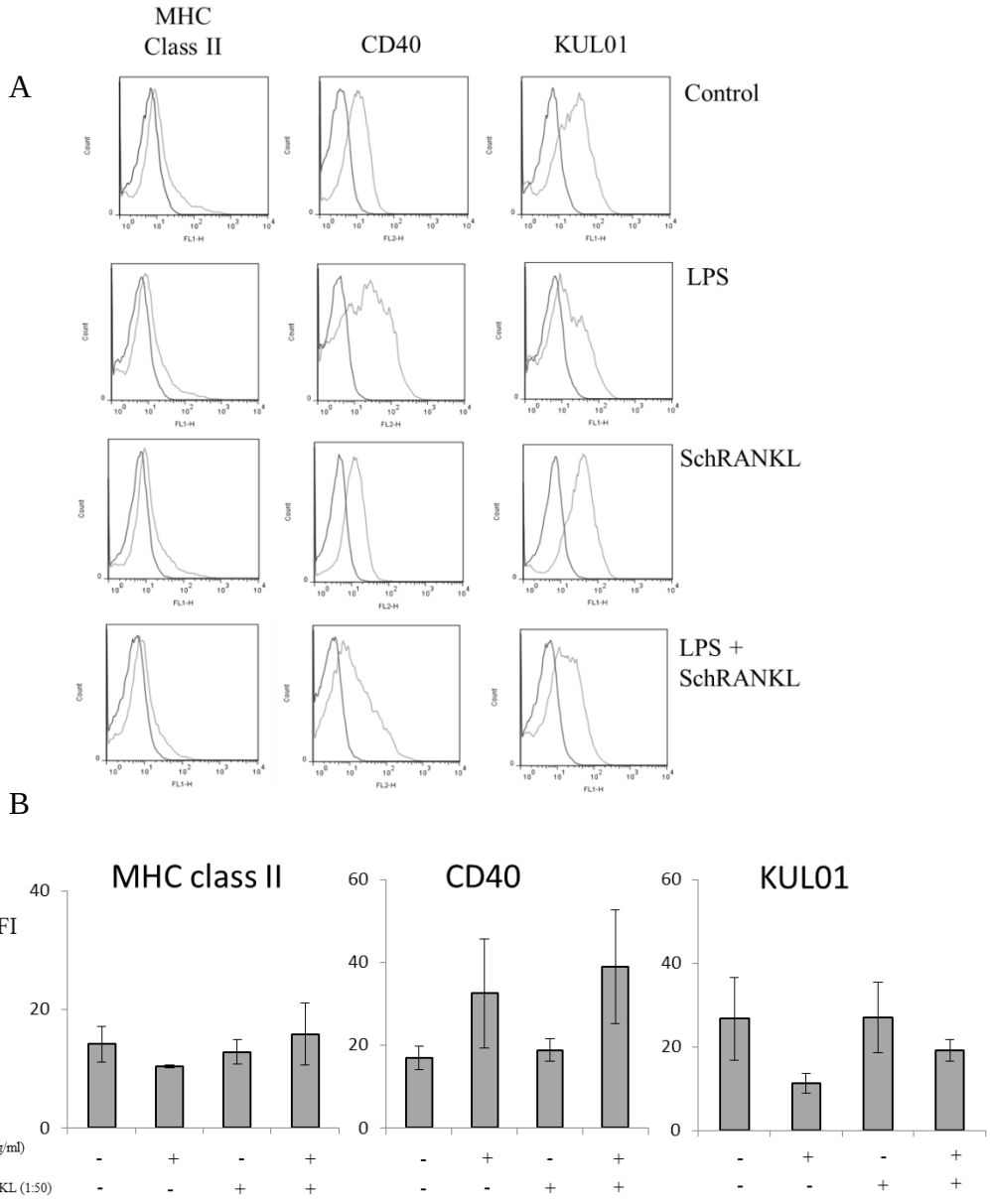

Figure 4.11 FACS analysis of BMDC stimulated with LPS and schRANKL for 24 h. *BMDC were unstimulated or stimulated with LPS (2 ng/ml), schRANKL (1:5 ex-COS) or both for 24 h. Cells were stained for activation markers (MHC class II, CD40 and KUL01) using mouse anti-chicken monoclonal antibodies and isotype controls and analysed by FACs.* **A)** *Data are represented as histograms comparing isotype controls (black lines) to surface staining (grey lines) and are representative of four independent experiments with similar results.* **B)** *Data are represented as the average geometric0mean fluorescence (GEO-MFI) of four independent experiments ± SEM.*

BMDM with LPS (1 ng/ml) alone or in combination with schRANKL (Figure 4.12). CD40 expression levels were increased in LPS-stimulated cells but were not enhanced by the addition of schRANKL (Figure 4.12A). KUL01 expression levels were decreased in LPS-stimulated cells compared to unstimulated cells and were not altered by the addition of schRANKL. Similarly to BMDC, schRANKL alone did not affect the expression levels of cell surface activation markers on BMDM. As there was no major difference in the expression levels of surface markers on BMDM stimulated with LPS and schRANKL, a more potent activator of macrophages, IFN-γ, was used to analyse the effects of schRANKL on mature BMDM.

As previous data indicated (Figure 4.12), schRANKL alone has no effect on the phenotype of BMDM and therefore this analysis is not shown. BMDM were unstimulated or stimulated with IFN-γ (1:100 exCOS) or IFN-γ and schRANKL, for 24 h and analysed by FACS. BMDM stimulated with IFN-γ increased surface expression of MHC class II indicating the potency of IFN-γ in stimulation of chicken macrophages (Figure 4.13). MHC class II expression levels on co-stimulated cells were increased compared to levels on unstimulated cells but were not significantly enhanced compared to levels on IFN-γ-stimulated cells (Figure 4.13). CD40 expression levels were increased in IFN-γ-stimulated cells and statistically significantly increased in co-stimulated cells compared to levels in unstimulated cells ($p=0.03$) (Figure 4.13). However, co-stimulated cells CD40 expression levels were slightly increased but were not statistically significantly altered compared to levels in IFN-γ-stimulated cells (Figure 4.13). KUL01 expression levels were statistically significantly decreased on IFN-γ and costimulated cells compare to levels in unstimulated cells. There were no statistically significant differences in levels between co-stimulated cells and IFN-γ-stimulated cells. Overall the data suggest that schRANKL does not stimulate differential expression of surface activation markers on BMDM.

4.3.11 Survival of BMDC treated with schRANKL

RANKL was first identified as a survival factor for DC (Anderson *et al.*, 1997; Wong *et al.*, 1997; Josien *et al*., 2000) through the anti-apoptotic serine/threonine kinase Akt/protein kinase B pathway (Wong *et al.*, 1998). To

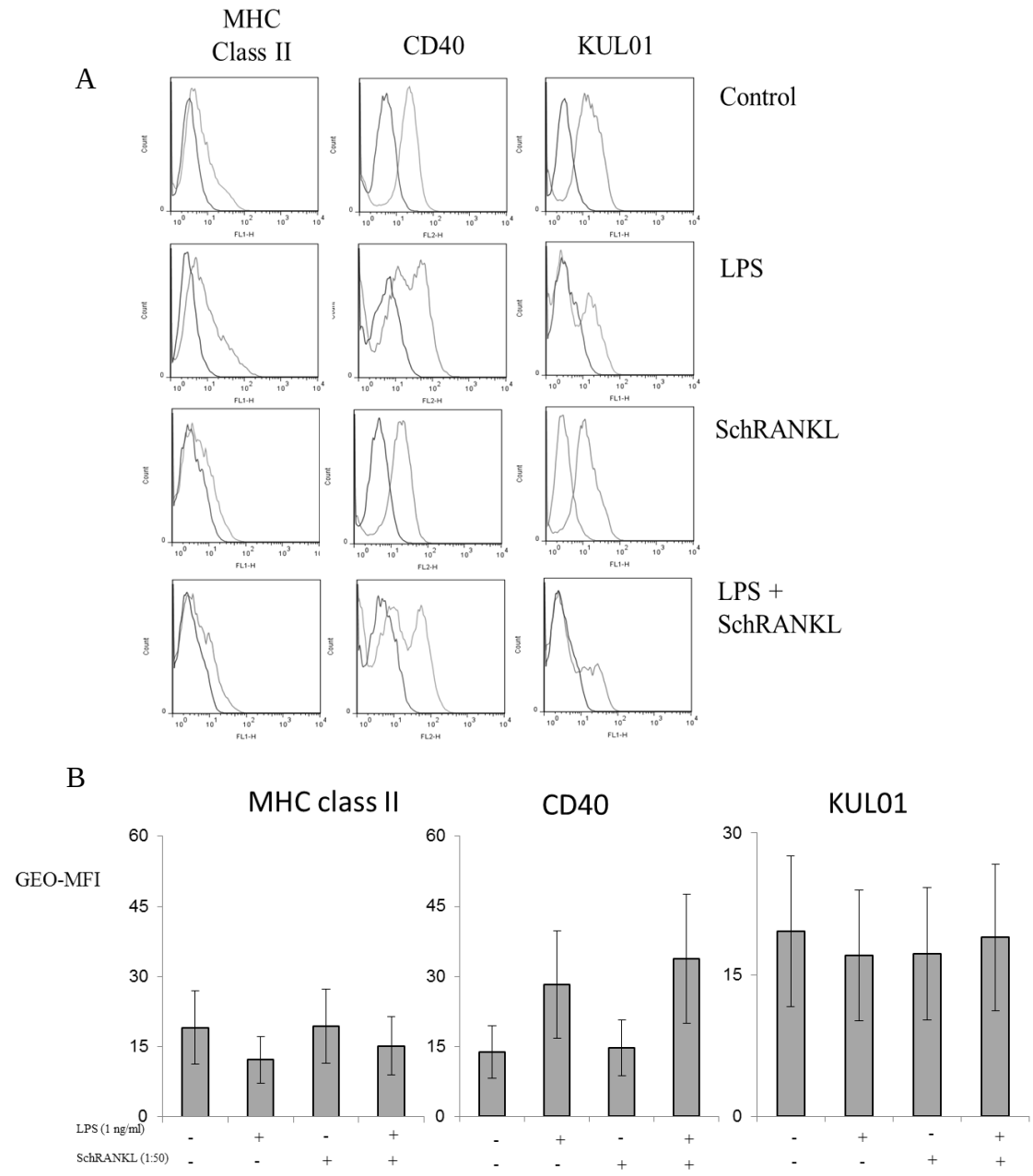

Figure 4.12 FACS analysis of BMDM stimulated with LPS and schRANKL for 24 h. *BMDM were unstimulated (control) or stimulated with LPS (1 ng/ml), schRANKL (1:5 ex-COS) or both for 24 h.* **A)** *Data are presented as histograms comparing isotype controls (black lines) to surface staining (grey lines) and are representative of four independent experiments with similar results.* **B)** *Data are represented as the average geometric-mean fluorescence intensity (GEO-MFI) of four independent experiments ± SEM.*

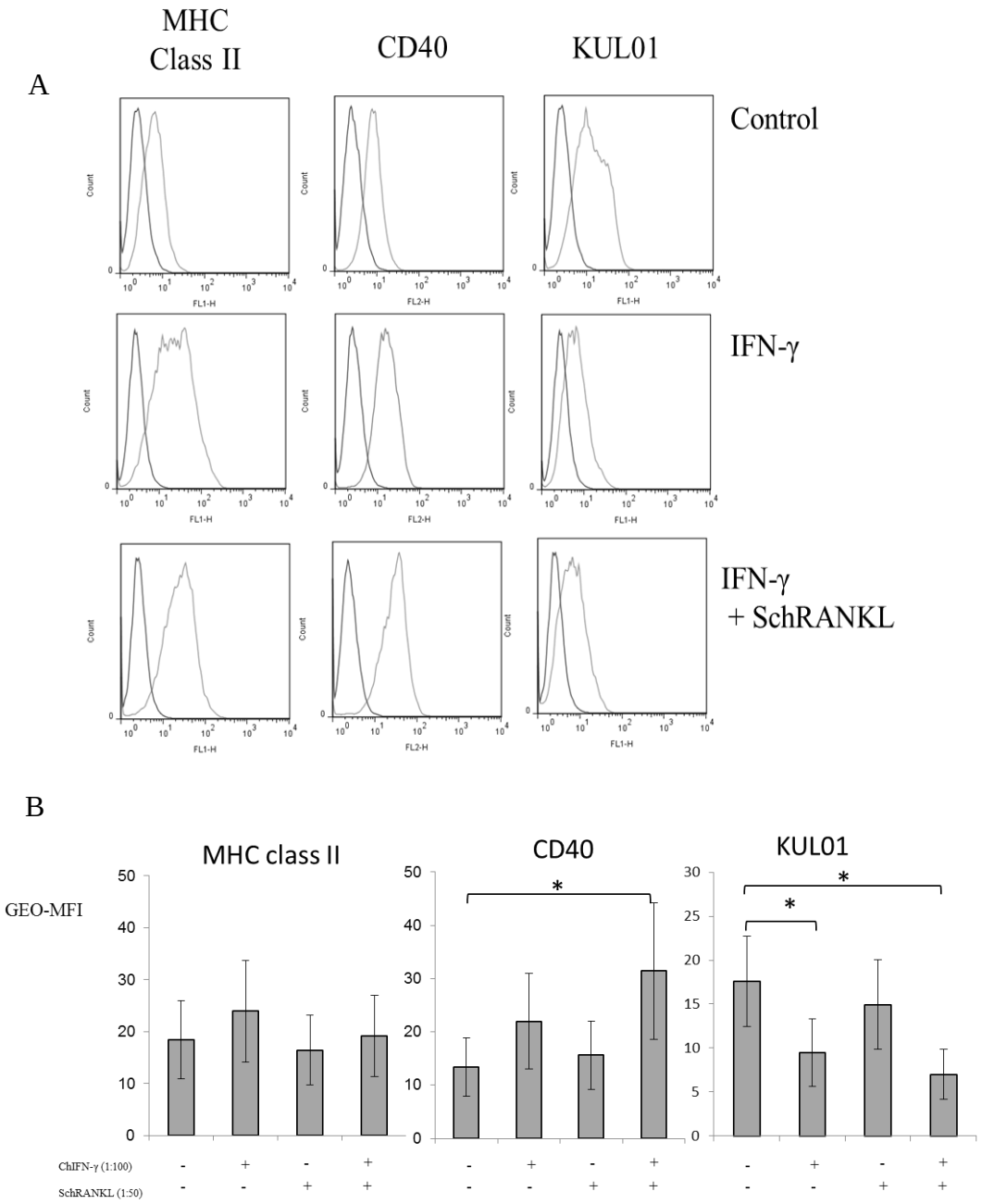

Figure 4.13 FACS analysis of BMDM stimulated with LPS and schRANKL for 24 h. *BMDM were unstimulated (control) and stimulated with LPS (1 ng/ml), schRANKL (1:5 ex-COS) or both for 24 h.* **A)** *Data are presented as histograms comparing isotype controls (black lines) to surface staining (grey lines) and are representative of six independent experiments with similar results.* **B)** *Data are represented as the average geometric-mean fluorescence intensity (GEO-MFI) intensity of six independent experiments ± SEM. *p<0.05(Mann-Whitney U test).*

examine whether chRANKL was a survival factor for BMDC, cells were treated with or without schRANKL (1:5 and 1:10 exCOS-7) for 24 and 48 h (Figure 4.14). Cell death and apoptosis were measured by Annexin-V and PI staining and analysed by FACs. Annexin-V and PI staining are commonly used to determine viable, apoptotic, necrotic and dead cells by flow cytometry. The PI stain can only enter cells that have damaged cellular membranes, so viable cells or cells undergoing early apoptosis cannot be stained with PI due to the nature of the cell death mechanism. Annexin-V can only bind to PS, which is usually found on the inner membrane of the cell and upon apoptosis-inducing signals flips to the outer membrane. This occurs at the early stages of apoptosis (Fadok *et al*., 1992).

After 24 h, 43% of untreated cells were viable (Annexin-V^-PI^-) and 42.8% positive for annexin-V (Annexin-V^+ + Annexin-V^+PI^+) (Figure 4.14). This indicates that nearly half of the cell population analysed under normal conditions were undergoing apoptosis. In contrast, 1:5 schRANKL-treated cells had 56.2% viable cells and 29.7% undergoing apoptosis. The 1:10 schRANKL-treated cells had similar levels of live cells (45.3%) and cells undergoing apoptosis (41.4%) as the untreated cells, indicating that the ability of schRANKL to enhance cell survival is dose-dependent. Although not statistically significant (n=3) (p=0.07), it is clear that schRANKL does enhance the survival of BMDC after 24 h of treatment compared to untreated cells. After 2 days (48 h), the number of viable untreated cells fell to 28.9% in comparison to schRANKL-treated cells where 37.2% were viable (Figure 4.14). The survival rates of 1:10 schRANKL-treated cells were similar to untreated cells at 48 h (Figure 4.14). Cells undergoing apoptosis in untreated cells increased to 56.4% but for schRANKL-treated cells apoptotic cells were 48.5%. Cells undergoing apoptosis reached 63% in 1:10 schRANKL-treated cells. Overall the data suggest that schRANKL acts as a survival factor for chicken BMDC.

4.3.12 Survival of BMDM treated with schRANKL

BMDM survival rates were analysed after 24 and 48 h of schRANKL treatment by FACs (Figure 4.15). After 24 h, cells untreated with schRANKL had very low number of viable cells (15.1%) whereas 1:5 and 1:10 schRANKL treated

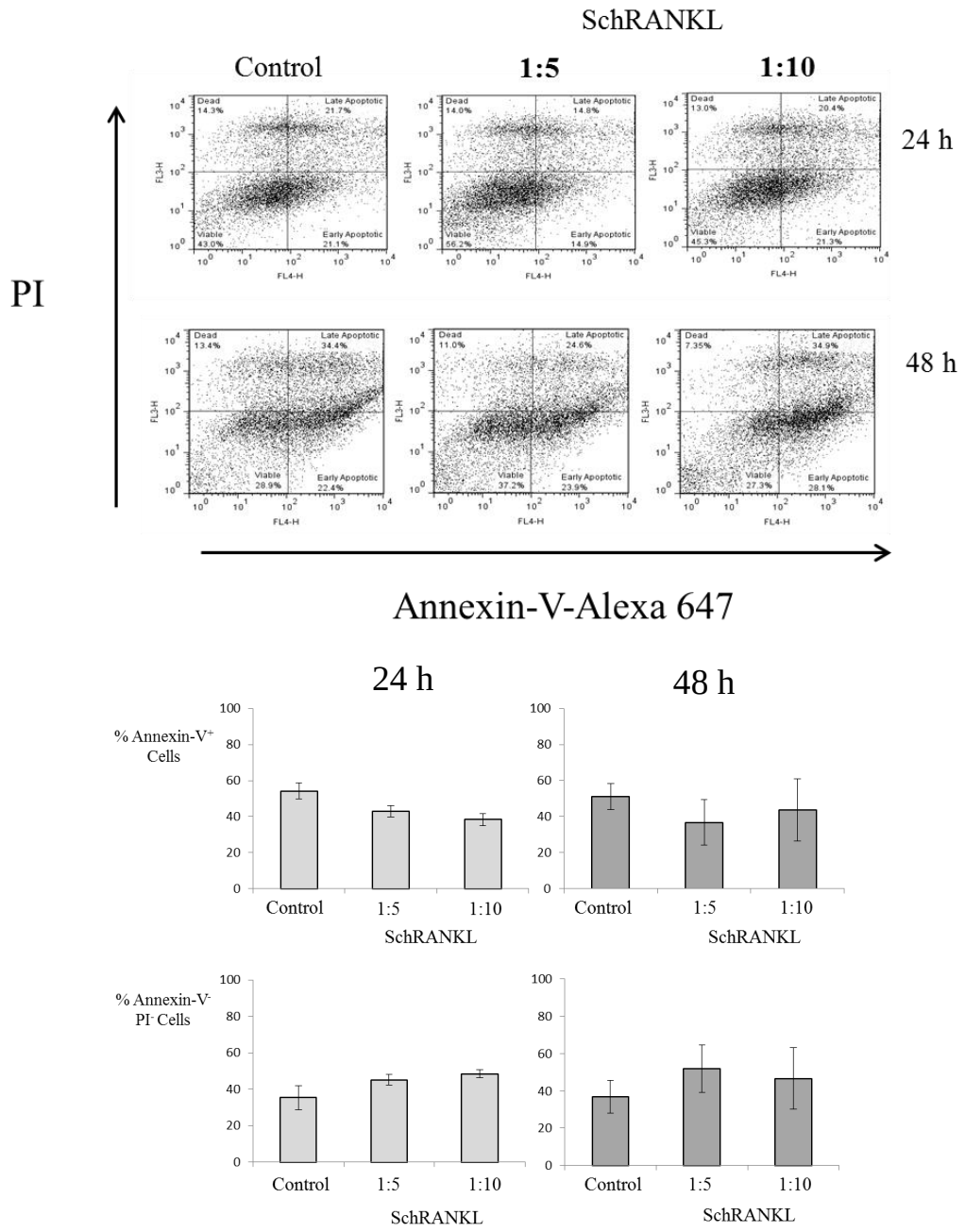

Figure 4.14 Survival of BMDC treated with schRANKL for 24 and 48 h. *BMDC were untreated or treated with schRANKL (1:5 or 1:10 ex-COS) for 24 and 48 h and cell survival was analysed by FACS after staining cells for Annexin-V (Alexa-647) and PI. Individual data are presented as dot plots (top) and data are summarised as bar charts representing the average percentages of Annexin-V$^+$ (apoptotic) and Annexin-V$^-$ and PI$^-$ (viable) cells of three independent experiments ± SEM (bottom).*

BMDM viability numbers were 29.5% and 30.2%, respectively. However, when apoptotic cell numbers were analysed in these cells, untreated and schRANKL-treated cells had similar percentages of cells undergoing cell death (Figure 4.15). A further 24 h of cell culture led to similar numbers of viable and apoptotic cells between untreated and schRANKL-treated cells. The average of three independent experiments indicates that after 48 h, cells treated with schRANKL had higher percentages of annexin-V^+ cells compare to control cells (Figure 4.15). Although the data are not statistically significant (n=3), there is evidence that schRANKL can enhance the survival of BMDM after 24 h of exposure but this enhanced survival is short-lived, as cells begin to undergo normal rates of apoptosis after 48 h.

4.3.13 Phagocytosis

As APCs, phagocytosis is an important function for DC. The effect of schRANKL on the phagocytic activity of BMDC was analysed by treating cells with schRANKL 24 h prior to exposure to zymosan A-FITC particles. The particles were incubated with untreated or schRANKL-treated cells for 1 h at 4°C or 41°C. Phagocytosis was inhibited by the addition of ice-cold PBS to the cells and the cells were then washed with trypan blue to quench external FITC expression. Cells were washed several times with PBS and the presence of ingested particles analysed by flow cytometry.

Cells incubated at 4°C did not phagocytose the zymosan A particles (control for surface binding) (Figure 4.16). When cells were exposed to the particles and incubated at 41°C, both untreated and treated BMDC ingested the particles. Cells pre-treated with schRANKL for 24 h had statistically significantly higher uptake of particles in comparison to the untreated cells ($p<0.01$). Although the previous data indicated that schRANKL did not enhance surface expression of antigen presenting MHC class II surface molecules, schRANKL can augment the phagocytic activity of BMDC. Murine BMDM can commit to the osteoclast lineage after 24 h of RANKL treatment and still have phagocytic potential (Mochizuki *et al.*, 2006). The BMDC cultures treated with schRANKL formed cluster of cells, whereas the untreated cells did not (Figure 4.17). BMDC cultures are heterogeneous and there could potentially be osteoclasts forming within these cultures when treated with schRANKL for 24 h.

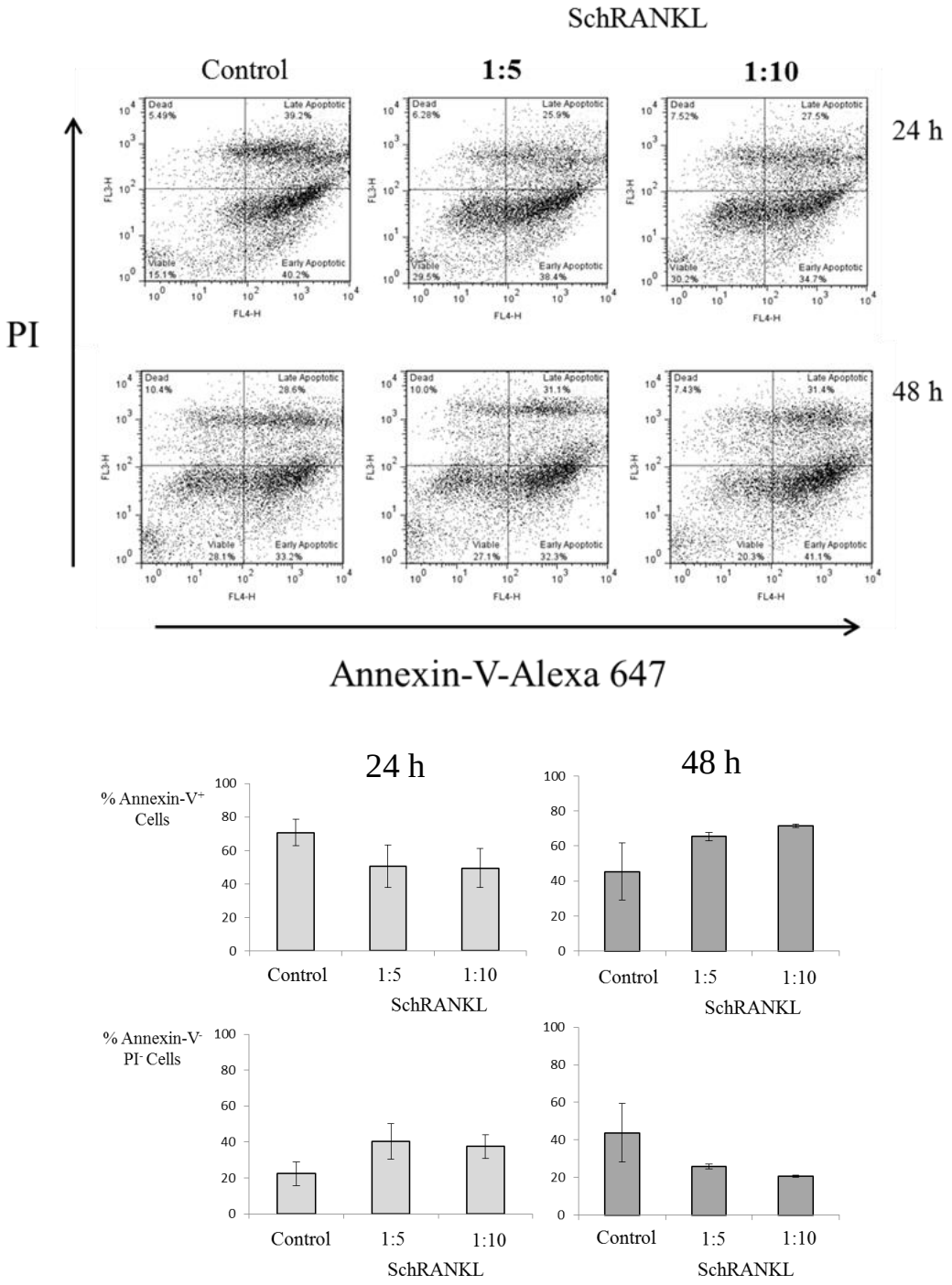

Figure 4.15 Survival of BMDM treated with schRANKL for 24 and 48 h. *BMDM were untreated or treated with schRANKL (1:5 or 1:10 ex-COS) for 24 and 48 h and cell survival was analysed by FACS after staining cells for Annexin-V (Alexa-647) and PI. Individual data are presented as dot plots (top) and bar charts representing the average percentages of Annexin-V$^+$ (apoptotic) and Annexin-V$^-$ and PI$^-$ (viable) cells of three independent experiments ± SEM (bottom).*

4.3.14 Pilot study: ChRANKL and osteoclasts

Since the discovery of mammalian RANKL, several studies have identified its requirement for osteoclast differentiation and activation (e.g. Simonet *et al.,* 1997; Yasuda *et al.,* 1998). Although the aim of this study was to investigate the bioactivity of chRANKL on chicken APCs, preliminary experiments were carried out towards establishing a protocol for differentiating chicken bone marrow cells into multinucleated osteoclasts. Osteoclast cells are derived from the mononuclear/macrophage lineage. Therefore, to drive bone marrow cells towards this lineage, cells were incubated with chCSF-1 for 2 days. On day 2, cells were removed from cultured plates, reseeded at 5 X 10^4 cells/well in 6-well plates and either untreated or treated with schRANKL (1:10 ex-COS) for 8 days. Twenty-four h after reseeding, an adherent monolayer of cells formed on the cultured plates (Figure 4.18A). There was no difference in cell numbers or cell clumping between untreated and schRANKL-treated cells (Figure 4.18A). After 4 days of culture, untreated cells became less confluent compared to schRANKL-treated cells. This could be linked to schRANKL being a survival factor for these undifferentiated cells, as it is for BMDC. On day eight, non-adherent cells were removed by gentle washing with PBS and stained with the nuclear stain Hoescht-33258. Stained cells were analysed by UV illumination to visualise multinucleated cells (Figure 4.18B). Untreated cells did not have multinucleated cells. However, schRANKL-treated cells had numerous large, multinucleated cells (Figure 4.18B). Although no functional studies were carried out on these cells for this study, these cells do express high amounts of chRANK mRNA and absorb bone (Garcia-Morales, unpublished results). This preliminary study indicates that schRANKL can differentiate bone marrow cells into osteoclasts.

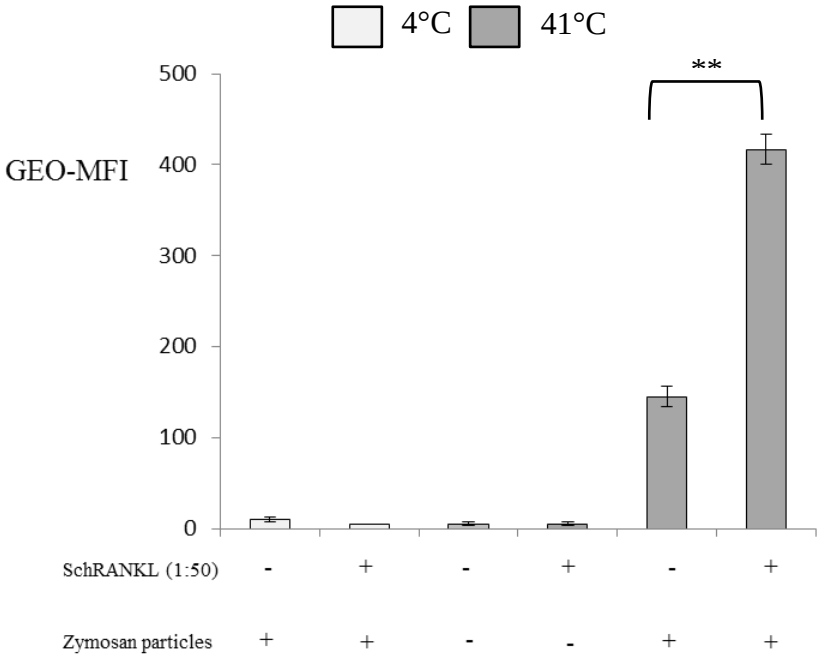

Figure 4.16 Phagocytosis by BMDC treated with schRANKL, analysed by FACS. *BMDC were untreated or pre-treated with schRANKL (1:50 exCOS-7) 24 h prior to exposure to zymosan A-FITC particles for 1 h at 4°C or 41°C. Particle ingestion was analysed by FACs. Data are presented as the average geometric-mean fluorescence intensity (GEO-MFI) of four independent experiments ± SEM. **p<0.01 (Student's t-test).*

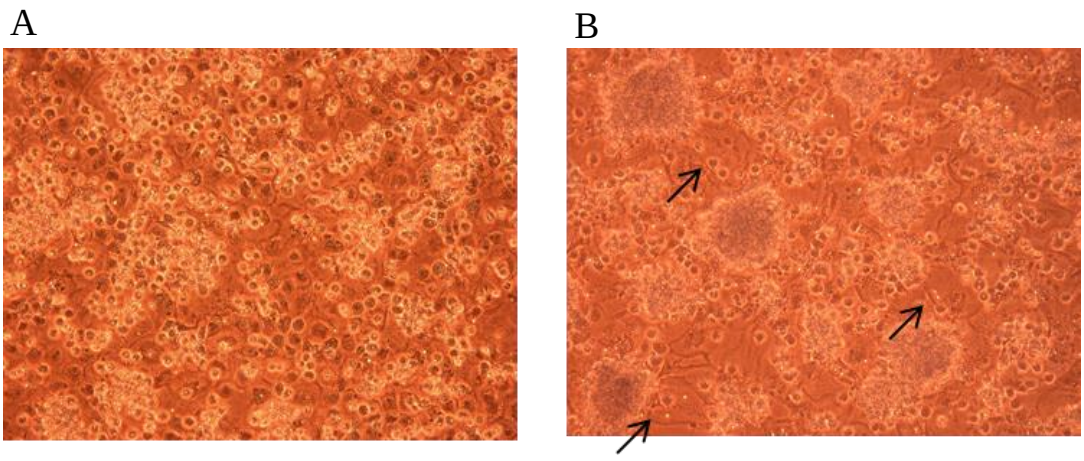

Figure 4.17 BMDC treated with schRANKL for 24 h. *BMDC were* **A)** *untreated or* **B)** *treated with schRANKL (1:50 ex-COS-7) for 24 h. Arrows indicate large cells underneath cell clumps in schRANKL-treated BMDC.*

4.4 Discussion

ChRANKL, chRANK and chOPG mRNA expression levels were ubiquitous across a range of lymphoid and non-lymphoid tissues and immune cells in the chicken. Studies examining the mRNA expression levels of mammalian RANKL are based on northern blot analysis. RANKL mRNA transcripts were only detected in the thymus and lymph nodes of mice (Wong *et al*., 1997). Mammalian OPG expression was not observed in the brain, muscle, thymocytes or naïve T and B cells (Yun *et al*., 1998). qRT-PCR is more sensitive than northern blot, and it would be interesting to revisit the expression of these molecules in mammals.

In the bone marrow, all three molecules were highly expressed at the mRNA level, which was not surprising as all three have vital roles in bone metabolism in mammalian species (Simonet *et al.*, 1997; Yasuda *et al.*, 1998). In non-lymphoid organs, chRANKL and chRANK mRNA expression levels were highest in muscle tissue, similar to mammalian RANKL and RANK (Anderson *et al.*, 1997; Wong *et al.*, 1997). The heart had the lowest mRNA expression levels of all three molecules amongst the non-lymphoid tissues examined. In contrast, mammalian OPG expression was strongest in smooth muscle tissue and the heart, which suggested that it may have a role in vascular development (Simonet *et al.*, 1997; Yun *et al.*, 1998). $OPG^{-/-}$ mice suffer from calcification of the renal arteries and aorta (Bucay *et al.*, 1998), due to OPG regulating RANKL-dependent IL-6 expression which promotes calcification (Callegari *et al.*, 2014).

In the spleen, mRNA expression levels of chRANKL, chRANK and chOPG levels were all similar. The chicken spleen contains a heterogeneous mix of T and B lymphocytes, macrophages and DC (Jeurissen, 1993; Quéré *et al.*, 2013). Purified splenocytes were also examined for the levels of chRANKL, chRANK and chOPG mRNA expression, either in unstimulated or in ConA-stimulated cells over four time-points. ConA stimulation did not significantly alter the mRNA expression levels of the three molecules compared to the levels in unstimulated cells (Figure 4.2A) but the culture conditions led to an increase in expression of all these molecules after 18 and 24 h. It may be as cells are cultured in media they undergo physiological changes, such as growth, differentiation or apoptosis, leading to the upregulation of

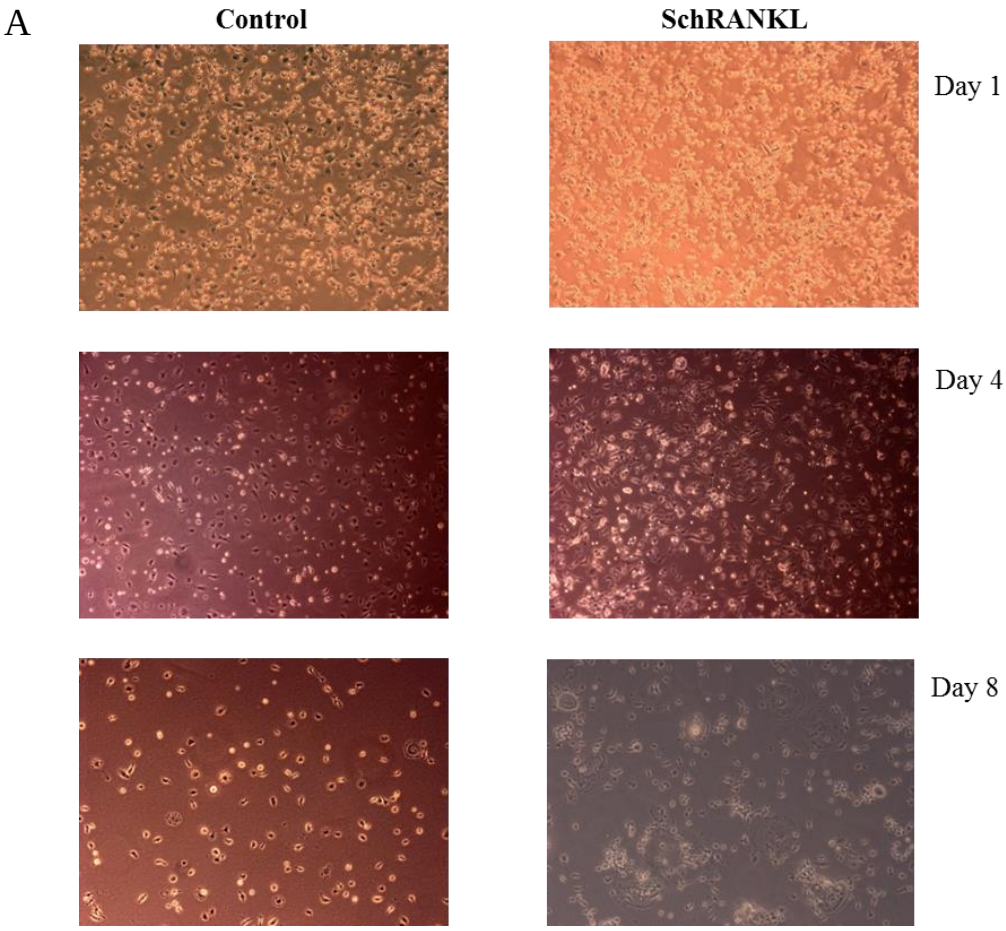

Figure 4.18 Differentiation of bone marrow cells into osteoclast cells by schRANKL. A) *Bone marrow cells were incubated for 2 days with rchCSF-1 and reseeded at 5 X* 10^4 *cells/ml with schRANKL (1:10 ex-COS) for up to 8 days.* **B)** *Hoechst*-33258 *staining of schRANKL-treated cells at day 8 of culture.*

these TNF and TNFR superfamily members. In mice, the co-culture of T cells and splenocytes stimulated with ConA induces osteoclast differentiation (Horwood *et al.,* 1999). It was not determined if this occurred in the chicken cultures but it could be the cause of the increase in the mRNA expression levels of the three molecules over time.

The mRNA expression levels of chRANKL, chRANK and chOPG were analysed in T cell subsets purified from chicken spleens (Figure 4.4). qRT-PCR analysis indicated that chRANKL mRNA expression levels were higher compared to those for chRANK and chOPG in $CD4^+$, $CD8\beta^+$, $TCR\gamma\delta^+$ and $TCR\alpha\beta1/\alpha\beta2^+$ cells. In murine lymph node-derived T cells, RANKL mRNA was not detected in resting $CD4^+$ or $CD8^+$ T cells but was expressed in $CD44^+$ memory T cells (Josien *et al.,* 1999). Mammalian RANKL cell surface expression was also identified on both stimulated murine Th1 and Th2 cell clones, with expression levels higher on Th1 cell clones. IL-4 treatment decreases the surface expression of RANKL, verifying that it is predominantly a Th1 surface marker (Josien *et al.,* 1999; Chen *et al.,* 2001). RANK surface expression was also detected on T cells but at much lower levels than its ligand (Josien *et al*., 1999). RANKL and RANK are not required for Th1/Th2 dichotomy but are required for optimal cytokine production in antigen receptor-activated Th1 cells (Kong *et al.,* 1999a; Chen *et al.,* 2001). $RANKL^{-/-}$ $CD4^+$ T cells produce lower levels of IL-4, IL-5, IL-6, IFN-γ and IL-2 (Kong *et al.*, 1999a). RANKL reverse-signalling has been linked to enhanced production of IFN-γ in Th1 cells, which in turn has been linked to activation of the p38 MAPK pathway (Chen *et al.*, 2001). Mammalian $CD4^+$ T cells express both the membrane and soluble forms of RANKL, and both can induce osteoclastogenesis (Kong *et al.,* 1999b). Various studies have shown that T cell-mediated inflammation is linked to arthritis in humans with symptoms of cartilage and bone erosion, severe joint pain and crippling (reviewed by Feldmann *et al.,* 1996). Having identified RANKL expression on the surface of activated $CD4^+$ T cells, Kong *et al*. (1999b) examined the expression of RANKL in adjuvant-induced arthritis in rats (Lewis rats). Within the hind paw of these rats, synovial and inflammatory cells expressed RANKL mRNA and $CD4^+$ inflammatory T cells expressed surface RANKL. When RANKL was blocked using OPG, bone and cartilage erosion were inhibited but not pro-inflammatory cytokine

expression, indicating that RANKL was the key mediator of joint destruction and bone loss in adjuvant arthritis (Kong *et al.,* 1999b). Although there is a lack of Th cell clones in the chicken, antibodies against chRANKL could help identify and differentiate between Th subsets.

ChRANKL mRNA expression levels were much higher than those of its receptors in both the upper-gut and Harderian gland (Figure 4.1). The intestinal surface is physically protected by tightly joined epithelial cells preventing enteric antigen from penetrating the host. Along the intestinal tract there are nodules or lymphoid follicles, such as Peyer's patches, Meckel's diverticulum and caecal tonsils, which are overlaid with epithelia required for immune surveillance. In the gut-associated lymphoid tissues (GALT), sampling of lumenal pathogens is achieved by M cells (reviewed by Mabbott *et al*., 2013). M cells are highly efficient phagocytic cells that uptake bacterial antigen from the lumen into the Payer's patches, priming $CD4^+$ T cells and IgA^+-committed B cells (VanCott *et al.,* 1996). RANKL is necessary for the differentiation of RANK expressing enterocytes into M cells (Knoop *et al.,* 2009). It would be interesting to determine if the high levels of chRANKL mRNA expressed in the upper gut correlated with the presence of large numbers of M cells in this tissue.

The Harderian gland is the major eye-associated lymphoid tissue and is rich in plasma cells at different stages of maturation. Birds used for the study were 6-weeks of age, coincident with high rates of plasma cell proliferation in the Harderian gland. In the chicken, the bursa of Fabricius is a specialised organ containing naïve B cells. qRT-PCR analysis indicated that all three molecules were similarly expressed in the bursa of Fabricius (Figure 4.1). Interestingly, in the kinetic studies where B cells were stimulated with ionomycin and PMA to activate MAPK kinases and the PKC pathway, inducing B cell proliferation, differentiation and effector functions, chRANK and chOPG mRNA expression levels were much lower than the levels of chRANKL mRNA expression. Notably, bursal cells had the highest levels of chRANKL mRNA expression compared to purified splenocytes and thymocytes. Early studies on bursal development found that epithelial tuffs overlaying the B cell follicles appear to be structurally and functionally similar to M cells (Bockman &

Copper, 1973). Mice with a germline deletion of either RANK or RANKL have serious defects in B cell development (Dougall *et al*., 1999; Kong *et al*., 1999) and mammalian RANKL is expressed on the surface of pre-B cells, where its expression is controlled by IL-7 (Kato *et al*., 2003). $OPG^{-/-}$ B cells have greater responses to IL-7 stimulation and higher numbers of pro-B cells and peripheral B cells compared to $OPG^{+/-}$ mice (Yun *et al.,* 2001). In a more recent study in $RANK^{-/-}$ mice (Perlot & Penninger, 2012), B cells were present in both the bone marrow and spleen and were of similar frequencies and types compared to B cells in wild-type mice. This strongly supported the hypothesis that in $RANKL^{-/-}$ and $RANK^{-/-}$ mice, defective B cell development may be due to the nature of osteoporosis where bones are denser and lack cavities, therefore creating secondary disorders not directly linked to RANKL-RANK signalling. In the chicken, B cell lymphopoiesis occurs in the bursa of Fabricius but early B cell progenitors have been identified in the embryonic, but not the adult, bone marrow. Two other TNF superfamily members are required for chicken B cell survival and proliferation, BAFF (Schneider *et al*., 2004) and CD40L (Kothlow *et al.,* 2008). ChRANKL may be a potential marker for identifying pro-B cells in the chicken, along with monoclonal antibodies against chicken IL-7Rα (van Haarlem *et al*., 2009).

In the chicken the highest levels of chRANKL mRNA expression were detected in the thymus, similarly to mammalian RANKL (Wong *et al.,* 1997). The development of T cells within the thymus depends on two cell types, cTEC and mTEC. TCR-expressing T cells are presented with peptide antigens expressed on both cell types, with cTEC required for positive selection and mTEC required for negative selection (Nitta *et al.,* 2008). mTEC are distinguished by the expression of the autoimmune regulator (AIRE), a transcriptional regulator required for the expression of tissue-specific antigens (TSA) and clonal deletion (Derbinski *et al*., 2001; reviewed by Kyewski & Klein, 2006), and are also distinguished by surface expression of MHC class II, CD80 and UEA-1 (Rossi *et al.,* 2007). mTEC express a wide range of TSA that bind to the TCR with either high affinity leading to apoptosis (negative selection) or with intermediate affinity which are then diverted to the regulatory T cell pool. A number of cytokines are involved in the development of mTEC including LT-β, CD40L (Dunn *et al*., 1997) and RANKL (Rossi *et al*., 2007).

TRAF6-dependent downstream NF-κB activation is required for mTEC development (Akiyama *et al.,* 2005) and the cell surface receptor required for that signalling is RANK (Rossi *et al*., 2007). Although the development of the medullary region of the thymus does not require RANKL-RANK interaction, $AIRE^+$ mTEC do require these cytokines in adult mice (Akiyama *et al.,* 2008). Mammalian RANKL is not expressed on the surface of $CD4^+CD8^+$, $CD4^+CD8^-$, $CD4^-CD8^+$ or $CD4^-CD8^-$ thymocytes but is expressed on LTi cells (Rossi *et al*., 2007). Although LTi cells have yet to be identified in the chicken, their identification may be possible in the future with the use of monoclonal antibodies against chRANKL.

The initial data suggested that ConA stimulation of splenocytes had no significant effect on the transcription of chRANKL. The expression of RANKL by mammalian T cells is induced by their activation and dependent on Ca^{2+} mobilisation (Wang *et al*., 2002). To understand whether the mechanism of chRANKL expression was conserved between mammals and birds, chicken splenocytes were stimulated with the intracellular calcium modulator, ionomycin, and the PKC activator, PMA, which mimic TCR activation, for 2, 4 and 18 h and levels of chRANKL mRNA expression were analysed by qRT-PCR (Figure 4.6A). In co-stimulated cell the levels of chRANKL mRNA expression were significantly increased at 4 and 18 h indicating that ionomycin and PMA work in synergy to induce chRANKL mRNA expression. In murine T cells, ionomycin alone was sufficient to induce RANKL expression and no synergy was found when cells were costimulated with ionomycin and PMA, although northern blot analysis was used and levels were not quantified (Wang *et al.,* 2002). In similar studies, murine T cell hybridomas weakly induced RANKL after PMA stimulation but a combination of PMA and ionomycin synergised and induced higher levels of RANKL expression (Fionda *et al.,* 2007; Bishop *et al*., 2011). TCR activation induced RANKL expression in T cells 2 h after activation and lasted up till 96 h (Josien *et al.,* 1999).

Calcium levels control a number of biological activities, such as gene expression, proliferation, differentiation and apoptosis. Two genes in particular that are upregulated by calcium levels in T cells are NFATc1 and NFATc3 (Lee *et al*., 2011). NFAT are a family of transcription factors (NFAT1-5) that express highly

conserved Rel/NF-κB DNA-binding domains. When either NFATc1 or NFATc3 were knocked down by siRNA in osteoblast cells, RANKL expression was ablated (Lee *et al*., 2011). There is no conclusive evidence that NFAT plays a role in transcriptional regulation of RANKL in mammalian lymphocytes (O'Brien, 2010). The transcriptional control of chRANKL and mammalian RANKL by Ca^{2+} modulation and PKC activation is conserved between species, as indicated by the inhibition studies (Figure 4.6B).

Since DC were first generated from chicken bone marrow cells, various markers and cytokines have be shown to be upregulated in mature BMDC, such as CCR7, TLRs and cell surface activation markers, after LPS, CpG or bacterial exposure (Wu *et al.*, 2010; Wu *et al.*, 2011; Lang *et al*., 2013; Rajput *et al*., 2014; Fu *et al*., 2014). CD40, a fellow TNF superfamily member with similar characteristics to RANK, is expressed on the surface of mature chicken BMDC (Wu *et al*., 2010) and mammalian RANK surface expression is predominantly found on mature DC in mammals (Anderson *et al*., 1997; Wong *et al.*, 1997; Josien *et al*., 1999). To investigate the expression patterns of the chRANKL receptors on chicken BMDC, cells were unstimulated or stimulated with various amounts of LPS and the levels of chRANK and chOPG mRNA expressions analysed by qRT-PCR (Figure 4.5). The data suggest that the mRNA expression levels of chRANK and chOPG in BMDC are both dose- and time-dependent. The more the cells matured, the lower the levels of chRANK expression and the higher the levels of chOPG expression observed. Also the dose of LPS used to stimulate BMDC affected the mRNA expression levels of chRANK and chOPG; lower concentrations led to lower mRNA expression levels of each receptor (Figure 4.5). Mammalian OPG expression is dependent on NF-κB pathway activation and increases as DC mature (Schoppet *et al.*, 2007). It is therefore possible that mature chicken BMDC increase levels of chOPG expression to regulate the magnitude of $chRANKL^{+}$ T cells interacting with $chRANK^{+}$ DC.

The ability of schRANKL to induce or enhance pro-inflammatory cytokine expression in immature or mature chicken APC was analysed by qRT-PCR. The exposure of chicken BMDC to LPS or chCD40L increased pro-inflammatory cytokine mRNA expression levels compared to those in unstimulated BMDC (Wu *et*

al., 2010). To examine whether schRANKL contributed to changes in pro-inflammatory cytokine levels, cells were either unstimulated or stimulated with LPS or chCD40L, schRANKL or both for 3, 6 or 24 h. Costimulation of cells with schRANKL and LPS led to a significant increase in pro-inflammatory cytokine mRNA expression levels compared to those in unstimulated cells, and in some cases, LPS-stimulated cells (Figure 4.7). The ability of schRANKL to drive IL-12α mRNA expression in costimulated cells could suggest that chRANKL enhances the differentiation of Th0 cells to the Th1 phenotype. SchRANKL-treatment alone did not alter the levels of IL-12α expression but did increase expression of IL-1β after 6 h of stimulation and IL-6 after 3 h of stimulation. Because schRANKL did not induce a large increase in pro-inflammatory cytokine mRNA expression levels in BMDC, anti-inflammatory cytokine mRNA expression levels were examined. Levels of IL-10 mRNA expression were low in schRANKL-treated cells (Figure 4.8), similar to the effects of mammalian RANKL (Izawa *et al.,* 2007), and it was therefore not likely to explain the inability of schRANKL alone to induce pro-inflammatory cytokine mRNA expression in BMDC. The mRNA expression levels of the receptors of chRANKL, chRANK and chOPG, were analysed to identify if their mRNA expression levels correlated with the lack of pro-inflammatory cytokine mRNA expression in schRANKL-treated cells. Interestingly, levels of chOPG expression were increased in schRANKL-treated cells at 3 h and decreased at 6 h (Figure 4.8), whereas levels of chRANK mRNA expression were very low in schRANKL-treated cells at both 3 and 6 h (Figure 4.8). Various studies have shown that in mammals DC surface expression levels of RANK were not altered by RANKL treatment (Wong *et al.,* 1999; Chino *et al.,* 2001; Williamson *et al.,* 2002). It is possible that immature BMDC express higher levels of chOPG to ensure DC do not mature under non-pathological conditions which could led to autoimmune disorders, as shown in $OPG^{-/-}$ mice which produce greater levels of IL-23, a cytokine associated with the induction of experimental autoimmune encephalomyelitis (EAE) due to activation of pro-inflammatory macrophages (Cua *et al.,* 2003).

To verify that schRANKL was a key mediator of enhanced pro-inflammatory cytokine expression in mature BMDC, soluble fusion proteins of chRANK-Fc or chOPG-Fc were pre-incubated with schRANKL prior to costimulating cells. Pre-

incubation with both chRANK-Fc and chOPG-Fc downregulated the schRANKL-mediated increase in pro-inflammatory cytokine mRNA expression levels (Figure 4.8). This also indicated that the soluble receptors of chRANKL were capable of interacting with their ligand. In mammalian studies, the bioactivity of RANKL is commonly verified by the ability of the soluble forms of either RANK or OPG to block its activity (Anderson *et al.,* 1997; Wong *et al,* 1999; Yun *et al*., 2001).

In mammals, RANKL increases the levels of pro-inflammatory cytokine mRNA expression in mature BMDC, such as IL-1β, IL-6, IL-12 (p70), IL-15 and TNF-α (Josien *et al.,* 1999), whereas RANKL-treated Mo-DC did not alter the mRNA expression levels of IL-3, IL-4, IL-6, IL-10, or IL-13 but did increase levels of IL-12β (Schiano de Colella *et al.,* 2008). In a similar study, RANKL-treated BMDC did not alter the mRNA expression levels of IFN-γ, IL-10 or IL-12β. However, $Fas^{-/-}$ BMDC significantly increased levels of IFN-γ and IL-12β mRNA expression when treated with RANKL, indicating the regulatory role of the death receptor on fellow TNF members (Izawa *et al.,* 2007). Mucosal-derived DC purified from spleen, Peyer's patches, mesenteric and peripheral lymph nodes of Flt-3L-injected mice all expressed surface RANK. However, the DC from these various anatomical sites reacted differently when incubated with RANKL for 18 h. Spleen-derived DC expressed the highest amounts of IL-12β and the lowest amounts of IL-10, whereas DC derived from Peyer's patches expressed the highest levels of IL-10. Levels of IL-18 mRNA expression were consistent across all mucosal-derived DC after RANKL treatment (Williamson *et al.,* 2002). It is important to note that DC may express RANK but react differently in their response to RANKL depending on their tissue of origin.

The synergistic effects of stimulation with two chicken TNF superfamily members, chCD40L and schRANKL, on the levels of pro-inflammatory cytokine mRNA expression by BMDC were investigated (Figure 4.10). BMDC costimulated with chCD40L and schRANKL had consistent levels of IL-1β mRNA expression at 3, 6 or 24 h and no significant difference was identified between unstimulated or chCD40L-stimulated cells. Levels of IL-6 mRNA expression were not statistically enhanced in costimulated cells. Similarly, levels of chRANK mRNA expression

were not significantly altered in either chCD40L- or co-stimulated cells. In mammals, the cooperation of CD40L and RANKL has been examined in survival assays and DC maturation (Josien *et al.*, 1999; Yu *et al.*, 2003). Treatment of Mo-DC with RANKL caused no change in the phenotype of cells but cells costimulated with CD40L and RANKL upregulated MHC class II and CD80 surface expression, which was further enhanced by the addition of TNF-α (Yu *et al.*, 2003). Various studies identifying the biological effect of mammalian RANKL in DC have produced contrasting evidence as to its effect on their phenotype. One of the first studies examining the biological role of mammalian RANKL proposed that RANKL-treated murine BMDC did not significantly increase the levels of MHC class II, CD80 or CD86 but did slightly (not significantly) upregulate the expression of CD40 after 48 h of stimulation (Anderson *et al.*, 1997). Surprisingly, this paper did not present the FACs data, making it difficult to assess their conclusions. A similar study followed (Wong *et al.*, 1997) in which RANKL-treated BMDC *in vitro* slightly down-regulated MHC class II, had no change in CD80 or CD86, CD11b or CD11c but increased CD40 expression, with similar data at 24 and 48 h of RANKL treatment. Mo-DC, cultured with IL-4 and CSF-2, treated with RANKL increased surface expression of MHC class II, CD80 and CD86 (Seshasayee *et al.*, 2004), suggesting that DC derived from various sources react differently to RANKL exposure, as previously identified in mucosal-derived DC (Williamson *et al.*, 2002). However, all three of the previous studies induced DC maturation prior to RANKL treatment by culturing cells for up to 7-8 days. Maturing BMDC by prolonged culturing only led 50% of the cell population to mature and express surface RANK (Wong *et al.*, 1999). Also, RANKL-treated BMDC do not increase the surface expression of RANK (Wong *et al.*, 1998). This may explain the different results seen for RANKL-mediated changes to DC phenotype in mammalian studies. Mo-DC, cultured with IL-4 and CSF-2, were stimulated with LTK murine cells previously transfected with full-length murine RANKL, or CD40L as a positive control. These cells were mixed with Mo-DC for 72 h and flow cytometric analysis indicated that RANKL-treated DC upregulated CD83, CD86, MHC class II and CD40 but not CD80 (Schiano de Colella *et al.*, 2008).

For chicken BMDC, schRANKL treatment did not affect the expression levels of MHC class II either alone or in combination with LPS (Figure 4.11). CD40 expression levels were increased in LPS-stimulated cells but its expression levels were not enhanced by the addition of schRANKL. The expression pattern of KUL01 was also analysed; although it is not an activation marker like CD40 and MHC class II, KUL01 expression decreases as chicken APC mature (Wu *et al.*, 2010). This was therefore a good marker to identify the ability of schRANKL to induce cell maturation. As expected, at 24 h LPS-treated cells had decreased KUL01 expression but were unaltered by schRANKL treatment. Overall schRANKL does not mediate the upregulation of cell surface activation markers in chicken BMDC, similarly to mammalian RANKL (Anderson *et al.*, 1997; Wong *et al.*, 1997).

BMDM cell phenotypes were analysed, similarly to BMDC, for 24 h (Figure 4.12). There were no changes in MHC class II or KUL01 expression in the presence of schRANKL alone or in co-stimulated cells. CD40 expression levels were increased in LPS-stimulated cells but not enhanced by the addition of schRANKL. A more potent activator of BMDM, IFN-γ, was also assessed for its ability to enhance surface expression of MHC class II, CD40 and KUL01, with schRANKL, after 24 h. IFN-γ-stimulated cells increased MHC class II expression but this was not enhanced in co-stimulated cells (Figure 4.13). Co-stimulated cells increased CD40 expression levels and decreased KUL01 expression levels but were not significantly different when compared to IFN-γ-stimulated cells. One study (Park *et al.*, 2005) of the bioactivity of mammalian RANKL on macrophages suggested that RANKL-treated cells upregulated MHC class II expression which was enhanced when cells were co-stimulated with LPS but not with IFN-γ. CD86 expression was also upregulated in cells costimulated with RANKL and LPS or IFN-γ (Park *et al.*, 2005). There are contrasting data on the ability of mammalian RANKL to alter the expression of the costimulatory molecules, CD80 and CD86. These are two of the best-characterised mammalian costimulatory molecules and are strongly and rapidly upregulated on activated APCs. Each interacts with their receptor, CD28, on naïve $CD4^+$ and $CD8^+$ T cells. Ligation of CD28 facilitates the progression of the cell-cycle and production of IL-2 (Sharpe & Freeman, 2002). Currently, a mouse anti-chicken CD86 monoclonal antibody is commercially available. However, this antibody is not very

efficient and studies using this antibody show little detection of surface chCD86 on BMDC (Wu *et al.,* 2010; Liang *et al.,* 2013), although chCD86 mRNA expression levels are increased in stimulated BMDC (Rajput *et al.*, 2014).

The lifespan of DC can influence the duration of lymphocyte activation, thereby affecting the outcome of immune responses. Limiting the lifespan of DC by inducing apoptosis is a means of regulating the interaction between antigen-bearing DC with T cells. Apoptosis is a physiological process of cell death that is required for tissue remodelling, development and homeostasis (Kerr *et al*., 1972). The survival of DC is affected by mediators of innate and adaptive immune responses, such as PAMPs interacting with their TLR ligands and co-stimulatory molecules expressed by T cells, such as CD40L (Hou & Parijs, 2004). Using trypan blue staining, Anderson *et al*. (1997) and Wong *et al*. (1997) concluded that cultures of murine DC treated with RANKL had more viable cells after 24 h of treatment. Park *et al*. (2005) analysed cell death and apoptosis by double-staining BMDM for annexin-V and PI after 24 h of RANKL treatment and found that treatment significantly increased the survival rates of cells but did not work in synergy with either LPS or IFN-γ. To determine the ability of schRANKL to enhance the survival rates of BMDC and BMDM, cells were untreated or treated with 1:5 or 1:10 (ex-COS) of schRANKL for 24 and 48 h (Figures 4.14 and 4.15). BMDC survival rates were increased in schRANKL-treated cells compared to untreated cells after 24 h and 48 h (Figure 4.14). After 24 h, the number of viable cells was increased in schRANKL-treated BMDM compared to untreated cells. However, after 48 h schRANKL-treated cells had fewer viable cells compared to untreated cells. It seems that the ability of schRANKL to enhance the survival of BMDM is short-lived. Although overall the data were not significant for either BMDC or BMDM (n=3), cells did undergo less apoptosis after 24 h of schRANKL treatment. The analysis did not identify the anti-apoptotic gene(s) linked to this enhanced survival, although various mammalian studies have shown that the upregulation of the Bcl-2 family members, Bcl-X_L and Bcl-2, is linked to RANKL-mediated cell survival (Wong *et al.,* 1998; Josien *et al.,* 1999; Cremer *et al*, 2002; Hou & Parijs, 2004; Izawa *et al.,* 2007). Bcl-2 and Bcl-X_L function to antagonise pro-apoptotic proteins such as BIM and BAX, regulate mitochondrial conductance and inhibit cell cycle progression.

Transgenic overexpression of Bcl-2 can prolong the survival of DC and is required for CD40L-mediated survival in murine BMDC (Hou & Parijs, 2004). Genetic and molecular analysis from nematodes to humans indicates that programmed cell death is highly conserved (Ellis *et al.*, 1991), so it is therefore plausible that chRANKL may upregulate the levels of anti-apoptotic chicken Bcl-2 family members in BMDC and BMDM.

The overall data suggest that schRANKL alone induces partial maturation of BMDC, by inducing low levels of pro-inflammatory cytokine mRNA expression and down-regulating KUL01. DC reside in the peripheral tissues in an immature state for optimal uptake and response to inflammatory signals (Banchereau & Steinman, 1998). The maintenance of DC, including apoptosis, cell growth and activation in the periphery, is in some ways regulated by RANKL and FAS (Izawa *et al.*, 2007). Chicken BMDC significantly phagocytosed more zymosan-A particles in the presence of schRANKL (Figure 4.16), although there was no change in MHC class II expression in schRANKL-stimulated BMDC. However, these cell cultures are heterogeneous and large cells can be seen in these cultures after 24 h of schRANKL-treatment (Figure 4.17). Osteoclast cells have APC properties, inducing expression of pro-inflammatory cytokines and cell surface markers and increasing phagocytosis (Li *et al.*, 2010). BMDM commit to the osteoclast lineage after 24 h of RANKL treatment and still have phagocytic potential (Mochizuki *et al.*, 2006). This may be the cause for the increased uptake of zymosan particles by schRANKL-treated chicken BMDC.

In a pilot study to investigate the ability of schRANKL protein to drive osteoclast differentiation, bone marrow cells were treated with chCSF-1 for 2 days to enrich for the monocyte/macrophage cell population (as described in mice by Takeshita *et al.*, 2000) and reseeded to ensure cells were in close proximity to fuse and generate multinucleated cells, in the presence of schRANKL for 8 days. The progenitor cells of osteoclasts are chemotactically attracted to sites of bone resorption, where they deposit in the mesenchyme surrounding the bone and proliferate and differentiate into mature osteoclasts by interacting with RANKL-expressing osteoblasts. Mature osteoclasts are very large cells containing multiple

nuclei, have abundant mitochondria, lysosomes and free ribosomes (Li *et al*., 2006) and have unique characteristics, such as expressing titrate-resistant acid phosphatase (TRAP), matrix metalloproteinases (MMP) and calcitonin and vitronectin receptors (Miyamoto & Suda, 2003). In preliminary studies, the presence of multinucleated cells was identified in chicken cell cultures using the nuclear stain Hoechst-33258. After 8 days of culture, schRANKL-treated cells had a variable morphology, from small to large cells. The large cells had a typical osteoclast morphology, large in size, flat and multinucleated. This study was not aimed to further characterise these cells but was carried out to identify an *in vitro* protocol for osteoclast differentiation using chCSF-1 and schRANKL and may be used in the future to understand osteoclast function in the chicken.

In summary, chRANKL, chRANK and chOPG mRNA expression levels have been analysed in different tissues and cells in the chicken. Of the triad of molecules, the ligand, chRANKL, is expressed at higher levels across a wider range of organs and cells in the chicken than its receptors, chRANK and chOPG. Both of the receptors for chRANKL are differentially expressed in mature BMDC. The bioactivity of chRANKL has been analysed in both BMDC and BMDM and has similar characteristics to its mammalian counterpart.

Chapter 5

Cloning and molecular characterisation of chicken TRAF2 (chTRAF2), chTRAF5, chTRAF6 and chTRAF7

5.1 Introduction

The TNFR superfamily members signal using adaptor proteins that bind directly to their cytoplasmic domains. TRAF1 and TRAF2 were first identified as signal transducers of TNFR2 (Rothe *et al.,* 1994). Four additional members of the TRAF family, TRAF3, TRAF4, TRAF5 and TRAF6, were identified in both mouse and human using yeast two-hybrid systems (Rothe *et al.,* 1994; Hu *et al.,* 1994; Regnier *et al.,* 1995; Nakano *et al.,* 1996; Cao *et al.,* 1996). A seventh potential member of the mammalian TRAF family was identified, TRAF7: potential as it does not contain a TRAF-C domain, but instead has seven WD40 repeat domains (Xu *et al.,* 2004). *In vitro* binding experiments revealed that TRAFs not only bind to and signal for TNFR superfamily members but also for Toll/IL-1R superfamily members via MyD88 or TRIF (Cao *et al.,* 1996; Naito *et al.,* 1999), NLR family members via RIP2 and RLR family members via MAVS (Paz *et al.,* 2011; Marinis *et al.,* 2011). The hallmark feature of TRAF family members is their highly conserved COOH-terminal TRAF domain of approximately 230 amino acids. The COOH-terminal domain can be subdivided into more divergent NH_2-proximal (TRAF-N) and highly conserved COOH-proximal (TRAF-C) subdomains. TRAF-N possesses a coiled-coil domain responsible for homo- and hetero-oligomerisation of TRAF proteins as well as for indirect and direct interactions with cognate surface receptors (Park *et al.,* 1999). TRAF proteins also possess an NH_2-terminal RING finger domain (TRAF2-TRAF7) which is highly conserved at the amino acid level. The RING finger domain is followed by several zinc finger motifs. These two domains are vital for activation of downstream signalling pathways, such as MAPK and NF-κB (Baud *et al.,* 1999). As described in Chapter 3, chRANK contains only four of the five TRAF peptide-binding motifs identified in mammalian RANK (Darnay *et al.,* 1998; Wong *et al.,* 1998). Importantly the "missing" TRAF peptide-binding motif was one of the three TRAF6-specific binding motifs. TRAF6 is vital for RANKL-mediated differentiation and activation of osteoclasts (Lomaga *et al.,* 1999; Naito *et al*., 1999). Here, the chRANK-specific signalling TRAFs, TRAF2, TRAF5, and TRAF6, were cloned and characterised, as well as the chicken orthologue of the newest member of the mammalian TRAF family, TRAF7.

5.2 Methods

5.2.1 In silico analysis

To identify the various domains within chicken TRAF proteins, the SMART prediction program was used to compare each to the known human and mouse sequences. Amino acid conservation and phylogenetic analyses were carried out using CLUSTALX v2 and MEGA v5, respectively (Chapter 2, section 2.1).

5.2.2 *In vitro* analysis

ChTRAF2, chTRAF5, chTRAF6 and chTRAF7 were cloned, using RNA from ConA-stimulated splenocytes as template by RT-PCR. The mRNA expression patterns of all TRAFs were analysed in a number of lymphoid and non-lymphoid organs by RT-PCR. RNA (100 ng) from each tissue was reverse-transcribed using Superscript III and analysed for the expression of the housekeeping gene, glyceraldehyde 3-phosphate dehydrogenase (GAPDH). Primers were designed to overlap intron-exon boundaries for the detection of mRNA for chTRAF2, chTRAF5, chTRAF6 and chTRAF7 (Chapter 2, section 2.8). Splenocyte subsets were purified and analysed for the mRNA expression of each TRAF and the kinetics of their mRNA expression levels were analysed in a time-course experiment comparing unstimulated and ConA-stimulated splenocytes. ChTRAF2 and chTRAF2S were sub-cloned into a modified pcDNA3-haemagglutinin (HA) vector to express NH_2-terminal-tagged HA-fusion proteins (Chapter 2, section 2.2). HEK-293T cells were transiently transfected with the chTRAF2 constructs and HA-tagged recombinant protein expression was analysed by dot blot (Chapter 2, section 2.4 & 2.5). Protein structures were analysed by SDS-PAGE under both reducing and non-reducing conditions. The bioactivity of the chTRAF2 isoforms were investigated using NF-κB reporter assays in HEK-293T cells (Chapter 2, section 2.12).

5.3 Results

5.3.1 Identification of the genes representing chTRAF2, chTRAF5, chTRAF6 and chTRAF7 in the chicken genome

ChTRAF5 had been previously cloned (Adballa *et al.*, 2004a). The Ensembl database (www.ensembl.org) was searched for chTRAF2, chTRAF6 and chTRAF7 cDNA sequences. All were present as predicted cDNA (Accession Numbers are given in Appendix 2, Table 5).

5.3.2 Amplification and molecular cloning of chTRAF5, chTRAF6 and chTRAF7

Primers were designed against the predicted full-length cDNAs of chTRAF5, chTRAF6 and chTRAF7 using the sequences available in the Ensembl database. cDNA was amplified using RNA from ConA-stimulated splenocytes as template for RT-PCR. The resulting products were a 1.7 kb cDNA product, corresponding to 557 amino acids for chTRAF5, a 1.6 kb cDNA product, corresponding to 545 amino acids for chTRAF6, and a 1.9 kb cDNA product, corresponding to 670 amino acids for chTRAF7 (Figure 5.1). Each band was excised and purified from the gel. All individual cDNA were ligated into the vector pGEM-T Easy. Sequences were verified for each for three individual clones and deposited into the Ensembl database (Accession Numbers: TRAF6, LM999953 and TRAF7, LM999954).

5.3.3 *In silico* analysis of chTRAF5, chTRAF6 and chTRAF7

TRAF proteins are composed of several highly conserved domains, such as a RING domain, several zinc finger motifs, a coiled-coil region and a TRAF-C domain. To determine the location and presence of these domains in chTRAF5, chTRAF6 and chTRAF7, SMART was used to graphically identify these regions in the chicken and human proteins (Figure 5.2). ChTRAF5 contains all regions characteristic of TRAF family members and has a longer coiled-coil region compared to human TRAF5 (Figure 5.2). The SMART prediction for chTRAF6 was very similar to that for human TRAF6 (Figure 5.2), indicating that the protein structures are conserved between the two species. TRAF7 does not express a TRAF-C domain, instead possessing seven WD40 repeat domains. All domains were

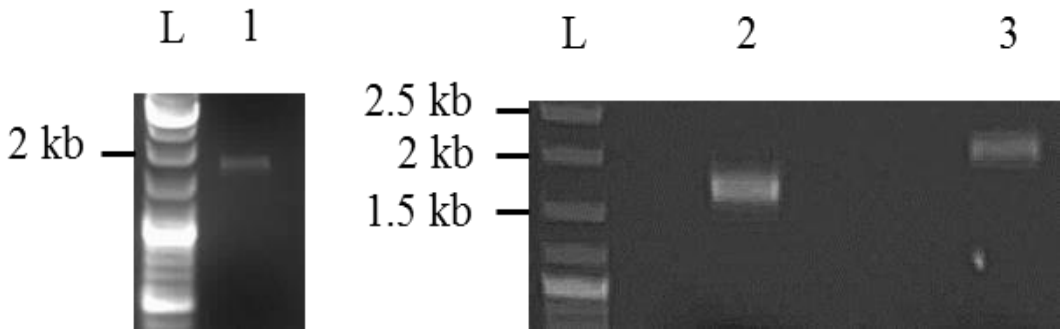

Figure 5.1 Gel electrophoresis of 1) chTRAF5, 2) chTRAF6 and 3) chTRAF7. *RT-PCR products of chTRAF5, chTRAF6 and chTRAF7 amplified from RNA from ConA-stimulated splenocytes. L = 5 kb DNA ladder (Invitrogen).*

predicted in the chTRAF7 protein along with a RING domain and one zinc finger motif (Figure 5.2).The degree of conservation between mammalian and chicken TRAF5, TRAF6 and TRAF7 proteins was analysed by CLUSTAL X. The consensus sequence for TRAF RING finger motifs is the $CX_2\,CX_{11}\,CX_1\,HX_2\,CX_2\,CX_9\,CX_2C$ motif (X being any amino acid). The TRAF zinc finger motif typical patterns are $CX_{2/3}\,CX_{11/12}\,HX_3C$ or $CX_6\,CX_{11}\,HX_3C$ with the last zinc finger motif differing slightly ($CX_6\,CX_{12}\,HX_8$). Sequence motifs for both the RING and zinc finger domains were identified in the mammalian and chicken TRAF proteins. ChTRAF5 has high identity with its mammalian counterparts (68-70%) with a highly conserved RING domain and five zinc finger motifs (Figure 5.3). ChTRAF6 shows relatively high amino acid similarity with its mammalian orthologues (70-72%) (Figure 5.4). The presence and location of five zinc finger motifs and the RING domain were conserved. Interestingly, chTRAF6 is slightly larger than mouse and human TRAF6 proteins. In the RING domain, chTRAF6 has three extra amino acids and an extra 23 amino acids within the coiled-coil, TRAF-N, domain.

ChTRAF7 is highly conserved across species (Figure 5.5), with 88% amino acid identity to human and mouse TRAF7 proteins. ChTRAF7 is slightly smaller than its mammalian orthologues, missing a small region before the first WD40 repeat domain. Overall, TRAF5, TRAF6 and TRAF7 are highly conserved across mammals and birds, which likely indicates strong conservation of bioactivity.

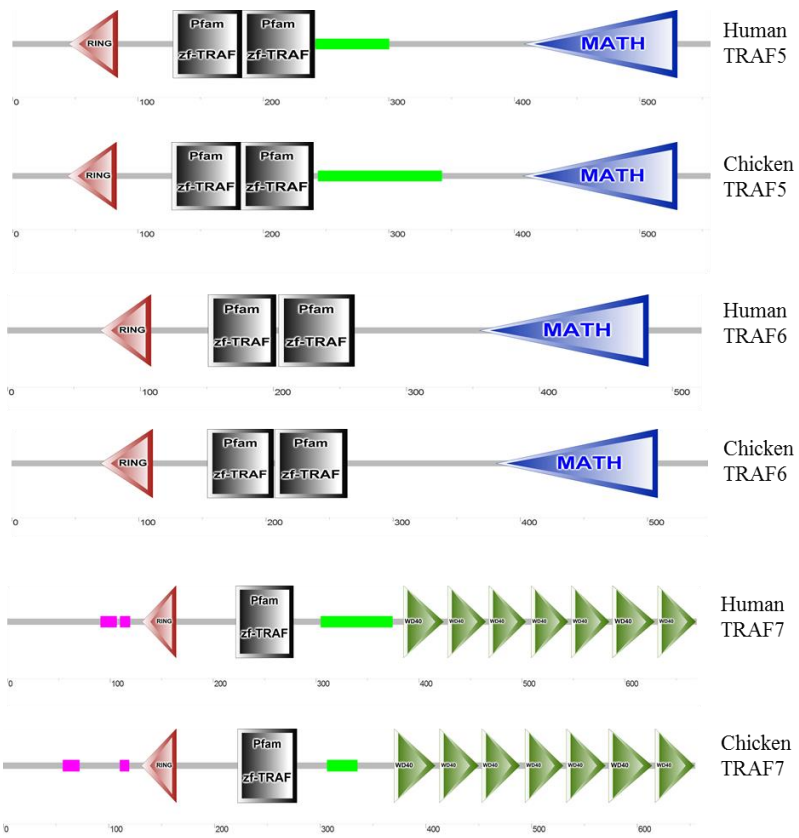

Figure 5.2 SMART prediction models of human and chicken TRAF5, TRAF6 and TRAF7 proteins. *Red triangles indicate RING domains, black boxes zinc finger motif regions, green boxes coiled-coil regions (TRAF-N), blue triangles MATH (TRAF-C) domains and green triangles the seven WD40 repeat domains in TRAF7.*

5.3.4 RT-PCR analysis of chTRAF5, chTRAF6 and chTRAF7 mRNA in chicken tissues

The mRNA expression of chTRAF5, chTRAF6 and chTRAF7 was analysed by RT-PCR. RNA (100 ng per sample) from various lymphoid and non-lymphoid organs was reverse-transcribed using Superscript III and an oligo dT_{20} primer to generate cDNA. To amplify regions of chTRAF5, chTRAF6 and chTRAF7, primers were designed to overlap intron and exon boundaries to generate a small amplicon of each gene (Appendix 2, Table 3). ChTRAF5 mRNA expression was detected in all lymphoid tissues examined except in the thymus (Figure 5.6). In the lymphoid tissue panel, the highest chTRAF5 mRNA expression levels were in the spleen caecal

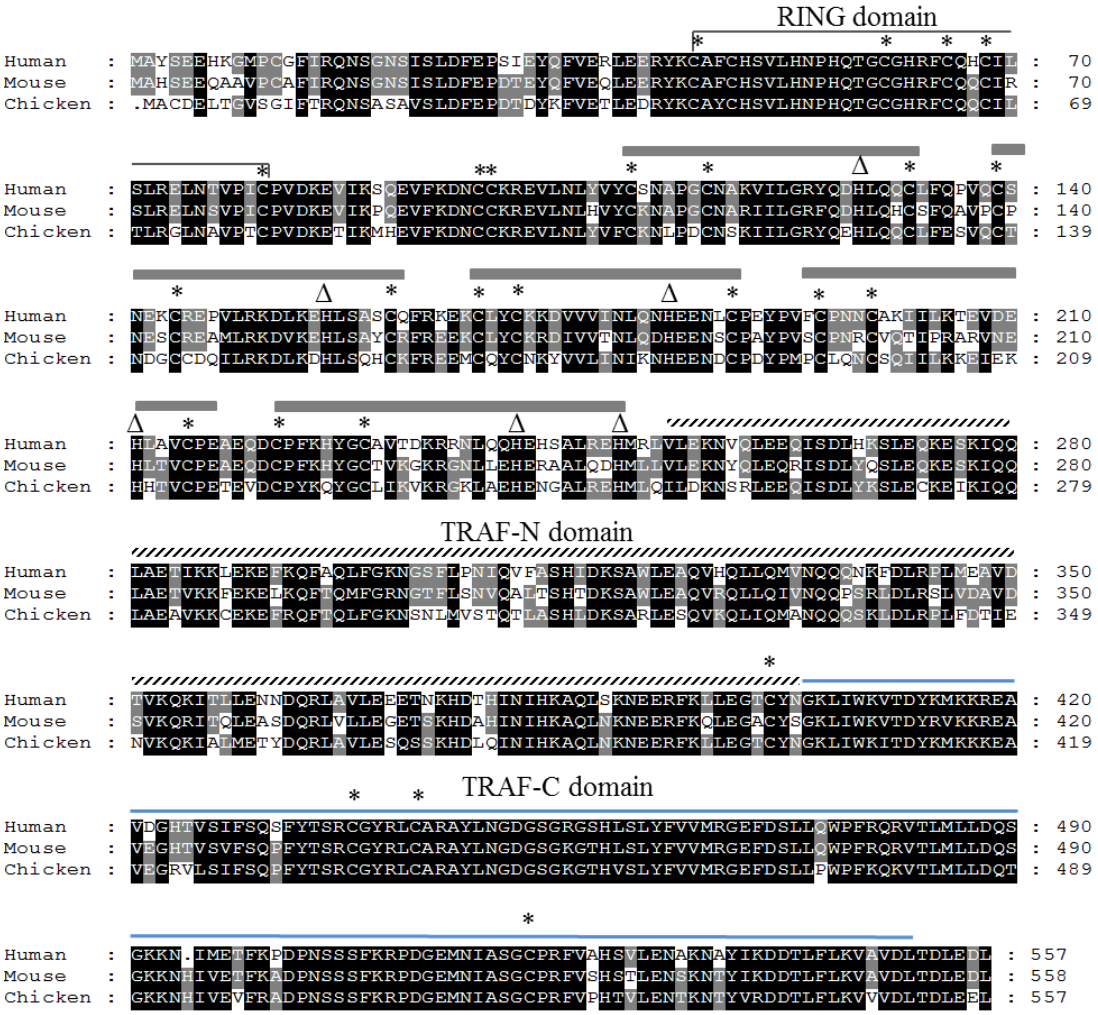

Figure 5.3 Amino acid alignment of the human, mouse and chicken TRAF5. *Shaded areas represent conservation of amino acids – the darker the shading, the more conserved the residue across species: black shading indicates conservation between all species, dark grey with white lettering indicates conservation between 2 species. Dots indicate gaps in the alignment. Black line above the sequence indicates the RING domain, asterisks conserved cysteine residues and open triangles conserved histidine residues characteristic of TRAF zinc finger motifs. Grey boxes above the sequence indicate the conserved zinc finger motif regions, the dashed line TRAF-N domains and the blue line the TRAF-C domains.*

tonsils, Meckel's diverticulum, caeca and upper-gut (Figure 5.6). ChTRAF6 mRNA expression was also not detected in the thymus but its expression was detected in all other lymphoid tissues examined (Figure 5.6). The highest chTRAF6 mRNA

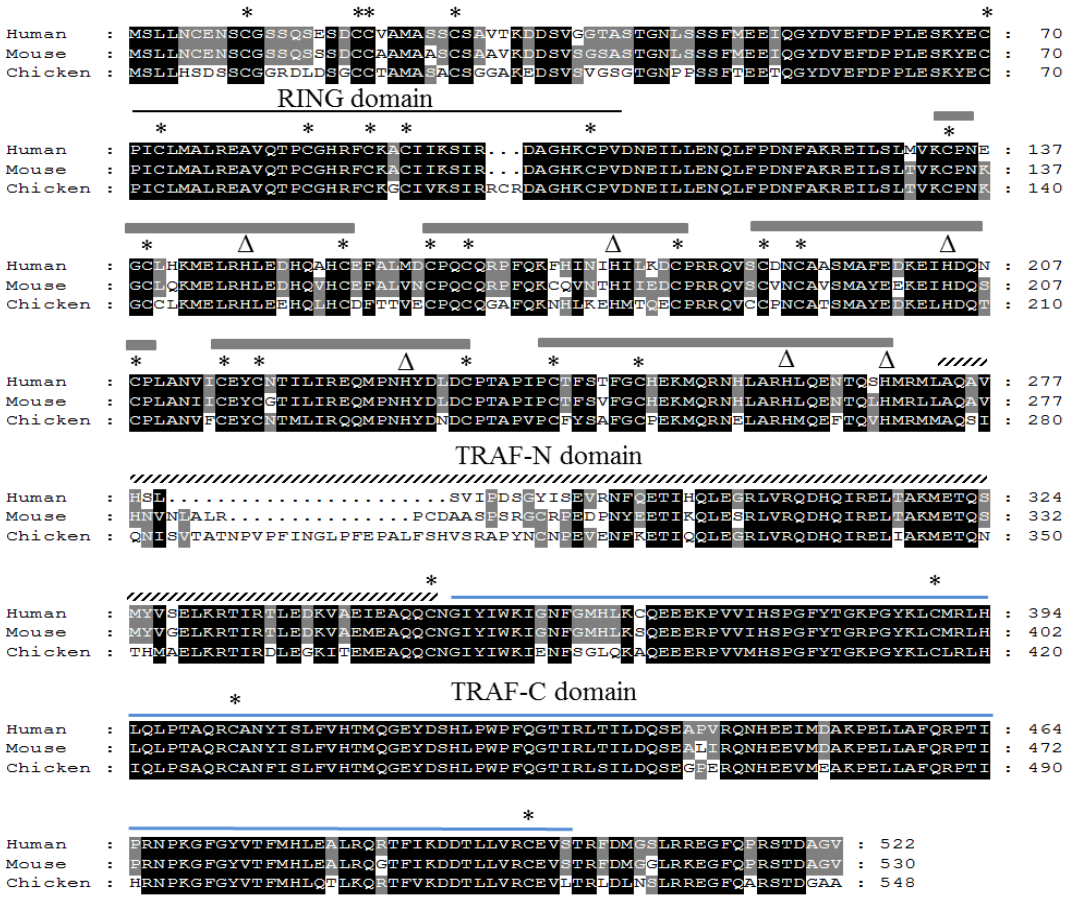

Figure 5.4 Amino acid alignment of the human, mouse and predicted chicken TRAF6. *Shaded areas represent conservation of amino acids – the darker the shading, the more conserved the residue across species: black shading indicates conservation between all species, dark grey with white lettering indicates conservation between 2 species. Dots indicate gaps in the alignment. Black line above the sequence indicates the RING domain, asterisks indicate conserved cysteine residues and open triangles conserved histidine residues characteristic of TRAF zinc finger motifs. Grey boxes above the sequence indicate the conserved zinc finger motif region, the dashed line TRAF-N domains and the blue line the TRAF-C domains.*

expression levels were in the spleen, bursa of Fabricius, Meckel's diverticulum, caeca and mid-gut. ChTRAF7 mRNA expression was ubiquitous across the lymphoid panel and levels were consistent for all tissues except for the crop, where

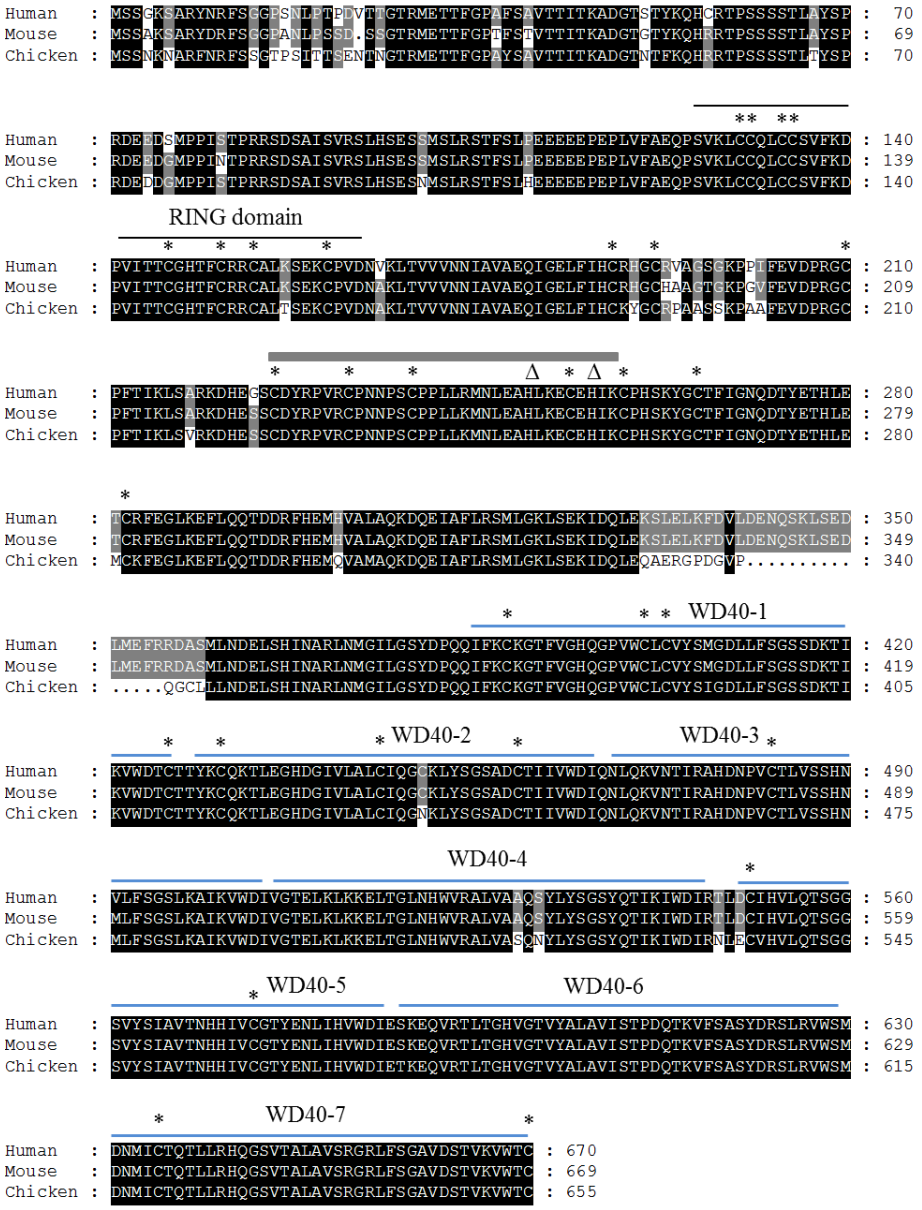

Figure 5.5 Amino acid alignment of the human, mouse and predicted chicken TRAF7. *Shaded areas represent conservation of amino acid – the darker the shading, the more conserved the residue across species: black shading indicates conservation between all species, dark grey with white lettering indicates conservation between 2 species. Dots indicate gaps in the alignment. Black line above the sequence indicates the RING domain, asterisks indicate conserved cysteine residues and open triangles conserved histidine residues characteristic of TRAF zinc finger motif regions. Grey boxes above the sequence indicate the conserved zinc finger motif and the blue line the WD40-repeat domains, labelled 1-7.*

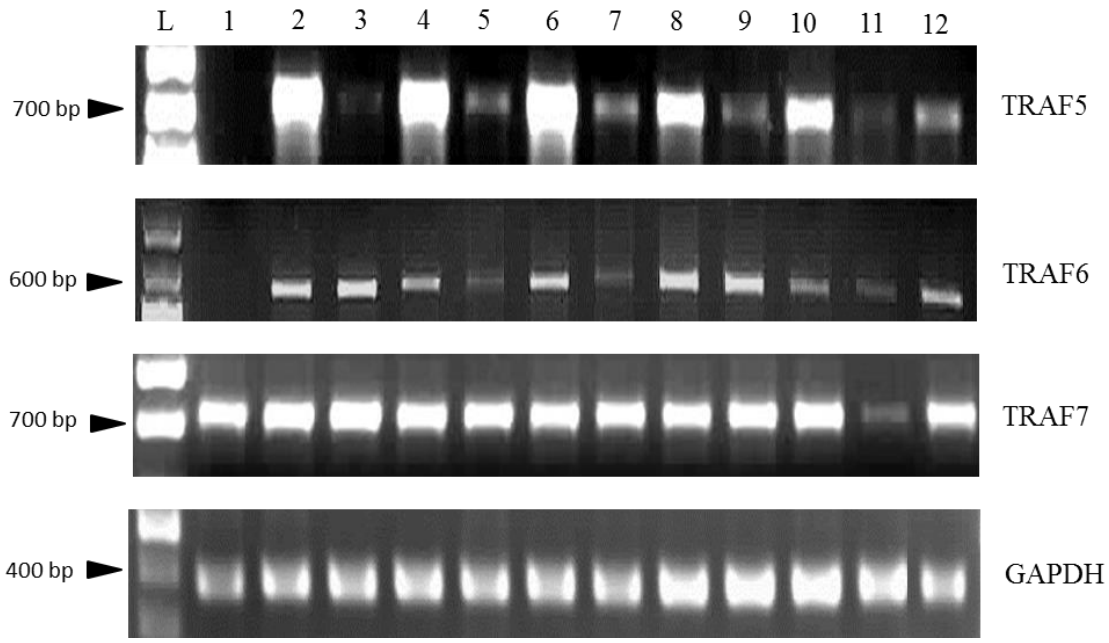

Figure 5.6 RT-PCR analysis of chTRAF5, chTRAF6 and chTRAF7 mRNA expression in lymphoid tissues. *ChTRAF5, chTRAF6 and chTRAF7 mRNA expression was measured by RT-PCR in lymphoid tissues: 1) thymus, 2) spleen, 3) bursa of Fabricius, 4) caecal tonsils, 5) bone marrow, 6) Meckel's diverticulum, 7) Harderian gland, 8) caeca, 9) mid-gut, 10) upper-gut, 11) crop, 12) gizzard. L = 1 kb DNA ladder (Invitrogen). Data represent results from one of three individual birds with similar results.*

levels were lower (Figure 5.6).

In non-lymphoid tissues, chTRAF5 mRNA expression was detected in all tissues except the muscle and the skin (Figure 5.7). ChTRAF5 mRNA expression was highest in the lung, consistent in the brain, heart, liver and kidney, and lowest in the heart (Figure 5.7). ChTRAF6 mRNA expression was detected in all non-lymphoid tissues examined (Figure 5.7), albeit only faintly in the brain. ChTRAF7 was ubiquitously expressed in non-lymphoid tissues (Figure 5.7).

5.3.5 RT-PCR analysis of chTRAF5, chTRAF6 and chTRAF7 mRNA in chicken cells

The mRNA expression of chTRAF5, chTRAF6 and chTRAF7 was examined in splenocyte subsets. Cells were purified using mouse anti-chicken CD4, CD8β,

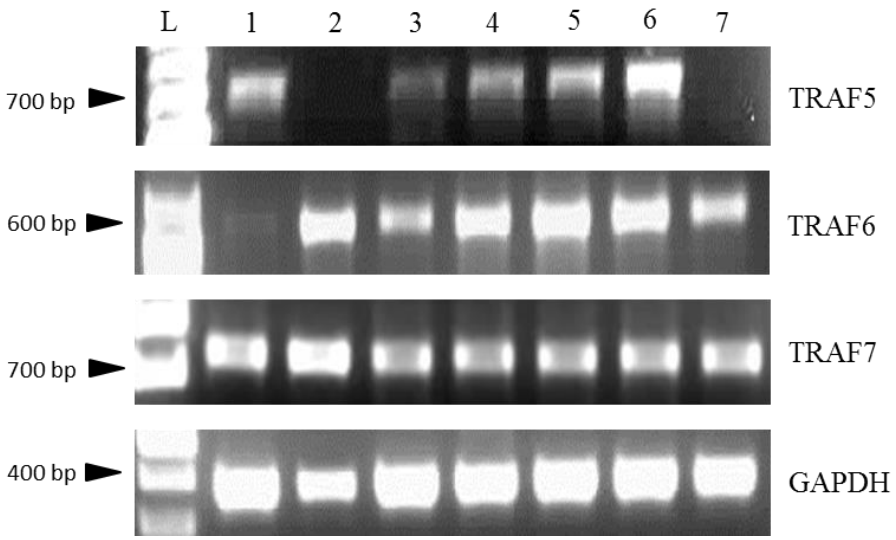

Figure 5.7 RT-PCR analysis of chTRAF5, chTRAF6 and chTRAF7 mRNA expression in non-lymphoid tissues. *ChTRAF5, chTRAF6 and chTRAF7 mRNA expression was measured by RT-PCR in non-lymphoid tissues; 1) brain, 2) muscle, 3) heart, 4) liver, 5) kidney, 6) lung, 7) skin. L = 1 kb DNA ladder (Invitrogen). Data represent results from one of three individual birds with similar results.*

TCRγδ, TCRαβ1, TCRαβ2, KUL01 and Bu1 mAb using an AutoMacs pro-separator and purity verified by FACs analysis (Appendix 4, Figure 2). ChTRAF5 mRNA expression was detected in all cell subsets except KUL01$^+$ cells. KUL01 is a marker for phagocytic cells and will predominantly represent DC and macrophages in the spleen. ChTRAF5 mRNA expression was highest in TCRγδ$^+$ cells.

ChTRAF6 mRNA expression was detected in all cells analysed. ChTRAF6 mRNA expression levels were highest in CD8β$^+$ and TCRγδ$^+$ cells, and lowest in TCRαβ2$^+$, Bu1$^+$ and KUL01$^+$ cells (Figure 5.8A). ChTRAF7 mRNA expression levels were similar in all cell subsets examined (Figure 5.8A) Next, the mRNA expression of chTRAF5, chTRAF6 and chTRAF7 was analysed in unstimulated or LPS-stimulated BMDC and BMDM, again by RT-PCR (Figure 5.8B). In BMDC, chTRAF5 mRNA expression levels were not altered between unstimulated and LPS-stimulated cells. In contrast, chTRAF5 mRNA expression levels were increased in LPS-stimulated BMDM compared to in unstimulated BMDM (Figure 5.8B). The

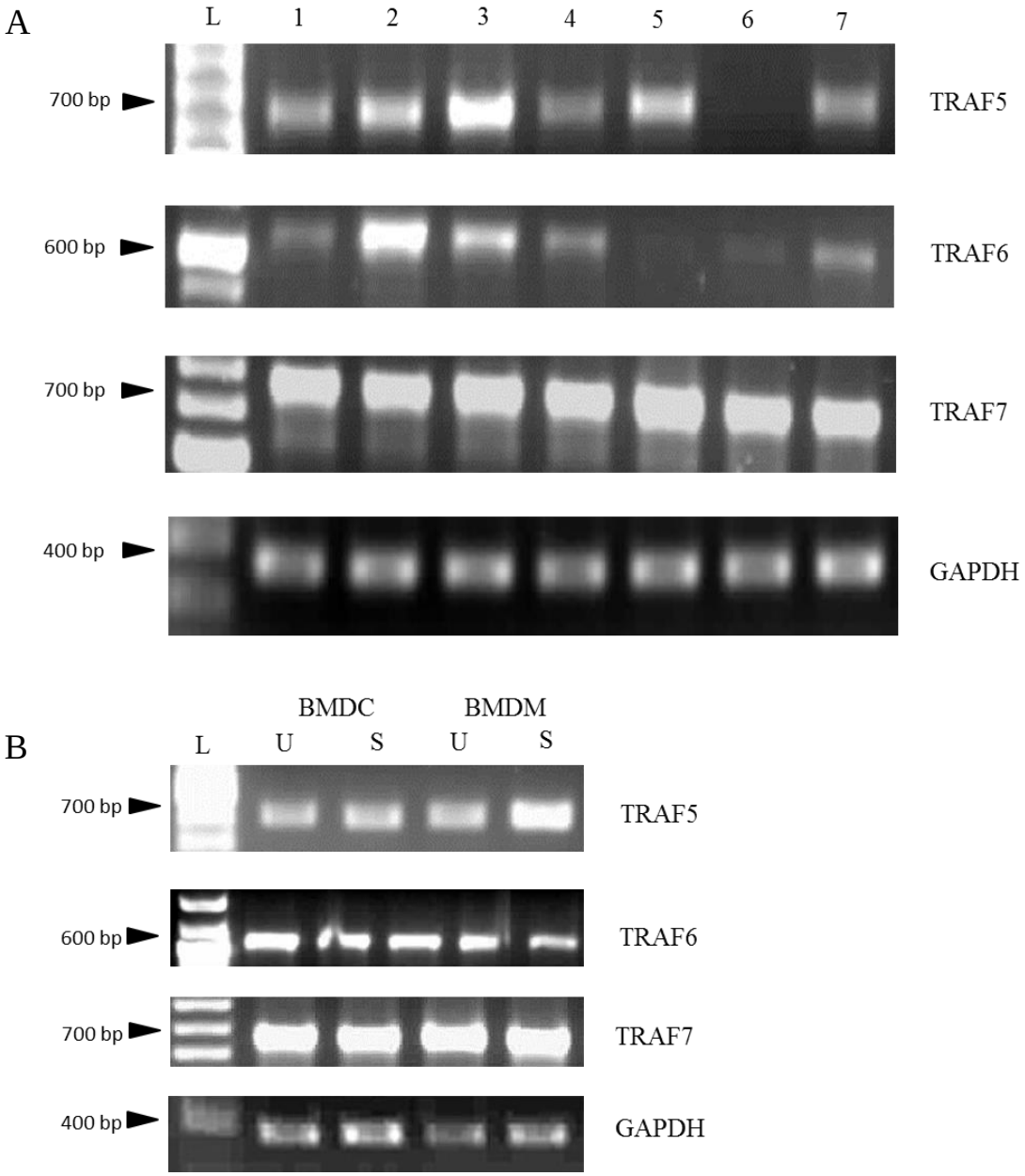

Figure 5.8 RT-PCR analysis of chTRAF5, chTRAF6 and chTRAF7 mRNA expression in chicken immune cells. *ChTRAF5, chTRAF6 and chTRAF7 mRNA expression was measured by RT-PCR in* **A)** *purified splenocytes; 1) CD4$^+$, 2) CD8β$^+$, 3) TCRγδ$^+$, 4) TCRαβ1$^+$, 5) TCR αβ2$^+$, 6) KUL01$^+$, 7) Bu1$^+$ and* **B)** *BMDC and BMDM unstimulated or stimulated with LPS (200 ng/ml) for 24 h. L = 1 kb DNA ladder (Invitrogen). Data represent results from one of three individual birds with similar results.*

mRNA expression levels of chTRAF6 and chTRAF7 were not altered between unstimulated or LPS-stimulated BMDC or BMDM (Figure 5.8B).

5.3.6 Kinetics of chTRAF5, chTRAF6 and chTRAF7 in stimulated splenocytes

The kinetics of mRNA expression of chTRAF5, chTRAF6 and chTRAF7 were analysed in splenocytes either unstimulated or stimulated with ConA (1 μg/ml) over a time-course of 2, 4, 6, 12, 18 and 24 h (Figure 5.9). ChTRAF5 mRNA expression was not altered in ConA-stimulated cells compared to unstimulated cells from 2 to 12 h. (Figure 5.9) At 18 and 24 h, chTRAF5 mRNA expression was low in unstimulated cells and was increased in Con-A stimulated cells. ChTRAF6 mRNA expression levels were similar between unstimulated and stimulated cells at 2 and 4 h (Figure 5.9). At 6 h, chTRAF6 mRNA expression was barely detectable in unstimulated cells but detectable in ConA-stimulated cells. At 12, 18 and 24 h, chTRAF6 mRNA expression was detected in unstimulated and was increased in ConA-stimulated cells (Figure 5.9). ChTRAF7 mRNA expression was detected in both unstimulated and stimulated cells at similar levels (Figure 5.9).

5.4 Identification of a novel chTRAF2 isoform

5.4.1 Amplification and molecular cloning of chTRAF2 and identification of a novel chTRAF2 isoform, chTRAF2S

Primers were designed to clone the full-length cDNA of chTRAF2 from the 5' ATG start codon to the 3' stop codon using the sequence extracted from the Ensembl database (Appendix 2, Table 5). RNA from ConA-stimulated splenocytes was used as template for RT-PCR. Gel electrophoresis of the PCR product revealed two distinct bands, an expected band at ~1.5 kb and a smaller band at ~1.4 kb (Figure 5.10). Both bands were gel purified and TA-cloned into pGEM-T Easy. Three independent clones of each cDNA were sequenced using the T7 forward and Sp6 reverse primers (Appendix 2, Table 1). Analyses of the cloned sequences of the large band indicated that the 1584 bp band was a 100% match to the predicted full-length chTRAF2 cDNA sequence in Ensembl. Analyses of the cloned sequences of the

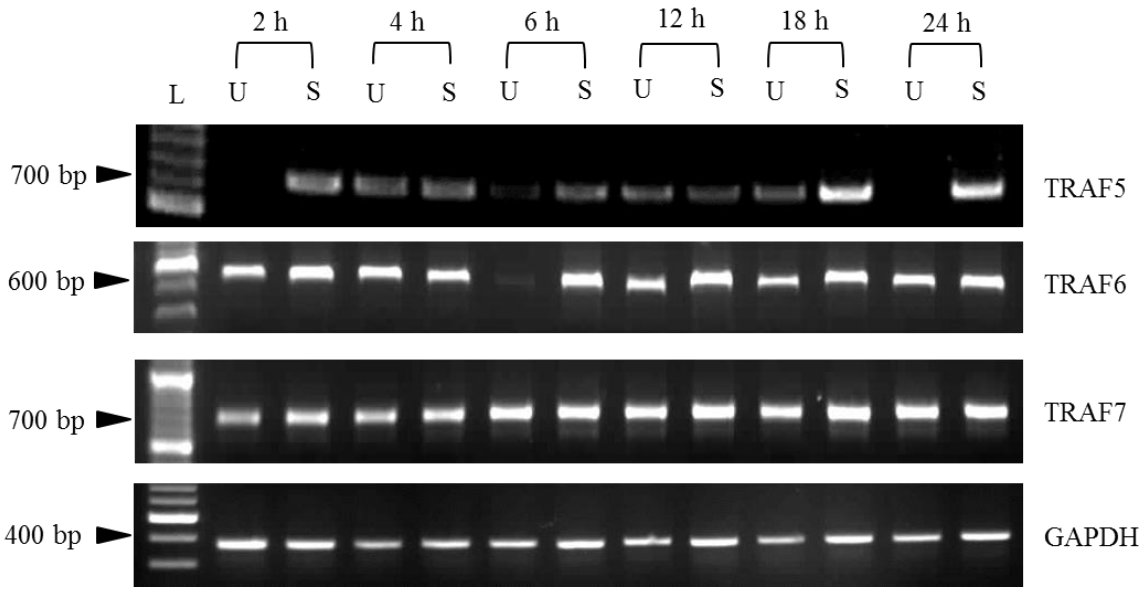

Figure 5.9 RT-PCR analysis of chTRAF5, chTRAF6 and chTRAF7 mRNA expression in unstimulated and ConA-stimulated splenocytes for 2, 4, 6, 12, 18 or 24 h. *ChTRAF5, chTRAF6 and chTRAF7 mRNA expression was measured by RT-PCR in splenocytes unstimulated (U) or stimulated (S) with ConA (1 µg/ml) for 2, 4, 6, 12, 18 or 24 h. L = 1 kb DNA ladder (Invitrogen). Data represent results from one of three individual birds with similar results.*

smaller band revealed the existence of a smaller chTRAF2 isoform 1422 bp in length, 162 bp smaller than the full-length cDNA of chTRAF2.

5.4.2 Analysis of conserved synteny of mammalian and avian TRAF2 genes

To date, very little information on the existence, conservation and bioactivity of avian TRAFs is available. Using the Ensembl database, the TRAF2 genes were identified in human, mouse and chicken (Figure 5.11). Genes that lie upstream and downstream of TRAF2 were conserved in synteny between the chicken and mammals (Figure 5.11). There was no evidence of gene duplication events suggesting that the smaller chTRAF2 isoform was generated by alternative splicing.

5.4.3 Identification of alternative splicing of chTRAF2

Alternative splicing can generate different isoforms of a single gene with

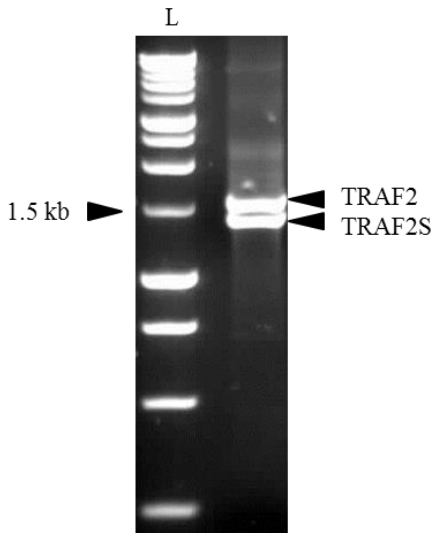

Figure 5.10 Gel electrophoresis of chTRAF2. *ChTRAF2 cDNA products from ConA-stimulated splenocytes. L = 5 kb DNA ladder (Invitrogen).*

different enzymatic activity, substrate specificity, subcellular localisation and altered abilities to interact with other proteins (Möröy & Heyd, 2007). To identify the type of splicing event that occurred for the generation of the smaller chTRAF2 isoform, the locations of each exon were identified. Using the SMART prediction model and the Ensembl database, the locations of the ten exons encoding chTRAF2 were identified in the cDNA sequence (Figure 5.12). The smaller chTRAF2 isoform lacks exon 4 (Figure 5.12). This suggests that the smaller chTRAF2 isoform is generated due to exon cassette splicing, characterised by an entire exon being skipped in the middle of the mRNA precursor, generating alternative isoforms of the same protein. SMART was used to identify if a protein domain would be in the region missing in the smaller TRAF2 isoform (Figure 5.13). Analysis of the two chTRAF2 proteins indicate that exon four translates into a portion of the zinc finger domain, and the smaller chTRAF2 isoform is therefore missing some zinc finger motifs. There is an alternative isoform of mouse TRAF2, TRAF2A, which has an additional seven amino acids in the RING domain. The chicken alternative isoform is obviously different, and shall henceforth be called chTRAF2S (S for short).

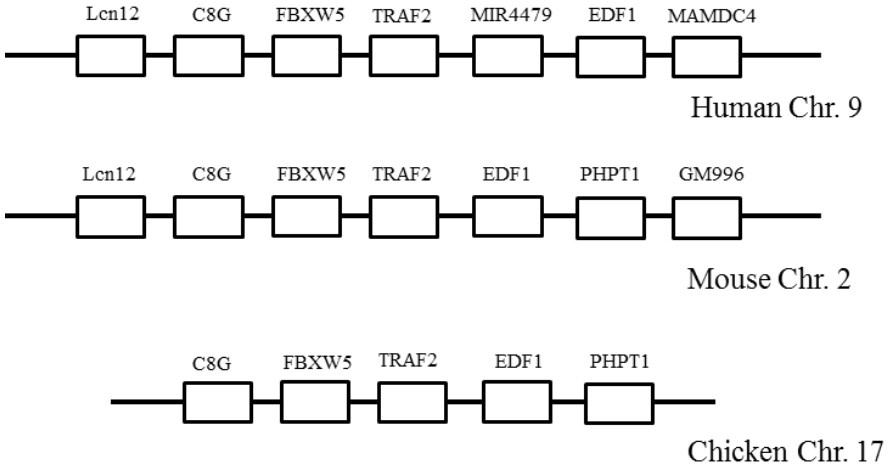

Figure 5.11 Conserved synteny of mammalian and chicken TRAF2 genes. *The location of genes upstream and downstream of mammalian and chicken TRAF2 were analysed using the Ensembl database*.

5.4.4 *In silico* analysis of chTRAF2 and chTRAF2S

To determine the amino acid conservation of chTRAF2 with its mammalian orthologues, sequence data for human TRAF2 (ENSP00000247668.2) and both of the mouse TRAF2 isoforms, TRAF2 (ENSMUSP00000028311) and TRAF2A (ENSMUSP00000109872), were extracted from the Ensembl database. TRAF family members are intracellular proteins and therefore do not possess a signal peptide cleavage site or a transmembrane domain. The amino acid sequences of the two chTRAF2 isoforms were predicted. The smaller chTRAF2 isoform translates into a protein with a stop codon in the same position as chTRAF2 (Figure 5.14). The two isoforms encode predicted proteins of 527 and 473 amino acids, respectively. When aligned with the mammalian TRAF2 sequences, chTRAF2 shares high amino acid identity (~66-69%) (Figure 5.14). Using the SMART prediction model, the locations of the various domains were identified within mammalian and chicken TRAF2 proteins (Figure 5.14). Mammalian TRAF2 contains an NH_2-terminal RING domain, five zinc finger motifs, a coiled-coil, TRAF-N, domain and a TRAF-C domain. ChTRAF2 also has these regions with high degrees of conservation. In contrast, chTRAF2S is missing a portion of the first zinc finger motif, all of the second zinc

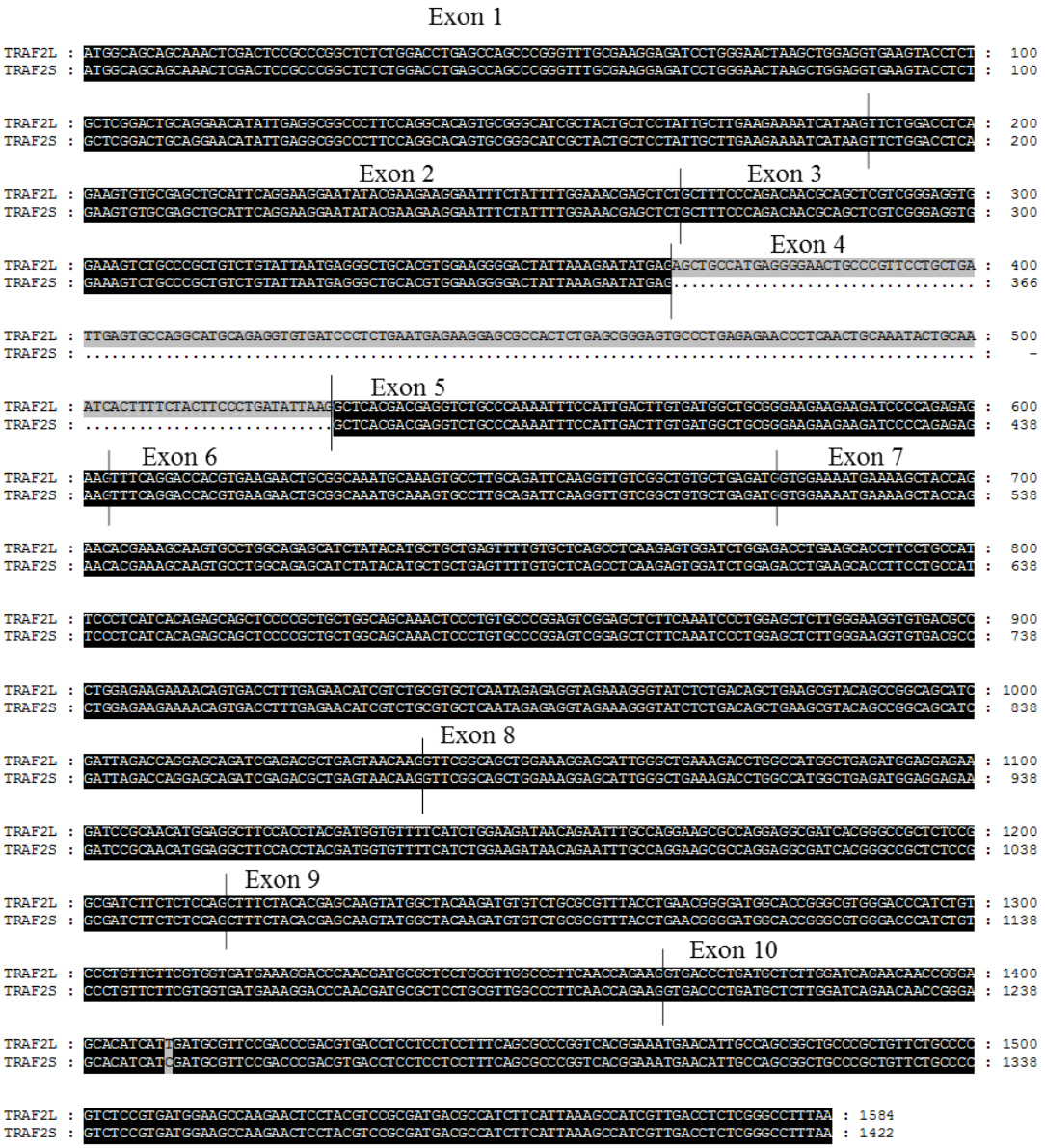

Figure 5.12 Nucleotide alignment of the chTRAF2 isoforms. *Using the SMART program and the Ensembl database, the ten chTRAF2 exons were annotated in the chicken cDNA sequence, labelled exons 1-10. Vertical lines indicate exon boundaries*

finger motif and a portion of the third zinc finger motif but has an intact RING domain, zinc finger motifs 4 and 5 and both of the TRAF-N and TRAF-C domains. The splicing of exon four from chTRAF2S would lead to the formation of a protein with a partial NH_2-terminal portion of zinc finger motif 1 connected to a COOH-

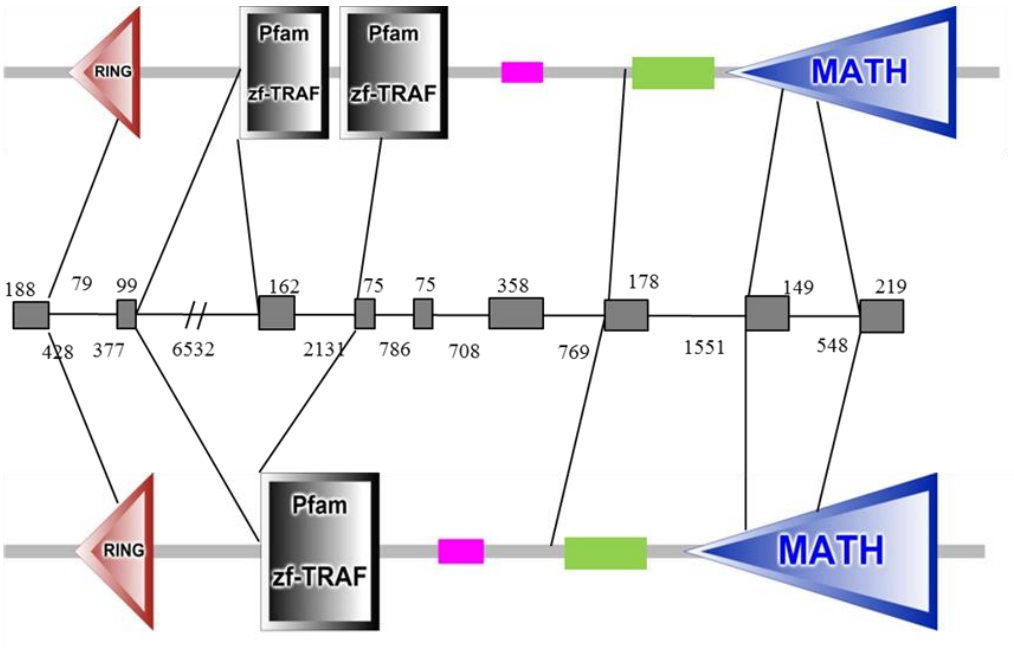

Figure 5.13 Genomic structure of the chTRAF2 isoforms. *Red triangles indicate the RING domains, black boxes the zinc finger motifs, green boxes the coiled-coil regions (TRAF-N) and blue triangles the MATH (TRAF-C) domain. In the gene model (centre) the grey boxes represent the ten exons and the numbers indicate the size (bp) of the exons and introns.*

terminal portion of zinc finger motif three (Figure 5.14). These two portions linked together may form a hybrid functional zinc finger.

5.4.5 Construction of pcDNA3-HA containing chTRAF2 or chTRAF2S

The two chTRAF2 isoforms were sub-cloned into a modified pcDNA3 vector containing a HA epitope (pcDNA3-HA) upstream of the cloning site (Poh *et al.*, 2008). Primers were designed to integrate an *Eco*R1 restriction site at the 5' end and an *Xba*I restriction site at the 3' end, downstream of the stop codon. The ATG start codon was removed from the chTRAF2 forward primer to generate NH_2-terminal tagged proteins with an ATG start codon upstream of the HA tag. The sub-cloning primers (Appendix 2, Table 2) were used in PCR using a 1:1000 dilution of plasmid DNA containing either gene previously TA-cloned into pGEM-T Easy. The

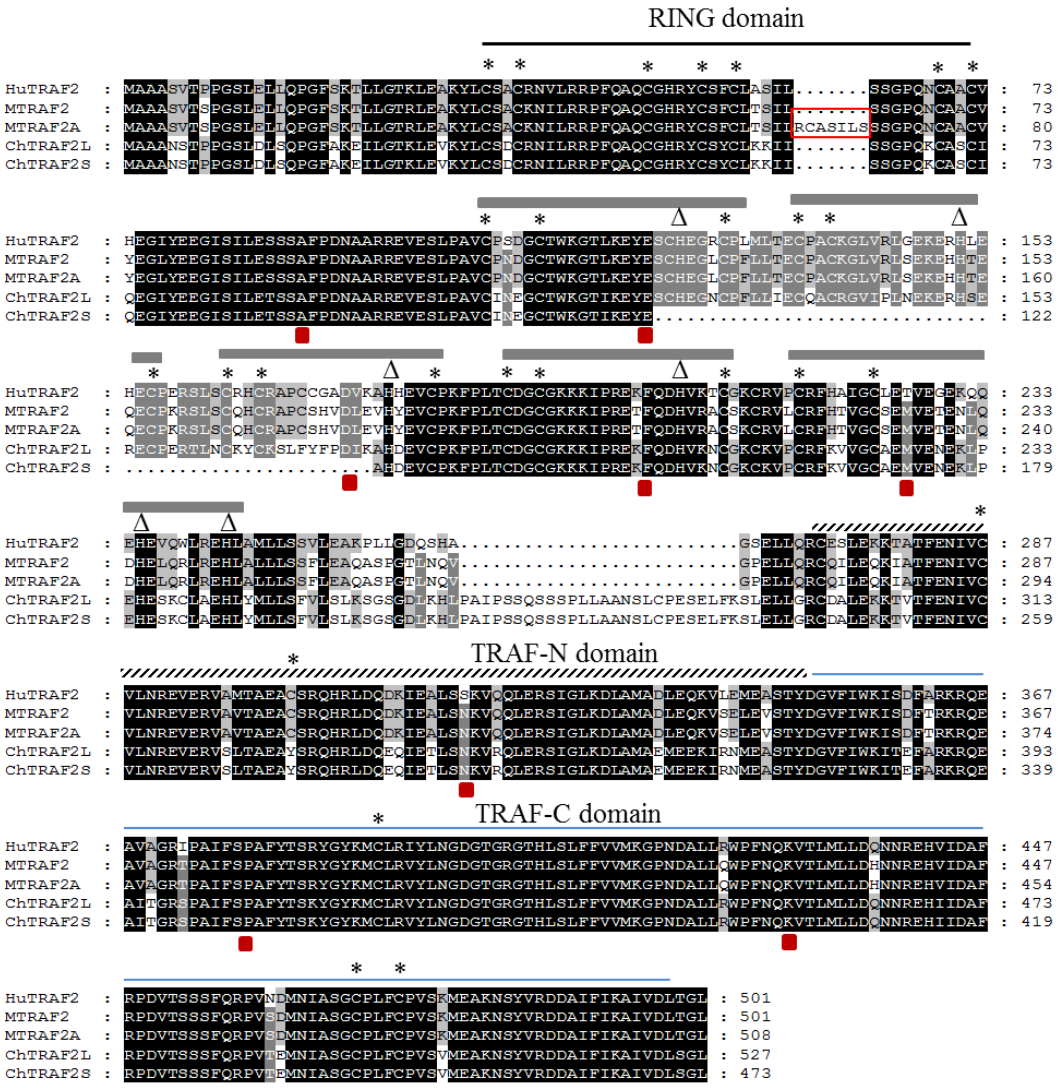

Figure 5.14 Amino acid alignment of mammalian and chicken TRAF2. *Shaded areas represent conservation of amino acid – the darker the shading, the more conserved the residue across species; black shading indicates conservation between all species, dark grey with white lettering indicates conservation between 2 species. Dots indicate gaps in the alignment. The red box indicates the 7 additional amino acids in the murine TRAF2A isoform. Asterisks indicate the conserved cysteine residues and open triangles conserved histidine residues characteristic of zinc finger motifs. Grey boxes above the sequence indicate the five conserved zinc finger motif regions, the dashed line the TRAF-N domain and blue line the TRAF-C domain.*

PCR products were gel electrophoresed and the resulting bands were gel purified. Both cDNAs were subjected to double restriction digestion using *Eco*R1 and *Xba*I restriction enzymes. The restriction product was visualised on an agarose gel and bands were excised and purified. The resulting products were ligated into linearized pcDNA3-HA and transformed into *E. coli* JM109 cells. Three independent colonies were sequenced and verified for chTRAF2 and chTRAF2S directional sub-cloning into pcDNA3-HA (Appendix 3, Figure 1).

5.3.6 Protein expression and analysis of chTRAF2 and chTRAF2S

To analyse the bioactivity of chTRAF2 and chTRAF2S, both cDNAs were sub-cloned separately into the modified pcDNA3-HA vector to examine protein expression. To generate recombinant proteins, each plasmid was transfected into HEK-293T cells using the calcium phosphate approach. Cells were transiently transfected and cell supernatants and lysates were collected after 48 h. The cell supernatants and lysates were examined for protein expression using mouse anti-HA mAb by western blot analysis. However, the expression of HA-tagged fusion proteins could not be detected. The samples were then analysed by dot blot, which allows concentration of the sample protein onto a small area of nitrocellulose membrane, and the HA-tagged recombinant proteins were then detected (Figure 5.15A). There was little or no detection of HA-tagged recombinant proteins in the cell supernatants, but expression was detected in the cell lysates of cells transfected with both isoforms, indicating that each protein is expressed intracellularly.

Cell lysates from transfected HEK-293T cells were analysed by SDS-PAGE followed by Coomassee blue staining under both reducing and non-reducing conditions (Figure 5.15B). The predicted molecular weight of the HA-chTRAF2 recombinant protein was 60.32 kDa and that of the HA-chTRAF2S recombinant protein was 54 kDa. Both bands were evident under both reducing and non-reducing conditions. No predominant larger proteins were identified on the gel indicating that chTRAF2 proteins do not form larger protein complexes under these conditions.

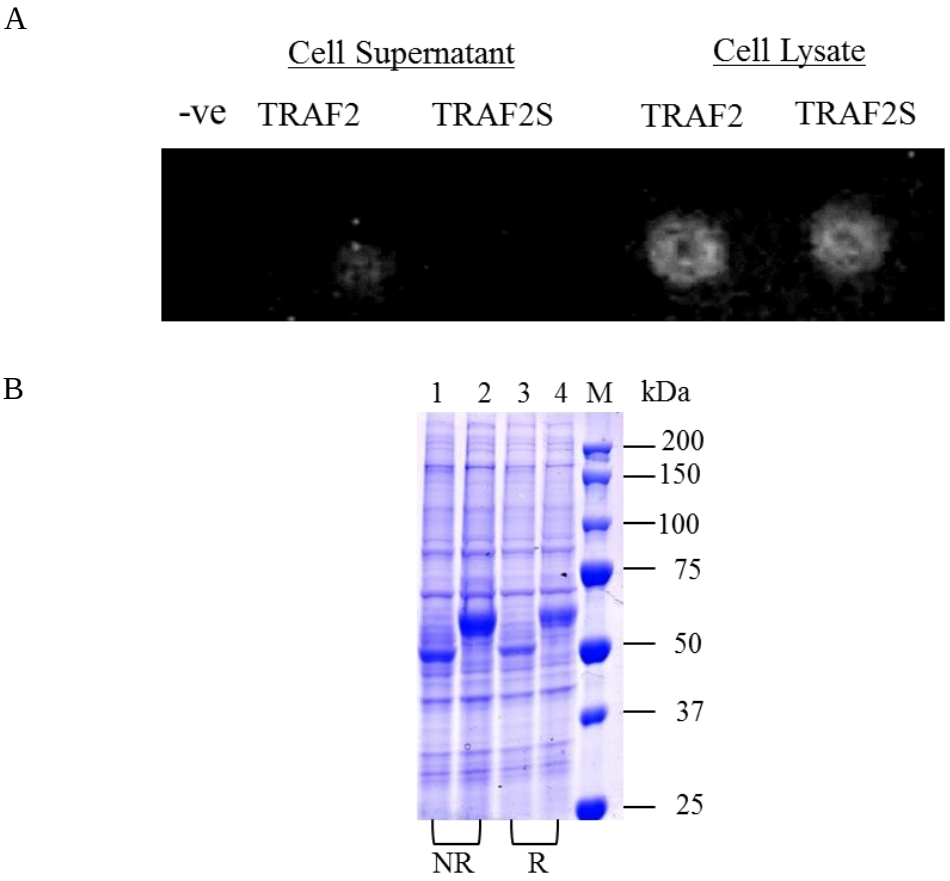

Figure 5.15 Protein expression analyses of HA-chTRAF2 and HA-chTRAF2S. ***A)*** *Dot blot analyses of cell supernatants and lysates from HEK-293T cells transiently transfected with pcDNA-HA-chTRAF2 and pcDNA-HA-chTRAF2S constructs. Protein expression was detected using mouse anti-HA mAb and goat anti-mouse HRP-conjugated mAb.* ***B)*** *SDS-PAGE analyses of cell lysates from HEK-293T cells transiently transfected with pcDNA-HA-chTRAF2 (lanes 2 and 4) and pcDNA-HA-chTRAF2S (lanes 1 and 3) under reducing (R) and non-reducing conditions (NR). M = Precision plus protein standard (BioRad).*

5.4.7 RT-PCR analysis of chTRAF2 and chTRAF2S mRNA expression in lymphoid and non-lymphoid tissues

The majority of eukaryotic genes are estimated to express several alternatively spliced forms that contribute to the complexity of the proteome. Protein isoforms may differ in their function, cellular and organ localisation and expression

pattern. RT-PCR analysis was carried out to examine the mRNA expression of chTRAF2 and chTRAF2S in lymphoid and non-lymphoid tissues. RNA samples (100 ng) were reverse-transcribed using an oligo-dT primer and then amplified by RT-PCR. A set of primers was designed for the amplification of both of the chTRAF2 isoforms (Appendix 2, Table 3). These primers overlapped exon 3 and exon 5 to amplify two bands, a large band at 350 bp representing chTRAF2 and a small band at 190 bp representing chTRAF2S.

In all the lymphoid tissues examined, both chTRAF2 and chTRAF2S mRNA expression were detected (Figure 5.16). ChTRAF2 mRNA expression levels was predominant compared to chTRAF2S mRNA expression in the lymphoid tissue panel (Figure 5.16). ChTRAF2S mRNA expression levels were low in the thymus, caecal tonsils, bone marrow, spleen, bursa of Fabricius and the crop and highest in Meckel's diverticulum (Figure 5.16). These data suggest that chTRAF2S mRNA expression levels are not as ubiquitous as those of chTRAF2 in a number of chicken lymphoid tissues.

In non-lymphoid tissues, chTRAF2 mRNA expression was not detected in the brain. ChTRAF2 and chTRAF2S mRNA expression was detected in the muscle, heart, liver, kidney, lung and skin (Figure 5.17). Interestingly, in the liver, kidney and lung, chTRAF2S mRNA expression was predominant compared to chTRAF2. In contrast, chTRAF2 mRNA expression levels were higher in the muscle and skin compared to those of chTRAF2S. These data suggest that chTRAF2 isoforms have differential expression in non-lymphoid tissues.

5.4.8 RT-PCR analysis of chTRAF2 and chTRAF2S mRNA expression in chicken immune cells

To examine whether there was a differences in expression of the two chTRAF2 isoforms in chicken splenocyte subsets, CD4, CD8β, TCRγδ, TCRαβ1, TCRαβ2, KUL01 and Bu1 cells were purified as previously described in section 5.3.6. RNA from these cell subsets were reverse-transcribed and chTRAF2 and chTRAF2S mRNA expression analysed by RT-PCR (Figure 5.18A). In both $CD4^+$ and $CD8\beta^+$ subsets, chTRAF2 mRNA expression levels were low. ChTRAF2S

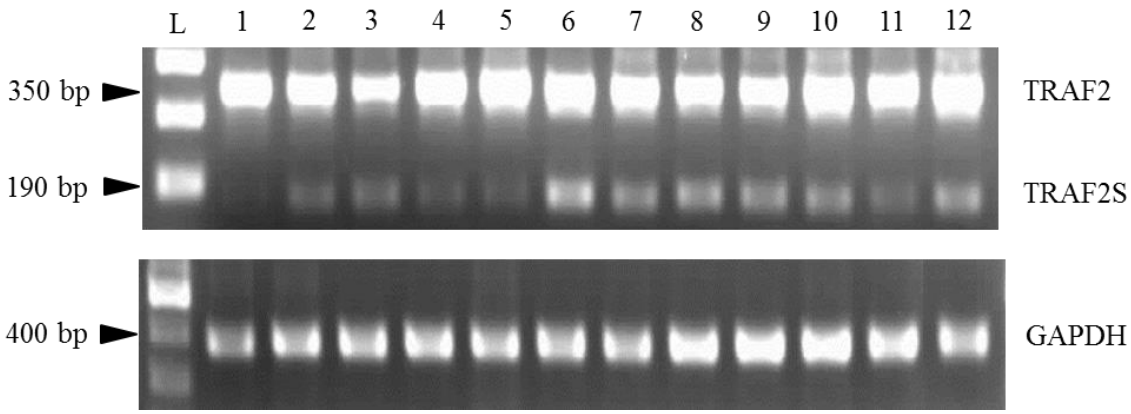

Figure 5.16 RT-PCR analysis of chTRAF2 and chTRAF2S mRNA expression in lymphoid tissues. *Primers were designed to overlap exon three and five of chTRAF2 to generate two cDNA products, a 350 bp product, representing chTRAF2, and a 190 bp product, representing chTRAF2S. ChTRAF2 and chTRAF2S mRNA expression was measured by RT-PCR in lymphoid tissues: 1) thymus, 2) spleen, 3) bursa of Fabricius, 4) caecal tonsils, 5) bone marrow, 6) Meckel's diverticulum, 7) Harderian gland, 8) caeca, 9) mid-gut, 10) upper-gut, 11) crop, 12) gizzard. L = 1 kb DNA ladder (Invitrogen). Data represent results from one of three individual birds with similar result.*

mRNA expression levels were high in $CD4^+$ and $KUL01^+$ subsets. Both chTRAF2 and chTRAF2S mRNA expression were detected in $TCR\gamma\delta^+$, $TCR\alpha\beta1^+$, $TCR\alpha\beta2^+$ and $Bu1^+$ subsets (Figure 5.18A). ChTRAF2 and chTRAF2S mRNA expression was examined in BMDC and BMDM either unstimulated or stimulated with LPS for 24 h, by RT-PCR (Figure 5.18B). In BMDC, there was no difference in the mRNA expression levels of either chTRAF2 isoform with or without stimulation. BMDM stimulated with LPS for 24 h had decreased chTRAF2 mRNA expression levels compared to those in unstimulated cells (Figure 5.18B), whereas chTRAF2S mRNA expression levels were unaltered.

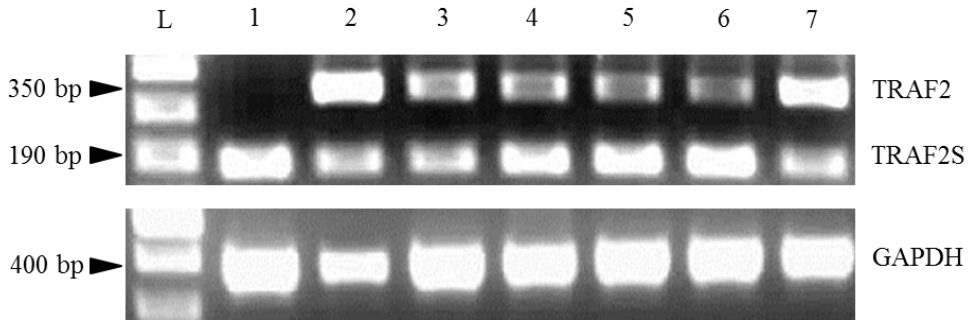

Figure 5.17 RT-PCR analysis of chTRAF2 and chTRAF2S mRNA expression in non-lymphoid tissues. *ChTRAF2 and chTRAF2S mRNA expression was analysed by RT-PCR in non-lymphoid tissues: 1) brain, 2) muscle, 3) heart, 4) liver, 5) kidney, 6) lung, 7) skin. L = 1 kb DNA ladder (Invitrogen). Data represent results from one of three individual birds with similar results.*

5.4.9 Kinetics of chTRAF2 and chTRAF2S mRNA expression in stimulated splenocytes

The kinetics of chTRAF2 and chTRAF2S mRNA expression in splenocytes unstimulated or stimulated with ConA for 2, 4, 6, 12, 18 or 24 h were examined by RT-PCR (Figure 5.19). ChTRAF2 mRNA expression levels were higher than chTRAF2S mRNA expression levels at all time-points examined (Figure 5.19). At all time-points, chTRAF2 mRNA expression levels were increased following stimulation. ChTRAF2S mRNA expression levels were increased in ConA-stimulated cells at most time-points but not as strongly as chTRAF2 mRNA.

5.4.10 Analysis of chTRAF2 and chTRAF2S bioactivity

To investigate the bioactivity of both chTRAF2 isoforms, NF-κB reporter assays were carried out in HEK-293T cells. The overexpression of receptors or signalling molecules can lead to the activation of their downstream signalling pathways in mammalian cells. Certain mammalian TRAFs positively regulate the NF-κB pathway, leading to its release from its inhibitor, IκB, in the cytoplasm and allowing it to translocate into the nuclease to bind to NF-κB DNA-binding motifs. HEK-293T cells were seeded at 1.5 X 10^4 cells/well and transiently transfected 24 h

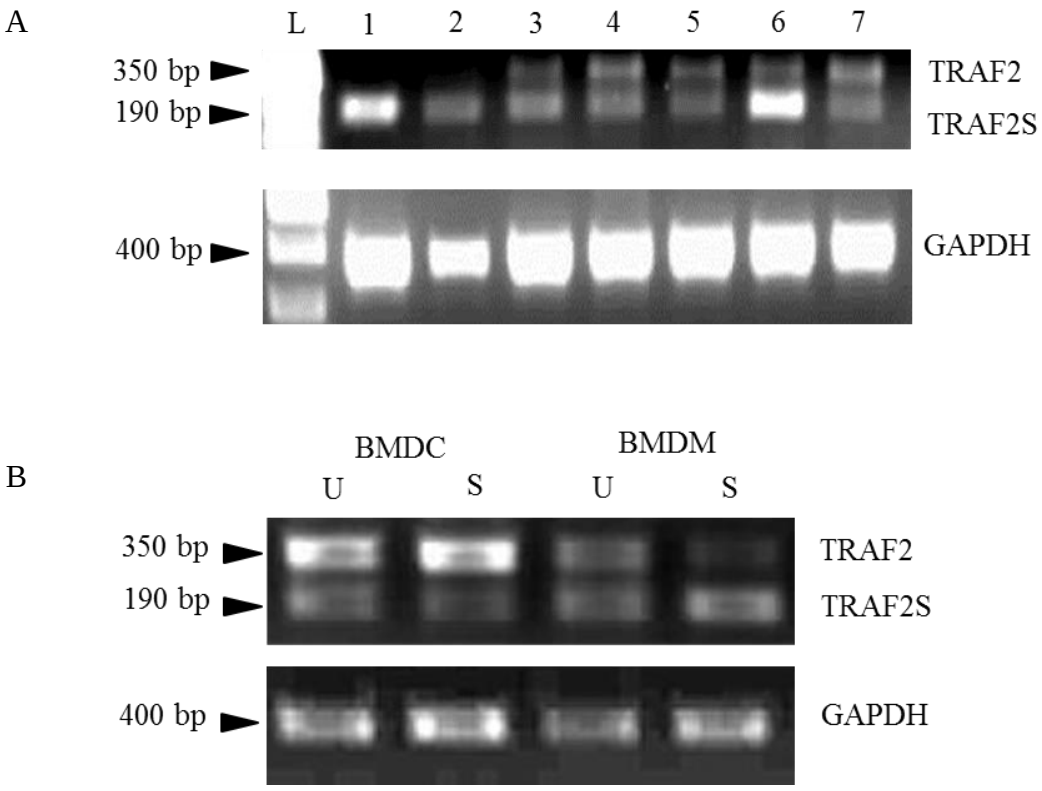

Figure 5.18 RT-PCR analysis of chTRAF2 and chTRAF2S mRNA expression in chicken immune cells. *ChTRAF2 and chTRAF2S mRNA expression was analysed by RT-PCR in* **A)** *purified splenocyte subsets: 1) CD4$^+$, 2) CD8β$^+$, 3) TCRγδ$^+$, 4) TCRαβ1$^+$, 5) TCRαβ2$^+$, 6) KUL01$^+$, 7) Bu1$^+$ and in* **B)** *BMDC and BMDM unstimulated or stimulated with LPS (200 ng/ml) for 24 h. L = 1 kb DNA ladder (Invitrogen). Data represent results from one of three individual birds with similar results.*

later with pGL4-NF-κB-Luc expressing the *Firefly* luciferase and the pcDNA3-HA constructs encoding chTRAF2 or/and chTRAF2S. To control for transfection efficiency and background signals, cells were cotransfected with a plasmid expressing *Renilla* luciferase. For each transfection, total DNA was adjusted to 200 ng using empty pcDNA3. To determine whether chTRAF2 or chTRAF2S could activate NF-κB in a dose-dependent manner, cells were transfected with 75 ng or 150 ng of each construct. To examine the ability of the chTRAF2 isoforms to synergise

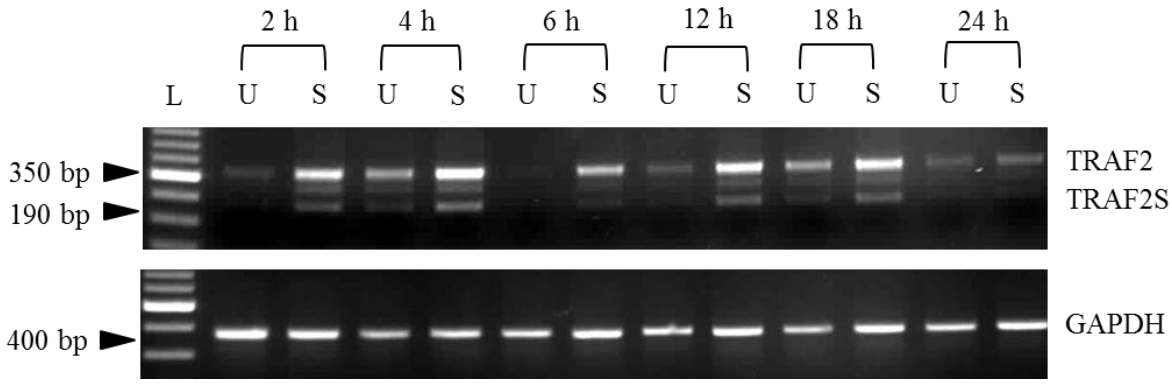

Figure 5.19 RT-PCR analysis of chTRAF2 and chTRAF2S mRNA expression in unstimulated and ConA-stimulated splenocytes for 2, 4, 6, 12, 18 or 24 h. *ChTRAF2 and chTRAF2S mRNA expression was analysed by RT-PCR in splenocytes unstimulated (U) or stimulated (S) with ConA (1 µg/ml) for 2, 4, 6, 12, 18 or 24 h L = 1 kb DNA ladder (Invitrogen). Data represent results from one of three individual birds with similar results.*

or inhibit NF-κB activation, cells were cotransfected with both chTRAF2 constructs at a total concentration of 75 ng (37.5 ng each) or 150 ng (75 ng each). *Firefly* and *Renilla* luciferase activation was analysed using a GloxMAX luminometer (Promega).

HEK-293T cells overexpressing either chTRAF2 or chTRAF2S significantly upregulated NF-κB activity in a dose-dependent manner compared to vector control cells (Figure 5.20). Cells transfected with empty pcDNA3 did not activate *Firefly* luciferase indicating that the vector did not contribute to the activation of NF-κB. ChTRAF2S activated NF-κB at higher levels that chTRAF2 but not to a statistically significant level. It is surprising that chTRAF2S can activate NF-κB as it does not express an intact primary zinc finger motif, lacks zinc finger motif two and a portion of the third zinc finger motif. Cotransfected cells significantly increased NF-κB activation in comparison to vector control cells at the two different DNA concentrations. However, NF-κB activation levels were not statistically significantly increased compared to levels in cells transfected with chTRAF2 or chTRAF2S alone

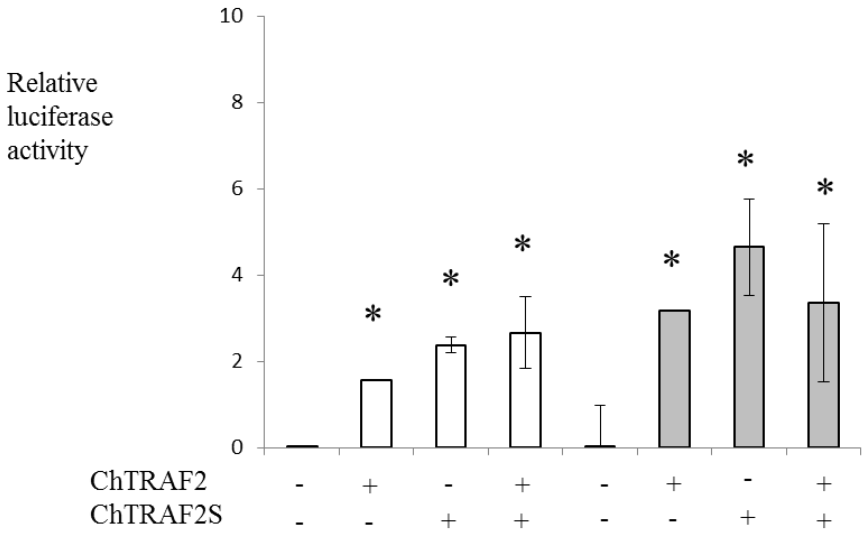

Figure 5.20 NF-κB reporter assays in HEK-293T cells. *The biological activity of chTRAF2 and chTRAF2S were determined using NF-κB reporter assays. Cells were transfected with 75 ng (white bars) or 150 ng of chTRAF2 and/or chTRAF2S (grey bars). Firefly and Renilla luciferase were detected in cell lysates 24 h after transfection. Data are presented as relative luciferase activity by normalising the data with Renilla luciferase activity. Data represent the average of four independent experiments and asterisks represents data that is statistically significantly ($p<0.05$) different compared to levels in pcDNA-3 empty control cells* ± *SEM (Mann-Whitney U test).*

(Figure 5.20). This suggests that the full-length chTRAF2 and chTRAF2S do not work in synergy to enhance the activation of NF-κB.

5.4.11 Phylogenetic analysis

In phylogenetic analysis, the TRAF family members are classified into five distinct clades (Figure 5.21). TRAF7 proteins cluster together, as do TRAF6 proteins and TRAF3 proteins. TRAF1 and TRAF2 proteins cluster separately but in the same clade, and TRAF4 and TRAF5 proteins also cluster separately but in a distinct clade. TRAF family members are therefore evolutionarily conserved across mammals and birds.

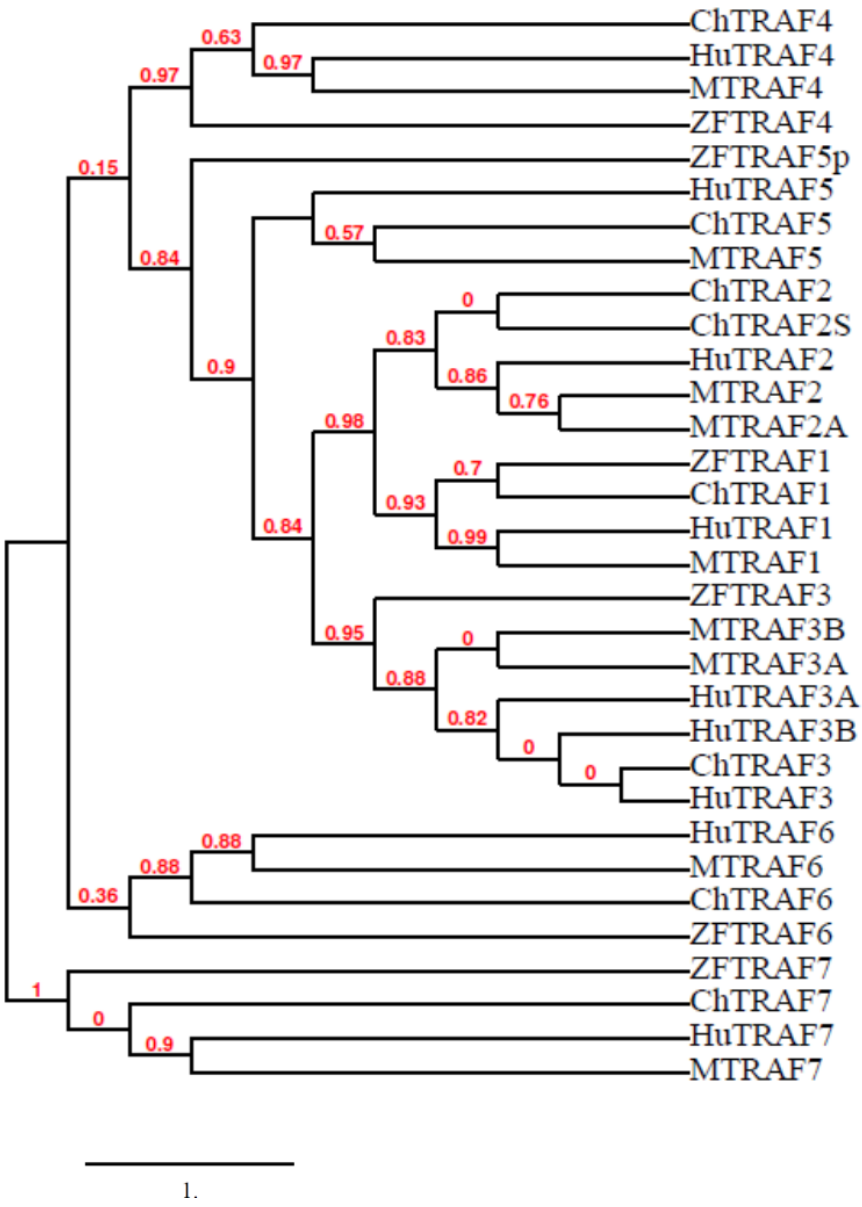

Figure 5.21 Phylogenetic tree showing the relationship between avian and mammalian TRAFs. *Numbers on the branches represent the boot-strap values. Analyses were performed using MEGA v5.0. Ch, chicken; Hu, human; M, mouse; ZF, zebra finch; p, partial: A, B, S; isoforms. Accession numbers are given in Appendix 2, Table 5.*

5.5 Discussion

Intracellular signalling by TNFR and Toll/IL-1R superfamilies is carried out by a number of TRAF family members. With some members of both the TNFR and IL-1R superfamilies absent from the chicken genome (Kaiser *et al.*, 2005), it is important to study the conservation of their downstream signalling proteins. Certain TRAF family members are important for development, as seen by the lethal phenotype in mice lacking TRAF2, TRAF3 and TRAF6 (Yeh *et al.*, 1997; Lomaga *et al.*, 1999). In the chicken, all members of the TRAF family (chTRAF1-chTRAF7) are present in the genome. The TRAF family of proteins are grouped together due to the presence of various domains such as a RING domain, zinc finger domains and the highly conserved TRAF-N and TRAF-C domains. The TRAF-N domain contains a coiled-coil region that mediates homo- or hetero-oligomerisation while the TRAF-C domains are involved in receptor binding (Pullen *et al.*, 1998). Despite sequence homology, each TRAF protein signals different outcomes which are non-redundant (Chung *et al.*, 2002). To begin to understand the downstream signalling pathways activated by chRANK, the cloning and molecular characterisation of chTRAF2, chTRAF5, chTRAF6 and chTRAF7 were attempted.

Mammalian TRAF5 shares similar functions to TRAF2 but is homologous to TRAF3 (Ishida *et al.*, 1996; Aizawa *et al.*, 1997). TRAF5$^{-/-}$ mice show no developmental abnormalities and survive as healthy adults. These mice do exhibit defects in CD40- and CD27-mediated activation of B cells (Nakano *et al.*, 1999) and GITR-mediated activation of NF-κB in T cells (Esparza *et al.*, 2006). TRAF5 overexpressed in the experimental rat model of inflammatory bowel disease was linked to the overexpression of the TNF-α receptors, TNFR1 and TNFR2, both of which bind to TRAF5 (Rojas-Cartagena *et al.*, 2005). It also regulates the expression of adhesion molecules and pro-inflammatory cytokines during early atherogenesis by enhancing JNK activation. TRAF5$^{-/-}$ BMDM can significantly uptake particulates more than wild-type cells by enhanced actin polymerisation (Missiou *et al.*, 2010). Crystal structure analysis of mammalian TRAF5 indicates that it can form homotrimers with the typical mushroom-shaped structure that is characteristic of TRAF proteins (Zhang *et al.*, 2012). Although TRAF5 is not required for lymphoid

organ or immune cell development, it is necessary for a number of biological activities in mammals. ChTRAF5 is highly conserved with its mammalian orthologues (Figure 5.3).

ChTRAF5 was cloned by Abdalla *et al.* (2004a), who analysed the expression pattern of chTRAF5 in a number of chicken tissues and cell types. The work presented here includes a more comprehensive panel of lymphoid and non-lymphoid organs, purified splenocytes and kinetics of expression in unstimulated and ConA-stimulated splenocytes. ChTRAF5 mRNA expression was detected in various organs of the chicken (Figure 5.6). ChTRAF5 mRNA expression was lowest in the thymus, as demonstrated by Abdalla *et al.* (2004a), bursa of Fabricius and the crop whereas the highest levels of mRNA expression were in the spleen, Meckel's diverticulum, caeca and upper-gut. In mammals, TRAF5 mRNA expression is limited to a few organs, such as the thymus and spleen, and was not found in the small intestine (Ishida *et al.,* 1996).

In non-lymphoid organs, chTRAF5 mRNA expression was barely detectable in the muscle and the skin (Figure 5.7), similar to mammalian TRAF5 mRNA expression patterns (Ishida *et al.,* 1996). In purified splenocytes, chTRAF5 mRNA expression was not detected in $KUL01^{+}$ cells. This could suggest that chTRAF5 is not highly expressed in phagocytic cells. In mice, $TRAF5^{-/-}$ DC have no defects in CD40- or TLR9-mediated activation of pro-inflammatory cytokine expression (Kraus *et al.*, 2008). In chicken LPS-stimulated BMDC, chTRAF5 mRNA expression levels were not altered compared to levels in unstimulated cells. However, chTRAF5 mRNA expression levels were increased in LPS-stimulated BMDM (Figure 5.8B). This suggest that chTRAF5 may have a role in the TLR4 downstream signalling pathway in BMDM. BMDM from $TRAF5^{-/-}$ knockout mice induced higher levels of IL-6 expression after TLR7 stimulation and TRAF5 was demonstrated to have a regulatory role in TLR signalling in B cells by interacting with and inhibiting MyD88 and TAK1 (Buchta & Bishop, 2014). ChTRAF5 mRNA expression levels were highest in $TCR\gamma\delta^{+}$ cells (Figure 5.8A). TCRγδ cells are the most abundant T cells in the chicken in contrast to mammals, where TCRαβ T cells are more abundant. TCRγδ cells are innate-like cells that increase in numbers upon

bacterial infection in human and chickens (Hara *et al.*, 1992; Berndt *et al.*, 2006). While naïve TRAF5$^{-/-}$ mice have normal lymphocyte cellularity, upon infection with intracellular pathogens, expansion of CD8^{+} T cells is defective (Kraus *et al.*, 2008), linked to an increase in cell apoptosis (Kraus *et al*., 2008), and they have a skewed and more enhanced Th2 immune response (So *et al.*, 2004). Mouse TRAF5 has a role in IL-17-mediated stabilisation of CXCL1 mRNA expression. This chemokine is released by neutrophils to attract cells to the site of injury and its long-term expression is required for an optimal immune response (Sun *et al.*, 2011). In ConA-stimulated splenocytes, chTRAF5 mRNA expression levels were increased at 18 and 24 h compared to levels in unstimulated cells (Figure 5.9). Activation of splenocytes therefore activates a downstream signalling pathway that involves chTRAF5. TRAF5 is involved in the regulation of T cell responses in mammals and it would be interesting to examine its role in chicken T cell biology.

TRAF6 expresses one of the most divergent TRAF-C domains of the TRAF family and binds to separate TRAF-binding peptides not recognised by TRAF1, TRAF2, TRAF3 or TRAF5. TRAF6 is the only TRAF family member that is associated with activating downstream signalling pathways for both the TNFR and Toll/IL-1R superfamilies (Cao *et al.*, 1996; Chung *et al.*, 2007). Structural analysis of TRAF6 identified that its zinc finger domain but not its RING domain is required for NF-κB activation (Cao *et al.*, 1996). ChTRAF6 mRNA expression was detected in all lymphoid organs examined except the thymus. The highest chTRAF6 mRNA expression levels were seen in the bursa of Fabricius and the mid- and upper-gut (Figure 5.6). The chicken intestine is rich in many cells of the innate immune system while the bursa of Fabricius is the site of development for the B cell receptor repertoire for chicken B cells, indicating that chTRAF6 may be involved in signalling in immune cells. It plays a vital role in CD40-mediated JNK activation in mammals (Rowland *et al.*, 2007). CD40 is a major player in B cell survival and Ig class switching, by binding to a number of TRAF molecules, such as TRAF2, TRAF3, TRAF5 and TRAF6 (Pullen *et al.*, 1998). TRAF6$^{-/-}$ mice have a lethal phenotype; such mice survive up to 2-3 weeks of age, lack osteoclasts, tooth eruption and normal bone marrow cavities (Lomaga *et al.*, 1999; Naito *et al*., 1999). To examine the role of TRAF6 in downstream signalling activities, mice were generated

to express mutations in the known TRAF-binding domains of CD40. The mutation of CD40 TRAF6-specific binding domains led to a 95% decrease in total plasma cell numbers (Ahonen *et al.,* 2002) and a decrease in the levels of IL-6 expression (Jalukar *et al.,* 2000). As described in Chapter 3, TRAF6 is necessary for RANKL-mediated osteoclastogenesis (Lomaga *et al.,* 1999).

ChTRAF6 mRNA expression was detected in all non-lymphoid tissues examined with the lowest expression levels seen in the brain (Figure 5.7). In purified splenocytes, chTRAF6 mRNA expression levels were low in TCRαβ2^{+} cells and the highest chTRAF6 mRNA expression levels were detected in CD8β^{+} cells (Figure 5.8A). In a time-course study of unstimulated and ConA-stimulated splenocytes, chTRAF6 mRNA expression levels were not altered between unstimulated or stimulated cells after 2 or 4 h (Figure 5.9). ChTRAF6 mRNA expression levels were increased in stimulated cells at 6, 12 and 18 h compared to levels in unstimulated cells, indicating that chTRAF6 mRNA expression levels are upregulated in activated splenocytes as they are in mammals (King *et al.,* 2006). TRAF6$^{-/-}$ mice have increased expression levels of Th2 and Treg cytokines, IL-4, IL-10 and TGF-β, in multiple organs but were still capable of differentiating Th1 cells. However, TRAF6$^{-/-}$ T cells could not induce IFN-γ production upon exposure to IL-18 which signals though an IL-1R superfamily member, the IL-18R, which requires TRAF6 for the activation of downstream signalling cascades (Chiffoleau *et al.,* 2003). TRAF6$^{-/-}$ T cells express higher levels of IL-4 and IL-5 upon stimulation (King *et al.,* 2006) and Treg cells lose the expression of FoxP3, becoming exFoxP3Treg cells, under inflammatory conditions (Muto *et al.,* 2013). These data indicate that TRAF6 has a role in the maintenance of Treg cells. TRAF6$^{-/-}$ T cells differentiated under Th1, Th2 or Th17 polarising conditions induced increased levels of the Th17 effector cytokine, IL-17, compared to Th1 (IFN-γ) and Th2 (IL-13) cells, due to the increase in ROR-γt transcription. The loss of Th17 regulation has been linked to a number of autoimmune diseases and the loss or malfunction of TRAF6 signalling may be linked to these diseases (Cejas *et al.,* 2010).

ChTRAF6 mRNA expression levels were not altered between unstimulated and LPS-stimulated BMDC and BMDM (Figure 5.8B). In mammals, TRAF6 is

required for the TLR- and CD40-mediated maturation of, pro-inflammatory cytokine production by and cell surface expression of CD80 and MHC class II in DC and is required for the development of $CD11c^+$ splenic DC (Kobayashi *et al.,* 2003). In a more recent study, $TRAF6^{-/-}$ gut-associated DC showed a substantial increase in Th2 immune responses. The main roles of mucosal DC are to control the induction and maintenance of iTreg cells (Pulendran *et al.,* 2010). In $TRAF6^{-/-}$ DC, the number of iTreg cells in the intestine was diminished due to the lack of IL-2 production by DC (Han *et al.,* 2013).

TRAF7 is the most recent member of the mammalian TRAF family to be identified (Bouwmeester *et al.,* 2004). The designation of this protein as TRAF7 has been controversial as it does not possess a TRAF-C domain but instead contains several WD40-repeat domains. It has been designated TRAF7 due to the high homology of its RING, zinc finger motif and coiled-coil domains with those of other TRAF proteins (Xu *et al.,* 2004). WD40-repeat domains are conserved WD dipeptides of approximately 44-60 amino acids. Each repeat comprises a four strand anti-parallel β-sheet (Wu *et al.,* 2010). The overall structure of WD40 domains is a β-propeller architecture which acts as a platform for multiple protein-protein interactions making these proteins good hubs in cellular interaction networks (Stirnimann *et al.,* 2010). WD40 domains are among the most abundant domain types across eukaryotic genomes. These proteins are involved in a number of biological processes such as apoptosis, signal transduction, cell cycle control and transcriptional regulation (Xu & Min, 2011). ChTRAF7 contains all seven WD40 repeat domains as found in mammalian TRAF7 (Xu *et al.,* 2004; Morita *et al.,* 2005). In mammals, TRAF7 WD40 domains are required for interacting with and driving the sumoylation of the transcription factor, c-Myb (Morita *et al.,* 2005). C-Myb is vital for several stages of T cell development and activation and requires tight regulatory control as its pro-oncogene, v-*myb,* induces anti-apoptotic signals leading to the development of T cell lymphomas (Gewirtz *et al.,* 1989).

ChTRAF7 mRNA expression was ubiquitous across chicken tissues and organs similar to mammalian TRAF7 (Xu *et al*., 2004; Morita *et al.,* 2005). ChTRAF7 mRNA expression levels were the lowest in the crop and its mRNA levels

were not different between unstimulated and ConA-stimulated splenocytes over the six time-points examined (Figure 5.9). To date, very little data are available on the role of mammalian TRAF7 in immunity. TRAF7$^{-/-}$ mice which would provide more insight into its biological functions have yet to be generated. Mammalian TRAF7 has not yet been implicated in binding to and signaling for members of the TNFR superfamily. Recently, an oyster homologue of TRAF7 was identified in *Crassostrea hongkongensis* (CrhTRAF7). Although no biological functions were examined, crhTRAF7 mRNA expression levels were significantly reduced in the first 12 h after challenge of hepatocytes with the Gram-ve bacteria, *Vibrio alginolyticus,* indicating a role for crhTRAF7 in fish immunity (Fu *et al.*, 2011).

When the full-length chTRAF2 cDNA was cloned, a smaller isoform was identified (Figure 5.10). Sequence analyses and the SMART prediction program indicated that the smaller isoform of chTRAF2 was missing exon four due to exon skipping (Figures 5.11 & 5.12). ChTRAF2S differs from the murine TRAF2A isoform, which expresses seven additional amino acids within the RING domain due to differential usage of a splice donor site at the 3' end of exon one (Brink & Lodish, 1998). Due to the difference between the murine and chicken TRAF2 isoforms, the chTRAF2 smaller isoform was named chTRAF2S. The splicing of exon four from chTRAF2 leads to a portion of the first zinc finger motif, the entire second zinc finger motif and a portion of the third zinc finger motif being excluded from the translated protein, generating chTRAF2S. The partial NH_2-terminal portion of zinc finger one may join to the partial COOH-terminal portion of zinc finger three to produce a slightly smaller hybrid zinc finger motif. Overall chTRAF2 showed high conservation with its mammalian orthologues and branched with the human and mouse TRAF2 proteins in phylogenetic analysis (Figure 5.21).

In RT-PCR analyses, chTRAF2 and chTRAF2S mRNA expression was analysed in a number of chicken lymphoid and non-lymphoid tissues (Figure 5.16). Across the lymphoid tissues examined, chTRAF2 mRNA expression levels were higher than those of chTRAF2S. ChTRAF2S mRNA expression levels were low across all tissues examined with the highest found in Meckel's diverticulum (Figure 5.16). In non-lymphoid tissues, chTRAF2 and chTRAF2S mRNA expression

patterns differ; chTRAF2 mRNA expression levels were low in the brain, heart, liver, kidney and lung (Figure 5.18). In contrast, chTRAF2S mRNA expression levels were highest in the brain and lung (Figure 5.17). Interestingly, in mice, TRAF2 mRNA expression levels were highest in the brain and lung whereas those of TRAF2A mRNA were lowest in these organs (Brink & Lodish, 1998).

In chicken splenocyte subsets, chTRAF2 mRNA expression levels were low in both $CD4^+$ and $CD8\beta^+$ cells (Figure 5.18A). Interestingly, chTRAF2S mRNA expression levels were higher than chTRAF2 mRNA expression levels in $KUL01^+$ cells. ChTRAF2 mRNA expression levels decreased in LPS-stimulated BMDM compared to chTRAF2S mRNA expression levels (Figure 5.18B). However, chTRAF2 mRNA expression levels increased in LPS-stimulated BMDC (Figure 5.18B). This indicates differential expression patterns between the chTRAF2 isoforms in chicken APC. ChTRAF2 and chTRAF2S mRNA expression levels were examined in a time-course assay of unstimulated and ConA-stimulated splenocytes by RT-PCR. Over all the time-points examined, chTRAF2 mRNA expression levels were predominantly increased in ConA-stimulated cells in comparison to chTRAF2S levels and levels of both isoforms in unstimulated cells (Figure 5.19). ChTRAF2 mRNA expression levels increased in cells stimulated with ConA, a lectin that non-specifically activates T cells, suggesting that chTRAF2 is associated with a pathway activated in chicken T cells. In mammals, TCR-activated T cells increase TRAF2 expression in a time- and dose-dependent manner and TRAF2 is required for regulation of the NF-κB2 pathway. Uncontrolled upregulation of the NF-κB2 pathway led to an increase in expression of Th17 cell effector cytokines, such as IL-21, and the transcription factor, ROR-γt (Lin *et al.*, 2011). The role of mammalian TRAF2 in Th17 cells was further demonstrated in $TRAF2^{-/-}$ mice where IL-17-producing T cell numbers were increased in the colonic lamina propria which led to colitis (Piao *et al.*, 2011). In mammals, TRAF2 expression was increased in stimulated lymphocytes and is not necessary for the development of either $CD4^+$ or $CD8^+$ T cells in the thymus but mice do exhibit an increase in B cell numbers when TRAF2 is expressed as a DNTRAF2 mutant (Lieberson *et al.*, 2001). Due to the lethality of $TRAF2^{-/-}$ mice, many studies have identified the role of TRAF2 signalling by generating DNTRAF2 mice. By only expressing the TRAF-C domain,

the DNTRAF2 protein can bind to receptors but not signal to activate pathways. Using this approach, it was demonstrated that TRAF2 was required for IL-2 production in T cells and mice were shown to have defects in both $CD4^+$ and $CD8^+$ T cell activation during a secondary response to influenza, indicating TRAF2 has a role in T cell memory (Cannons *et al.*, 2002). TRAF2 also regulates Th2 differentiation by binding to and inhibiting NIP45, a member of the NFAT family, required for the activation of IL-4 (Lieberson *et al.*, 2001). Mammalian TRAF2 is required for a number of T cell activities and with high conservation between mammals and chickens, chTRAF2 may have similar roles.

Mouse TRAF2 and TRAF3 isoforms have been identified and demonstrated to have a role in the regulation of NF-κB activation (van Eyndhoven *et al.*, 1998; Brink & Lodish, 1998). The bioactivity of intracellular signalling proteins can be investigated by overexpressing these genes in non-immune, transformed cell lines, such as HEK-293T cells, in combination with reporter genes, signalling molecules or receptors. This approach was used to analyse the bioactivity of chTRAF2 and chTRAF2S using NF-κB as a reporter gene. The overexpression of chTRAF2 or chTRAF2S proteins in HEK-293T cells led to a significant upregulation of NF-κB activation in a dose-dependent manner, compared to levels in empty vector control cells (Figure 5.20). Cells cotransfected with both chTRAF2 constructs at a total concentration of 75 ng (37.5 ng each) significantly increased NF-κB activation compared to levels in vector control cells but not compared to levels in chTRAF2 or chTRAF2S singly transfected cells (Figure 5.20). Cells cotransfected with higher concentrations of the chTRAF2 constructs (75 ng each) only slightly enhanced NF-κB activation compared to chTRAF2 and chTRAF2S levels (Figure 5.20). This suggests that chTRAF2 and chTRAF2S do not synergise to enhance NF-κB activation. ChTRAF2S overexpression induced higher levels of NF-κB activation than those induced by chTRAF2 but not to a statistically significant level (Figure 5.20). The chTRAF2S isoform lacks internal zinc fingers compared to chTRAF2 (Figures 5.12 & 5.14). Mammalian TRAF2 requires an intact RING domain and zinc finger domains for NF-κB activation (Takeuchi *et al.*, 1996). In NF-κB reporter systems, the replacement of the RING and zinc finger motifs one and two of TRAF3 with the TRAF2 equivalent domains induced NF-κB activation compared to wild-

type TRAF3, which cannot activate NF-κB (Takeuchi *et al.,* 1996), indicating the importance of TRAF2 RING domain and zinc finger motifs for activating downstream signalling cascades. In mice, the TRAF2 isoform, TRAF2A, does not activate NF-κB, due to an additional seven amino acids within the RING domain (Brink & Lodish, 1998). It is hypothesised that the non-signalling TRAF2A isoform competitively binds to TRAF-binding peptides, inhibiting TRAF2 and other TRAF members from binding and signalling downstream pathways. Thus TRAF2A regulates the activation of downstream NK-κB but can activate JNK (Dadgostar & Cheng, 1998), suggesting a regulatory role for this isoform on specific downstream signalling pathways. The data indicate that chTRAF2S is capable of activating NF-κB. The absence of exon four from chTRAF2S generates a protein expressing three zinc finger motifs, as compared to the five expressed in mammalian TRAF2 and chTRAF2 (Figure 5.14). Exon 4 of chTRAF2 translates the COOH-terminal portion of zinc finger motif one and the NH_2-terminal portion of zinc finger motif three. It is hypothesised that these two zinc finger portions form a hybrid zinc finger motif with biological functions similar to the chTRAF2 protein which expresses five zinc finger motifs. ChTRAF2S is biologically active and may competitively bind to TRAF-binding motifs in the intracellular domains of members of the TNFR superfamily, where it could send a more enhanced signal downstream during certain cellular processes.

Overall, this Chapter describes the cloning and molecular characterisation of a number of chicken TRAF family members. These intracellular proteins share high amino acid conservation with their mammalian orthologues which could indicate conserved bioactivities. Although this Chapter describes their mRNA expression in a number of lymphoid and non-lymphoid tissues, along with immune cells, by RT-PCR, future work should be aimed at quantifying their mRNA expression levels in cells activated by various stimuli, such as TLR, TNFR or IL-1R. Analysis of TRAF family member mRNA expression levels in chicken immune responses will help elucidate the downstream signalling pathways used by various cell surface receptors.

Chapter 6

Discussion

6.1 Overall perspective

The main aim of this thesis was to clone and characterise the TNF family members RANKL, RANK and OPG in the chicken. Once the three genes were cloned, their transcriptional regulation, protein structure and bioactivity were investigated. In mammals, the TNF superfamily is made up of 19 ligands and 29 receptors that have multiple roles in lymphoid organ development and immunity. In 2005, genomic analysis identified a reduced number of TNF family members in the chicken genome (Kaiser *et al.*, 2005). The missing members have roles in T cell costimulation, activation and effector cytokine production. It is possible that the chicken genome expresses a minimal essential TNF superfamily. Prior to this study, avian orthologues of five members of the TNF superfamily- CD30L, TRAIL, BAFF, CD40L and VEGI- had been characterised. These studies indicated high conservation of biological activity of TNF family members between mammals and birds.

The chicken mounts a Th1 and Th2 immune response to infection with intracellular and extracellular pathogens, respectively (Degen *et al.*, 2004; Powell *et al.*, 2009). However, the tools and reagents required to identify polarised Th cells in the chicken are still largely not available. Certain members of the TNF superfamily are predominantly expressed on different $CD4^+$ T cell subsets and can be used to help differentiate between them. Mammalian RANKL is predominantly expressed on the surface of Th1 cells and induces pro-inflammatory cytokine expression in RANK-expressing DC and macrophages. RANKL is a multitasking cytokine, having roles in immune organ development (lymph nodes, M cells, mTEC), pro-inflammatory immune responses and bone remodelling. Its importance within human physiology is underscored by the use of monoclonal antibodies against RANKL (denosumab, Amgen Inc., USA) to treat post-menopausal osteoporosis and cancer-related osteolysis. It is currently under phase IV clinical trials for use in alleviating RA (Lacey *et al.*, 2012). The conservation of RANKL bioactivity in the chicken was identified in this study and therefore RANKL has a role in both chicken Th1 immune responses and bone metabolism.

6.2 Cloning and analysis of chRANKL, chRANK and chOPG

The presence of RANKL, RANK and OPG in the chicken genome indicates the conservation of these genes from before the divergence of mammals and birds from a common ancestor over 300 million years ago. Using the sequence data from the Ensembl database, chRANK and chOPG cDNA were amplified by RT-PCR (Chapter 3). The predicted chRANKL sequence in the Ensembl database was annotated incorrectly, lacking a predicted transmembrane domain. Using the human RANKL sequence, the full-length correct chRANKL sequence was mined from the chicken genome and cDNA cloned from RNA from ConA-stimulated splenocytes. Like mammals, chRANKL is a 318 amino acid, type II transmembrane protein with an extracellular, TNF homology, domain. ChRANK is a type I transmembrane protein with highly conserved extracellular CRDs, characteristic of TNFR superfamily members (Anderson *et al.*, 1997). ChOPG is produced as a soluble protein that contains two DD and four CRD, similar to mammalian OPG (Yasuda *et al.*, 1998).

Protein-protein interactions are central to biological processes from cellular communication to programmed cell death. The correct folding and assembly of protein complexes are vital for ligand and receptor interactions. Members of the TNF superfamily characteristically form homotrimers to induce the oligomerisation of their respective receptor(s). The geometry of the resulting TNF ligand-receptor interaction is favourable for the recruitment of intracellular adaptor proteins. It is therefore important to ensure that members of the TNF family are folded correctly to interact with their receptor(s) and activate appropriate downstream signalling pathways. The extracellular, soluble domain of chRANKL predominantly forms homotrimers with the assistance of an isoleucine zipper sequence in the expression plasmid. Mammalian OPG is produced as a dimeric soluble protein excreted from cells to interrupt the interaction between RANKL and RANK (Yasuda *et al.*, 1998). ChOPG shares these characteristic by being expressed as a secreted homodimeric protein.

All three molecules were ubiquitously expressed across a number of lymphoid and non-lymphoid tissues in the chicken, as shown by qRT-PCR. Primary

immune cells stimulated with a number of mitogens associated with the activation and proliferation of T and B cells did not affect the mRNA expression levels of these molecules in the chicken, indicating their mRNA is transcriptionally regulated by specific biological pathways. In mammals, RANKL transcription is regulated in murine T cells by Ca^{2+} mobilisation and activation of the PKC pathway (Wang *et al.*, 2002; Fionda *et al.*, 2007). Chicken splenocytes stimulated with ionomycin and PMA increased the mRNA expression levels of chRANKL which was verified by the blockade of Ca^{2+} mobilisation and PKC activation by TMB-8 treatment. The data indicate the conserved transcriptional regulation of RANKL in mammals and birds (Wang *et al.*, 2002; Fionda *et al.*, 2007; Bishop *et al*., 2011). Similar to mammals, chOPG is expressed in LPS-stimulated BMDC and its mRNA expression levels were increased in a time- and dose-dependent manner (Schoppet *et al.*, 2007). The mRNA expression levels of chRANK were also affected by the level of BMDC maturation, with mRNA expression levels decreasing as the cells matured. The data suggest that chOPG mRNA expression levels increase as BMDC mature, possibly regulating the interaction between chRANKL-expressing T cells and chRANK-expressing DC, similar to mammals. In osteoblast cells, the OPG promoter region is transcriptionally regulated by activation of the PKC pathway (Yang *et al.*, 2002). It would be interesting to investigate the transcriptional regulation of chRANKL and chOPG in chicken osteoblast and stromal cells.

6.3 The biological activity of chRANKL

Mammalian RANKL enhances the expression levels of pro-inflammatory cytokines and the survival of DC and macrophages (Anderson *et al.*, 1997; Wong *et al.*, 1997; Park *et al.*, 2005). In chicken BMDC, mRNA expression levels of the pro-inflammatory cytokines IL-1β, IL-6 and IL-12α were enhanced in cells co-stimulated with LPS and schRANKL (Chapter 4). Mammalian IL-12 is a key player in governing the development of Th1 responses and is a cytokine that is largely produced by DC. IL-12 induces the activation of the Th1 transcription factor, STAT4, and synergises with IL-2 to drive Th1 differentiation (Athie-Morales *et al.*, 2004). Chicken IL-1β mRNA expression is increased in response to bacterial, viral and parasite infection, demonstrating its role as a rapidly induced pro-inflammatory

cytokine (Gibson *et al.,* 2014). To verify that the enhanced pro-inflammatory cytokine mRNA expression levels were due to treatment of cells with schRANKL, schRANKL was pre-incubated with soluble chRANK-Fc and chOPG-Fc before addition to cells with LPS. The schRANKL-mediated increase in pro-inflammatory cytokine mRNA expression levels was inhibited by both soluble chRANK-Fc and chOPG-Fc. This provides evidence that the recombinant schRANKL protein is biologically active and that its receptors, recombinant chRANK-Fc and chOPG-Fc, are folded correctly and capable of interacting with their ligand. SchRANKL bioactivity was also investigated in BMDM. mRNA expression levels of the pro-inflammatory cytokine, IL-1β, were enhanced by schRANKL and LPS co-stimulation. However, IL-6 mRNA expression levels were not enhanced to a statistically significant level compared to those in unstimulated cells.

BMDC and BMDM stimulated with schRANKL or co-stimulated with schRANKL and LPS did not enhance the expression levels of cell surface markers associated with antigen presentation (MHC class II) or costimulatory capacities (CD40) which is similar to various studies in mammals (Anderson *et al.,* 1997; Wong *et al.,* 1997). To investigate whether the stimulant was a factor in the inability of schRANKL to enhance cell surface marker expression levels, a more potent activator of macrophages, IFN-γ, was used to induce M1 (classical) macrophage activation. However, schRANKL did not affect surface expression of MHC class II or KUL01 and only slightly enhanced CD40 surface expression. The data suggest that chicken APC matured with microbial components (LPS) or cytokines (IFN-γ) do not alter the surface expression of activation markers when in the presence of schRANKL. In mammalian studies, the treatment of APC with RANKL induces different outcomes depending on the anatomical location of DC. For example, RANKL induces IL-12 expression in spleen-derived DC but not in Peyer's patch-derived DC (Williamson *et al.,* 2002) and upregulated MHC class II, CD80 and CD86 expression levels in Mo-DC (Schiano de Colella *et al.,* 2008) but not BMDC (Anderson *et al.,* 1997; Wong *et al.,* 1997). Although this study did not investigate the expression levels of chCD80 and chCD86, it cannot be ruled out that schRANKL does not alter the phenotype of APC in the chicken. Future work is required for the

analysis of chRANKL bioactivity on Mo-DC, spleen-derived DC and other various anatomical-derived DC in the chicken.

Similar to mammalian RANKL, chRANKL is a survival factor for chicken BMDC and BMDM. Cells treated with schRANKL for 24 and 48 h had increased numbers of viable cells compared to untreated cells. This study did not measure the mRNA expression levels of the anti-apoptotic genes, Bcl-X_L or Bcl-2, involved in mammalian RANKL-mediated cell survival (Cremer *et al.,* 2002). Apoptosis is an evolutionary conserved form of programmed cell death and plays vital roles in development, tissue homeostasis and cell defence against pathogens. Apoptosis occurs by two signals, extrinsic and intrinsic (mitochondrial). Extrinsic apoptosis is initiated by ligand-receptor interaction, such as that of the DD-containing TNF family members, FASL and FAS, which leads to the formation of the death-inducing signalling complex (DISC) that can activate caspase-8 and caspase-3 (Lamkanfi *et al.,* 2007). Intrinsic apoptosis is initiated by intracellular perturbations in homeostasis, such as DNA damage, Ca^{2+} overload and oxidative stress (Taylor *et al.,* 2008). Mammalian Bcl-X_L and Bcl-2 are localized to the membrane surface of ER, mitochondria and the nucleus. Both regulate Ca^{2+} levels by reducing the capacity of ER Ca^{2+} stores (Szegezdi *et al.,* 2003; Distelhorst & Bootman, 2011). Both counteract the mitochondrial pore-forming activities of the pro-apoptotic molecules, BAK and BAX, whose function is to induce mitochondrial outer membrane permeabilisation that drives the loss of mitochondrial transmembrane potential (Michels *et al.,* 2013). In osteoclast cells, a fellow member of the anti-apoptotic Bcl-2 family, myeloid cell leukemia-1 (Mcl-1), has been implicated in RANKL-mediated osteoclast cell survival, rather than Bcl-X_L or Bcl-2 (Sutherland *et al.,* 2009; Masuda *et al.,* 2014). Mcl-1 is essential for embryonic development and survival of a number of cell lineages in the adult, such as lymphocytes, neurons, cardiomyocytes, hepatocytes and immunoglobulin-secreting plasma cells. Mcl-1 expression is tightly regulated at the transcriptional, post-transcriptional and post-translational levels (Mojsa *et al.,* 2014).

Similar to mammalian RANKL, chRANKL enhances the phagocytic activity of chicken BMDC. However, more research is required to fully investigate the ability

of schRANKL to differentiate BMDC into osteoclast cells which have phagocytic potential (Li *et al.,* 2010). Murine RANKL signals the differentiation of macrophages and DC into osteoclasts, a process that requires NF-κB and NFATc1 (Walsh *et al.,* 2003). These cells have properties that include the expression of pro-inflammatory cytokines, MHC class II and phagocytic potential (Li *et al.,* 2010). BMDM commit to the osteoclast cell lineage after 24 h of RANKL treatment (Mochizuki *et al.,* 2006). There are two types of macrophage-derived multinucleated giant cells (MNG), osteoclasts in bone and MNG in chronic inflammatory reactions (Anderson, 2000). Various proteins have been implicated in the cell-cell fusion required for MNG formation, such as DC-STAMP, RANKL, CD47 and CD36 (Yagi *et al.,* 2005; Yu *et al.,* 2011; Miyamoto, 2011). In a pilot study, bone marrow cells incubated with chCSF-1 prior to exposure to chRANKL were capable of differentiating into large multinucleated cells characteristic of osteoclasts. Although a more detailed analysis of these cells is required, the ability of chRANKL to induce osteoclast-like cell differentiation indicates its conserved bioactivity both in immunity and bone metabolism in the chicken.

Overall the data presented in this thesis suggest the conserved bioactivity of RANKL, RANK and OPG across mammals and birds. It provides a platform for understanding the roles of these TNF molecules in various biological processes in the chicken.

6.4 The cloning of TRAF-binding proteins which bind intracellularly to RANK

Members of the TNFR superfamily do not possess intracellular catalytic domains for downstream signalling upon ligand interaction; instead they rely on the recruitment of adaptor proteins called TNF receptor-associated factors (TRAFs). Differently to mammalian RANK, chRANK lacks one of three TRAF6-specific binding motifs. RANK-mediated TRAF6 signalling is crucial for osteoclastogenesis (Koda *et al.,* 2004). TRAF2, TRAF3 and TRAF6 knockout mice are all phenotypically lethal indicating the important roles of these molecules in development (Xu *et al.,* 1996; Yeh *et al.,* 1997; Lomaga *et al.,* 1999; Naito *et al.,* 1999). Specifically, TRAF2, TRAF5 and TRAF6 serve as adaptor proteins that link

cell surface receptors to downstream signalling cascades involved in activating transcription factors, such as NF-κB, resulting in cytokine expression.

To date, the only member of the chicken TRAF family cloned and studied is chTRAF5 (Abdalla *et al.,* 2004a). To begin to understand the biological effects of chRANK, which contains two out of the three mammalian TRAF6-binding motifs, and chRANK intracellular signalling, the identification and molecular characterisation of chicken TRAFs was required. All seven TRAF family members are present in the chicken genome and this study focused on three members involved in mammalian RANK signalling, TRAF2, TRAF5 and TRAF6 (Wong *et al.,* 1999; Darnay *et al.,* 1999) and the newest member, TRAF7 (Xu *et al.,* 2004).

Using the sequences from the Ensembl database, chTRAF5, chTRAF6 and chTRAF7 cDNA were cloned and found to be highly conserved across mammals and chickens (Chapter 5). The cloning of chTRAF2 led to the identification of a novel splice isoform missing exon four, named chTRAF2S (Chapter 5). ChTRAF5, chTRAF6 and chTRAF7 mRNA expression levels across a number of lymphoid and non-lymphoid tissues were similar to those in mammals. In kinetic experiments comparing unstimulated and ConA-stimulated splenocytes, chTRAF5 mRNA expression levels were increased at 18 and 24 h in stimulated cells, chTRAF6 mRNA expression levels were increased at 6 h in stimulated cells whereas chTRAF7 mRNA expression was constant in unstimulated and stimulated cells. This suggests that chTRAF5 and chTRAF6 may be involved in intracellular pathways associated with T cell activation and proliferation in the chicken. The biological role of mammalian TRAF7 in immunity has yet to be identified but it plays a role in fish immunity against bacterial infection (Fu *et al.,* 2011).

6.5 The identification of a novel chTRAF2 isoform

Mammalian TRAF2 is one on the best characterised members of the TRAF family. As described in Chapter 5, chicken TRAF2 undergoes alternative splicing to produce a smaller isoform lacking exon 4, which encodes a partial portion of the first zinc finger motif, omits the entire second zinc finger motif and a partial portion of the third zinc finger motif. This splice isoform has not been reported in mammalian

species. A murine TRAF2 splice isoform has previously been described, TRAF2A, which contains an additional seven amino acids within the RING domain which affect its ability to activate the NF-κB pathway (Brink & Lodish, 1998) but not the JNK pathway (Dadgostar & Cheng, 1998).

Messenger RNA is transcribed as a precursor containing intron sequences which are removed so that the flanking regions, exons, are spliced together to form a mature mRNA. Alternative splicing of mRNA precursors is a versatile mechanism that increases the complexity of the resulting protein localisation and/or function. There are a number of alternative splicing mechanisms, such as exon skipping, mutually exclusive exons, alternative acceptor and alternative donor sites. Exon skipping is one of the most common forms of alternative splicing. As the name implies, exon or exons are spliced out of the precursor mRNA resulting in a smaller mature mRNA being generated. The mutually exclusive exon approach sees one of two exons retained but never both exons in the final mature mRNA. Use of alternative acceptor and alternative donor sites is where an alternative 5' splice junction is used changing the 3' acceptor site of the upstream exon or an alternative 3' splice junction is used altering the 5' boundary of the downstream exon. It is clear that the chTRAF2S isoform is generated from exon skipping, splicing out exon 4 and joining exon 3 to exon 5.

RT-PCR analyses indicated that chTRAF2 is the constitutive form expressed in lymphoid tissues but not in non-lymphoid tissues, where chTRAF2S is predominantly expressed. In splenocyte subsets, the mRNA expression levels of chTRAF2S were higher in $CD4^+$, $CD8^+$ and $KUL01^+$ cells compared to chTRAF2 (Chapter 5). ChTRAF2 mRNA expression levels increased to higher levels than chTRAF2S in ConA-stimulated splenocytes, indicating that chTRAF2 is the predominant form expressed in activated chicken lymphoid cells. In chicken BMDM, chTRAF2 mRNA expression levels were unaltered after stimulation. ChTRAF2S mRNA expression levels were increased in LPS-stimulated BMDM but not BMDC.

The bioactivity of chTRAF2 and chTRAF2S was investigated by analysing their ability to activate a reporter gene in HEK-293T cells. The reporter gene used for the analysis was NF-κB, known to be positively regulated by mammalian TRAF2

(Lee *et al.,* 1997; Takeuchi *et al.,* 1996). Interestingly, chTRAF2S activated NF-κB. It is surprising that chTRAF2S can activate NF-κB when lacking zinc finger motifs. Mammalian TRAF2 RING and zinc finger motifs one, two and three are vital for NF-κB activation (Takeuchi *et al.,* 1996). It may be plausible that the joining of the NH_2-terminal piece of zinc finger motif one with the COOH-terminal portion of zinc finger motif three in chTRAF2S creates a composite zinc finger motif with biological activity. Overexpressing chTRAF2 or chTRAF2S in HEK-293T cells increased levels of NF-κB activation in a dose-dependent manner. However, when both chTRAF2 isoforms were overexpressed together, enhanced levels of NF-κB was not observed. Although NF-κB expression levels were increased in cotransfected cells compared to vector control wells, levels were not statistically significantly different between chTRAF2- or chTRAF2S-mediated NF-κB activation levels. More likely, the two isoforms bind to the same adaptor proteins, and therefore one may block the other. However, the two isoforms could form homo- or heterodimers, and any such interaction could hamper their respective bioactivities.

Overall the data suggest that chTRAF2, chTRAF5, chTRAF6 and chTRAF7 are highly conserved between mammals and birds. Importantly, chicken TRAF2 is alternatively spliced to generate a protein that is bioactive, inducing NF-κB activation, which may be relevant during certain immune responses.

6.6 Future experiments

Additional experiments could have been carried to better understand the role of chRANKL, chRANK and chOPG in avian immunity during these studies. One of the most informative approaches would have been the use of chOPG to detect chRANKL surface expression. Mammalian OPG binds to RANKL 1000-fold higher than RANK binds to RANKL (Lam *et al.,* 2001) making it the more sensitive receptor to use. The purified chOPG-Fc could be used to detect the surface expression of chRANKL on a number of immune cells by FACS analysis and in a number of tissues by histology. These studies will give a broader understanding of the protein expression of chRANKL in the chicken.

The mRNA expression levels of chTRAF2 isoforms should be quantified to give a better understanding of the differential expression of these adaptor proteins in

the chicken. Further analysis on the role of chTRAF2 and chTRAF2S during various biological processes would have provided more insight into the regulation of their mRNA expression in various signalling pathways, such as downstream signalling induced TLR and TCR activation in splenocytes, BMDC and BMDM. It would have also been interesting to test the ability of the chTRAF2 isoforms to form homo- or hetrodimers with themselves and other TRAF family members.

6.7 ChRANKL and its potential application to chicken immunity

6.7.1 ChRANKL as a potential marker for chicken Th1 cells

Mammalian RANKL is predominantly expressed on the surface of Th1 cells and increases the expression of Th1 effector cytokines, such as IL-12 and IFN-γ, in DC (Wong *et al.*, 1999; Josien *et al.*, 1999). This study identified the ability of chRANKL to enhance the mRNA expression levels of chIL-12α that may in turn enhance the Th1 immune response in the chicken. Due to the role of mammalian RANKL in bone metabolism, research into RANKL and immunity is angled towards $CD4^+$ T cells expressing RANKL under pro-inflammatory conditions linked to autoimmune diseases, such as RA and periodontal infection (Terheyden *et al.*, 2014). Mammalian $CD4^+$ Th1 and Th17 cells express RANKL under inflammatory conditions that activate osteoclasts, which degrade and destroy bone and tissue (Vernal *et al.*, 2014). More recently, under arthritic conditions, $FoxP3^+$ Treg cells differentiate into $FoxP3^-$ Th17 cells that upregulate the expression of RANKL, thought to contribute to the pathogenesis of RA (Komatsu *et al.*, 2014).

In the future, mAb against chRANKL will be developed by the avian toolbox initiative at The Roslin Institute. Antibodies against chRANKL and chRANK will help further develop the understanding of DC and T cell interactions in the chicken. Antibodies against chRANKL could be used to isolate cells expressing this molecule during a Th1 infection model, to test if they are expressing other Th1-specfic molecules and therefore if RANKL is a marker for Th1 cells in the chicken.

6.7.2 Understanding M cells in the chicken

The self-renewing epithelial cells of the small intestine are organised into crypts and villi. A huge rate of cell production occurs in the crypts and is balanced by a large amount of apoptosis at the tips of the villi. In the crypts, self-renewing cells produce rapidly proliferating transit-amplifying cells that can differentiate into any of the four cell linages (Paneth cells, enterocytes, goblet cells and enteroendocrine cells) (Barker *et al.*, 2008). M cells are a unique set of epithelial cells restricted to the FAE which overlays the gut-associated lymphoid tissues (GALT), such as Peyer's patches, ILF and tonsils. M cells are phagocytic and take up particulates from the luminal environment and present them to cells in immune-inductive Peyer's patches, initiating the intestinal immune response. RANKL is necessity for murine M cell differentiation and maintenance (Knoop *et al.*, 2009). Bacteria can exploit the plasticity of cells to alter their activity and transform them to suit their requirements. This has been demonstrated in intestinal epithelial cells, which can undergo a reversible epithelial-mesenchymal transition (EMT) after exposure to bacteria (Thiery *et al.*, 2009). The potential for the understanding of the role of M cells in host-pathogen interactions in the intestine can be seen in a study by Tahoun *et al.* (2012). *S.* Typhimurium can bind to epithelial cells and engage effector proteins to alter the cell's cytoskeleton to uptake the bacterium (Galan & Zhou, 2000) and it preferably targets M cells in the intestine (Jones *et al.*, 1994). Tahoun *et al.* (2012) demonstrated that *S.* Typhimurium interacts with bovine intestinal cells expressing the M cell marker, vimentin, and vimentin$^-$ cells. The exposure of M cells to *S.* Typhimurium increased expression levels of RANKL, RANK and vimentin that could be controlled by OPG treatment. *S.* Typhimurium-mediated upregulation of RANKL was associated with RANKL-induced transformation of epithelial cells into M cells, a process allowing the bacteria to cross the intestinal mucosa. Aging mice have a slow decline of M cell numbers in the gut, causing defects in the mucosal immune response (Kobayashi *et al.*, 2013). These studies indicate the importance of M cells in intestinal immunity and that they are good candidates for the investigation of how microbes evade the mucosal immune response in the chicken.

There is a need for intestinal culture systems in the chicken to enable the understanding of host-pathogen interactions. There are methods that have existed for some time to culture primary epithelial cells from mice as three-dimensional structures, called organoids (Macartney *et al.*, 2000; Sato *et al.*, 2009) (Figure 6.1). Since the discovery of the leucine-rich repeat-containing G-protein coupled receptor 5 (Lrg5), as a marker for intestinal stem cells (Barker *et al.*, 2007; Barker *et al.*, 2008), there have been unprecedented developments in the use of human tissue surrogates *in vitro* (reviewed by Sachs & Clevers, 2014). Intestinal stem cells divide every 24 h generating rapidly proliferating progenitor cells that fill up pocket-like crypts. These cells migrate up the crypt becoming nutrient absorbing enterocytes, secretory cells and M cells (Koo & Clevers, 2014). Organoids were first identified by mimicking the intestinal environment, leading to the discovery of culture conditions for mouse $Lgr5^{+}$ intestinal cells (Sato *et al.*, 2009). R-spondin-1, Noggin, EGF and Matrigel are the minimal requirements for the culture of murine organoids which led to the generation of crypt-like domains harbouring all four of the common intestinal cell lineages (Figure 6.1). These cell cultures are unique compared to cell lines; they efficiently form, self-renew and are genetically stable in long-term cultures (Sato *et al.*, 2011). Recently, M cells were differentiated in these organoid systems by the addition of RANKL (De Lau *et al.*, 2012).

The ability to culture M cells as organoids has great potential for understanding host-pathogen interactions in the chicken gut. Organoid systems are useful for modelling of disease. There are many examples of human organoids being used to examine diseases, such as cystic fibrosis. The clustered regularly interspaced short palindromic repeats (CRISPR) RNA-guided Cas9 nuclease system was applied to amend the missing amino acid in cystic fibrosis transmembrane conductor regulator (CFTR) (F508) protein, a mutation linked to the common form of cystic fibrosis in humans. In organoid cultures generated from two mutant-expressing patients, the induction of double-stranded breaks and the insertion of the correct sequence led to the resultant organoids to regain CFTR functionality (Schwank *et al.*, 2013). Organoid cultures can be used as experimental platforms, using transgenic and knockout organoid systems to understand and study a gene of interest. These culture systems have the potential to reduce animal use and can feature *ex vivo* model

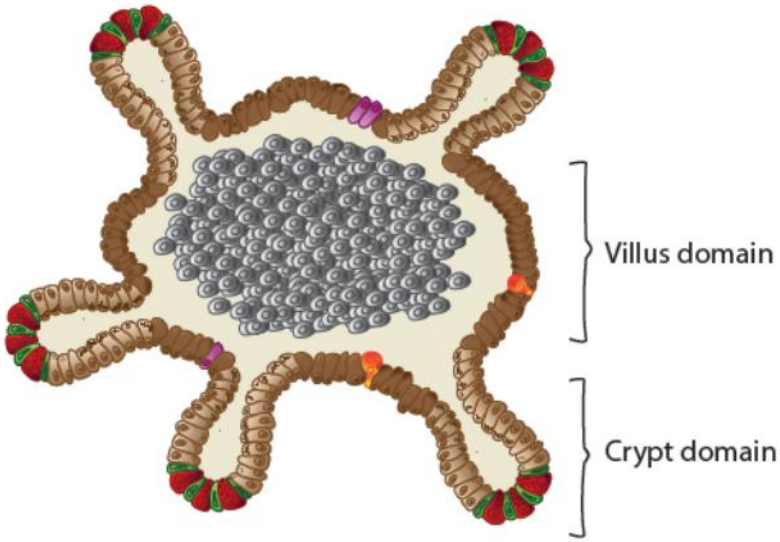

Figure 6.1 Schematic diagram of intestinal organoid. *Intestinal organoids can be generated from a single Lrg5^{+} cell or from a portion of a crypt. Differentiated cells are found in the villus domain while stem cells (red cells) and Paneth cells (green cells) are found in the crypt domain of the organoid similar to the gastro-intestinal architecture. Cells move up the crypt, differentiating as they reach the villus domain, and are shed into the lumen (grey cells) (adapted from Koo & Clevers, 2014).*

systems. Efforts are now being made to generate these organoids in the chicken in our laboratory.

6.7.3 Understanding bone metabolism in the chicken

Femoral head separation is a common bone disorder seen in broilers that can lead to bacterial chondronecrosis with osteomyelitis. Excessive weight gain is thought to be the main cause of femoral head separation, as the pressure of the ball and joint of the femur restricts the flow of blood. The rapid increase in body mass is linked to the inability of the femur to keep pace with bone formation, leading to excessive osteoclast activity (Prisby *et al.*, 2014). Skeletal disorders in broilers are linked to the inability of the skeleton to mature at rates sufficient to support the rapid growth of body mass. In the EU, there are over 350 million laying hens producing

100 billion eggs, annually. Over a third of these hens are reared under free-range conditions while the remaining two thirds are housed in furnished cages, a number likely to decrease due to the 2012 EU directive banning battery cage systems (Tarlton *et al.,* 2013). The main concern about the increase in free-range chicken numbers is that up to 95% of these animals suffer bone breakage due to bone weakness and hazards of housing (Wilkins *et al.,* 2011). Laying hens also require high amounts of calcium for the formation of the eggshells and therefore undergo extraordinarily intense calcium metabolism. Laying hens use nearly 10% of their body calcium levels for egg formation and around 50% of this is dietary derived. Therefore a considerable amount of calcium is taken from skeletal stores. During oviposition, osteoblast activity alters from cortical bone formation to medullary bone formation, a characteristic unique to birds and dinosaurs. Medullary bone is a source of calcium for egg shell formation usually found in the long bones of hens (legs), thereby contributing to bone weakness causing fractures. These fractures cause considerable pain and discomfort to the chickens, a serious animal welfare issue. There is evidence that the deficiency of dietary fatty acids may contribute to bone loss (Das, 2000). In mice, the lack of omega-3 leads to a reduction in osteoclastogenesis (Rahman *et al.,* 2009) and in a more recent study an increase in omega-3 in the diet of free range chickens led to reduction in bone breakages (Tarlton *et al.,* 2013).

Osteoblast and osteoclast cell culture systems can be used to investigate the mechanism of bone formation and metabolism, allowing researchers to probe the cellular and molecular basis of bone diseases. Osteoblasts originate from the mesenchymal cell precursors whereas osteoclasts are derived from haematopoietic precursors of the myeloid lineage, present in the bone marrow and circulation (Collin-Osdoby & Osdoby, 2012). The essential osteoclast differentiation signal comes from RANKL, expressed by osteoblast cells, stromal cells and various cells in the bone marrow, causing osteoclast precursor cells to fuse and differentiate into large multinucleated cells with morphological features, such as membrane polarisation, ion pumps, enzyme activities and antigenic potential (Hall *et al.,* 1996; Roodman, 1996). Osteoclasts perform bone pit reabsorption which needs to be carefully balanced with bone-forming osteoblast activity. The chicken is used as a

model for adolescent idiopathic scoliosis (AIS), a disease characterised by the lateral curvature of the spine (Machida *et al.,* 1993; Coillard & Rivard, 1996). Thillard *et al.* (1959) reported the development of AID in pinealectomized chickens at 2 to 3 days old, called experimental pinealectomy (PNX) birds. The PNX birds had increased osteoclast cell numbers at the front of the growth plate three days post-pinealectomization, which disappeared by day 6. This osteoclast activity is linked to the degradation of chondrocytes, leaving minimal cartilage matrix for osteoblasts to form new bone. Hypertrophic and proliferative chondrocyte cell numbers are increased in PTX chickens, leading to the increase in the thickness of the growth plate, leading to AIS (Aota *et al.,* 2013).

This thesis describes the ability of schRANKL and chCSF-1 to induce primary osteoclast cell differentiation from bone marrow-derived cells. These culture systems can be used study osteoclast phenotypes associated with knockout culture systems and will allow researchers to use *in vitro* culture systems to understand bone metabolism and effects of treatments, biomaterial safety and therapies in the chicken.

6.7.4 ChRANKL as a potential vaccine adjuvant

The emergence of antibiotic-resistant bacteria has led to the need for alternative treatments for poultry diseases. The previous strategies to control disease in poultry flocks worldwide included in-feed antibiotics whose use has now been banned by the EU, which now relies heavily on vaccination and biosecurity. Feed additives have been extensively explored in chickens with growth promoters, immunomodulators or both being used to control disease in large commercial flocks. However, they are not cost-effective and can be a waste of energy in non-challenged birds (Guo *et al.*, 2003; Huff *et al.*, 2006; Kumar *et al.*, 2011). Vaccination is considered the most effective way to control diseases in chickens. In recent years the development and use of subunit vaccines has increased due to the evidence that in some cases vaccination with live attenuated vaccines lead to higher virulence (Witter. 1997). Sub-unit vaccines can express a number of antigens with their production simpler, faster and safer than conventional vaccines. However, subunit vaccines are less immunogenic than conventional vaccines. Numerous studies have revealed the importance of the local cytokine microenvironment for the quality and

magnitude of the initial and ongoing responses to subunit vaccines. Therefore, certain cytokines have great appeal as potential vaccine adjuvants.

ChCD40L expressed with M2e, an integral membrane protein of influenza A viruses (Pinto *et al.,* 1992), conferred protection against low pathogenic avian influenza virus in chickens (Layton *et al.,* 2009) and also contributed to reduced *Salmonella* colonisation and organ invasion in turkeys (O'Meara *et al.,* 2010). The fusion of chCD40L with extracellular segments of HA increased the humoral response of chickens to H_5N_1 infection (Pose *et al.,* 2011). These studies indicate the potential adjuvant properties of TNF superfamily members in the chicken. ChIL-2 adjuvant properties have been described for a number of sub-unit vaccines. For example, the *Eimeria tenella* rhomboid protein and chIL-2 vaccine conferred partial protection against *Eimeria* infection compared to the vaccine not expressing chIL-2 (Min *et al.,* 2001).

DNA immunisation is another effective way of inducing specific innate and humoral immune responses against various pathogens (Dunachie *et al.,* 2006; Keitel *et al.,* 2009). The use of plasmid DNA allows for precise immunisation against a plasmid expressing the gene or genes encoding the antigen, driving the synthesis of the antigen protein within the vaccinated host that will induce the production of antibodies. Cytokine adjuvants enhance the efficacy of DNA immunisation improving the immune response to the candidate DNA vaccine. For example, CSF-2 enhances the immunogenicity of a HIV-1P24-Nef vaccine by recruiting DC to the site of the immune response and increasing the number of CTL (Mahdavi *et al.,* 2011). Recently, the adjuvant properties of chIL-18 were analysed in chickens vaccinated with a DNA vaccine expressing the VP243 gene from infectious bursal disease virus (IBDV). Compared to chickens immunized with the plasmid expressing only VP243, the administration of a plasmid expressing both VP243 and chIL-18 induced higher levels of antibody production and increased levels of IL-4 and IFN-γ expression (Li *et al.,* 2013). ChIL-6 adjuvant properties were demonstrated in animals vaccinated with the fimbrail Fae gene from the enterotoxigenic *E. coli* K88 strain. Co-administration of Fae and chIL-6 expressing plasmids induced higher titres of anti-Fae mAb over a longer period than immunizing with Fae-expressing plasmid

alone (Cho *et al.*, 2004). The adjuvant potential of chIL-1β has been demonstrated with tetanus toxoid where increased antibody production levels were induced compared to levels in chickens administered the antigen alone (Schijns *et al.*, 2000).

The adjuvant properties of mammalian RANKL have been analysed in vaccination programs. Plasmids encoding murine RANKL and the epitope trans-sialidase surface antigen from *Trypanosoma cruzi (T. cruzi),* enhanced the induction of $CD8^+$ T cells and improved the survival of mice infected with lethal doses of *T. cruzi* (Miyahira *et al.*, 2003). Using an adenoviral vector, a model tumour antigen was co-expressed with either RANKL or CD40L to generate transgenic mice. Mice immunised with transgenic DC co-expressing the antigen and RANKL increased IFN-γ-producing cells, RANKL and RANK expression and CTL cell numbers compared to antigen alone and antigen co-expressed with CD40L-transgenic DC (Wiethe *et al.*, 2003). Mice immunised against the HIV-1 Gag gene vaccine co-expressing RANKL induced higher numbers of $CD8^+$ T cells, IFN-γ production and enhanced T cell memory compared to mice immunized with the HIV-1 Gag gene vaccine alone. However, co-expression of RANKL was not as effective at inducing higher levels of IL-2 and anti-Gag mAb production as co-expression of other TNF superfamily members, such as CD40L, LIGHT and OX40L, with that antigen (Kanagavelu *et al.*, 2012).

The use of subunit vaccination in chickens is evolving and recent developments in the understanding of chicken innate immunity have seen an increase in vaccine adjuvant-based research (Xu *et al.*, 2013; Li *et al.*, 2013; Gupta *et al.*, 2014a; Gupta *et al.*, 2014b; Zhao *et al.*, 2014). The ability of chRANKL to enhance the expression of pro-inflammatory cytokines and survival of DC makes it a good candidate as a vaccine adjuvant.

6.7.5 Understanding TRAF intracellular signalling induced by TNFR and Toll/IL-1R superfamilies in the chicken

TRAF family members are required for a number of biological processes activated by TNFR, Toll/IL-1R, RLR and NLR family members, either by direct binding or indirect binding via adaptor proteins. TRAF family members are therefore

critically involved in inflammation, innate and adaptive immune responses, and cell death (Inoue *et al.,* 2000). However, in exaggerated immune responses, TRAF-mediated cytokine expression has been linked to multiorgan failure and shock. Hence, TRAF proteins have central roles in signal transduction involved in the transactivation of genes linked to a multitude of biological processes involved in immunity.

Viruses and bacteria have developed a variety of mechanisms to hijack or target TRAF family members to invade the immune response. For example, *Mycobacterium tuberculosis*-infected macrophages have an increased lifespan due to the upregulation of TRAF1 and TRAF2, linked to the upregulation of NF-κB (Ordway *et al.,* 2005). *Leishmania donovani* neutralises the macrophage defence machinery by inhibiting TRAF3-mediated ubquitination of TAK-1, which is required for the activation of the TLR4-MyD88-Ubc13-TAK-1-TRAF6-cIAP1/2 complex leading to downstream activation of the MAPK kinases, JNK, ERK and p38 (Gupta *et al.,* 2014). T cell-specific oncoproteins encoded by the old world monkey viruses *Herpesvirus saimiri and Herpesvirus ateles* utilise TRAF proteins to drive NF-κB activation. The herpesvirus oncoprotein, Tio, induces T cell leukaemia in humans by recruiting TRAF6 and blocking TRAF3, leading to the concomitant activation of NF-κB (de Jong *et al.*, 2010; de Jong *et al.*, 2013). The HIV-encoded protein, Nef, binds to TRAF2 which is necessary for Nef-mediated activation of NF-κB in macrophages (Mangino *et al.,* 2011).

The overexpression of TRAF family members has been linked to a number of mammalian diseases. CD30 is a characteristic cell surface marker for T cells and the malignant cells of Hodgkin's disease. High expression of CD30 leads to its aggregation and recruitment of TRAF2 and TRAF5 to its intracellular domain, constitutively activating NF-κB, characteristic of Hodgkin's disease (Izban *et al.,* 2000; Horie *et al.,* 2002). In B cell-chronic lymphocytic leukaemia (B-CLL), the inhibition of B cell apoptosis is linked to the overexpression of TRAF1 and TRAF2, which mediate the activation of NF-κB (Munzert *et al.,* 2002).

Understanding the pathogenesis and the immune mechanisms of protection against the pathogen is a prerequisite for preventing the disease. Chicken TRAF

family members may be targeted by avian viruses and bacteria to evade chicken immune responses. Similar to Hodgkin's disease, chCD30 overexpression is seen on MDV-infected cells (Burgess *et al.*, 2004). The induction of lymphomas due to MDV infection may involve the enhanced recruitment of TRAF family members, chTRAF2 and chTRAF5, to the intracellular domain of chCD30 leading to the enhanced activation of NF-κB. *Clostridium perfringens*-infected chickens increased mRNA expression levels of chTRAF6 (Lu *et al.*, 2009). In a recent study, chTLR7 activation significantly increased chTRAF6 mRNA expression levels in the spleens of MDV-infected chickens after 14 days but no change in chTRAF3 mRNA expression levels was observed (Jie *et al.*, 2013). In BMDC, chTRAF6 mRNA expression levels were also significantly increased by stimulation with LPS, *Bacillus subtilis* and *Saccharomyces boulardii*, demonstrating that chTRAF6 is involved in TLR signalling in chicken APC (Rajput *et al.*, 2013).

In avian research, the detection of TRAF family members is becoming a means to understand the downstream signalling pathways initiated by viruses, yeast and bacterial infections (Rajput *et al.*, 2013; Jie *et al.*, 2013). However, with the identification of a novel chTRAF2 isoform and various chTRAF3 isoforms (unpublished data, Kate Sutton), the avian research community needs to be cautious in measuring chicken TRAFs before the full repertoire has been cloned and characterised and potential alternative isoforms have been identified. Exploiting TNFR family members for control of avian diseases will require a precise understanding of their *in vivo* regulation and downstream signalling pathways for a targeted approach to ensure improved antigen-specific responses.

References

ABDALLA, S. A., HORIUCHI, H., FURUSAWA, S. & MATSUDA, H. 2004. Molecular study on chicken tumor necrosis factor receptor-II and tumor necrosis factor receptor-associated factor-5. *Vet Immunol Immunopathol,* 98**,** 31-41. a

ABDALLA, S. A., HORIUCHI, H., FURUSAWA, S. & MATSUDA, H. 2004. Molecular cloning and characterization of chicken tumor necrosis factor (TNF)-superfamily ligands, CD30L and TNF-related apoptosis inducing ligand (TRAIL). J Vet Med Sci, 66, 643-50. b

ABI-RACHED, L., GILLES, A., SHIINA, T., PONTAROTTI, P. & INOKO, H. 2002. Evidence of en bloc duplication in vertebrate genomes. *Nat Genet,* 31**,** 100-5.

AGEMATSU, K., NAGUMO, H., OGUCHI, Y., NAKAZAWA, T., FUKUSHIMA, K., YASUI, K., ITO, S., KOBATA, T., MORIMOTO, C. & KOMIYAMA, A. 1998. Generation of plasma cells from peripheral blood memory B cells: synergistic effect of interleukin-10 and CD27/CD70 interaction. *Blood,* 91**,** 173-80.

AGGARWAL, B. B. 2003. Signalling pathways of the TNF superfamily: a double-edged sword. *Nat Rev Immunol,* 3**,** 745-56.

AGGARWAL, B. B., GUPTA, S. C. & KIM, J. H. 2012. Historical perspectives on tumor necrosis factor and its superfamily: 25 years later, a golden journey. *Blood,* 119**,** 651-65.

AHONEN, C., MANNING, E., ERICKSON, L. D., O'CONNOR, B., LIND, E. F., PULLEN, S. S., KEHRY, M. R. & NOELLE, R. J. 2002. The CD40-TRAF6 axis controls affinity maturation and the generation of long-lived plasma cells. *Nat Immunol,* 3**,** 451-6.

AIZAWA, S., NAKANO, H., ISHIDA, T., HORIE, R., NAGAI, M., ITO, K., YAGITA, H., OKUMURA, K., INOUE, J. & WATANABE, T. 1997. Tumor necrosis factor receptor-associated factor (TRAF) 5 and TRAF2 are involved in CD30-mediated NFkappaB activation. *J Biol Chem,* 272**,** 2042-5.

AKIBA, H., NAKANO, H., NISHINAKA, S., SHINDO, M., KOBATA, T., ATSUTA, M., MORIMOTO, C., WARE, C. F., MALININ, N. L., WALLACH, D., YAGITA, H. & OKUMURA, K. 1998. CD27, a member of the tumor necrosis factor receptor superfamily, activates NF-kappaB and stress-activated protein kinase/c-Jun N-terminal kinase via TRAF2, TRAF5, and NF-kappaB-inducing kinase. *J Biol Chem,* 273**,** 13353-8.

AKIYAMA, T., MAEDA, S., YAMANE, S., OGINO, K., KASAI, M., KAJIURA, F., MATSUMOTO, M. & INOUE, J. 2005. Dependence of self-tolerance on TRAF6-directed development of thymic stroma. *Science,* 308**,** 248-51.

AKIYAMA, T., SHIMO, Y., YANAI, H., QIN, J., OHSHIMA, D., MARUYAMA, Y., ASAUMI, Y., KITAZAWA, J., TAKAYANAGI, H., PENNINGER, J. M., MATSUMOTO, M., NITTA, T., TAKAHAMA, Y. & INOUE, J. 2008. The tumor necrosis factor family receptors RANK and CD40 cooperatively establish the thymic medullary microenvironment and self-tolerance. *Immunity,* 29**,** 423-37.

AKIYAMA, T., SHINZAWA, M. & AKIYAMA, N. 2012. TNF receptor family signaling in the development and functions of medullary thymic epithelial cells. *Front Immunol,* 3**,** 278.

ALEXOPOULOU, L., HOLT, A. C., MEDZHITOV, R. & FLAVELL, R. A. 2001.

Recognition of double-stranded RNA and activation of NF-kappaB by Toll-like receptor 3. *Nature,* 413**,** 732-8.
ANDERSON, D. M., MARASKOVSKY, E., BILLINGSLEY, W. L., DOUGALL, W. C., TOMETSKO, M. E., ROUX, E. R., TEEPE, M. C., DUBOSE, R. F., COSMAN, D. & GALIBERT, L. 1997. A homologue of the TNF receptor and its ligand enhance T-cell growth and dendritic-cell function. *Nature,* 390**,** 175-9.
ANDERSON, J. M. 2000. Multinucleated giant cells. *Curr Opin Hematol,* 7**,** 40-7.
ANDRADE, W. A., SOUZA MDO, C., RAMOS-MARTINEZ, E., NAGPAL, K., DUTRA, M. S., MELO, M. B., BARTHOLOMEU, D. C., GHOSH, S., GOLENBOCK, D. T. & GAZZINELLI, R. T. 2013. Combined action of nucleic acid-sensing Toll-like receptors and TLR11/TLR12 heterodimers imparts resistance to Toxoplasma gondii in mice. *Cell Host Microbe,* 13**,** 42-53.
ANFOSSI, N., ANDRE, P., GUIA, S., FALK, C. S., ROETYNCK, S., STEWART, C. A., BRESO, V., FRASSATI, C., REVIRON, D., MIDDLETON, D., ROMAGNE, F., UGOLINI, S. & VIVIER, E. 2006. Human NK cell education by inhibitory receptors for MHC class I. *Immunity,* 25**,** 331-42.
AOTA, Y., TERAYAMA, H., SAITO, T. & ITOH, M. 2013. Pinealectomy in a broiler chicken model impairs endochondral ossification and induces rapid cancellous bone loss. *Spine J,* 13**,** 1607-16.
APOSTOLOU, I., SARUKHAN, A., KLEIN, L. & VON BOEHMER, H. 2002. Origin of regulatory T cells with known specificity for antigen. *Nat Immunol,* 3**,** 756-63.
ARCH, R. H., GEDRICH, R. W. & THOMPSON, C. B. 1998. Tumor necrosis factor receptor-associated factors (TRAFs)-a family of adapter proteins that regulates life and death. *Genes Dev,* 12**,** 2821-30.
ARMITAGE, R. J., SATO, T. A., MACDUFF, B. M., CLIFFORD, K. N., ALPERT, A. R., SMITH, C. A. & FANSLOW, W. C. 1992. Identification of a source of biologically active CD40 ligand. *Eur J Immunol,* 22**,** 2071-6.
ARRON, J. R. & CHOI, Y. 2000. Bone versus immune system. *Nature,* 408**,** 535-6.
ATHIE-MORALES, V., SMITS, H. H., CANTRELL, D. A. & HILKENS, C. M. 2004. Sustained IL-12 signalling is required for Th1 development. *J Immunol,* 172**,** 61-9.
AUFFRAY, C., FOGG, D. K., NARNI-MANCINELLI, E., SENECHAL, B., TROUILLET, C., SAEDERUP, N., LEEMPUT, J., BIGOT, K., CAMPISI, L., ABITBOL, M., MOLINA, T., CHARO, I., HUME, D. A., CUMANO, A., LAUVAU, G. & GEISSMANN, F. 2009. CX3CR1+ CD115+ CD135+ common macrophage/DC precursors and the role of CX3CR1 in their response to inflammation. *J Exp Med,* 206**,** 595-606.
AVERY, S., ROTHWELL, L., DEGEN, W. D., SCHIJNS, V. E., YOUNG, J., KAUFMAN, J. & KAISER, P. 2004. Characterization of the first nonmammalian T2 cytokine gene cluster: the cluster contains functional single-copy genes for IL-3, IL-4, IL-13, and GM-CSF, a gene for IL-5 that appears to be a pseudogene, and a gene encoding another cytokinelike transcript, KK34. *J Interferon Cytokine Res,* 24**,** 600-10.
AWASTHI, A., CARRIER, Y., PERON, J. P., BETTELLI, E., KAMANAKA, M., FLAVELL, R. A., KUCHROO, V. K., OUKKA, M. & WEINER, H. L. 2007.

A dominant function for interleukin 27 in generating interleukin 10-producing anti-inflammatory T cells. *Nat Immunol,* 8**,** 1380-9.
BACHMANN, M. F., WONG, B. R., JOSIEN, R., STEINMAN, R. M., OXENIUS, A. & CHOI, Y. 1999. TRANCE, a tumor necrosis factor family member critical for CD40 ligand-independent T helper cell activation. *J Exp Med,* 189**,** 1025-31.
BALDWIN, A. S., JR. 1996. The NF-kappa B and I kappa B proteins: new discoveries and insights. *Annu Rev Immunol,* 14**,** 649-83.
BANCHEREAU, J. & STEINMAN, R. M. 1998. Dendritic cells and the control of immunity. *Nature,* 392**,** 245-52.
BANKS, T. A., ROUSE, B. T., KERLEY, M. K., BLAIR, P. J., GODFREY, V. L., KUKLIN, N. A., BOULEY, D. M., THOMAS, J., KANANGAT, S. & MUCENSKI, M. L. 1995. Lymphotoxin-alpha-deficient mice. Effects on secondary lymphoid organ development and humoral immune responsiveness. *J Immunol,* 155**,** 1685-93.
BANNER, D. W., D'ARCY, A., JANES, W., GENTZ, R., SCHOENFELD, H. J., BROGER, C., LOETSCHER, H. & LESSLAUER, W. 1993. Crystal structure of the soluble human 55 kd TNF receptor-human TNF beta complex: implications for TNF receptor activation. *Cell,* 73**,** 431-45.
BARBER, M. R., ALDRIDGE, J. R., JR., WEBSTER, R. G. & MAGOR, K. E. 2010. Association of RIG-I with innate immunity of ducks to influenza. *Proc Natl Acad Sci U S A,* 107**,** 5913-8.
BARKER, N., VAN ES, J. H., JAKS, V., KASPER, M., SNIPPERT, H., TOFTGARD, R. & CLEVERS, H. 2008. Very long-term self-renewal of small intestine, colon, and hair follicles from cycling Lgr5+ve stem cells. *Cold Spring Harb Symp Quant Biol,* 73**,** 351-6.
BARKER, N., VAN ES, J. H., KUIPERS, J., KUJALA, P., VAN DEN BORN, M., COZIJNSEN, M., HAEGEBARTH, A., KORVING, J., BEGTHEL, H., PETERS, P. J. & CLEVERS, H. 2007. Identification of stem cells in small intestine and colon by marker gene Lgr5. *Nature,* 449**,** 1003-7.
BAUD, V., LIU, Z. G., BENNETT, B., SUZUKI, N., XIA, Y. & KARIN, M. 1999. Signaling by proinflammatory cytokines: oligomerization of TRAF2 and TRAF6 is sufficient for JNK and IKK activation and target gene induction via an amino-terminal effector domain. *Genes Dev,* 13**,** 1297-308.
BAUD'HUIN, M., LAMOUREUX, F., DUPLOMB, L., REDINI, F. & HEYMANN, D. 2007. RANKL, RANK, osteoprotegerin: key partners of osteoimmunology and vascular diseases. *Cell Mol Life Sci,* 64**,** 2334-50.
BEAN, A. G., BAKER, M. L., STEWART, C. R., COWLED, C., DEFFRASNES, C., WANG, L. F. & LOWENTHAL, J. W. 2013. Studying immunity to zoonotic diseases in the natural host - keeping it real. *Nat Rev Immunol,* 13**,** 851-61.
BELGNAOUI, S. M., PAZ, S. & HISCOTT, J. 2011. Orchestrating the interferon antiviral response through the mitochondrial antiviral signaling (MAVS) adapter. *Curr Opin Immunol,* 23**,** 564-72.
BEN-ALI, M., CORRE, B., MANRY, J., BARREIRO, L. B., QUACH, H., BONIOTTO, M., PELLEGRINI, S. & QUINTANA-MURCI, L. 2011. Functional characterization of naturally occurring genetic variants in the human TLR1-2-6 gene family. *Hum Mutat,* 32**,** 643-52.

BENDTSEN, J. D., NIELSEN, H., VON HEIJNE, G. & BRUNAK, S. 2004. Improved prediction of signal peptides: SignalP 3.0. *J Mol Biol,* 340**,** 783-95.
BERNDT, A., PIEPER, J. & METHNER, U. 2006. Circulating gamma delta T cells in response to Salmonella enterica serovar enteritidis exposure in chickens. *Infect Immun,* 74**,** 3967-78.
BERNOT, A. & AUFFRAY, C. 1991. Primary structure and ontogeny of an avian CD3 transcript. *Proc Natl Acad Sci U S A,* 88**,** 2550-4.

BERRY, R., HEADEY, S. J., CALL, M. J., MCCLUSKEY, J., TREGASKES, C. A., KAUFMAN, J., KOH, R., SCANLON, M. J., CALL, M. E. & ROSSJOHN, J. 2014. Structure of the chicken CD3epsilondelta/gamma heterodimer and its assembly with the alphabetaT cell receptor. *J Biol Chem,* 289**,** 8240-51.
BIGGS, P. M. & NAIR, V. 2012. The long view: 40 years of Marek's disease research and Avian Pathology. *Avian Pathol,* 41**,** 3-9.
BISHOP, K. A., COY, H. M., NERENZ, R. D., MEYER, M. B. & PIKE, J. W. 2011. Mouse Rankl expression is regulated in T cells by c-Fos through a cluster of distal regulatory enhancers designated the T cell control region. *J Biol Chem,* 286**,** 20880-91.
BISWAS, S. K. & MANTOVANI, A. 2010. Macrophage plasticity and interaction with lymphocyte subsets: cancer as a paradigm. *Nat Immunol,* 11**,** 889-96.
BOCKER, W., RADIC, T., SCHONITZER, V., HAASTERS, F., MUTSCHLER, W. & SCHIEKER, M. 2012. Molecular cloning and functional characterization of the porcine extracellular domain of Receptor Activator of NF-kappaB Ligand (sRANKL). *Gene,* 492**,** 296-304.
BOCKMAN, D. E. & COOPER, M. D. 1973. Pinocytosis by epithelium associated with lymphoid follicles in the bursa of Fabricius, appendix, and Peyer's patches. An electron microscopic study. *Am J Anat,* 136**,** 455-77.
BOSSEN, C., INGOLD, K., TARDIVEL, A., BODMER, J. L., GAIDE, O., HERTIG, S., AMBROSE, C., TSCHOPP, J. & SCHNEIDER, P. 2006. Interactions of tumor necrosis factor (TNF) and TNF receptor family members in the mouse and human. *J Biol Chem,* 281**,** 13964-71.
BOSSEN, C. & SCHNEIDER, P. 2006. BAFF, APRIL and their receptors: structure, function and signaling. *Semin Immunol,* 18**,** 263-75.
BOURS, V., VILLALOBOS, J., BURD, P. R., KELLY, K. & SIEBENLIST, U. 1990. Cloning of a mitogen-inducible gene encoding a kappa B DNA-binding protein with homology to the rel oncogene and to cell-cycle motifs. *Nature,* 348**,** 76-80.
BOUWMEESTER, T., BAUCH, A., RUFFNER, H., ANGRAND, P. O., BERGAMINI, G., CROUGHTON, K., CRUCIAT, C., EBERHARD, D., GAGNEUR, J., GHIDELLI, S., HOPF, C., HUHSE, B., MANGANO, R., MICHON, A. M., SCHIRLE, M., SCHLEGL, J., SCHWAB, M., STEIN, M. A., BAUER, A., CASARI, G., DREWES, G., GAVIN, A. C., JACKSON, D. B., JOBERTY, G., NEUBAUER, G., RICK, J., KUSTER, B. & SUPERTI-FURGA, G. 2004. A physical and functional map of the human TNF-alpha/NF-kappa B signal transduction pathway. *Nat Cell Biol,* 6**,** 97-105.
BOYD, A., PHILBIN, V. J. & SMITH, A. L. 2007. Conserved and distinct aspects of the avian Toll-like receptor (TLR) system: implications for transmission and control of bird-borne zoonoses. *Biochem Soc Trans,* 35**,** 1504-7.

BOYD, Y., GOODCHILD, M., MORROLL, S. & BUMSTEAD, N. 2001. Mapping of the chicken and mouse genes for toll-like receptor 2 (TLR2) to an evolutionarily conserved chromosomal segment. *Immunogenetics,* 52**,** 294-8.

BOYLE, J. P., MAYLE, S., PARKHOUSE, R. & MONIE, T. P. 2013. Comparative Genomic and Sequence Analysis Provides Insight into the Molecular Functionality of NOD1 and NOD2. *Front Immunol,* 4**,** 317.

BRAGGIO, E., KEATS, J. J., LELEU, X., VAN WIER, S., JIMENEZ-ZEPEDA, V. H., VALDEZ, R., SCHOP, R. F., PRICE-TROSKA, T., HENDERSON, K., SACCO, A., AZAB, F., GREIPP, P., GERTZ, M., HAYMAN, S., RAJKUMAR, S. V., CARPTEN, J., CHESI, M., BARRETT, M., STEWART, A. K., DOGAN, A., BERGSAGEL, P. L., GHOBRIAL, I. M. & FONSECA, R. 2009. Identification of copy number abnormalities and inactivating mutations in two negative regulators of nuclear factor-kappaB signaling pathways in Waldenstrom's macroglobulinemia. *Cancer Res,* 69**,** 3579-88.

BRANDTZAEG, P., HALSTENSEN, T. S., KETT, K., KRAJCI, P., KVALE, D., ROGNUM, T. O., SCOTT, H. & SOLLID, L. M. 1989. Immunobiology and immunopathology of human gut mucosa: humoral immunity and intraepithelial lymphocytes. *Gastroenterology,* 97**,** 1562-84.

BRIDGHAM, J. T. & JOHNSON, A. L. 2001. Expression and regulation of Fas antigen and tumor necrosis factor receptor type I in hen granulosa cells. *Biol Reprod,* 65**,** 733-9.

BRIDGHAM, J. T. & JOHNSON, A. L. 2003. Characterization of chicken TNFR superfamily decoy receptors, DcR3 and osteoprotegerin. *Biochem Biophys Res Commun,* 307, 956-61.

BRINK, R. & LODISH, H. F. 1998. Tumor necrosis factor receptor (TNFR)-associated factor 2A (TRAF2A), a TRAF2 splice variant with an extended RING finger domain that inhibits TNFR2-mediated NF-kappaB activation. *J Biol Chem,* 273**,** 4129-34.

BRINKMANN, M. M., SPOONER, E., HOEBE, K., BEUTLER, B., PLOEGH, H. L. & KIM, Y. M. 2007. The interaction between the ER membrane protein UNC93B and TLR3, 7, and 9 is crucial for TLR signaling. *J Cell Biol,* 177**,** 265-75.

BROMBACHER, F., DORFMULLER, A., MAGRAM, J., DAI, W. J., KOHLER, G., WUNDERLIN, A., PALMER-LEHMANN, K., GATELY, M. K. & ALBER, G. 1999. IL-12 is dispensable for innate and adaptive immunity against low doses of Listeria monocytogenes. *Int Immunol,* 11**,** 325-32.

BROWN, G. D. 2006. Macrophage receptors and innate immunity: insights from dectin-1. *Novartis Found Symp,* 279**,** 114-23; discussion 123-6, 216-9.

BROWNING, J. L., NGAM-EK, A., LAWTON, P., DEMARINIS, J., TIZARD, R., CHOW, E. P., HESSION, C., O'BRINE-GRECO, B., FOLEY, S. F. & WARE, C. F. 1993. Lymphotoxin beta, a novel member of the TNF family that forms a heteromeric complex with lymphotoxin on the cell surface. *Cell,* 72**,** 847-56.

BROWNLIE, R., ZHU, J., ALLAN, B., MUTWIRI, G. K., BABIUK, L. A., POTTER, A. & GRIEBEL, P. 2009. Chicken TLR21 acts as a functional homologue to mammalian TLR9 in the recognition of CpG oligodeoxynucleotides. *Mol Immunol,* 46**,** 3163-70.

BRUNIQUEL, D., BORIE, N., HANNIER, S. & TRIEBEL, F. 1998. Regulation of expression of the human lymphocyte activation gene-3 (LAG-3) molecule, a ligand for MHC class II. *Immunogenetics,* 48**,** 116-24.

BUCAY, N., SAROSI, I., DUNSTAN, C. R., MORONY, S., TARPLEY, J., CAPPARELLI, C., SCULLY, S., TAN, H. L., XU, W., LACEY, D. L., BOYLE, W. J. & SIMONET, W. S. 1998. osteoprotegerin-deficient mice develop early onset osteoporosis and arterial calcification. *Genes Dev,* 12**,** 1260-8.

BUCHTA, C. M. & BISHOP, G. A. 2014. TRAF5 negatively regulates TLR signaling in B lymphocytes. *J Immunol,* 192**,** 145-50.

BURGESS, S. C., YOUNG, J. R., BAATEN, B. J., HUNT, L., ROSS, L. N., PARCELLS, M. S., KUMAR, P. M., TREGASKES, C. A., LEE, L. F. & DAVISON, T. F. 2004. Marek's disease is a natural model for lymphomas overexpressing Hodgkin's disease antigen (CD30). *Proc Natl Acad Sci U S A,* 101**,** 13879-84.

BURTRUM, D. B., KIM, S., DUDLEY, E. C., HAYDAY, A. C. & PETRIE, H. T. 1996. TCR gene recombination and alpha beta-gamma delta lineage divergence: productive TCR-beta rearrangement is neither exclusive nor preclusive of gamma delta cell development. *J Immunol,* 157**,** 4293-6.

CAI, G. & FREEMAN, G. J. 2009. The CD160, BTLA, LIGHT/HVEM pathway: a bidirectional switch regulating T-cell activation. *Immunol Rev,* 229**,** 244-58.

CALLEGARI, A., COONS, M. L., RICKS, J. L., ROSENFELD, M. E. & SCATENA, M. 2014. Increased Calcification in Osteoprotegerin-Deficient Smooth Muscle Cells: Dependence on Receptor Activator of NF-kappaB Ligand and Interleukin 6. *J Vasc Res,* 51**,** 118-31.

CAMBI, A., GIJZEN, K., DE VRIES L, J., TORENSMA, R., JOOSTEN, B., ADEMA, G. J., NETEA, M. G., KULLBERG, B. J., ROMANI, L. & FIGDOR, C. G. 2003. The C-type lectin DC-SIGN (CD209) is an antigen-uptake receptor for Candida albicans on dendritic cells. *Eur J Immunol,* 33**,** 532-8.

CAMERINI, D., WALZ, G., LOENEN, W. A., BORST, J. & SEED, B. 1991. The T cell activation antigen CD27 is a member of the nerve growth factor/tumor necrosis factor receptor gene family. *J Immunol,* 147**,** 3165-9.

CAO, Z., XIONG, J., TAKEUCHI, M., KURAMA, T. & GOEDDEL, D. V. 1996. TRAF6 is a signal transducer for interleukin-1. *Nature,* 383**,** 443-6.

CARPENTIER, I. & BEYAERT, R. 1999. TRAF1 is a TNF inducible regulator of NF-kappaB activation. *FEBS Lett,* 460**,** 246-50.

CEJAS, P. J., WALSH, M. C., PEARCE, E. L., HAN, D., HARMS, G. M., ARTIS, D., TURKA, L. A. & CHOI, Y. 2010. TRAF6 inhibits Th17 differentiation and TGF-beta-mediated suppression of IL-2. *Blood,* 115**,** 4750-7.

CHAN, F. K., CHUN, H. J., ZHENG, L., SIEGEL, R. M., BUI, K. L. & LENARDO, M. J. 2000. A domain in TNF receptors that mediates ligand-independent receptor assembly and signaling. *Science,* 288**,** 2351-4.

CHANG, S. H. & DONG, C. 2011. Signaling of interleukin-17 family cytokines in immunity and inflammation. *Cell Signal,* 23**,** 1069-75.

CHEN, N. J., HUANG, M. W. & HSIEH, S. L. 2001. Enhanced secretion of IFN-gamma by activated Th1 cells occurs via reverse signaling through TNF-related activation-induced cytokine. *J Immunol,* 166**,** 270-6.

CHEN, W., JIN, W., HARDEGEN, N., LEI, K. J., LI, L., MARINOS, N., MCGRADY, G. & WAHL, S. M. 2003. Conversion of peripheral CD4+CD25- naive T cells to CD4+CD25+ regulatory T cells by TGF-beta induction of transcription factor Foxp3. *J Exp Med,* 198**,** 1875-86.

CHENG, T., PAVLOS, N. J., WANG, C., TAN, J. W., LIN, J. M., CORNISH, J., ZHENG, M. H. & XU, J. 2009. Mutations within the TNF-like core domain of RANKL impair osteoclast differentiation and activation. *Mol Endocrinol,* 23**,** 35-46.

CHERFILS-VICINI, J., VINGERT, B., VARIN, A., TARTOUR, E., FRIDMAN, W. H., SAUTES-FRIDMAN, C., REGNIER, C. H. & CREMER, I. 2008. Characterization of immune functions in TRAF4-deficient mice. *Immunology,* 124**,** 562-74.

CHICHEPORTICHE, Y., BOURDON, P. R., XU, H., HSU, Y. M., SCOTT, H., HESSION, C., GARCIA, I. & BROWNING, J. L. 1997. TWEAK, a new secreted ligand in the tumor necrosis factor family that weakly induces apoptosis. *J Biol Chem,* 272**,** 32401-10.

CHIFFOLEAU, E., KOBAYASHI, T., WALSH, M. C., KING, C. G., WALSH, P. T., HANCOCK, W. W., CHOI, Y. & TURKA, L. A. 2003. TNF receptor-associated factor 6 deficiency during hemopoiesis induces Th2-polarized inflammatory disease. *J Immunol,* 171**,** 5751-9.

CHILDS, K., STOCK, N., ROSS, C., ANDREJEVA, J., HILTON, L., SKINNER, M., RANDALL, R. & GOODBOURN, S. 2007. mda-5, but not RIG-I, is a common target for paramyxovirus V proteins. *Virology,* 359**,** 190-200.

CHINO, T., DRAVES, K. E. & CLARK, E. A. 2009. Regulation of dendritic cell survival and cytokine production by osteoprotegerin. *J Leukoc Biol,* 86**,** 933-40.

CHO, S. H., LOEWEN, P. C. & MARQUARDT, R. R. 2004. A plasmid DNA encoding chicken interleukin-6 and Escherichia coli K88 fimbrial protein FaeG stimulates the production of anti-K88 fimbrial antibodies in chickens. *Poult Sci,* 83**,** 1973-8.

CHRZASTEK, K., BOROWSKA, D., KAISER, P. & VERVELDE, L. 2014. Class B CpG ODN stimulation upregulates expression of TLR21 and IFN-gamma in chicken Harderian gland cells. *Vet Immunol Immunopathol,* 160, 293-9.

CHUAMMITRI, P., OSTOJIC, J., ANDREASEN, C. B., REDMOND, S. B., LAMONT, S. J. & PALIC, D. 2009. Chicken heterophil extracellular traps (HETs): novel defense mechanism of chicken heterophils. *Vet Immunol Immunopathol,* 129**,** 126-31.

CHUANG, H. C., LAY, J. D., CHUANG, S. E., HSIEH, W. C., CHANG, Y. & SU, I. J. 2007. Epstein-Barr virus (EBV) latent membrane protein-1 down-regulates tumor necrosis factor-alpha (TNF-alpha) receptor-1 and confers resistance to TNF-alpha-induced apoptosis in T cells: implication for the progression to T-cell lymphoma in EBV-associated hemophagocytic syndrome. *Am J Pathol,* 170**,** 1607-17.

CHUNG, J. Y., PARK, Y. C., YE, H. & WU, H. 2002. All TRAFs are not created equal: common and distinct molecular mechanisms of TRAF-mediated signal transduction. *J Cell Sci,* 115**,** 679-88.

CIRACI, C. & LAMONT, S. J. 2011. Avian-specific TLRs and downstream effector responses to CpG-induction in chicken macrophages. *Dev Comp Immunol,*

35**,** 392-8.
CLARK, V. E., ERSON-OMAY, E. Z., SERIN, A., YIN, J., COTNEY, J., OZDUMAN, K., AVSAR, T., LI, J., MURRAY, P. B., HENEGARIU, O., YILMAZ, S., GUNEL, J. M., CARRION-GRANT, G., YILMAZ, B., GRADY, C., TANRIKULU, B., BAKIRCIOGLU, M., KAYMAKCALAN, H., CAGLAYAN, A. O., SENCAR, L., CEYHUN, E., ATIK, A. F., BAYRI, Y., BAI, H., KOLB, L. E., HEBERT, R. M., OMAY, S. B., MISHRA-GORUR, K., CHOI, M., OVERTON, J. D., HOLLAND, E. C., MANE, S., STATE, M. W., BILGUVAR, K., BAEHRING, J. M., GUTIN, P. H., PIEPMEIER, J. M., VORTMEYER, A., BRENNAN, C. W., PAMIR, M. N., KILIC, T., LIFTON, R. P., NOONAN, J. P., YASUNO, K. & GUNEL, M. 2013. Genomic analysis of non-NF2 meningiomas reveals mutations in TRAF7, KLF4, AKT1, and SMO. *Science,* 339**,** 1077-80.
COILLARD, C. & RIVARD, C. H. 1996. Vertebral deformities and scoliosis. *Eur Spine J,* 5**,** 91-100.
COLLIN-OSDOBY, P. & OSDOBY, P. 2012. Isolation and culture of primary chicken osteoclasts. *Methods Mol Biol,* 816**,** 119-43.
COURTOIS, G. & GILMORE, T. D. 2006. Mutations in the NF-kappaB signaling pathway: implications for human disease. *Oncogene,* 25**,** 6831-43.
CREMER, I., DIEU-NOSJEAN, M. C., MARECHAL, S., DEZUTTER-DAMBUYANT, C., GODDARD, S., ADAMS, D., WINTER, N., MENETRIER-CAUX, C., SAUTES-FRIDMAN, C., FRIDMAN, W. H. & MUELLER, C. G. 2002. Long-lived immature dendritic cells mediated by TRANCE-RANK interaction. *Blood,* 100**,** 3646-55.
CROFT, M. 2014. The TNF family in T cell differentiation and function - Unanswered questions and future directions. *Semin Immunol,* 26, 183-90.
CUA, D. J., SHERLOCK, J., CHEN, Y., MURPHY, C. A., JOYCE, B., SEYMOUR, B., LUCIAN, L., TO, W., KWAN, S., CHURAKOVA, T., ZURAWSKI, S., WIEKOWSKI, M., LIRA, S. A., GORMAN, D., KASTELEIN, R. A. & SEDGWICK, J. D. 2003. Interleukin-23 rather than interleukin-12 is the critical cytokine for autoimmune inflammation of the brain. *Nature,* 421**,** 744-8.
CUPEDO, T. & MEBIUS, R. E. 2005. Cellular interactions in lymph node development. *J Immunol,* 174**,** 21-5.
DADGOSTAR, H. & CHENG, G. 1998. An intact zinc ring finger is required for tumor necrosis factor receptor-associated factor-mediated nuclear factor-kappaB activation but is dispensable for c-Jun N-terminal kinase signaling. *J Biol Chem,* 273**,** 24775-80.
DAI, X. M., ZONG, X. H., SYLVESTRE, V. & STANLEY, E. R. 2004. Incomplete restoration of colony-stimulating factor 1 (CSF-1) function in CSF-1-deficient Csf1op/Csf1op mice by transgenic expression of cell surface CSF-1. *Blood,* 103**,** 1114-23.
DALLOUL, R. A., LONG, J. A., ZIMIN, A. V., ASLAM, L., BEAL, K., BLOMBERG LE, A., BOUFFARD, P., BURT, D. W., CRASTA, O., CROOIJMANS, R. P., COOPER, K., COULOMBE, R. A., DE, S., DELANY, M. E., DODGSON, J. B., DONG, J. J., EVANS, C., FREDERICKSON, K. M., FLICEK, P., FLOREA, L., FOLKERTS, O., GROENEN, M. A., HARKINS, T. T., HERRERO, J., HOFFMANN, S.,

MEGENS, H. J., JIANG, A., DE JONG, P., KAISER, P., KIM, H., KIM, K. W., KIM, S., LANGENBERGER, D., LEE, M. K., LEE, T., MANE, S., MARCAIS, G., MARZ, M., MCELROY, A. P., MODISE, T., NEFEDOV, M., NOTREDAME, C., PATON, I. R., PAYNE, W. S., PERTEA, G., PRICKETT, D., PUIU, D., QIOA, D., RAINERI, E., RUFFIER, M., SALZBERG, S. L., SCHATZ, M. C., SCHEURING, C., SCHMIDT, C. J., SCHROEDER, S., SEARLE, S. M., SMITH, E. J., SMITH, J., SONSTEGARD, T. S., STADLER, P. F., TAFER, H., TU, Z. J., VAN TASSELL, C. P., VILELLA, A. J., WILLIAMS, K. P., YORKE, J. A., ZHANG, L., ZHANG, H. B., ZHANG, X., ZHANG, Y. & REED, K. M. 2010. Multi-platform next-generation sequencing of the domestic turkey (Meleagris gallopavo): genome assembly and analysis. *PLoS Biol,* 8, e1000475.

DARDALHON, V., AWASTHI, A., KWON, H., GALILEOS, G., GAO, W., SOBEL, R. A., MITSDOERFFER, M., STROM, T. B., ELYAMAN, W., HO, I. C., KHOURY, S., OUKKA, M. & KUCHROO, V. K. 2008. IL-4 inhibits TGF-beta-induced Foxp3+ T cells and, together with TGF-beta, generates IL-9+ IL-10+ Foxp3(-) effector T cells. *Nat Immunol,* 9**,** 1347-55.

DARNAY, B. G., HARIDAS, V., NI, J., MOORE, P. A. & AGGARWAL, B. B. 1998. Characterization of the intracellular domain of receptor activator of NF-kappaB (RANK). Interaction with tumor necrosis factor receptor-associated factors and activation of NF-kappab and c-Jun N-terminal kinase. *J Biol Chem,* 273**,** 20551-5.

DARNAY, B. G., NI, J., MOORE, P. A. & AGGARWAL, B. B. 1999. Activation of NF-kappaB by RANK requires tumor necrosis factor receptor-associated factor (TRAF) 6 and NF-kappaB-inducing kinase. Identification of a novel TRAF6 interaction motif. *J Biol Chem,* 274**,** 7724-31.

DAS, U. N. 2010. Do long-chain unsaturated fatty acids function as endogenous anti-trypanosomal molecules? *Med Hypotheses,* 74**,** 676-8.

DE GEUS, E. D., TEFSEN, B., VAN HAARLEM, D. A., VAN EDEN, W., VAN DIE, I. & VERVELDE, L. 2013. Glycans from avian influenza virus are recognized by chicken dendritic cells and are targets for the humoral immune response in chicken. *Mol Immunol,* 56**,** 452-62.

DE JONG, S. J., ALBRECHT, J. C., GIEHLER, F., KIESER, A., STICHT, H. & BIESINGER, B. 2013. Noncanonical NF-kappaB activation by the oncoprotein Tio occurs through a nonconserved TRAF3-binding motif. *Sci Signal,* 6**,** ra27.

DE JONG, S. J., ALBRECHT, J. C., SCHMIDT, M., MULLER-FLECKENSTEIN, I. & BIESINGER, B. 2010. Activation of noncanonical NF-kappaB signaling by the oncoprotein Tio. *J Biol Chem,* 285**,** 16495-503.

DE LAU, W., KUJALA, P., SCHNEEBERGER, K., MIDDENDORP, S., LI, V. S., BARKER, N., MARTENS, A., HOFHUIS, F., DEKOTER, R. P., PETERS, P. J., NIEUWENHUIS, E. & CLEVERS, H. 2012. Peyer's patch M cells derived from Lgr5(+) stem cells require SpiB and are induced by RankL in cultured "miniguts". *Mol Cell Biol,* 32**,** 3639-47.

DE MENDONCA, F. L., DA FONSECA, P. C., PHILLIPS, R. M., SALDANHA, J. W., WILLIAMS, T. J. & PEASE, J. E. 2005. Site-directed mutagenesis of CC chemokine receptor 1 reveals the mechanism of action of UCB 35625, a

small molecule chemokine receptor antagonist. *J Biol Chem,* 280**,** 4808-16.
DE ZOETE, M. R., BOUWMAN, L. I., KEESTRA, A. M. & VAN PUTTEN, J. P. 2011. Cleavage and activation of a Toll-like receptor by microbial proteases. *Proc Natl Acad Sci U S A,* 108**,** 4968-73.
DEGEN, W. G., DAAL, N., ROTHWELL, L., KAISER, P. & SCHIJNS, V. E. 2005. Th1/Th2 polarization by viral and helminth infection in birds. *Vet Microbiol,* 105**,** 163-7.
DENG, L., WANG, C., SPENCER, E., YANG, L., BRAUN, A., YOU, J., SLAUGHTER, C., PICKART, C. & CHEN, Z. J. 2000. Activation of the IkappaB kinase complex by TRAF6 requires a dimeric ubiquitin-conjugating enzyme complex and a unique polyubiquitin chain. *Cell,* 103**,** 351-61.
DERBINSKI, J., SCHULTE, A., KYEWSKI, B. & KLEIN, L. 2001. Promiscuous gene expression in medullary thymic epithelial cells mirrors the peripheral self. *Nat Immunol,* 2**,** 1032-9.
DEVERGNE, O., HATZIVASSILIOU, E., IZUMI, K. M., KAYE, K. M., KLEIJNEN, M. F., KIEFF, E. & MOSIALOS, G. 1996. Association of TRAF1, TRAF2, and TRAF3 with an Epstein-Barr virus LMP1 domain important for B-lymphocyte transformation: role in NF-kappaB activation. *Mol Cell Biol,* 16**,** 7098-108.
DEWHIRST, F. E., STASHENKO, P. P., MOLE, J. E. & TSURUMACHI, T. 1985. Purification and partial sequence of human osteoclast-activating factor: identity with interleukin 1 beta. *J Immunol,* 135**,** 2562-8.
DI NOIA, J. M., WILLIAMS, G. T., CHAN, D. T., BUERSTEDDE, J. M., BALDWIN, G. S. & NEUBERGER, M. S. 2007. Dependence of antibody gene diversification on uracil excision. *J Exp Med,* 204**,** 3209-19.
DIECKMANN, D., PLOTTNER, H., BERCHTOLD, S., BERGER, T. & SCHULER, G. 2001. Ex vivo isolation and characterization of CD4(+)CD25(+) T cells with regulatory properties from human blood. *J Exp Med,* 193**,** 1303-10.
DIGBY, M. R. & LOWENTHAL, J. W. 1995. Cloning and expression of the chicken interferon-gamma gene. *J Interferon Cytokine Res,* 15**,** 939-45.
DISTELHORST, C. W. & BOOTMAN, M. D. 2011. Bcl-2 interaction with the inositol 1,4,5-trisphosphate receptor: role in Ca(2+) signaling and disease. *Cell Calcium,* 50**,** 234-41.
DOUGALL, W. C., GLACCUM, M., CHARRIER, K., ROHRBACH, K., BRASEL, K., DE SMEDT, T., DARO, E., SMITH, J., TOMETSKO, M. E., MALISZEWSKI, C. R., ARMSTRONG, A., SHEN, V., BAIN, S., COSMAN, D., ANDERSON, D., MORRISSEY, P. J., PESCHON, J. J. & SCHUH, J. 1999. RANK is essential for osteoclast and lymph node development. *Genes Dev,* 13**,** 2412-24.
DUHEN, T., GEIGER, R., JARROSSAY, D., LANZAVECCHIA, A. & SALLUSTO, F. 2009. Production of interleukin 22 but not interleukin 17 by a subset of human skin-homing memory T cells. *Nat Immunol,* 10**,** 857-63.
DUNACHIE, S. J., WALTHER, M., EPSTEIN, J. E., KEATING, S., BERTHOUD, T., ANDREWS, L., ANDERSEN, R. F., BEJON, P., GOONETILLEKE, N., POULTON, I., WEBSTER, D. P., BUTCHER, G., WATKINS, K., SINDEN, R. E., LEVINE, G. L., RICHIE, T. L., SCHNEIDER, J., KASLOW, D., GILBERT, S. C., CARUCCI, D. J. & HILL, A. V. 2006. A DNA prime-

modified vaccinia virus ankara boost vaccine encoding thrombospondin-related adhesion protein but not circumsporozoite protein partially protects healthy malaria-naive adults against Plasmodium falciparum sporozoite challenge. *Infect Immun,* 74**,** 5933-42.

DUNN, R. J., LUEDECKER, C. J., HAUGEN, H. S., CLEGG, C. H. & FARR, A. G. 1997. Thymic overexpression of CD40 ligand disrupts normal thymic epithelial organization. *J Histochem Cytochem,* 45**,** 129-41.

ELINAV, E., STROWIG, T., HENAO-MEJIA, J. & FLAVELL, R. A. 2011. Regulation of the antimicrobial response by NLR proteins. *Immunity,* 34**,** 665-79.

ELLIS, R. E., YUAN, J. Y. & HORVITZ, H. R. 1991. Mechanisms and functions of cell death. *Annu Rev Cell Biol,* 7**,** 663-98.

EMERY, J. G., MCDONNELL, P., BURKE, M. B., DEEN, K. C., LYN, S., SILVERMAN, C., DUL, E., APPELBAUM, E. R., EICHMAN, C., DIPRINZIO, R., DODDS, R. A., JAMES, I. E., ROSENBERG, M., LEE, J. C. & YOUNG, P. R. 1998. Osteoprotegerin is a receptor for the cytotoxic ligand TRAIL. *J Biol Chem,* 273**,** 14363-7.

ETEMADI, N., HOLIEN, J. K., CHAU, D., DEWSON, G., MURPHY, J. M., ALEXANDER, W. S., PARKER, M. W., SILKE, J. & NACHBUR, U. 2013. Lymphotoxin alpha induces apoptosis, necroptosis and inflammatory signals with the same potency as tumour necrosis factor. *FEBS J,* 280**,** 5283-97.

FADOK, V. A., VOELKER, D. R., CAMPBELL, P. A., COHEN, J. J., BRATTON, D. L. & HENSON, P. M. 1992. Exposure of phosphatidylserine on the surface of apoptotic lymphocytes triggers specific recognition and removal by macrophages. *J Immunol,* 148**,** 2207-16.

FARHAT, K., RIEKENBERG, S., HEINE, H., DEBARRY, J., LANG, R., MAGES, J., BUWITT-BECKMANN, U., ROSCHMANN, K., JUNG, G., WIESMULLER, K. H. & ULMER, A. J. 2008. Heterodimerization of TLR2 with TLR1 or TLR6 expands the ligand spectrum but does not lead to differential signaling. *J Leukoc Biol,* 83**,** 692-701.

FELDMANN, M., BRENNAN, F. M. & MAINI, R. N. 1996. Role of cytokines in rheumatoid arthritis. *Annu Rev Immunol,* 14**,** 397-440.

FENNEWALD, S., VAN SANTEN, V. & KIEFF, E. 1984. Nucleotide sequence of an mRNA transcribed in latent growth-transforming virus infection indicates that it may encode a membrane protein. *J Virol,* 51**,** 411-9.

FIONDA, C., NAPPI, F., PICCOLI, M., FRATI, L., SANTONI, A. & CIPPITELLI, M. 2007. 15-deoxy-Delta12,14-prostaglandin J2 negatively regulates rankl gene expression in activated T lymphocytes: role of NF-kappaB and early growth response transcription factors. *J Immunol,* 178**,** 4039-50.

FONTENOT, J. D., GAVIN, M. A. & RUDENSKY, A. Y. 2003. Foxp3 programs the development and function of CD4+CD25+ regulatory T cells. *Nat Immunol,* 4**,** 330-6.

FRATTINI, A., VEZZONI, P., VILLA, A. & SOBACCHI, C. 2007. The Dissection of Human Autosomal Recessive Osteopetrosis Identifies an Osteoclast-Poor Form due to RANKL Deficiency. *Cell Cycle,* 6**,** 3027-33.

FU, D., ZHANG, Y., XIAO, S. & YU, Z. 2011. The first homolog of a TRAF7 (TNF receptor-associated factor 7) gene in a mollusk, *Crassostrea hongkongensis*. *Fish Shellfish Immunol,* 31**,** 1208-10.

GALAN, J. E. & FU, Y. 2000. Modulation of actin cytoskeleton by Salmonella GTPase activating protein SptP. *Methods Enzymol,* 325**,** 496-504.
GALIBERT, L., TOMETSKO, M. E., ANDERSON, D. M., COSMAN, D. & DOUGALL, W. C. 1998. The involvement of multiple tumor necrosis factor receptor (TNFR)-associated factors in the signaling mechanisms of receptor activator of NF-kappaB, a member of the TNFR superfamily. *J Biol Chem,* 273**,** 34120-7.
GAO, H., WU, L., SUN, J. S., GENG, X. Y. & PAN, B. P. 2013. Molecular characterization and expression analysis of Toll-like receptor 21 cDNA from Paralichthys olivaceus. *Fish Shellfish Immunol,* 35**,** 1138-45.
GARCEAU, V., SMITH, J., PATON, I. R., DAVEY, M., FARES, M. A., SESTER, D. P., BURT, D. W. & HUME, D. A. 2010. Pivotal Advance: Avian colony-stimulating factor 1 (CSF-1), interleukin-34 (IL-34), and CSF-1 receptor genes and gene products. *J Leukoc Biol,* 87**,** 753-64.
GEISSMANN, F., MANZ, M. G., JUNG, S., SIEWEKE, M. H., MERAD, M. & LEY, K. 2010. Development of monocytes, macrophages, and dendritic cells. *Science,* 327**,** 656-61.
GENOVESE, K. J., HE, H., SWAGGERTY, C. L. & KOGUT, M. H. 2013. The avian heterophil. *Dev Comp Immunol,* 41**,** 334-40.
GEWIRTZ, A. M., ANFOSSI, G., VENTURELLI, D., VALPREDA, S., SIMS, R. & CALABRETTA, B. 1989. G1/S transition in normal human T-lymphocytes requires the nuclear protein encoded by c-myb. *Science,* 245**,** 180-3.
GIBSON, M. S., KAISER, P. & FIFE, M. 2014. The chicken IL-1 family: evolution in the context of the studied vertebrate lineage. *Immunogenetics,* 66**,** 427-38.
GIL, J., GARCIA, M. A., GOMEZ-PUERTAS, P., GUERRA, S., RULLAS, J., NAKANO, H., ALCAMI, J. & ESTEBAN, M. 2004. TRAF family proteins link PKR with NF-kappa B activation. *Mol Cell Biol,* 24**,** 4502-12.
GILL, J., MALIN, M., SUTHERLAND, J., GRAY, D., HOLLANDER, G. & BOYD, R. 2003. Thymic generation and regeneration. *Immunol Rev,* 195**,** 28-50.
GLENNEY, G. W. & WIENS, G. D. 2007. Early diversification of the TNF superfamily in teleosts: genomic characterization and expression analysis. *J Immunol,* 178**,** 7955-73.
GLICK, B. 1991. Historical perspective: the bursa of Fabricius and its influence on B-cell development, past and present. *Vet Immunol Immunopathol,* 30**,** 3-12.
GOHDA, J., AKIYAMA, T., KOGA, T., TAKAYANAGI, H., TANAKA, S. & INOUE, J. 2005. RANK-mediated amplification of TRAF6 signaling leads to NFATc1 induction during osteoclastogenesis. *EMBO J,* 24**,** 790-9.
GONZALVEZ, F., LAWRENCE, D., YANG, B., YEE, S., PITTI, R., MARSTERS, S., PHAM, V. C., STEPHAN, J. P., LILL, J. & ASHKENAZI, A. 2012. TRAF2 Sets a threshold for extrinsic apoptosis by tagging caspase-8 with a ubiquitin shutoff timer. *Mol Cell,* 48**,** 888-99.
GORDON, S. 2003. Alternative activation of macrophages. *Nat Rev Immunol,* 3**,** 23-35.
GOULD, H. J. & SUTTON, B. J. 2008. IgE in allergy and asthma today. *Nat Rev Immunol,* 8**,** 205-17.
GRAHAM, J. P., MOORE, C. R. & BISHOP, G. A. 2009. Roles of the TRAF2/3 binding site in differential B cell signaling by CD40 and its viral oncogenic

mimic, LMP1. *J Immunol,* 183**,** 2966-73.
GRECH, A., QUINN, R., SRINIVASAN, D., BADOUX, X. & BRINK, R. 2000. Complete structural characterisation of the mammalian and Drosophila TRAF genes: implications for TRAF evolution and the role of RING finger splice variants. *Mol Immunol,* 37**,** 721-34.
GRECH, A. P., AMESBURY, M., CHAN, T., GARDAM, S., BASTEN, A. & BRINK, R. 2004. TRAF2 differentially regulates the canonical and noncanonical pathways of NF-kappaB activation in mature B cells. *Immunity,* 21**,** 629-42.
GUAN, Y., RANOA, D. R., JIANG, S., MUTHA, S. K., LI, X., BAUDRY, J. & TAPPING, R. I. 2010. Human TLRs 10 and 1 share common mechanisms of innate immune sensing but not signaling. *J Immunol,* 184**,** 5094-103.
GUERDER, S., VIRET, C., LUCHE, H., ARDOUIN, L. & MALISSEN, B. 2012. Differential processing of self-antigens by subsets of thymic stromal cells. *Curr Opin Immunol,* 24**,** 99-104.
GUO, Y., ALI, R. A. & QURESHI, M. A. 2003. The influence of beta-glucan on immune responses in broiler chicks. *Immunopharmacol Immunotoxicol,* 25**,** 461-72.
GUPTA, P., GIRI, J., SRIVASTAV, S., CHANDE, A. G., MUKHOPADHYAYA, R., DAS, P. K. & UKIL, A. 2014. Leishmania donovani targets tumor necrosis factor receptor-associated factor (TRAF) 3 for impairing TLR4-mediated host response. *FASEB J,* 28**,** 1756-68.
GUPTA, S. K., BAJWA, P., DEB, R., CHELLAPPA, M. M. & DEY, S. 2014. Flagellin a toll-like receptor 5 agonist as an adjuvant in chicken vaccines. *Clin Vaccine Immunol,* 21**,** 261-70.
HAAS, J. D., GONZALEZ, F. H., SCHMITZ, S., CHENNUPATI, V., FOHSE, L., KREMMER, E., FORSTER, R. & PRINZ, I. 2009. CCR6 and NK1.1 distinguish between IL-17A and IFN-gamma-producing gammadelta effector T cells. *Eur J Immunol,* 39**,** 3488-97.
HAKOZAKI, A., YODA, M., TOHMONDA, T., FURUKAWA, M., HIKATA, T., UCHIKAWA, S., TAKAISHI, H., MATSUMOTO, M., CHIBA, K., HORIUCHI, K. & TOYAMA, Y. 2010. Receptor activator of NF-kappaB (RANK) ligand induces ectodomain shedding of RANK in murine RAW264.7 macrophages. *J Immunol,* 184**,** 2442-8.
HALL, T. J. & CHAMBERS, T. J. 1996. Molecular aspects of osteoclast function. *Inflamm Res,* 45**,** 1-9.
HAN, D., WALSH, M. C., CEJAS, P. J., DANG, N. N., KIM, Y. F., KIM, J., CHARRIER-HISAMUDDIN, L., CHAU, L., ZHANG, Q., BITTINGER, K., BUSHMAN, F. D., TURKA, L. A., SHEN, H., REIZIS, B., DEFRANCO, A. L., WU, G. D. & CHOI, Y. 2013. Dendritic cell expression of the signaling molecule TRAF6 is critical for gut microbiota-dependent immune tolerance. *Immunity,* 38**,** 1211-22.
HARA, J. & KAWA-HA, K. 1992. T-cell receptor alpha and delta gene assembly in B-cell precursor acute lymphoblastic leukemia. *Leuk Lymphoma,* 7**,** 363-70.
HARBURY, P. B., KIM, P. S. & ALBER, T. 1994. Crystal structure of an isoleucine-zipper trimer. *Nature,* 371**,** 80-3.
HARFORD, I. D., PAVLIDIS, H. O. & ANTHONY, N. B. 2014. Divergent selection for muscle color in broilers. *Poult Sci,* 93**,** 1059-66.

HARRINGTON, L. E., HATTON, R. D., MANGAN, P. R., TURNER, H., MURPHY, T. L., MURPHY, K. M. & WEAVER, C. T. 2005. Interleukin 17-producing CD4+ effector T cells develop via a lineage distinct from the T helper type 1 and 2 lineages. *Nat Immunol,* 6**,** 1123-32.

HARROP, J. A., MCDONNELL, P. C., BRIGHAM-BURKE, M., LYN, S. D., MINTON, J., TAN, K. B., DEDE, K., SPAMPANATO, J., SILVERMAN, C., HENSLEY, P., DIPRINZIO, R., EMERY, J. G., DEEN, K., EICHMAN, C., CHABOT-FLETCHER, M., TRUNEH, A. & YOUNG, P. R. 1998. Herpesvirus entry mediator ligand (HVEM-L), a novel ligand for HVEM/TR2, stimulates proliferation of T cells and inhibits HT29 cell growth. *J Biol Chem,* 273**,** 27548-56.

HE, H., GENOVESE, K. J., SWAGGERTY, C. L., MACKINNON, K. M. & KOGUT, M. H. 2012. Co-stimulation with TLR3 and TLR21 ligands synergistically up-regulates Th1-cytokine IFN-gamma and regulatory cytokine IL-10 expression in chicken monocytes. *Dev Comp Immunol,* 36**,** 756-60.

HE, H., LOWRY, V. K., FERRO, P. J. & KOGUT, M. H. 2005. CpG-oligodeoxynucleotide-stimulated chicken heterophil degranulation is serum cofactor and cell surface receptor dependent. *Dev Comp Immunol,* 29**,** 255-64.

HE, Y., WU, K., HU, Y., SHENG, L., TIE, R., WANG, B. & HUANG, H. 2014. γδ T cell and other immune cells crosstalk in cellular immunity.J Immunol Res, 960252.

HENDRIKS, J., GRAVESTEIN, L. A., TESSELAAR, K., VAN LIER, R. A., SCHUMACHER, T. N. & BORST, J. 2000. CD27 is required for generation and long-term maintenance of T cell immunity. *Nat Immunol,* 1**,** 433-40.

HEYD, F. & LYNCH, K. W. 2010. Phosphorylation-dependent regulation of PSF by GSK3 controls CD45 alternative splicing. *Mol Cell,* 40**,** 126-37.

HIGGS, R., CORMICAN, P., CAHALANE, S., ALLAN, B., LLOYD, A. T., MEADE, K., JAMES, T., LYNN, D. J., BABIUK, L. A. & O'FARRELLY, C. 2006. Induction of a novel chicken Toll-like receptor following Salmonella enterica serovar Typhimurium infection. *Infect Immun,* 74**,** 1692-8.

HIGUCHI, M., MATSUO, A., SHINGAI, M., SHIDA, K., ISHII, A., FUNAMI, K., SUZUKI, Y., OSHIUMI, H., MATSUMOTO, M. & SEYA, T. 2008. Combinational recognition of bacterial lipoproteins and peptidoglycan by chicken Toll-like receptor 2 subfamily. *Dev Comp Immunol,* 32**,** 147-55.

HIKOSAKA, Y., NITTA, T., OHIGASHI, I., YANO, K., ISHIMARU, N., HAYASHI, Y., MATSUMOTO, M., MATSUO, K., PENNINGER, J. M., TAKAYANAGI, H., YOKOTA, Y., YAMADA, H., YOSHIKAI, Y., INOUE, J., AKIYAMA, T. & TAKAHAMA, Y. 2008. The cytokine RANKL produced by positively selected thymocytes fosters medullary thymic epithelial cells that express autoimmune regulator. *Immunity,* 29**,** 438-50.

HO, I. C., LO, D. & GLIMCHER, L. H. 1998. c-maf promotes T helper cell type 2 (Th2) and attenuates Th1 differentiation by both interleukin 4-dependent and -independent mechanisms. *J Exp Med,* 188**,** 1859-66.

HOCKING, P. M. 2014. Unexpected consequences of genetic selection in broilers and turkeys: problems and solutions. *Br Poult Sci,* 55**,** 1-12.

HOLEN, I., CROUCHER, P. I., HAMDY, F. C. & EATON, C. L. 2002. Osteoprotegerin (OPG) is a survival factor for human prostate cancer cells. *Cancer Res,* 62**,** 1619-23.
HORI, S., NOMURA, T. & SAKAGUCHI, S. 2003. Control of regulatory T cell development by the transcription factor Foxp3. *Science,* 299**,** 1057-61.
HORIE, R., WATANABE, T., ITO, K., MORISITA, Y., WATANABE, M., ISHIDA, T., HIGASHIHARA, M., KADIN, M. & WATANABE, T. 2002. Cytoplasmic aggregation of TRAF2 and TRAF5 proteins in the Hodgkin-Reed-Sternberg cells. *Am J Pathol,* 160**,** 1647-54.
HOROWITZ, M., VIGNERY, A., GERSHON, R. K. & BARON, R. 1984. Thymus-derived lymphocytes and their interactions with macrophages are required for the production of osteoclast-activating factor in the mouse. *Proc Natl Acad Sci U S A,* 81**,** 2181-5.
HORWOOD, N. J., KARTSOGIANNIS, V., QUINN, J. M., ROMAS, E., MARTIN, T. J. & GILLESPIE, M. T. 1999. Activated T lymphocytes support osteoclast formation in vitro. *Biochem Biophys Res Commun,* 265**,** 144-50.
HOU, L., HOU, J., YAO, J. & ZHOU, Z. 2011. Effects of osteoprotegerin from transfection of pcDNA3.1(+)/chOPG on bioactivity of chicken osteoclasts. *Acta Vet Scand,* 53**,** 21.
HOU, W. S. & VAN PARIJS, L. 2004. A Bcl-2-dependent molecular timer regulates the lifespan and immunogenicity of dendritic cells. *Nat Immunol,* 5**,** 583-9.
HSU, H., SOLOVYEV, I., COLOMBERO, A., ELLIOTT, R., KELLEY, M. & BOYLE, W. J. 1997. ATAR, a novel tumor necrosis factor receptor family member, signals through TRAF2 and TRAF5. *J Biol Chem,* 272**,** 13471-4.
HU, H. M., O'ROURKE, K., BOGUSKI, M. S. & DIXIT, V. M. 1994. A novel RING finger protein interacts with the cytoplasmic domain of CD40. *J Biol Chem,* 269**,** 30069-72.
HUANG, X. D., LIU, W. G., GUAN, Y. Y., SHI, Y., WANG, Q., ZHAO, M., WU, S. Z. & HE, M. X. 2012. Molecular cloning, characterization and expression analysis of tumor necrosis factor receptor-associated factor 3 (TRAF3) from pearl oyster Pinctada fucata. *Fish Shellfish Immunol,* 33**,** 652-8.
HUANG, Y., LI, Y., BURT, D. W., CHEN, H., ZHANG, Y., QIAN, W., KIM, H., GAN, S., ZHAO, Y., LI, J., YI, K., FENG, H., ZHU, P., LI, B., LIU, Q., FAIRLEY, S., MAGOR, K. E., DU, Z., HU, X., GOODMAN, L., TAFER, H., VIGNAL, A., LEE, T., KIM, K. W., SHENG, Z., AN, Y., SEARLE, S., HERRERO, J., GROENEN, M. A., CROOIJMANS, R. P., FARAUT, T., CAI, Q., WEBSTER, R. G., ALDRIDGE, J. R., WARREN, W. C., BARTSCHAT, S., KEHR, S., MARZ, M., STADLER, P. F., SMITH, J., KRAUS, R. H., ZHAO, Y., REN, L., FEI, J., MORISSON, M., KAISER, P., GRIFFIN, D. K., RAO, M., PITEL, F., WANG, J. & LI, N. 2013. The duck genome and transcriptome provide insight into an avian influenza virus reservoir species. *Nat Genet,* 45**,** 776-83.
HUFF, G. R., HUFF, W. E., RATH, N. C. & TELLEZ, G. 2006. Limited treatment with beta-1,3/1,6-glucan improves production values of broiler chickens challenged with Escherichia coli. *Poult Sci,* 85**,** 613-8.
HUSEBYE, H., HALAAS, O., STENMARK, H., TUNHEIM, G., SANDANGER, O., BOGEN, B., BRECH, A., LATZ, E. & ESPEVIK, T. 2006. Endocytic pathways regulate Toll-like receptor 4 signaling and link innate and adaptive

immunity. *EMBO J,* 25**,** 683-92.
HYMOWITZ, S. G., CHRISTINGER, H. W., FUH, G., ULTSCH, M., O'CONNELL, M., KELLEY, R. F., ASHKENAZI, A. & DE VOS, A. M. 1999. Triggering cell death: the crystal structure of Apo2L/TRAIL in a complex with death receptor 5. *Mol Cell,* 4**,** 563-71.
IKEDA, T., KASAI, M., UTSUYAMA, M. & HIROKAWA, K. 2001. Determination of three isoforms of the receptor activator of nuclear factor-kappaB ligand and their differential expression in bone and thymus. *Endocrinology,* 142**,** 1419-26.
INABA, K., INABA, M., ROMANI, N., AYA, H., DEGUCHI, M., IKEHARA, S., MURAMATSU, S. & STEINMAN, R. M. 1992. Generation of large numbers of dendritic cells from mouse bone marrow cultures supplemented with granulocyte/macrophage colony-stimulating factor. *J Exp Med,* 176**,** 1693-702.
INOUE, J., ISHIDA, T., TSUKAMOTO, N., KOBAYASHI, N., NAITO, A., AZUMA, S. & YAMAMOTO, T. 2000. Tumor necrosis factor receptor-associated factor (TRAF) family: adapter proteins that mediate cytokine signaling. *Exp Cell Res,* 254**,** 14-24.
IQBAL, M., PHILBIN, V. J., WITHANAGE, G. S., WIGLEY, P., BEAL, R. K., GOODCHILD, M. J., BARROW, P., MCCONNELL, I., MASKELL, D. J., YOUNG, J., BUMSTEAD, N., BOYD, Y. & SMITH, A. L. 2005. Identification and functional characterization of chicken toll-like receptor 5 reveals a fundamental role in the biology of infection with Salmonella enterica serovar typhimurium. *Infect Immun,* 73**,** 2344-50.
IRIE, A., TAKAMI, M., KUBO, H., SEKINO-SUZUKI, N., KASAHARA, K. & SANAI, Y. 2007. Heparin enhances osteoclastic bone resorption by inhibiting osteoprotegerin activity. *Bone,* 41**,** 165-74.
ISHIDA, N., HAYASHI, K., HOSHIJIMA, M., OGAWA, T., KOGA, S., MIYATAKE, Y., KUMEGAWA, M., KIMURA, T. & TAKEYA, T. 2002. Large scale gene expression analysis of osteoclastogenesis in vitro and elucidation of NFAT2 as a key regulator. *J Biol Chem,* 277**,** 41147-56.
ISHIDA, T., MIZUSHIMA, S., AZUMA, S., KOBAYASHI, N., TOJO, T., SUZUKI, K., AIZAWA, S., WATANABE, T., MOSIALOS, G., KIEFF, E., YAMAMOTO, T. & INOUE, J. 1996. Identification of TRAF6, a novel tumor necrosis factor receptor-associated factor protein that mediates signaling from an amino-terminal domain of the CD40 cytoplasmic region. *J Biol Chem,* 271**,** 28745-8.
ISHIDA, T. K., TOJO, T., AOKI, T., KOBAYASHI, N., OHISHI, T., WATANABE, T., YAMAMOTO, T. & INOUE, J. 1996. TRAF5, a novel tumor necrosis factor receptor-associated factor family protein, mediates CD40 signaling. *Proc Natl Acad Sci U S A,* 93**,** 9437-42.
IVANOV, II, ZHOU, L. & LITTMAN, D. R. 2007. Transcriptional regulation of Th17 cell differentiation. *Semin Immunol,* 19**,** 409-17.
IZAWA, T., ISHIMARU, N., MORIYAMA, K., KOHASHI, M., ARAKAKI, R. & HAYASHI, Y. 2007. Crosstalk between RANKL and Fas signaling in dendritic cells controls immune tolerance. *Blood,* 110**,** 242-50.
IZBAN, K. F., ERGIN, M., MARTINEZ, R. L. & ALKAN, S. 2000. Expression of the tumor necrosis factor receptor-associated factors (TRAFs) 1 and 2 is a

characteristic feature of Hodgkin and Reed-Sternberg cells. *Mod Pathol,* 13**,** 1324-31.
IZON, D., RUDD, K., DEMUTH, W., PEAR, W. S., CLENDENIN, C., LINDSLEY, R. C. & ALLMAN, D. 2001. A common pathway for dendritic cell and early B cell development. *J Immunol,* 167**,** 1387-92.
JALKANEN, S., JALKANEN, M., GRANFORS, K. & TOIVANEN, P. 1984. Defect in the generation of light-chain diversity in bursectomized chickens. *Nature,* 311**,** 69-71.
JALUKAR, S. V., HOSTAGER, B. S. & BISHOP, G. A. 2000. Characterization of the roles of TNF receptor-associated factor 6 in CD40-mediated B lymphocyte effector functions. *J Immunol,* 164**,** 623-30.
JEURISSEN, S. H. 1993. The role of various compartments in the chicken spleen during an antigen-specific humoral response. *Immunology,* 80**,** 29-33.
JIE, H., LIAN, L., QU, L. J., ZHENG, J. X., HOU, Z. C., XU, G. Y., SONG, J. Z. & YANG, N. 2013. Differential expression of Toll-like receptor genes in lymphoid tissues between Marek's disease virus-infected and noninfected chickens. *Poult Sci,* 92**,** 645-54.
JONES, B. D., GHORI, N. & FALKOW, S. 1994. Salmonella typhimurium initiates murine infection by penetrating and destroying the specialized epithelial M cells of the Peyer's patches. *J Exp Med,* 180**,** 15-23.
JONES, E. Y., STUART, D. I. & WALKER, N. P. 1990. The structure of tumour necrosis factor--implications for biological function. *J Cell Sci Suppl,* 13**,** 11-8.
JONES, K. E., PATEL, N. G., LEVY, M. A., STOREYGARD, A., BALK, D., GITTLEMAN, J. L. & DASZAK, P. 2008. Global trends in emerging infectious diseases. *Nature,* 451**,** 990-3.
JOSIEN, R., WONG, B. R., LI, H. L., STEINMAN, R. M. & CHOI, Y. 1999. TRANCE, a TNF family member, is differentially expressed on T cell subsets and induces cytokine production in dendritic cells. *J Immunol,* 162**,** 2562-8.
JOSIEN, R., LI, H. L., INGULLI, E., SARMA, S., WONG, B. R., VOLOGODSKAIA, M., STEINMAN, R. M. & CHOI, Y. 2000. TRANCE, a tumor necrosis factor family member, enhances the longevity and adjuvant properties of dendritic cells in vivo. *J Exp Med,* 191, 495-502.
KADOWAKI, N., HO, S., ANTONENKO, S., MALEFYT, R. W., KASTELEIN, R. A., BAZAN, F. & LIU, Y. J. 2001. Subsets of human dendritic cell precursors express different toll-like receptors and respond to different microbial antigens. *J Exp Med,* 194**,** 863-9.
KAISER, P. 2010. Advances in avian immunology--prospects for disease control: a review. *Avian Pathol,* 39**,** 309-24.
KAISER, P. 2012. The long view: a bright past, a brighter future? Forty years of chicken immunology pre- and post-genome. *Avian Pathol,* 41**,** 511-8.
KAISER, P., POH, T. Y., ROTHWELL, L., AVERY, S., BALU, S., PATHANIA, U. S., HUGHES, S., GOODCHILD, M., MORRELL, S., WATSON, M., BUMSTEAD, N., KAUFMAN, J. & YOUNG, J. R. 2005. A genomic analysis of chicken cytokines and chemokines. *J Interferon Cytokine Res,* 25**,** 467-84.
KAISHO, T. & AKIRA, S. 2006. Toll-like receptor function and signaling. *J Allergy Clin Immunol,* 117**,** 979-87; quiz 988.

KALETA, E. & BALDAUF, C. 1988. Newcastle Disease in Free-Living and Pet Birds. *In:* ALEXANDER, D. J. (ed.) *Newcastle Disease.* Springer US.
KANAGAVELU, S. K., SNARSKY, V., TERMINI, J. M., GUPTA, S., BARZEE, S., WRIGHT, J. A., KHAN, W. N., KORNBLUTH, R. S. & STONE, G. W. 2012. Soluble multi-trimeric TNF superfamily ligand adjuvants enhance immune responses to a HIV-1 Gag DNA vaccine. *Vaccine,* 30**,** 691-702.
KANAZAWA, K. & KUDO, A. 2005. Self-assembled RANK induces osteoclastogenesis ligand-independently. *J Bone Miner Res,* 20**,** 2053-60.
KANG, D. C., GOPALKRISHNAN, R. V., WU, Q., JANKOWSKY, E., PYLE, A. M. & FISHER, P. B. 2002. mda-5: An interferon-inducible putative RNA helicase with double-stranded RNA-dependent ATPase activity and melanoma growth-suppressive properties. *Proc Natl Acad Sci U S A,* 99**,** 637-42.
KARPALA, A. J., STEWART, C., MCKAY, J., LOWENTHAL, J. W. & BEAN, A. G. 2011. Characterization of chicken Mda5 activity: regulation of IFN-beta in the absence of RIG-I functionality. *J Immunol,* 186**,** 5397-405.
KARPUSAS, M., HSU, Y. M., WANG, J. H., THOMPSON, J., LEDERMAN, S., CHESS, L. & THOMAS, D. 1995. 2 A crystal structure of an extracellular fragment of human CD40 ligand. *Structure,* 3**,** 1426.
KATAGIRI, T. & TAKAHASHI, N. 2002. Regulatory mechanisms of osteoblast and osteoclast differentiation. *Oral Dis,* 8**,** 147-59.
KATO, I., SATO, H. & KUDO, A. 2003. TRANCE together with IL-7 induces pre-B cells to proliferate. *Eur J Immunol,* 33**,** 334-41.
KAWAMATA, S., HORI, T., IMURA, A., TAKAORI-KONDO, A. & UCHIYAMA, T. 1998. Activation of OX40 signal transduction pathways leads to tumor necrosis factor receptor-associated factor (TRAF) 2- and TRAF5-mediated NF-kappaB activation. *J Biol Chem,* 273**,** 5808-14.
KEESTRA, A. M., DE ZOETE, M. R., BOUWMAN, L. I. & VAN PUTTEN, J. P. 2010. Chicken TLR21 is an innate CpG DNA receptor distinct from mammalian TLR9. *J Immunol,* 185**,** 460-7.
KEITEL, W. A., TREANOR, J. J., EL SAHLY, H. M., EVANS, T. G., KOPPER, S., WHITLOW, V., SELINSKY, C., KASLOW, D. C., ROLLAND, A., SMITH, L. R. & LALOR, P. A. 2009. Evaluation of a plasmid DNA-based anthrax vaccine in rabbits, nonhuman primates and healthy adults. *Hum Vaccin,* 5**,** 536-44.
KERR, J. F., WYLLIE, A. H. & CURRIE, A. R. 1972. Apoptosis: a basic biological phenomenon with wide-ranging implications in tissue kinetics. *Br J Cancer,* 26**,** 239-57.
KEYEL, P. A. 2014. How is inflammation initiated? Individual influences of IL-1, IL-18 and HMGB1. *Cytokine,* 69, 136-45.
KILLAR, L. M., HATFIELD, C. A., CARDING, S. R., PAN, M., WINTERROWD, G. E. & BOTTOMLY, K. 1989. In vivo administration of interleukin 1 elicits increased Ia antigen expression on B cells through the induction of interleukin 4. *Eur J Immunol,* 19**,** 2205-10.
KIM, D., MEBIUS, R. E., MACMICKING, J. D., JUNG, S., CUPEDO, T., CASTELLANOS, Y., RHO, J., WONG, B. R., JOSIEN, R., KIM, N., RENNERT, P. D. & CHOI, Y. 2000. Regulation of peripheral lymph node genesis by the tumor necrosis factor family member TRANCE. *J Exp Med,*

192**,** 1467-78.
KIM, H. H., LEE, D. E., SHIN, J. N., LEE, Y. S., JEON, Y. M., CHUNG, C. H., NI, J., KWON, B. S. & LEE, Z. H. 1999. Receptor activator of NF-kappaB recruits multiple TRAF family adaptors and activates c-Jun N-terminal kinase. *FEBS Lett,* 443**,** 297-302.
KIM, M. H., BILLIAR, T. R. & SEOL, D. W. 2004. The secretable form of trimeric TRAIL, a potent inducer of apoptosis. *Biochem Biophys Res Commun,* 321**,** 930-5.
KIM, N., KADONO, Y., TAKAMI, M., LEE, J., LEE, S. H., OKADA, F., KIM, J. H., KOBAYASHI, T., ODGREN, P. R., NAKANO, H., YEH, W. C., LEE, S. K., LORENZO, J. A. & CHOI, Y. 2005. Osteoclast differentiation independent of the TRANCE-RANK-TRAF6 axis. *J Exp Med,* 202**,** 589-95.
KIM, W. H., JEONG, J., PARK, A. R., YIM, D., KIM, Y. H., KIM, K. D., CHANG, H. H., LILLEHOJ, H. S., LEE, B. H. & MIN, W. 2012. Chicken IL-17F: identification and comparative expression analysis in Eimeria-infected chickens. *Dev Comp Immunol,* 38**,** 401-9.
KIM, W. L., KIM, M. S. & KIM, K. H. 2011. Molecular cloning of rock bream's (Oplegnathus fasciatus) tumor necrosis factor receptor-associated factor 2 and its role in NF-kappaB activiation. *Fish Shellfish Immunol,* 30**,** 1178-83.
KIM, Y. M., BRINKMANN, M. M., PAQUET, M. E. & PLOEGH, H. L. 2008. UNC93B1 delivers nucleotide-sensing toll-like receptors to endolysosomes. *Nature,* 452**,** 234-8.
KING, C. G., KOBAYASHI, T., CEJAS, P. J., KIM, T., YOON, K., KIM, G. K., CHIFFOLEAU, E., HICKMAN, S. P., WALSH, P. T., TURKA, L. A. & CHOI, Y. 2006. TRAF6 is a T cell-intrinsic negative regulator required for the maintenance of immune homeostasis. *Nat Med,* 12**,** 1088-92.
KITAMURA, K., TAKAHIRA, K., INARI, M., SATOH, Y., HAYAKAWA, K., TABUCHI, Y., OGAI, K., NISHIUCHI, T., KONDO, T., MIKUNI-TAKAGAKI, Y., CHEN, W., HATTORI, A. & SUZUKI, N. 2013. Zebrafish scales respond differently to in vitro dynamic and static acceleration: analysis of interaction between osteoblasts and osteoclasts. *Comp Biochem Physiol A Mol Integr Physiol,* 166**,** 74-80.
KNOOP, K. A., KUMAR, N., BUTLER, B. R., SAKTHIVEL, S. K., TAYLOR, R. T., NOCHI, T., AKIBA, H., YAGITA, H., KIYONO, H. & WILLIAMS, I. R. 2009. RANKL is necessary and sufficient to initiate development of antigen-sampling M cells in the intestinal epithelium. *J Immunol,* 183**,** 5738-47.
KOBAYASHI, A., DONALDSON, D. S., ERRIDGE, C., KANAYA, T., WILLIAMS, I. R., OHNO, H., MAHAJAN, A. & MABBOTT, N. A. 2013. The functional maturation of M cells is dramatically reduced in the Peyer's patches of aged mice. *Mucosal Immunol,* 6**,** 1027-37.
KOBAYASHI, T., WALSH, P. T., WALSH, M. C., SPEIRS, K. M., CHIFFOLEAU, E., KING, C. G., HANCOCK, W. W., CAAMANO, J. H., HUNTER, C. A., SCOTT, P., TURKA, L. A. & CHOI, Y. 2003. TRAF6 is a critical factor for dendritic cell maturation and development. *Immunity,* 19**,** 353-63.
KOGA, T., INUI, M., INOUE, K., KIM, S., SUEMATSU, A., KOBAYASHI, E., IWATA, T., OHNISHI, H., MATOZAKI, T., KODAMA, T., TANIGUCHI, T., TAKAYANAGI, H. & TAKAI, T. 2004. Costimulatory signals mediated

by the ITAM motif cooperate with RANKL for bone homeostasis. *Nature,* 428**,** 758-63.
KOGUT, M. H., HE, H. & KAISER, P. 2005. Lipopolysaccharide binding protein/CD14/ TLR4-dependent recognition of salmonella LPS induces the functional activation of chicken heterophils and up-regulation of pro-inflammatory cytokine and chemokine gene expression in these cells. *Anim Biotechnol,* 16**,** 165-81.
KOGUT, M. H., IQBAL, M., HE, H., PHILBIN, V., KAISER, P. & SMITH, A. 2005. Expression and function of Toll-like receptors in chicken heterophils. *Dev Comp Immunol,* 29**,** 791-807.
KOGUT, M. H., MCGRUDER, E. D., HARGIS, B. M., CORRIER, D. E. & DELOACH, J. R. 1994. Dynamics of avian inflammatory response to Salmonella-immune lymphokines. Changes in avian blood leukocyte populations. *Inflammation,* 18**,** 373-88.
KOMAROVA, S. V., PILKINGTON, M. F., WEIDEMA, A. F., DIXON, S. J. & SIMS, S. M. 2003. RANK ligand-induced elevation of cytosolic Ca2+ accelerates nuclear translocation of nuclear factor kappa B in osteoclasts. *J Biol Chem,* 278**,** 8286-93.
KOMATSU, N., OKAMOTO, K., SAWA, S., NAKASHIMA, T., OH-HORA, M., KODAMA, T., TANAKA, S., BLUESTONE, J. A. & TAKAYANAGI, H. 2014. Pathogenic conversion of Foxp3+ T cells into TH17 cells in autoimmune arthritis. *Nat Med,* 20**,** 62-8.
KONG, Y. Y., YOSHIDA, H., SAROSI, I., TAN, H. L., TIMMS, E., CAPPARELLI, C., MORONY, S., OLIVEIRA-DOS-SANTOS, A. J., VAN, G., ITIE, A., KHOO, W., WAKEHAM, A., DUNSTAN, C. R., LACEY, D. L., MAK, T. W., BOYLE, W. J. & PENNINGER, J. M. 1999a. OPGL is a key regulator of osteoclastogenesis, lymphocyte development and lymph-node organogenesis. *Nature,* 397**,** 315-23.
KONG, Y. Y., FEIGE, U., SAROSI, I., BOLON, B., TAFURI, A., MORONY, S., CAPPARELLI, C., LI, J., ELLIOTT, R., MCCABE, S., WONG, T., CAMPAGNUOLO, G., MORAN, E., BOGOCH, E. R., VAN, G., NGUYEN, L. T., OHASHI, P. S., LACEY, D. L., FISH, E., BOYLE, W. J. & PENNINGER, J. M. 1999b. Activated T cells regulate bone loss and joint destruction in adjuvant arthritis through osteoprotegerin ligand. *Nature,* 402, 304-9. b
KOO, B. K. & CLEVERS, H. 2014. Stem cells marked by the R-spondin receptor Lgr5. *Gastroenterology,* 147, 289-302.
KOTHLOW, S., MORGENROTH, I., GRAEF, Y., SCHNEIDER, K., RIEHL, I., STAEHELI, P., SCHNEIDER, P. & KASPERS, B. 2007. Unique and conserved functions of B cell-activating factor of the TNF family (BAFF) in the chicken. *Int Immunol,* 19**,** 203-15.
KRAUS, Z. J., NAKANO, H. & BISHOP, G. A. 2009. TRAF5 is a critical mediator of in vitro signals and in vivo functions of LMP1, the viral oncogenic mimic of CD40. *Proc Natl Acad Sci U S A,* 106**,** 17140-5.
KRIEG, A. M. & VOLLMER, J. 2007. Toll-like receptors 7, 8, and 9: linking innate immunity to autoimmunity. *Immunol Rev,* 220**,** 251-69.
KUDSK, K. A. 2002. Current aspects of mucosal immunology and its influence by nutrition. *Am J Surg,* 183**,** 390-8.

KUMAR, S., CIRACI, C., REDMOND, S. B., CHUAMMITRI, P., ANDREASEN, C. B., PALIC, D. & LAMONT, S. J. 2011. Immune response gene expression in spleens of diverse chicken lines fed dietary immunomodulators. *Poult Sci,* 90**,** 1009-13.

KYEWSKI, B. & KLEIN, L. 2006. A central role for central tolerance. *Annu Rev Immunol,* 24**,** 571-606.

LACEY, D. L., BOYLE, W. J., SIMONET, W. S., KOSTENUIK, P. J., DOUGALL, W. C., SULLIVAN, J. K., SAN MARTIN, J. & DANSEY, R. 2012. Bench to bedside: elucidation of the OPG-RANK-RANKL pathway and the development of denosumab. *Nat Rev Drug Discov,* 11**,** 401-19.

LACEY, D. L., TIMMS, E., TAN, H. L., KELLEY, M. J., DUNSTAN, C. R., BURGESS, T., ELLIOTT, R., COLOMBERO, A., ELLIOTT, G., SCULLY, S., HSU, H., SULLIVAN, J., HAWKINS, N., DAVY, E., CAPPARELLI, C., ELI, A., QIAN, Y. X., KAUFMAN, S., SAROSI, I., SHALHOUB, V., SENALDI, G., GUO, J., DELANEY, J. & BOYLE, W. J. 1998. Osteoprotegerin ligand is a cytokine that regulates osteoclast differentiation and activation. *Cell,* 93**,** 165-76.

LAM, J., NELSON, C. A., ROSS, F. P., TEITELBAUM, S. L. & FREMONT, D. H. 2001. Crystal structure of the TRANCE/RANKL cytokine reveals determinants of receptor-ligand specificity. *J Clin Invest,* 108**,** 971-9.

LAMKANFI, M., FESTJENS, N., DECLERCQ, W., VANDEN BERGHE, T. & VANDENABEELE, P. 2007. Caspases in cell survival, proliferation and differentiation. *Cell Death Differ,* 14**,** 44-55.

LARSSON, K., LINDSTEDT, M., LUNDBERG, K., DEXLIN, L., WINGREN, C., KORSGREN, M., GREIFF, L. & BORREBAECK, C. A. 2009. CD4+ T cells have a key instructive role in educating dendritic cells in allergy. *Int Arch Allergy Immunol,* 149**,** 1-15.

LAUN, K., COGGILL, P., PALMER, S., SIMS, S., NING, Z., RAGOUSSIS, J., VOLPI, E., WILSON, N., BECK, S., ZIEGLER, A. & VOLZ, A. 2006. The leukocyte receptor complex in chicken is characterized by massive expansion and diversification of immunoglobulin-like Loci. *PLoS Genet,* 2**,** e73.

LAWTON, P., NELSON, J., TIZARD, R. & BROWNING, J. L. 1995. Characterization of the mouse lymphotoxin-beta gene. *J Immunol,* 154**,** 239-46.

LAYTON, S. L., KAPCZYNSKI, D. R., HIGGINS, S., HIGGINS, J., WOLFENDEN, A. D., LILJEBJELKE, K. A., BOTTJE, W. G., SWAYNE, D., BERGHMAN, L. R., KWON, Y. M., HARGIS, B. M. & COLE, K. 2009. Vaccination of chickens with recombinant Salmonella expressing M2e and CD154 epitopes increases protection and decreases viral shedding after low pathogenic avian influenza challenge. *Poult Sci,* 88**,** 2244-52.

LEE, B. L., MOON, J. E., SHU, J. H., YUAN, L., NEWMAN, Z. R., SCHEKMAN, R. & BARTON, G. M. 2013. UNC93B1 mediates differential trafficking of endosomal TLRs. *Elife,* 2**,** e00291.

LEE, M. Y., GARVEY, S. M., RIPLEY, M. L. & WAMHOFF, B. R. 2011. Genome-wide microarray analyses identify the protein C receptor as a novel calcineurin/nuclear factor of activated T cells-dependent gene in vascular smooth muscle cell phenotypic modulation. *Arterioscler Thromb Vasc Biol,* 31**,** 2665-75.

LEE, N. K. & LEE, S. Y. 2002. Modulation of life and death by the tumor necrosis factor receptor-associated factors (TRAFs). *J Biochem Mol Biol,* 35**,** 61-6.
LEE, S. C., JU, S. A., PACK, H. N., HEO, S. K., SUH, J. H., PARK, S. M., CHOI, B. K., KWON, B. S. & KIM, B. S. 2005. 4-1BB (CD137) is required for rapid clearance of Listeria monocytogenes infection. *Infect Immun,* 73**,** 5144-51.
LEE, S. Y., REICHLIN, A., SANTANA, A., SOKOL, K. A., NUSSENZWEIG, M. C. & CHOI, Y. 1997. TRAF2 is essential for JNK but not NF-kappaB activation and regulates lymphocyte proliferation and survival. *Immunity,* 7**,** 703-13.
LEIBUNDGUT-LANDMANN, S., GROSS, O., ROBINSON, M. J., OSORIO, F., SLACK, E. C., TSONI, S. V., SCHWEIGHOFFER, E., TYBULEWICZ, V., BROWN, G. D., RULAND, J. & REIS E SOUSA, C. 2007. Syk- and CARD9-dependent coupling of innate immunity to the induction of T helper cells that produce interleukin 17. *Nat Immunol,* 8**,** 630-8.
LEMAITRE, B., NICOLAS, E., MICHAUT, L., REICHHART, J. M. & HOFFMANN, J. A. 1996. The dorsoventral regulatory gene cassette spatzle/Toll/cactus controls the potent antifungal response in Drosophila adults. *Cell,* 86**,** 973-83.
LETUNIC, I., DOERKS, T. & BORK, P. 2012. SMART 7: recent updates to the protein domain annotation resource. *Nucleic Acids Res,* 40**,** D302-5.
LEUNG, S., LIU, X., FANG, L., CHEN, X., GUO, T. & ZHANG, J. 2010. The cytokine milieu in the interplay of pathogenic Th1/Th17 cells and regulatory T cells in autoimmune disease. *Cell Mol Immunol,* 7**,** 182-9.
LEVEQUE, G., FORGETTA, V., MORROLL, S., SMITH, A. L., BUMSTEAD, N., BARROW, P., LOREDO-OSTI, J. C., MORGAN, K. & MALO, D. 2003. Allelic variation in TLR4 is linked to susceptibility to Salmonella enterica serovar Typhimurium infection in chickens. *Infect Immun,* 71**,** 1116-24.
LI, J. Y., TAWFEEK, H., BEDI, B., YANG, X., ADAMS, J., GAO, K. Y., ZAYZAFOON, M., WEITZMANN, M. N. & PACIFICI, R. 2011. Ovariectomy disregulates osteoblast and osteoclast formation through the T-cell receptor CD40 ligand. *Proc Natl Acad Sci U S A,* 108**,** 768-73.
LI, K., GAO, H., GAO, L., QI, X., GAO, Y., QIN, L., WANG, Y. & WANG, X. 2013. Adjuvant effects of interleukin-18 in DNA vaccination against infectious bursal disease virus in chickens. *Vaccine,* 31**,** 1799-805.
LI, S., STRELOW, A., FONTANA, E. J. & WESCHE, H. 2002. IRAK-4: a novel member of the IRAK family with the properties of an IRAK-kinase. *Proc Natl Acad Sci U S A,* 99**,** 5567-72.
LI, X. D. & CHEN, Z. J. 2012. Sequence specific detection of bacterial 23S ribosomal RNA by TLR13. *Elife,* 1**,** e00102.
LI, Y. W., LI, X., XIAO, X. X., ZHAO, F., LUO, X. C., DAN, X. M. & LI, A. X. 2014. Molecular characterization and functional analysis of TRAF6 in orange-spotted grouper (Epinephelus coioides). *Dev Comp Immunol,* 44**,** 217-25.
LI, Z., KONG, K. & QI, W. 2006. Osteoclast and its roles in calcium metabolism and bone development and remodeling. *Biochem Biophys Res Commun,* 343**,** 345-50.
LIANG, J., FU, J., KANG, H., LIN, J., YU, Q. & YANG, Q. 2013. Comparison of 3

kinds of Toll-like receptor ligands for inactivated avian H5N1 influenza virus intranasal immunization in chicken. *Poult Sci,* 92**,** 2651-60.
LIANG, J., FU, J., KANG, H., LIN, J., YU, Q. & YANG, Q. 2013. The stimulatory effect of TLRs ligands on maturation of chicken bone marrow-derived dendritic cells. *Vet Immunol Immunopathol,* 155**,** 205-10.
LIANG, S. C., TAN, X. Y., LUXENBERG, D. P., KARIM, R., DUNUSSI-JOANNOPOULOS, K., COLLINS, M. & FOUSER, L. A. 2006. Interleukin (IL)-22 and IL-17 are coexpressed by Th17 cells and cooperatively enhance expression of antimicrobial peptides. *J Exp Med,* 203**,** 2271-9.
LIEBERSON, R., MOWEN, K. A., MCBRIDE, K. D., LEAUTAUD, V., ZHANG, X., SUH, W. K., WU, L. & GLIMCHER, L. H. 2001. Tumor necrosis factor receptor-associated factor (TRAF)2 represses the T helper cell type 2 response through interaction with NFAT-interacting protein (NIP45). *J Exp Med,* 194**,** 89-98.
LIEBERSON, R., MOWEN, K. A., MCBRIDE, K. D., LEAUTAUD, V., ZHANG, X., SUH, W. K., WU, L. & GLIMCHER, L. H. 2001. Tumor necrosis factor receptor-associated factor (TRAF)2 represses the T helper cell type 2 response through interaction with NFAT-interacting protein (NIP45). *J Exp Med,* 194**,** 89-98.
LIN, W. J., SU, Y. W., LU, Y. C., HAO, Z., CHIO, II, CHEN, N. J., BRUSTLE, A., LI, W. Y. & MAK, T. W. 2011. Crucial role for TNF receptor-associated factor 2 (TRAF2) in regulating NFkappaB2 signaling that contributes to autoimmunity. *Proc Natl Acad Sci U S A,* 108**,** 18354-9.
LIN, W. W., HILDEBRAND, J. M. & BISHOP, G. A. 2013. A Complex Relationship between TRAF3 and Non-Canonical NF-kappaB2 Activation in B Lymphocytes. *Front Immunol,* 4**,** 477.
LINIGER, M., SUMMERFIELD, A. & RUGGLI, N. 2012. MDA5 can be exploited as efficacious genetic adjuvant for DNA vaccination against lethal H5N1 influenza virus infection in chickens. *PLoS One,* 7**,** e49952.
LIU, D., RHEBERGEN, A. M. & EISENBARTH, S. C. 2013. Licensing adaptive immunity by NOD-like receptors. *Front Immunol,* 4**,** 486.
LOCKSLEY, R. M., KILLEEN, N. & LENARDO, M. J. 2001. The TNF and TNF receptor superfamilies: integrating mammalian biology. *Cell,* 104**,** 487-501.
LOMAGA, M. A., YEH, W. C., SAROSI, I., DUNCAN, G. S., FURLONGER, C., HO, A., MORONY, S., CAPPARELLI, C., VAN, G., KAUFMAN, S., VAN DER HEIDEN, A., ITIE, A., WAKEHAM, A., KHOO, W., SASAKI, T., CAO, Z., PENNINGER, J. M., PAIGE, C. J., LACEY, D. L., DUNSTAN, C. R., BOYLE, W. J., GOEDDEL, D. V. & MAK, T. W. 1999. TRAF6 deficiency results in osteopetrosis and defective interleukin-1, CD40, and LPS signaling. *Genes Dev,* 13**,** 1015-24.
LOO, Y. M., FORNEK, J., CROCHET, N., BAJWA, G., PERWITASARI, O., MARTINEZ-SOBRIDO, L., AKIRA, S., GILL, M. A., GARCIA-SASTRE, A., KATZE, M. G. & GALE, M., JR. 2008. Distinct RIG-I and MDA5 signaling by RNA viruses in innate immunity. *J Virol,* 82**,** 335-45.
LOPEZ-FRAGA, M., FERNANDEZ, R., ALBAR, J. P. & HAHNE, M. 2001. Biologically active APRIL is secreted following intracellular processing in the Golgi apparatus by furin convertase. *EMBO Rep,* 2**,** 945-51.
LUAN, X., LU, Q., JIANG, Y., ZHANG, S., WANG, Q., YUAN, H., ZHAO, W.,

WANG, J. & WANG, X. 2012. Crystal structure of human RANKL complexed with its decoy receptor osteoprotegerin. *J Immunol,* 189**,** 245-52.
LUM, L., WONG, B. R., JOSIEN, R., BECHERER, J. D., ERDJUMENT-BROMAGE, H., SCHLONDORFF, J., TEMPST, P., CHOI, Y. & BLOBEL, C. P. 1999. Evidence for a role of a tumor necrosis factor-alpha (TNF-alpha)-converting enzyme-like protease in shedding of TRANCE, a TNF family member involved in osteoclastogenesis and dendritic cell survival. *J Biol Chem,* 274**,** 13613-8.
MABBOTT, N. A., DONALDSON, D. S., OHNO, H., WILLIAMS, I. R. & MAHAJAN, A. 2013. Microfold (M) cells: important immunosurveillance posts in the intestinal epithelium. *Mucosal Immunol,* 6**,** 666-77.
MACARTNEY, K. K., BAUMGART, D. C., CARDING, S. R., BRUBAKER, J. O. & OFFIT, P. A. 2000. Primary murine small intestinal epithelial cells, maintained in long-term culture, are susceptible to rotavirus infection. *J Virol,* 74**,** 5597-603.
MACHIDA, M., DUBOUSSET, J., IMAMURA, Y., IWAYA, T., YAMADA, T. & KIMURA, J. 1993. An experimental study in chickens for the pathogenesis of idiopathic scoliosis. *Spine (Phila Pa 1976),* 18**,** 1609-15.
MAHDAVI, M., EBTEKAR, M., KHORRAM KHORSHID, H. R., AZADMANESH, K., HARTOONIAN, C. & HASSAN, Z. M. 2011. ELISPOT analysis of a new CTL based DNA vaccine for HIV-1 using GM-CSF in DNA prime/peptide boost strategy: GM-CSF induced long-lived memory responses. *Immunol Lett,* 140**,** 14-20.
MAIA, S., PELLETIER, M., DING, J., HSU, Y. M., SALLAN, S. E., RAO, S. P., NADLER, L. M. & CARDOSO, A. A. 2011. Aberrant expression of functional BAFF-system receptors by malignant B-cell precursors impacts leukemia cell survival. *PLoS One,* 6**,** e20787.
MALI, B. & FRANK, U. 2004. Hydroid TNF-receptor-associated factor (TRAF) and its splice variant: a role in development. *Mol Immunol,* 41**,** 377-84.
MANGINO, G., PERCARIO, Z. A., FIORUCCI, G., VACCARI, G., ACCONCIA, F., CHIARABELLI, C., LEONE, S., NOTO, A., HORENKAMP, F. A., MANRIQUE, S., ROMEO, G., POLTICELLI, F., GEYER, M. & AFFABRIS, E. 2011. HIV-1 Nef induces proinflammatory state in macrophages through its acidic cluster domain: involvement of TNF alpha receptor associated factor 2. *PLoS One,* 6**,** e22982.
MANTOVANI, A., SOZZANI, S., LOCATI, M., ALLAVENA, P. & SICA, A. 2002. Macrophage polarization: tumor-associated macrophages as a paradigm for polarized M2 mononuclear phagocytes. *Trends Immunol,* 23**,** 549-55.
MAO, D., EPPLE, H., UTHGENANNT, B., NOVACK, D. V. & FACCIO, R. 2006. PLCgamma2 regulates osteoclastogenesis via its interaction with ITAM proteins and GAB2. *J Clin Invest,* 116**,** 2869-79.
MARINIS, J. M., HOMER, C. R., MCDONALD, C. & ABBOTT, D. W. 2011. A novel motif in the Crohn's disease susceptibility protein, NOD2, allows TRAF4 to down-regulate innate immune responses. *J Biol Chem,* 286**,** 1938-50.
MARSTERS, S. A., AYRES, T. M., SKUBATCH, M., GRAY, C. L., ROTHE, M. & ASHKENAZI, A. 1997. Herpesvirus entry mediator, a member of the tumor necrosis factor receptor (TNFR) family, interacts with members of the TNFR-

associated factor family and activates the transcription factors NF-kappaB and AP-1. *J Biol Chem,* 272**,** 14029-32.
MARTIN-FONTECHA, A., THOMSEN, L. L., BRETT, S., GERARD, C., LIPP, M., LANZAVECCHIA, A. & SALLUSTO, F. 2004. Induced recruitment of NK cells to lymph nodes provides IFN-gamma for T(H)1 priming. *Nat Immunol,* 5**,** 1260-5.
MAST, J., GODDEERIS, B. M., PEETERS, K., VANDESANDE, F. & BERGHMAN, L. R. 1998. Characterisation of chicken monocytes, macrophages and interdigitating cells by the monoclonal antibody KUL01. *Vet Immunol Immunopathol,* 61**,** 343-57.
MASUDA, H., HIROSE, J., OMATA, Y., TOKUYAMA, N., YASUI, T., KADONO, Y., MIYAZAKI, T. & TANAKA, S. 2014. Anti-apoptotic Bcl-2 family member Mcl-1 regulates cell viability and bone-resorbing activity of osteoclasts. *Bone,* 58**,** 1-10.
MAURER, D., HOLTER, W., MAJDIC, O., FISCHER, G. F. & KNAPP, W. 1990. CD27 expression by a distinct subpopulation of human B lymphocytes. *Eur J Immunol,* 20**,** 2679-84.
MCCORMACK, W. T. & THOMPSON, C. B. 1990. Chicken IgL variable region gene conversions display pseudogene donor preference and 5' to 3' polarity. *Genes Dev,* 4**,** 548-58.
MCCORMACK, W. T., TJOELKER, L. W., CARLSON, L. M., PETRYNIAK, B., BARTH, C. F., HUMPHRIES, E. H. & THOMPSON, C. B. 1989. Chicken IgL gene rearrangement involves deletion of a circular episome and addition of single nonrandom nucleotides to both coding segments. *Cell,* 56**,** 785-91.
MCPHERSON, A. J., SNELL, L. M., MAK, T. W. & WATTS, T. H. 2012. Opposing roles for TRAF1 in the alternative versus classical NF-kappaB pathway in T cells. *J Biol Chem,* 287**,** 23010-9.
MICHELS, J., KEPP, O., SENOVILLA, L., LISSA, D., CASTEDO, M., KROEMER, G. & GALLUZZI, L. 2013. Functions of BCL-X L at the Interface between cell death and metabolism. *Int J Cell Biol***,** 705294.
MIN W, LILLEJOJ HS, BURNSIDE J, WEINING KC, STAEHELI P, ZHU JJ. Adjuvant effects of IL-1beta, IL-2, IL-8, IL-15, IFN-alpha, IFN-gamma TGF-beta4 and lymphotactin on DNA vaccination against Eimeria acervulina. *Vaccine,* 12;20(1-2):267-74.
MIN, W., KIM, W. H., LILLEHOJ, E. P. & LILLEHOJ, H. S. 2013. Recent progress in host immunity to avian coccidiosis: IL-17 family cytokines as sentinels of the intestinal mucosa. *Dev Comp Immunol,* 41**,** 418-28.
MIN, W. & LILLEHOJ, H. S. 2002. Isolation and characterization of chicken interleukin-17 cDNA. *J Interferon Cytokine Res,* 22**,** 1123-8.
MISSIOU, A., RUDOLF, P., STACHON, P., WOLF, D., VARO, N., AICHELE, P., COLBERG, C., HOPPE, N., ERNST, S., MUNKEL, C., WALTER, C., SOMMER, B., HILGENDORF, I., NAKANO, H., BODE, C. & ZIRLIK, A. 2010. TRAF5 deficiency accelerates atherogenesis in mice by increasing inflammatory cell recruitment and foam cell formation. *Circ Res,* 107**,** 757-66.
MIYAHIRA, Y., AKIBA, H., KATAE, M., KUBOTA, K., KOBAYASHI, S., TAKEUCHI, T., GARCIA-SASTRE, A., FUKUCHI, Y., OKUMURA, K., YAGITA, H. & AOKI, T. 2003. Cutting edge: a potent adjuvant effect of

ligand to receptor activator of NF-kappa B gene for inducing antigen-specific CD8+ T cell response by DNA and viral vector vaccination. *J Immunol,* 171**,** 6344-8.

MIYAMOTO, T. 2011. Regulators of osteoclast differentiation and cell-cell fusion. *Keio J Med,* 60**,** 101-5.

MIYAMOTO, T. & SUDA, T. 2003. Differentiation and function of osteoclasts. *Keio J Med,* 52**,** 1-7.

MOCHIZUKI, A., TAKAMI, M., KAWAWA, T., SUZUMOTO, R., SASAKI, T., SHIBA, A., TSUKASAKI, H., ZHAO, B., YASUHARA, R., SUZAWA, T., MIYAMOTO, Y., CHOI, Y. & KAMIJO, R. 2006. Identification and characterization of the precursors committed to osteoclasts induced by TNF-related activation-induced cytokine/receptor activator of NF-kappa B ligand. *J Immunol,* 177**,** 4360-8.

MONREAL, A. W., FERGUSON, B. M., HEADON, D. J., STREET, S. L., OVERBEEK, P. A. & ZONANA, J. 1999. Mutations in the human homologue of mouse dl cause autosomal recessive and dominant hypohidrotic ectodermal dysplasia. *Nat Genet,* 22**,** 366-9.

MORITA, Y., KANEI-ISHII, C., NOMURA, T. & ISHII, S. 2005. TRAF7 sequesters c-Myb to the cytoplasm by stimulating its sumoylation. *Mol Biol Cell,* 16**,** 5433-44.

MORRIS, A. E., REMMELE, R. L., JR., KLINKE, R., MACDUFF, B. M., FANSLOW, W. C. & ARMITAGE, R. J. 1999. Incorporation of an isoleucine zipper motif enhances the biological activity of soluble CD40L (CD154). *J Biol Chem,* 274**,** 418-23.

MOSHEIMER, B. A., KANEIDER, N. C., FEISTRITZER, C., STURN, D. H. & WIEDERMANN, C. J. 2004. Expression and function of RANK in human monocyte chemotaxis. *Arthritis Rheum,* 50**,** 2309-16.

MOSMANN, T. R. & COFFMAN, R. L. 1989. TH1 and TH2 cells: different patterns of lymphokine secretion lead to different functional properties. *Annu Rev Immunol,* 7**,** 145-73.

MOTEGI, H., SHIMO, Y., AKIYAMA, T. & INOUE, J. 2011. TRAF6 negatively regulates the Jak1-Erk pathway in interleukin-2 signaling. *Genes Cells,* 16**,** 179-89.

MUIR, J. M., ANDREW, M., HIRSH, J., WEITZ, J. I., YOUNG, E., DESCHAMPS, P. & SHAUGHNESSY, S. G. 1996. Histomorphometric analysis of the effects of standard heparin on trabecular bone in vivo. *Blood,* 88**,** 1314-20.

MUNZERT, G., KIRCHNER, D., STOBBE, H., BERGMANN, L., SCHMID, R. M., DOHNER, H. & HEIMPEL, H. 2002. Tumor necrosis factor receptor-associated factor 1 gene overexpression in B-cell chronic lymphocytic leukemia: analysis of NF-kappa B/Rel-regulated inhibitors of apoptosis. *Blood,* 100**,** 3749-56.

MURPHY, C. A., LANGRISH, C. L., CHEN, Y., BLUMENSCHEIN, W., MCCLANAHAN, T., KASTELEIN, R. A., SEDGWICK, J. D. & CUA, D. J. 2003. Divergent pro- and antiinflammatory roles for IL-23 and IL-12 in joint autoimmune inflammation. *J Exp Med,* 198**,** 1951-7.

MURPHY, K. M., MURPHY, T. L., SZABO, S. J., JACOBSON, N. G., GULER, M. L., GORHAM, J. D. & GUBLER, U. 1997. Regulation of IL-12 receptor expression in early T-helper responses implies two phases of Th1

differentiation: capacitance and development. *Chem Immunol,* 68**,** 54-69.
MURPHY, K. M. & REINER, S. L. 2002. The lineage decisions of helper T cells. *Nat Rev Immunol,* 2**,** 933-44.
MUTO, G., KOTANI, H., KONDO, T., MORITA, R., TSURUTA, S., KOBAYASHI, T., LUCHE, H., FEHLING, H. J., WALSH, M., CHOI, Y. & YOSHIMURA, A. 2013. TRAF6 is essential for maintenance of regulatory T cells that suppress Th2 type autoimmunity. *PLoS One,* 8**,** e74639.
MUZIO, M., BOSISIO, D., POLENTARUTTI, N., D'AMICO, G., STOPPACCIARO, A., MANCINELLI, R., VAN'T VEER, C., PENTON-ROL, G., RUCO, L. P., ALLAVENA, P. & MANTOVANI, A. 2000. Differential expression and regulation of toll-like receptors (TLR) in human leukocytes: selective expression of TLR3 in dendritic cells. *J Immunol,* 164**,** 5998-6004.
NAGASHIMA, H., OKUYAMA, Y., ASAO, A., KAWABE, T., YAMAKI, S., NAKANO, H., CROFT, M., ISHII, N. & SO, T. 2014. The adaptor TRAF5 limits the differentiation of inflammatory CD4(+) T cells by antagonizing signaling via the receptor for IL-6. *Nat Immunol,* 15**,** 449-56.
NAGATA, S. 1997. Apoptosis by death factor. *Cell,* 88**,** 355-65.
NAIR, V. 2005. Evolution of Marek's disease -- a paradigm for incessant race between the pathogen and the host. *Vet J,* 170**,** 175-83.
NAISMITH, J. H. & SPRANG, S. R. 1998. Modularity in the TNF-receptor family. *Trends Biochem Sci,* 23**,** 74-9.
NAITO, A., AZUMA, S., TANAKA, S., MIYAZAKI, T., TAKAKI, S., TAKATSU, K., NAKAO, K., NAKAMURA, K., KATSUKI, M., YAMAMOTO, T. & INOUE, J. 1999. Severe osteopetrosis, defective interleukin-1 signalling and lymph node organogenesis in TRAF6-deficient mice. *Genes Cells,* 4**,** 353-62.
NAKANO, H., SAKON, S., KOSEKI, H., TAKEMORI, T., TADA, K., MATSUMOTO, M., MUNECHIKA, E., SAKAI, T., SHIRASAWA, T., AKIBA, H., KOBATA, T., SANTEE, S. M., WARE, C. F., RENNERT, P. D., TANIGUCHI, M., YAGITA, H. & OKUMURA, K. 1999. Targeted disruption of Traf5 gene causes defects in CD40- and CD27-mediated lymphocyte activation. *Proc Natl Acad Sci U S A,* 96**,** 9803-8.
NAKASHIMA, T., KOBAYASHI, Y., YAMASAKI, S., KAWAKAMI, A., EGUCHI, K., SASAKI, H. & SAKAI, H. 2000. Protein expression and functional difference of membrane-bound and soluble receptor activator of NF-kappaB ligand: modulation of the expression by osteotropic factors and cytokines. *Biochem Biophys Res Commun,* 275**,** 768-75.
NAKAYAMA, M., KAYAGAKI, N., YAMAGUCHI, N., OKUMURA, K. & YAGITA, H. 2000. Involvement of TWEAK in interferon gamma-stimulated monocyte cytotoxicity. *J Exp Med,* 192**,** 1373-80.
NEEFJES, J., JONGSMA, M. L., PAUL, P. & BAKKE, O. 2011. Towards a systems understanding of MHC class I and MHC class II antigen presentation. *Nat Rev Immunol,* 11**,** 823-36.
NEIGHBORS, M., XU, X., BARRAT, F. J., RUULS, S. R., CHURAKOVA, T., DEBETS, R., BAZAN, J. F., KASTELEIN, R. A., ABRAMS, J. S. & O'GARRA, A. 2001. A critical role for interleukin 18 in primary and memory effector responses to Listeria monocytogenes that extends beyond its effects on Interferon gamma production. *J Exp Med,* 194**,** 343-54.

NELSON, C. A., WARREN, J. T., WANG, M. W., TEITELBAUM, S. L. & FREMONT, D. H. 2012. RANKL employs distinct binding modes to engage RANK and the osteoprotegerin decoy receptor. *Structure,* 20**,** 1971-82.
NERREN, J. R., SWAGGERTY, C. L., MACKINNON, K. M., GENOVESE, K. J., HE, H., PEVZNER, I. & KOGUT, M. H. 2009. Differential mRNA expression of the avian-specific toll-like receptor 15 between heterophils from Salmonella-susceptible and -resistant chickens. *Immunogenetics,* 61**,** 71-7.
NEUTRA, M. R., FREY, A. & KRAEHENBUHL, J. P. 1996. Epithelial M cells: gateways for mucosal infection and immunization. *Cell,* 86**,** 345-8.
NIKOLAEV, A., MCLAUGHLIN, T., O'LEARY, D. D. & TESSIER-LAVIGNE, M. 2009. APP binds DR6 to trigger axon pruning and neuron death via distinct caspases. *Nature,* 457**,** 981-9.
NITTA, T., MURATA, S., UENO, T., TANAKA, K. & TAKAHAMA, Y. 2008. Thymic microenvironments for T-cell repertoire formation. *Adv Immunol,* 99**,** 59-94.
NOVATCHKOVA, M., LEIBBRANDT, A., WERZOWA, J., NEUBUSER, A. & EISENHABER, F. 2003. The STIR-domain superfamily in signal transduction, development and immunity. *Trends Biochem Sci,* 28**,** 226-9.
NURIEVA, R. I., CHUNG, Y., HWANG, D., YANG, X. O., KANG, H. S., MA, L., WANG, Y. H., WATOWICH, S. S., JETTEN, A. M., TIAN, Q. & DONG, C. 2008. Generation of T follicular helper cells is mediated by interleukin-21 but independent of T helper 1, 2, or 17 cell lineages. *Immunity,* 29**,** 138-49.
O'BRIEN, C. A. 2010. Control of RANKL gene expression. *Bone,* 46**,** 911-9.
OETTINGER, M. A., SCHATZ, D. G., GORKA, C. & BALTIMORE, D. 1990. RAG-1 and RAG-2, adjacent genes that synergistically activate V(D)J recombination. *Science,* 248**,** 1517-23.
O'MEARA, K. M., KREMER, C. J., LAYTON, S. L., BERGHMAN, L. R., HARGIS, B. M. & COLE, K. 2010. Evaluation of recombinant Salmonella expressing CD154 for persistence and enhanced antibody response in commercial turkeys. *Poult Sci,* 89**,** 1399-405.
O'NEILL, L. A. & BOWIE, A. G. 2007. The family of five: TIR-domain-containing adaptors in Toll-like receptor signalling. *Nat Rev Immunol,* 7**,** 353-64.
OPPMANN, B., LESLEY, R., BLOM, B., TIMANS, J. C., XU, Y., HUNTE, B., VEGA, F., YU, N., WANG, J., SINGH, K., ZONIN, F., VAISBERG, E., CHURAKOVA, T., LIU, M., GORMAN, D., WAGNER, J., ZURAWSKI, S., LIU, Y., ABRAMS, J. S., MOORE, K. W., RENNICK, D., DE WAAL-MALEFYT, R., HANNUM, C., BAZAN, J. F. & KASTELEIN, R. A. 2000. Novel p19 protein engages IL-12p40 to form a cytokine, IL-23, with biological activities similar as well as distinct from IL-12. *Immunity,* 13**,** 715-25.
ORDWAY, D., HENAO-TAMAYO, M., ORME, I. M. & GONZALEZ-JUARRERO, M. 2005. Foamy macrophages within lung granulomas of mice infected with Mycobacterium tuberculosis express molecules characteristic of dendritic cells and antiapoptotic markers of the TNF receptor-associated factor family. *J Immunol,* 175**,** 3873-81.
OTA, T. & NEI, M. 1995. Evolution of immunoglobulin VH pseudogenes in chickens. *Mol Biol Evol,* 12**,** 94-102.

OUYANG, W., LOHNING, M., GAO, Z., ASSENMACHER, M., RANGANATH, S., RADBRUCH, A. & MURPHY, K. M. 2000. Stat6-independent GATA-3 autoactivation directs IL-4-independent Th2 development and commitment. *Immunity,* 12**,** 27-37.

OUYANG, W., RANGANATH, S. H., WEINDEL, K., BHATTACHARYA, D., MURPHY, T. L., SHA, W. C. & MURPHY, K. M. 1998. Inhibition of Th1 development mediated by GATA-3 through an IL-4-independent mechanism. *Immunity,* 9**,** 745-55.

OVEN, I., RESMAN RUS, K., DUSANIC, D., BENCINA, D., KEELER, C. L., JR. & NARAT, M. 2013. Diacylated lipopeptide from Mycoplasma synoviae mediates TLR15 induced innate immune responses. *Vet Res,* 44**,** 99.

OWEN, R. L. & JONES, A. L. 1974. Epithelial cell specialization within human Peyer's patches: an ultrastructural study of intestinal lymphoid follicles. *Gastroenterology,* 66**,** 189-203.

OZINSKY, A., UNDERHILL, D. M., FONTENOT, J. D., HAJJAR, A. M., SMITH, K. D., WILSON, C. B., SCHROEDER, L. & ADEREM, A. 2000. The repertoire for pattern recognition of pathogens by the innate immune system is defined by cooperation between toll-like receptors. *Proc Natl Acad Sci U S A,* 97**,** 13766-71.

PADIGEL, U. M., KIM, N., CHOI, Y. & FARRELL, J. P. 2003. TRANCE-RANK costimulation is required for IL-12 production and the initiation of a Th1-type response to Leishmania major infection in CD40L-deficient mice. *J Immunol,* 171**,** 5437-41.

PARK, H. J., PARK, O. J. & SHIN, J. 2005. Receptor activator of NF-kappaB ligand enhances the activity of macrophages as antigen presenting cells. *Exp Mol Med,* 37**,** 524-32.

PARK, Y. C., BURKITT, V., VILLA, A. R., TONG, L. & WU, H. 1999. Structural basis for self-association and receptor recognition of human TRAF2. *Nature,* 398**,** 533-8.

PASPARAKIS, M., ALEXOPOULOU, L., EPISKOPOU, V. & KOLLIAS, G. 1996. Immune and inflammatory responses in TNF alpha-deficient mice: a critical requirement for TNF alpha in the formation of primary B cell follicles, follicular dendritic cell networks and germinal centers, and in the maturation of the humoral immune response. *J Exp Med,* 184**,** 1397-411.

PAZ, S., VILASCO, M., WERDEN, S. J., ARGUELLO, M., JOSEPH-PILLAI, D., ZHAO, T., NGUYEN, T. L., SUN, Q., MEURS, E. F., LIN, R. & HISCOTT, J. 2011. A functional C-terminal TRAF3-binding site in MAVS participates in positive and negative regulation of the IFN antiviral response. *Cell Res,* 21**,** 895-910.

PEIRIS, J. S., DE JONG, M. D. & GUAN, Y. 2007. Avian influenza virus (H5N1): a threat to human health. *Clin Microbiol Rev,* 20**,** 243-67.

PERA, M. F., BENNETT, W. & CERRETTI, D. P. 1998. CD30 and its ligand: possible role in regulation of teratoma stem cells. *APMIS,* 106**,** 169-72; discussion 173.

PERLOT, T. & PENNINGER, J. M. 2012. Development and function of murine B cells lacking RANK. *J Immunol,* 188**,** 1201-5.

PHILBIN, V. J., IQBAL, M., BOYD, Y., GOODCHILD, M. J., BEAL, R. K., BUMSTEAD, N., YOUNG, J. & SMITH, A. L. 2005. Identification and

characterization of a functional, alternatively spliced Toll-like receptor 7 (TLR7) and genomic disruption of TLR8 in chickens. *Immunology,* 114**,** 507-21.

PIAO, J. H., HASEGAWA, M., HEISSIG, B., HATTORI, K., TAKEDA, K., IWAKURA, Y., OKUMURA, K., INOHARA, N. & NAKANO, H. 2011. Tumor necrosis factor receptor-associated factor (TRAF) 2 controls homeostasis of the colon to prevent spontaneous development of murine inflammatory bowel disease. *J Biol Chem,* 286**,** 17879-88.

PIEPER, J., METHNER, U. & BERNDT, A. 2011. Characterization of avian gammadelta T-cell subsets after Salmonella enterica serovar Typhimurium infection of chicks. *Infect Immun,* 79**,** 822-9.

PINTO, L. H., HOLSINGER, L. J. & LAMB, R. A. 1992. Influenza virus M2 protein has ion channel activity. *Cell,* 69**,** 517-28.

PIPPIG, D. A., HELLMUTH, J. C., CUI, S., KIRCHHOFER, A., LAMMENS, K., LAMMENS, A., SCHMIDT, A., ROTHENFUSSER, S. & HOPFNER, K. P. 2009. The regulatory domain of the RIG-I family ATPase LGP2 senses double-stranded RNA. *Nucleic Acids Res,* 37**,** 2014-25.

PONTING, C. P., SCHULTZ, J., MILPETZ, F. & BORK, P. 1999. SMART: identification and annotation of domains from signalling and extracellular protein sequences. *Nucleic Acids Res,* 27**,** 229-32.

POWELL, F. L., ROTHWELL, L., CLARKSON, M. J. & KAISER, P. 2009. The turkey, compared to the chicken, fails to mount an effective early immune response to Histomonas meleagridis in the gut. *Parasite Immunol,* 31**,** 312-27.

POWLESLAND, A. S., WARD, E. M., SADHU, S. K., GUO, Y., TAYLOR, M. E. & DRICKAMER, K. 2006. Widely divergent biochemical properties of the complete set of mouse DC-SIGN-related proteins. *J Biol Chem,* 281**,** 20440-9.

PRADET-BALADE, B., MEDEMA, J. P., LOPEZ-FRAGA, M., LOZANO, J. C., KOLFSCHOTEN, G. M., PICARD, A., MARTINEZ, A. C., GARCIA-SANZ, J. A. & HAHNE, M. 2002. An endogenous hybrid mRNA encodes TWE-PRIL, a functional cell surface TWEAK-APRIL fusion protein. *EMBO J,* 21**,** 5711-20.

PRISBY, R., MENEZES, T., CAMPBELL, J., BENSON, T., SAMRAJ, E., PEVZNER, I. & WIDEMAN, R. F., JR. 2014. Kinetic examination of femoral bone modeling in broilers. *Poult Sci,* 93**,** 1122-9.

PROIETTO, A. I., O'KEEFFE, M., GARTLAN, K., WRIGHT, M. D., SHORTMAN, K., WU, L. & LAHOUD, M. H. 2004. Differential production of inflammatory chemokines by murine dendritic cell subsets. *Immunobiology,* 209**,** 163-72.

PUGH, C. W., MACPHERSON, G. G. & STEER, H. W. 1983. Characterization of nonlymphoid cells derived from rat peripheral lymph. *J Exp Med,* 157**,** 1758-79.

PULENDRAN, B., TANG, H. & MANICASSAMY, S. 2010. Programming dendritic cells to induce T(H)2 and tolerogenic responses. *Nat Immunol,* 11**,** 647-55.

PULLEN, S. S., MILLER, H. G., EVERDEEN, D. S., DANG, T. T., CRUTE, J. J. & KEHRY, M. R. 1998. CD40-tumor necrosis factor receptor-associated factor

(TRAF) interactions: regulation of CD40 signaling through multiple TRAF binding sites and TRAF hetero-oligomerization. *Biochemistry,* 37**,** 11836-45.
QIU, L., SONG, L., YU, Y., ZHAO, J., WANG, L. & ZHANG, Q. 2009. Identification and expression of TRAF6 (TNF receptor-associated factor 6) gene in Zhikong scallop Chlamys farreri. *Fish Shellfish Immunol,* 26**,** 359-67.
QUERE, P., PIERRE, J., HOANG, M. D., ESNAULT, E., DOMENECH, J., SIBILLE, P. & DIMIER-POISSON, I. 2013. Presence of dendritic cells in chicken spleen cell preparations and their functional interaction with the parasite Toxoplasma gondii. *Vet Immunol Immunopathol,* 153**,** 57-69.
RAHMAN, M. M., BHATTACHARYA, A., BANU, J., KANG, J. X. & FERNANDES, G. 2009. Endogenous n-3 fatty acids protect ovariectomy induced bone loss by attenuating osteoclastogenesis. *J Cell Mol Med,* 13**,** 1833-44.
RAJPUT, M. K., DARWEESH, M. F., PARK, K., BRAUN, L. J., MWANGI, W., YOUNG, A. J. & CHASE, C. C. 2014. The effect of bovine viral diarrhea virus (BVDV) strains on bovine monocyte-derived dendritic cells (Mo-DC) phenotype and capacity to produce BVDV. *Virol J,* 11**,** 44.
RAMASAMY, K. T., REDDY, M. R., VERMA, P. C. & MURUGESAN, S. 2012. Expression analysis of turkey (Meleagris gallopavo) toll-like receptors and molecular characterization of avian specific TLR15. *Mol Biol Rep,* 39**,** 8539-49.
RAO, A., LUO, C. & HOGAN, P. G. 1997. Transcription factors of the NFAT family: regulation and function. *Annu Rev Immunol,* 15**,** 707-47.
RATCLIFFE, M. J. 2006. Antibodies, immunoglobulin genes and the bursa of Fabricius in chicken B cell development. *Dev Comp Immunol,* 30**,** 101-18.
REDDY, S. K., HU, T., GUDIVADA, R., STAINES, K. A., WRIGHT, K. E., VICKERSTAFF, L., KOTHLOW, S., HUNT, L. G., BUTTER, C., KASPERS, B. & YOUNG, J. R. 2008. The BAFF-interacting receptors of chickens. *Dev Comp Immunol,* 32**,** 1076-87.
REGNIER, C. H., MASSON, R., KEDINGER, V., TEXTORIS, J., STOLL, I., CHENARD, M. P., DIERICH, A., TOMASETTO, C. & RIO, M. C. 2002. Impaired neural tube closure, axial skeleton malformations, and tracheal ring disruption in TRAF4-deficient mice. *Proc Natl Acad Sci U S A,* 99**,** 5585-90.
REGNIER, C. H., TOMASETTO, C., MOOG-LUTZ, C., CHENARD, M. P., WENDLING, C., BASSET, P. & RIO, M. C. 1995. Presence of a new conserved domain in CART1, a novel member of the tumor necrosis factor receptor-associated protein family, which is expressed in breast carcinoma. *J Biol Chem,* 270**,** 25715-21.
REUSS, D. E., PIRO, R. M., JONES, D. T., SIMON, M., KETTER, R., KOOL, M., BECKER, A., SAHM, F., PUSCH, S., MEYER, J., HAGENLOCHER, C., SCHWEIZER, L., CAPPER, D., KICKINGEREDER, P., MUCHA, J., KOELSCHE, C., JAGER, N., SANTARIUS, T., TARPEY, P. S., STEPHENS, P. J., ANDREW FUTREAL, P., WELLENREUTHER, R., KRAUS, J., LENARTZ, D., HEROLD-MENDE, C., HARTMANN, C., MAWRIN, C., GIESE, N., EILS, R., COLLINS, V. P., KONIG, R., WIESTLER, O. D., PFISTER, S. M. & VON DEIMLING, A. 2013. Secretory meningiomas are defined by combined KLF4 K409Q and TRAF7 mutations. *Acta Neuropathol,* 125**,** 351-8.

REYNAUD, C. A., ANQUEZ, V., GRIMAL, H. & WEILL, J. C. 1987. A hyperconversion mechanism generates the chicken light chain preimmune repertoire. *Cell,* 48**,** 379-88.

REYNAUD, C. A., ANQUEZ, V. & WEILL, J. C. 1991. The chicken D locus and its contribution to the immunoglobulin heavy chain repertoire. *Eur J Immunol,* 21**,** 2661-70.

RIEGEL, A., MAURER, T., PRIOR, B., STEGMAIER, S., HEPPERT, V., WAGNER, C. & HANSCH, G. M. 2012. Human polymorphonuclear neutrophils express RANK and are activated by its ligand, RANKL. *Eur J Immunol,* 42**,** 975-81.

ROACH, J. C., GLUSMAN, G., ROWEN, L., KAUR, A., PURCELL, M. K., SMITH, K. D., HOOD, L. E. & ADEREM, A. 2005. The evolution of vertebrate Toll-like receptors. *Proc Natl Acad Sci U S A,* 102**,** 9577-82.

ROBINSON, D., SHIBUYA, K., MUI, A., ZONIN, F., MURPHY, E., SANA, T., HARTLEY, S. B., MENON, S., KASTELEIN, R., BAZAN, F. & O'GARRA, A. 1997. IGIF does not drive Th1 development but synergizes with IL-12 for interferon-gamma production and activates IRAK and NF-kappaB. *Immunity,* 7**,** 571-81.

ROJAS-CARTAGENA, C., FLORES, I. & APPLEYARD, C. B. 2005. Role of tumor necrosis factor receptors in an animal model of acute colitis. *Cytokine,* 32**,** 85-93.

ROSSI, S. W., KIM, M. Y., LEIBBRANDT, A., PARNELL, S. M., JENKINSON, W. E., GLANVILLE, S. H., MCCONNELL, F. M., SCOTT, H. S., PENNINGER, J. M., JENKINSON, E. J., LANE, P. J. & ANDERSON, G. 2007. RANK signals from CD4(+)3(-) inducer cells regulate development of Aire-expressing epithelial cells in the thymic medulla. *J Exp Med,* 204**,** 1267-72.

ROTHE, M., PAN, M. G., HENZEL, W. J., AYRES, T. M. & GOEDDEL, D. V. 1995. The TNFR2-TRAF signaling complex contains two novel proteins related to baculoviral inhibitor of apoptosis proteins. *Cell,* 83**,** 1243-52.

ROTHENFUSSER, S., GOUTAGNY, N., DIPERNA, G., GONG, M., MONKS, B. G., SCHOENEMEYER, A., YAMAMOTO, M., AKIRA, S. & FITZGERALD, K. A. 2005. The RNA helicase Lgp2 inhibits TLR-independent sensing of viral replication by retinoic acid-inducible gene-I. *J Immunol,* 175**,** 5260-8.

ROTHWELL, L., HU, T., WU, Z. & KAISER, P. 2012. Chicken interleukin-21 is costimulatory for T cells and blocks maturation of dendritic cells. *Dev Comp Immunol,* 36**,** 475-82.

ROTHWELL, L., YOUNG, J. R., ZOOROB, R., WHITTAKER, C. A., HESKETH, P., ARCHER, A., SMITH, A. L. & KAISER, P. 2004. Cloning and characterization of chicken IL-10 and its role in the immune response to Eimeria maxima. *J Immunol,* 173**,** 2675-82.

ROWLAND, S. L., TREMBLAY, M. M., ELLISON, J. M., STUNZ, L. L., BISHOP, G. A. & HOSTAGER, B. S. 2007. A novel mechanism for TNFR-associated factor 6-dependent CD40 signaling. *J Immunol,* 179**,** 4645-53.

RUBIN, C., XU, G. & JUDEX, S. 2001. The anabolic activity of bone tissue, suppressed by disuse, is normalized by brief exposure to extremely low-magnitude mechanical stimuli. *FASEB J,* 15**,** 2225-9.

RUDDLE, N. H. & AKIRAV, E. M. 2009. Secondary lymphoid organs: responding to genetic and environmental cues in ontogeny and the immune response. *J Immunol,* 183**,** 2205-12.
SACHS, N. & CLEVERS, H. 2014. Organoid cultures for the analysis of cancer phenotypes. *Curr Opin Genet Dev,* 24**,** 68-73.
SAKAGUCHI, S., YAMAGUCHI, T., NOMURA, T. & ONO, M. 2008. Regulatory T cells and immune tolerance. *Cell,* 133**,** 775-87.
SALLUSTO, F., CELLA, M., DANIELI, C. & LANZAVECCHIA, A. 1995. Dendritic cells use macropinocytosis and the mannose receptor to concentrate macromolecules in the major histocompatibility complex class II compartment: downregulation by cytokines and bacterial products. *J Exp Med,* 182**,** 389-400.
SALLUSTO, F. & LANZAVECCHIA, A. 1994. Efficient presentation of soluble antigen by cultured human dendritic cells is maintained by granulocyte/macrophage colony-stimulating factor plus interleukin 4 and downregulated by tumor necrosis factor alpha. *J Exp Med,* 179**,** 1109-18.
SAMELSON, L. E. 2002. Signal transduction mediated by the T cell antigen receptor: the role of adapter proteins. *Annu Rev Immunol,* 20**,** 371-94.
SAMUEL, C. E. 2001. Antiviral actions of interferons. *Clin Microbiol Rev,* 14**,** 778-809.
SANUKI, R., MITSUI, N., SUZUKI, N., KOYAMA, Y., YAMAGUCHI, A., ISOKAWA, K., SHIMIZU, N. & MAENO, M. 2007. Effect of compressive force on the production of prostaglandin E(2) and its receptors in osteoblastic Saos-2 cells. *Connect Tissue Res,* 48**,** 246-53.
SATO, K. & TAKAYANAGI, H. 2006. Osteoclasts, rheumatoid arthritis, and osteoimmunology. *Curr Opin Rheumatol,* 18**,** 419-26.
SATO, T., STANGE, D. E., FERRANTE, M., VRIES, R. G., VAN ES, J. H., VAN DEN BRINK, S., VAN HOUDT, W. J., PRONK, A., VAN GORP, J., SIERSEMA, P. D. & CLEVERS, H. 2011. Long-term expansion of epithelial organoids from human colon, adenoma, adenocarcinoma, and Barrett's epithelium. *Gastroenterology,* 141**,** 1762-72.
SATO, T., VRIES, R. G., SNIPPERT, H. J., VAN DE WETERING, M., BARKER, N., STANGE, D. E., VAN ES, J. H., ABO, A., KUJALA, P., PETERS, P. J. & CLEVERS, H. 2009. Single Lgr5 stem cells build crypt-villus structures in vitro without a mesenchymal niche. *Nature,* 459**,** 262-5.
SCHIANO DE COLELLA, J. M., BARBARAT, B., SWEET, R., GASTAUT, J. A., OLIVE, D. & COSTELLO, R. T. 2008. Rank ligand stimulation induces a partial but functional maturation of human monocyte-derived dendritic cells. *Eur Cytokine Netw,* 19**,** 81-8.
SCHIJNS, V. E., WEINING, K. C., NUIJTEN, P., RIJKE, E. O. & STAEHELI, P. 2000. Immunoadjuvant activities of E. coli- and plasmid-expressed recombinant chicken IFN-alpha/beta, IFN-gamma and IL-1beta in 1-day- and 3-week-old chickens. *Vaccine,* 18**,** 2147-54.
SCHNEEWEIS, L. A., WILLARD, D. & MILLA, M. E. 2005. Functional dissection of osteoprotegerin and its interaction with receptor activator of NF-kappaB ligand. *J Biol Chem,* 280**,** 41155-64.
SCHNEIDER, K., KOTHLOW, S., SCHNEIDER, P., TARDIVEL, A., GOBEL, T., KASPERS, B. & STAEHELI, P. 2004. Chicken BAFF--a highly conserved

cytokine that mediates B cell survival. *Int Immunol,* 16**,** 139-48.
SCHNEIDER, P. 2005. The role of APRIL and BAFF in lymphocyte activation. *Curr Opin Immunol,* 17**,** 282-9.
SCHOPPET, M., HENSER, S., RUPPERT, V., STUBIG, T., AL-FAKHRI, N., MAISCH, B. & HOFBAUER, L. C. 2007. Osteoprotegerin expression in dendritic cells increases with maturation and is NF-kappaB-dependent. *J Cell Biochem,* 100**,** 1430-9.
SCHWANDNER, R., YAMAGUCHI, K. & CAO, Z. 2000. Requirement of tumor necrosis factor receptor-associated factor (TRAF)6 in interleukin 17 signal transduction. *J Exp Med,* 191**,** 1233-40.
SCHWANK, G., KOO, B. K., SASSELLI, V., DEKKERS, J. F., HEO, I., DEMIRCAN, T., SASAKI, N., BOYMANS, S., CUPPEN, E., VAN DER ENT, C. K., NIEUWENHUIS, E. E., BEEKMAN, J. M. & CLEVERS, H. 2013. Functional repair of CFTR by CRISPR/Cas9 in intestinal stem cell organoids of cystic fibrosis patients. *Cell Stem Cell,* 13**,** 653-8.
SCUDIERO, I., ZOTTI, T., FERRAVANTE, A., VESSICHELLI, M., REALE, C., MASONE, M. C., LEONARDI, A., VITO, P. & STILO, R. 2012. Tumor necrosis factor (TNF) receptor-associated factor 7 is required for TNFalpha-induced Jun NH2-terminal kinase activation and promotes cell death by regulating polyubiquitination and lysosomal degradation of c-FLIP protein. *J Biol Chem,* 287**,** 6053-61.
SEN, R. & BALTIMORE, D. 1986. Inducibility of kappa immunoglobulin enhancer-binding protein Nf-kappa B by a posttranslational mechanism. *Cell,* 47**,** 921-8.
SERFLING, E., BERBERICH-SIEBELT, F., CHUVPILO, S., JANKEVICS, E., KLEIN-HESSLING, S., TWARDZIK, T. & AVOTS, A. 2000. The role of NF-AT transcription factors in T cell activation and differentiation. *Biochim Biophys Acta,* 1498**,** 1-18.
SESHASAYEE, D., WANG, H., LEE, W. P., GRIBLING, P., ROSS, J., VAN BRUGGEN, N., CARANO, R. & GREWAL, I. S. 2004. A novel in vivo role for osteoprotegerin ligand in activation of monocyte effector function and inflammatory response. *J Biol Chem,* 279, 30202-9.
SESSLER, T., HEALY, S., SAMALI, A. & SZEGEZDI, E. 2013. Structural determinants of DISC function: new insights into death receptor-mediated apoptosis signalling. *Pharmacol Ther,* 140**,** 186-99.
SETA, N., OKAZAKI, Y. & KUWANA, M. 2008. Human circulating monocytes can express receptor activator of nuclear factor-kappaB ligand and differentiate into functional osteoclasts without exogenous stimulation. *Immunol Cell Biol,* 86**,** 453-9.
SHANMUGASUNDARAM, R. & SELVARAJ, R. K. 2011. Regulatory T cell properties of chicken CD4+CD25+ cells. *J Immunol,* 186**,** 1997-2002.
SHARPE, A. H. & FREEMAN, G. J. 2002. The B7-CD28 superfamily. *Nat Rev Immunol,* 2**,** 116-26.
SHAUGHNESSY, R. G., MEADE, K. G., CAHALANE, S., ALLAN, B., REIMAN, C., CALLANAN, J. J. & O'FARRELLY, C. 2009. Innate immune gene expression differentiates the early avian intestinal response between Salmonella and Campylobacter. *Vet Immunol Immunopathol,* 132**,** 191-8.
SHEVACH, E. M. 2009. Mechanisms of foxp3+ T regulatory cell-mediated

suppression. *Immunity,* 30**,** 636-45.
SHIELS, H., LI, X., SCHUMACKER, P. T., MALTEPE, E., PADRID, P. A., SPERLING, A., THOMPSON, C. B. & LINDSTEN, T. 2000. TRAF4 deficiency leads to tracheal malformation with resulting alterations in air flow to the lungs. *Am J Pathol,* 157**,** 679-88.
SILVERMAN, N. & MANIATIS, T. 2001. NF-kappaB signaling pathways in mammalian and insect innate immunity. *Genes Dev,* 15**,** 2321-42.
SIMONET, W. S., LACEY, D. L., DUNSTAN, C. R., KELLEY, M., CHANG, M. S., LUTHY, R., NGUYEN, H. Q., WOODEN, S., BENNETT, L., BOONE, T., SHIMAMOTO, G., DEROSE, M., ELLIOTT, R., COLOMBERO, A., TAN, H. L., TRAIL, G., SULLIVAN, J., DAVY, E., BUCAY, N., RENSHAW-GEGG, L., HUGHES, T. M., HILL, D., PATTISON, W., CAMPBELL, P., SANDER, S., VAN, G., TARPLEY, J., DERBY, P., LEE, R. & BOYLE, W. J. 1997. Osteoprotegerin: a novel secreted protein involved in the regulation of bone density. *Cell,* 89**,** 309-19.
SMITH, C. A., FARRAH, T. & GOODWIN, R. G. 1994. The TNF receptor superfamily of cellular and viral proteins: activation, costimulation, and death. *Cell,* 76**,** 959-62.
SO, T., SALEK-ARDAKANI, S., NAKANO, H., WARE, C. F. & CROFT, M. 2004. TNF receptor-associated factor 5 limits the induction of Th2 immune responses. *J Immunol,* 172**,** 4292-7.
SOBACCHI, C., FRATTINI, A., GUERRINI, M. M., ABINUN, M., PANGRAZIO, A., SUSANI, L., BREDIUS, R., MANCINI, G., CANT, A., BISHOP, N., GRABOWSKI, P., DEL FATTORE, A., MESSINA, C., ERRIGO, G., COXON, F. P., SCOTT, D. I., TETI, A., ROGERS, M. J., VEZZONI, P., VILLA, A. & HELFRICH, M. H. 2007. Osteoclast-poor human osteopetrosis due to mutations in the gene encoding RANKL. *Nat Genet,* 39**,** 960-2.
STAINES, K., YOUNG, J. R. & BUTTER, C. 2013. Expression of chicken DEC205 reflects the unique structure and function of the avian immune system. *PLoS One,* 8**,** e51799.
STEINMAN, R. M. 1991. The dendritic cell system and its role in immunogenicity. *Annu Rev Immunol,* 9**,** 271-96.
STIRNIMANN, C. U., PETSALAKI, E., RUSSELL, R. B. & MULLER, C. W. 2010. WD40 proteins propel cellular networks. *Trends Biochem Sci,* 35**,** 565-74.
STRAUB, C., NEULEN, M. L., SPERLING, B., WINDAU, K., ZECHMANN, M., JANSEN, C. A., VIERTLBOECK, B. C. & GOBEL, T. W. 2013. Chicken NK cell receptors. *Dev Comp Immunol,* 41**,** 324-33.
SUN, D., NOVOTNY, M., BULEK, K., LIU, C., LI, X. & HAMILTON, T. 2011. Treatment with IL-17 prolongs the half-life of chemokine CXCL1 mRNA via the adaptor TRAF5 and the splicing-regulatory factor SF2 (ASF). *Nat Immunol,* 12**,** 853-60.
SUN, Y., DING, N., DING, S. S., YU, S., MENG, C., CHEN, H., QIU, X., ZHANG, S., YU, Y., ZHAN, Y. & DING, C. 2013. Goose RIG-I functions in innate immunity against Newcastle disease virus infections. *Mol Immunol,* 53**,** 321-7.
SUTHERLAND, K. A., ROGERS, H. L., TOSH, D. & ROGERS, M. J. 2009. RANKL increases the level of Mcl-1 in osteoclasts and reduces

bisphosphonate-induced osteoclast apoptosis in vitro. *Arthritis Res Ther,* 11**,** R58.

SZABO, S. J., SULLIVAN, B. M., STEMMANN, C., SATOSKAR, A. R., SLECKMAN, B. P. & GLIMCHER, L. H. 2002. Distinct effects of T-bet in TH1 lineage commitment and IFN-gamma production in CD4 and CD8 T cells. *Science,* 295**,** 338-42.

SZEGEZDI, E., FITZGERALD, U. & SAMALI, A. 2003. Caspase-12 and ER-stress-mediated apoptosis: the story so far. *Ann N Y Acad Sci,* 1010**,** 186-94.

TAGUCHI, Y., GOHDA, J., KOGA, T., TAKAYANAGI, H. & INOUE, J. 2009. A unique domain in RANK is required for Gab2 and PLCgamma2 binding to establish osteoclastogenic signals. *Genes Cells,* 14**,** 1331-45.

TAHOUN, A., MAHAJAN, S., PAXTON, E., MALTERER, G., DONALDSON, D. S., WANG, D., TAN, A., GILLESPIE, T. L., O'SHEA, M., ROE, A. J., SHAW, D. J., GALLY, D. L., LENGELING, A., MABBOTT, N. A., HAAS, J. & MAHAJAN, A. 2012. Salmonella transforms follicle-associated epithelial cells into M cells to promote intestinal invasion. *Cell Host Microbe,* 12**,** 645-56.

TAKAESU, G., KISHIDA, S., HIYAMA, A., YAMAGUCHI, K., SHIBUYA, H., IRIE, K., NINOMIYA-TSUJI, J. & MATSUMOTO, K. 2000. TAB2, a novel adaptor protein, mediates activation of TAK1 MAPKKK by linking TAK1 to TRAF6 in the IL-1 signal transduction pathway. *Mol Cell,* 5**,** 649-58.

TAKAYANAGI, H. 2007. [Osteoclast differentiation and activation]. *Clin Calcium,* 17**,** 484-92.

TAKAYANAGI, H., KIM, S., KOGA, T., NISHINA, H., ISSHIKI, M., YOSHIDA, H., SAIURA, A., ISOBE, M., YOKOCHI, T., INOUE, J., WAGNER, E. F., MAK, T. W., KODAMA, T. & TANIGUCHI, T. 2002. Induction and activation of the transcription factor NFATc1 (NFAT2) integrate RANKL signalling in terminal differentiation of osteoclasts. *Dev Cell,* 3**,** 889-901.

TAKESHITA, F., ISHII, K. J., KOBIYAMA, K., KOJIMA, Y., COBAN, C., SASAKI, S., ISHII, N., KLINMAN, D. M., OKUDA, K., AKIRA, S. & SUZUKI, K. 2005. TRAF4 acts as a silencer in TLR-mediated signalling through the association with TRAF6 and TRIF. *Eur J Immunol,* 35**,** 2477-85.

TAKEUCHI, M., ROTHE, M. & GOEDDEL, D. V. 1996. Anatomy of TRAF2. Distinct domains for nuclear factor-kappaB activation and association with tumor necrosis factor signaling proteins. *J Biol Chem,* 271**,** 19935-42.

TAKIMOTO, T., TAKAHASHI, K., SATO, K. & AKIBA, Y. 2005. Molecular cloning and functional characterizations of chicken TL1A. *Dev Comp Immunol,* 29**,** 895-905.

TAMADA, K., NI, J., ZHU, G., FISCELLA, M., TENG, B., VAN DEURSEN, J. M. & CHEN, L. 2002. Cutting edge: selective impairment of CD8+ T cell function in mice lacking the TNF superfamily member LIGHT. *J Immunol,* 168**,** 4832-5.

TARLTON, J. F., WILKINS, L. J., TOSCANO, M. J., AVERY, N. C. & KNOTT, L. 2013. Reduced bone breakage and increased bone strength in free range laying hens fed omega-3 polyunsaturated fatty acid supplemented diets. *Bone,* 52**,** 578-86.

TERHEYDEN, H., STADLINGER, B., SANZ, M., GARBE, A. I. & MEYLE, J. 2014. Inflammatory reaction-communication of cells. *Clin Oral Implants Res,*

25**,** 399-407.
THAMAMONGOOD, T. A., FURUYA, R., FUKUBA, S., NAKAMURA, M., SUZUKI, N. & HATTORI, A. 2012. Expression of osteoblastic and osteoclastic genes during spontaneous regeneration and autotransplantation of goldfish scale: a new tool to study intramembranous bone regeneration. *Bone,* 50**,** 1240-9.
THIERY, J. P., ACLOQUE, H., HUANG, R. Y. & NIETO, M. A. 2009. Epithelial-mesenchymal transitions in development and disease. *Cell,* 139**,** 871-90.

THILLARD, M. J. 1959. [Vertebral column deformities following epiphysectomy in the chick]. *C R Hebd Seances Acad Sci,* 248**,** 1238-40.
TING, J. P., DUNCAN, J. A. & LEI, Y. 2010. How the noninflammasome NLRs function in the innate immune system. *Science,* 327**,** 286-90.
TONEGAWA, S. 1983. Somatic generation of antibody diversity. *Nature,* 302**,** 575-81.
TRAVASSOS, L. H., CARNEIRO, L. A., GIRARDIN, S. & PHILPOTT, D. J. 2010. Nod proteins link bacterial sensing and autophagy. *Autophagy,* 6**,** 409-11.
TREGASKES, C. A., GLANSBEEK, H. L., GILL, A. C., HUNT, L. G., BURNSIDE, J. & YOUNG, J. R. 2005. Conservation of biological properties of the CD40 ligand, CD154 in a non-mammalian vertebrate. *Dev Comp Immunol,* 29**,** 361-74.
TSITSIKOV, E. N., LAOUINI, D., DUNN, I. F., SANNIKOVA, T. Y., DAVIDSON, L., ALT, F. W. & GEHA, R. S. 2001. TRAF1 is a negative regulator of TNF signaling. enhanced TNF signaling in TRAF1-deficient mice. *Immunity,* 15**,** 647-57.
TSITSIKOV, E. N., WRIGHT, D. A. & GEHA, R. S. 1997. CD30 induction of human immunodeficiency virus gene transcription is mediated by TRAF2. *Proc Natl Acad Sci U S A,* 94**,** 1390-5.
TSUKAMOTO, N., KOBAYASHI, N., AZUMA, S., YAMAMOTO, T. & INOUE, J. 1999. Two differently regulated nuclear factor kappaB activation pathways triggered by the cytoplasmic tail of CD40. *Proc Natl Acad Sci U S A,* 96**,** 1234-9.
TURCHINOVICH, G. & PENNINGTON, D. J. 2011. T cell receptor signalling in gammadelta cell development: strength isn't everything. *Trends Immunol,* 32**,** 567-73.
UPADHYAY, V. & FU, Y. X. 2014. Lymphotoxin organizes contributions to host defense and metabolic illness from innate lymphoid cells. *Cytokine Growth Factor Rev,* 25**,** 227-33.
VAN EYNDHOVEN, W. G., FRANK, D., KALACHIKOV, S., CLEARY, A. M., HONG, D. I., CHO, E., NASR, S., PEREZ, A. J., MACKUS, W. J., CAYANIS, E., WELLINGTON, S., FISCHER, S. G., WARBURTON, D. & LEDERMAN, S. 1998. A single gene for human TRAF-3 at chromosome 14q32.3 encodes a variety of mRNA species by alternative polyadenylation, mRNA splicing and transcription initiation. *Mol Immunol,* 35**,** 1189-206.
VAN EYNDHOVEN, W. G., GAMPER, C. J., CHO, E., MACKUS, W. J. & LEDERMAN, S. 1999. TRAF-3 mRNA splice-deletion variants encode isoforms that induce NF-kappaB activation. *Mol Immunol,* 36**,** 647-58.
VAN HAARLEM, D. A., VAN KOOTEN, P. J., ROTHWELL, L., KAISER, P. &

VERVELDE, L. 2009. Characterisation and expression analysis of the chicken interleukin-7 receptor alpha chain. *Dev Comp Immunol,* 33**,** 1018-26.
VANCOTT, J. L., STAATS, H. F., PASCUAL, D. W., ROBERTS, M., CHATFIELD, S. N., YAMAMOTO, M., COSTE, M., CARTER, P. B., KIYONO, H. & MCGHEE, J. R. 1996. Regulation of mucosal and systemic antibody responses by T helper cell subsets, macrophages, and derived cytokines following oral immunization with live recombinant Salmonella. *J Immunol,* 156**,** 1504-14.
VERNAL, R., DIAZ-ZUNIGA, J., MELGAR-RODRIGUEZ, S., PUJOL, M., DIAZ-GUERRA, E., SILVA, A., SANZ, M. & GARCIA-SANZ, J. A. 2014. Activation of RANKL-induced osteoclasts and memory T lymphocytes by Porphyromonas gingivalis is serotype dependant. *J Clin Periodontol,* 41**,** 451-9.
VERVELDE, L., REEMERS, S. S., VAN HAARLEM, D. A., POST, J., CLAASSEN, E., REBEL, J. M. & JANSEN, C. A. 2013. Chicken dendritic cells are susceptible to highly pathogenic avian influenza viruses which induce strong cytokine responses. *Dev Comp Immunol,* 39**,** 198-206.
VIERTLBOECK, B. C. & GOBEL, T. W. 2011. The chicken leukocyte receptor cluster. *Vet Immunol Immunopathol,* 144**,** 1-10.
VITOVSKI, S., PHILLIPS, J. S., SAYERS, J. & CROUCHER, P. I. 2007. Investigating the interaction between osteoprotegerin and receptor activator of NF-kappaB or tumor necrosis factor-related apoptosis-inducing ligand: evidence for a pivotal role for osteoprotegerin in regulating two distinct pathways. *J Biol Chem,* 282**,** 31601-9.
VIVIER, E., NUNES, J. A. & VELY, F. 2004. Natural killer cell signaling pathways. *Science,* 306**,** 1517-9.
VLEUGELS, B., VERVERKEN, C. & GODDEERIS, B. M. 2002. Stimulatory effect of CpG sequences on humoral response in chickens. *Poult Sci,* 81**,** 1317-21.
VYAS, J. M., VAN DER VEEN, A. G. & PLOEGH, H. L. 2008. The known unknowns of antigen processing and presentation. *Nat Rev Immunol,* 8**,** 607-18.
WAJANT, H., PFIZENMAIER, K. & SCHEURICH, P. 2003. Tumor necrosis factor signaling. *Cell Death Differ,* 10**,** 45-65.
WALLIS, J. W., AERTS, J., GROENEN, M. A., CROOIJMANS, R. P., LAYMAN, D., GRAVES, T. A., SCHEER, D. E., KREMITZKI, C., FEDELE, M. J., MUDD, N. K., CARDENAS, M., HIGGINBOTHAM, J., CARTER, J., MCGRANE, R., GAIGE, T., MEAD, K., WALKER, J., ALBRACHT, D., DAVITO, J., YANG, S. P., LEONG, S., CHINWALLA, A., SEKHON, M., WYLIE, K., DODGSON, J., ROMANOV, M. N., CHENG, H., DE JONG, P. J., OSOEGAWA, K., NEFEDOV, M., ZHANG, H., MCPHERSON, J. D., KRZYWINSKI, M., SCHEIN, J., HILLIER, L., MARDIS, E. R., WILSON, R. K. & WARREN, W. C. 2004. A physical map of the chicken genome. Nature, 432, 761-4.
WALSH, N. C., ALEXANDER, K. A., MANNING, C. A., KARMAKAR, S., WANG, J. F., WEYAND, C. M., PETTIT, A. R. & GRAVALLESE, E. M. 2013. Activated human T cells express alternative mRNA transcripts encoding a secreted form of RANKL. *Genes Immun,* 14**,** 336-45.

WALSH, N. C., CAHILL, M., CARNINCI, P., KAWAI, J., OKAZAKI, Y., HAYASHIZAKI, Y., HUME, D. A. & CASSADY, A. I. 2003. Multiple tissue-specific promoters control expression of the murine tartrate-resistant acid phosphatase gene. *Gene,* 307**,** 111-23.

WANG, C., LIN, G. H., MCPHERSON, A. J. & WATTS, T. H. 2009. Immune regulation by 4-1BB and 4-1BBL: complexities and challenges. *Immunol Rev,* 229**,** 192-215.

WANG, L., WANG, L., ZHANG, S., QU, G., ZHANG, D., LI, S. & LIU, S. 2013. Downregulation of ubiquitin E3 ligase TNF receptor-associated factor 7 leads to stabilization of p53 in breast cancer. *Oncol Rep,* 29**,** 283-7.

WANG, R., ZHANG, L., ZHANG, X., MORENO, J., CELLUZZI, C., TONDRAVI, M. & SHI, Y. 2002. Regulation of activation-induced receptor activator of NF-kappaB ligand (RANKL) expression in T cells. *Eur J Immunol,* 32**,** 1090-8.

WANG, Y. J., YAO, F. R., ZHANG & HOU, J. F. 2008. Cloning, Expression and bioactivity analysis of chicken receptor activator of NF-kB Ligand (chRANKL). *J. Agric Biotechnol,* 16**,** 32-36.

WARREN, W. C., CLAYTON, D. F., ELLEGREN, H., ARNOLD, A. P., HILLIER, L. W., KUNSTNER, A., SEARLE, S., WHITE, S., VILELLA, A. J., FAIRLEY, S., HEGER, A., KONG, L., PONTING, C. P., JARVIS, E. D., MELLO, C. V., MINX, P., LOVELL, P., VELHO, T. A., FERRIS, M., BALAKRISHNAN, C. N., SINHA, S., BLATTI, C., LONDON, S. E., LI, Y., LIN, Y. C., GEORGE, J., SWEEDLER, J., SOUTHEY, B., GUNARATNE, P., WATSON, M., NAM, K., BACKSTROM, N., SMEDS, L., NABHOLZ, B., ITOH, Y., WHITNEY, O., PFENNING, A. R., HOWARD, J., VOLKER, M., SKINNER, B. M., GRIFFIN, D. K., YE, L., MCLAREN, W. M., FLICEK, P., QUESADA, V., VELASCO, G., LOPEZ-OTIN, C., PUENTE, X. S., OLENDER, T., LANCET, D., SMIT, A. F., HUBLEY, R., KONKEL, M. K., WALKER, J. A., BATZER, M. A., GU, W., POLLOCK, D. D., CHEN, L., CHENG, Z., EICHLER, E. E., STAPLEY, J., SLATE, J., EKBLOM, R., BIRKHEAD, T., BURKE, T., BURT, D., SCHARFF, C., ADAM, I., RICHARD, H., SULTAN, M., SOLDATOV, A., LEHRACH, H., EDWARDS, S. V., YANG, S. P., LI, X., GRAVES, T., FULTON, L., NELSON, J., CHINWALLA, A., HOU, S., MARDIS, E. R. & WILSON, R. K. 2010. The genome of a songbird. *Nature,* 464**,** 757-62.

WATTS, T. H. 2005. TNF/TNFR family members in costimulation of T cell responses. *Annu Rev Immunol,* 23**,** 23-68.

WEI, J., GUO, M., GAO, P., JI, H., LI, P., YAN, Y. & QIN, Q. 2014. Isolation and characterization of tumor necrosis factor receptor-associated factor 6 (TRAF6) from grouper, Epinephelus tauvina. *Fish Shellfish Immunol,* 39**,** 61-8.

WEI, L., CUI, J., SONG, Y., ZHANG, S., HAN, F., YUAN, R., GONG, L., JIAO, P. & LIAO, M. 2014. Duck MDA5 functions in innate immunity against H5N1 highly pathogenic avian influenza virus infections. *Vet Res,* 45**,** 66.

WELLS, L. L., LOWRY, V. K., DELOACH, J. R. & KOGUT, M. H. 1998. Age-dependent phagocytosis and bactericidal activities of the chicken heterophil. *Dev Comp Immunol,* 22**,** 103-9.

WIETHE, C., DITTMAR, K., DOAN, T., LINDENMAIER, W. & TINDLE, R.

2003. Enhanced effector and memory CTL responses generated by incorporation of receptor activator of NF-kappa B (RANK)/RANK ligand costimulatory molecules into dendritic cell immunogens expressing a human tumor-specific antigen. *J Immunol,* 171**,** 4121-30.

WILCOX, R. A., TAMADA, K., STROME, S. E. & CHEN, L. 2002. Signaling through NK cell-associated CD137 promotes both helper function for CD8+ cytolytic T cells and responsiveness to IL-2 but not cytolytic activity. *J Immunol,* 169**,** 4230-6.

WILKINS, L. J., MCKINSTRY, J. L., AVERY, N. C., KNOWLES, T. G., BROWN, S. N., TARLTON, J. & NICOL, C. J. 2011. Influence of housing system and design on bone strength and keel bone fractures in laying hens. *Vet Rec,* 169**,** 414.

WILLIAMSON, E., BILSBOROUGH, J. M. & VINEY, J. L. 2002. Regulation of mucosal dendritic cell function by receptor activator of NF-kappa B (RANK)/RANK ligand interactions: impact on tolerance induction. *J Immunol,* 169**,** 3606-12.

WILSON, N. S., EL-SUKKARI, D. & VILLADANGOS, J. A. 2004. Dendritic cells constitutively present self-antigens in their immature state in vivo and regulate antigen presentation by controlling the rates of MHC class II synthesis and endocytosis. *Blood,* 103**,** 2187-95.

WING, K., ONISHI, Y., PRIETO-MARTIN, P., YAMAGUCHI, T., MIYARA, M., FEHERVARI, Z., NOMURA, T. & SAKAGUCHI, S. 2008. CTLA-4 control over Foxp3+ regulatory T cell function. *Science,* 322**,** 271-5.

WITTEN, P. E. & HUYSSEUNE, A. 2009. A comparative view on mechanisms and functions of skeletal remodelling in teleost fish, with special emphasis on osteoclasts and their function. *Biol Rev Camb Philos Soc,* 84**,** 315-46.

WITTER, R. L. 1997. Increased virulence of Marek's disease virus field isolates. *Avian Dis,* 41**,** 149-63.

WONG, B. R., BESSER, D., KIM, N., ARRON, J. R., VOLOGODSKAIA, M., HANAFUSA, H. & CHOI, Y. 1999. TRANCE, a TNF family member, activates Akt/PKB through a signaling complex involving TRAF6 and c-Src. *Mol Cell,* 4**,** 1041-9.

WONG, B. R., JOSIEN, R., LEE, S. Y., VOLOGODSKAIA, M., STEINMAN, R. M. & CHOI, Y. 1998. The TRAF family of signal transducers mediates NF-kappaB activation by the TRANCE receptor. *J Biol Chem,* 273**,** 28355-9.

WONG, B. R., RHO, J., ARRON, J., ROBINSON, E., ORLINICK, J., CHAO, M., KALACHIKOV, S., CAYANI, E., BARTLETT, F. S., 3RD, FRANKEL, W. N., LEE, S. Y. & CHOI, Y. 1997. TRANCE is a novel ligand of the tumor necrosis factor receptor family that activates c-Jun N-terminal kinase in T cells. *J Biol Chem,* 272**,** 25190-4.

WORKMAN, C. J., SZYMCZAK-WORKMAN, A. L., COLLISON, L. W., PILLAI, M. R. & VIGNALI, D. A. 2009. The development and function of regulatory T cells. *Cell Mol Life Sci,* 66**,** 2603-22.

WU, Z., HU, T. & KAISER, P. 2011. Chicken CCR6 and CCR7 are markers for immature and mature dendritic cells respectively. *Dev Comp Immunol,* 35**,** 563-7.

WU, Z., ROTHWELL, L., YOUNG, J. R., KAUFMAN, J., BUTTER, C. & KAISER, P. 2010. Generation and characterization of chicken bone marrow-

derived dendritic cells. *Immunology,* 129**,** 133-45.
WYNN, T. A., CHAWLA, A. & POLLARD, J. W. 2013. Macrophage biology in development, homeostasis and disease. *Nature,* 496**,** 445-55.
XIE, P. 2013. TRAF molecules in cell signaling and in human diseases. J Mol Signal, 8, 7.
XIE, P., HOSTAGER, B. S. & BISHOP, G. A. 2004. Requirement for TRAF3 in signaling by LMP1 but not CD40 in B lymphocytes. *J Exp Med,* 199**,** 661-71.
XIE, P., STUNZ, L. L., LARISON, K. D., YANG, B. & BISHOP, G. A. 2007. Tumor necrosis factor receptor-associated factor 3 is a critical regulator of B cell homeostasis in secondary lymphoid organs. *Immunity,* 27**,** 253-67.
XU, C. & MIN, J. 2011. Structure and function of WD40 domain proteins. *Protein Cell,* 2**,** 202-14.
XU, D., WANG, S., LIU, W., LIU, J. & FENG, X. 2006. A novel receptor activator of NF-kappaB (RANK) cytoplasmic motif plays an essential role in osteoclastogenesis by committing macrophages to the osteoclast lineage. *J Biol Chem,* 281**,** 4678-90.
XU, L. G., LI, L. Y. & SHU, H. B. 2004. TRAF7 potentiates MEKK3-induced AP1 and CHOP activation and induces apoptosis. *J Biol Chem,* 279**,** 17278-82.
XU, Y., CHENG, G. & BALTIMORE, D. 1996. Targeted disruption of TRAF3 leads to postnatal lethality and defective T-dependent immune responses. *Immunity,* 5**,** 407-15.
YAGI, M., MIYAMOTO, T., SAWATANI, Y., IWAMOTO, K., HOSOGANE, N., FUJITA, N., MORITA, K., NINOMIYA, K., SUZUKI, T., MIYAMOTO, K., OIKE, Y., TAKEYA, M., TOYAMA, Y. & SUDA, T. 2005. DC-STAMP is essential for cell-cell fusion in osteoclasts and foreign body giant cells. *J Exp Med,* 202**,** 345-51.
YAMAMOTO, H., KISHIMOTO, T. & MINAMOTO, S. 1998. NF-kappaB activation in CD27 signaling: involvement of TNF receptor-associated factors in its signaling and identification of functional region of CD27. *J Immunol,* 161**,** 4753-9.
YANG, G. X., LIAN, Z. X., KIKUCHI, K., MORITOKI, Y., ANSARI, A. A., LIU, Y. J., IKEHARA, S. & GERSHWIN, M. E. 2005. Plasmacytoid dendritic cells of different origins have distinct characteristics and function: studies of lymphoid progenitors versus myeloid progenitors. *J Immunol,* 175**,** 7281-7.
YANG, X., HALLADAY, D., ONYIA, J. E., MARTIN, T. J. & CHANDRASEKHAR, S. 2002. Protein Kinase C is a mediator of the synthesis and secretion of osteoprotegerin in osteoblast-like cells. *Biochem Biophys Res Commun,* 290**,** 42-6.
YANO, S., KITAMURA, K., SATOH, Y., NAKANO, M., HATTORI, A., SEKIGUCHI, T., IKEGAME, M., NAKASHIMA, H., OMORI, K., HAYAKAWA, K., CHIBA, A., SASAYAMA, Y., EJIRI, S., MIKUNI-TAKAGAKI, Y., MISHIMA, H., FUNAHASHI, H., SAKAMOTO, T. & SUZUKI, N. 2013. Static and dynamic hypergravity responses of osteoblasts and osteoclasts in medaka scales. *Zoolog Sci,* 30**,** 217-23.
YASUDA, H., SHIMA, N., NAKAGAWA, N., YAMAGUCHI, K., KINOSAKI, M., MOCHIZUKI, S., TOMOYASU, A., YANO, K., GOTO, M., MURAKAMI, A., TSUDA, E., MORINAGA, T., HIGASHIO, K., UDAGAWA, N., TAKAHASHI, N. & SUDA, T. 1998. Osteoclast differentiation factor is a

ligand for osteoprotegerin/osteoclastogenesis-inhibitory factor and is identical to TRANCE/RANKL. *Proc Natl Acad Sci U S A,* 95**,** 3597-602.

YE, H., ARRON, J. R., LAMOTHE, B., CIRILLI, M., KOBAYASHI, T., SHEVDE, N. K., SEGAL, D., DZIVENU, O. K., VOLOGODSKAIA, M., YIM, M., DU, K., SINGH, S., PIKE, J. W., DARNAY, B. G., CHOI, Y. & WU, H. 2002. Distinct molecular mechanism for initiating TRAF6 signalling. *Nature,* 418**,** 443-7.

YEH, D. W., LIU, Y. L., LO, Y. C., YUH, C. H., YU, G. Y., LO, J. F., LUO, Y., XIANG, R. & CHUANG, T. H. 2013. Toll-like receptor 9 and 21 have different ligand recognition profiles and cooperatively mediate activity of CpG-oligodeoxynucleotides in zebrafish. *Proc Natl Acad Sci U S A,* 110**,** 20711-6.

YEH, W. C., SHAHINIAN, A., SPEISER, D., KRAUNUS, J., BILLIA, F., WAKEHAM, A., DE LA POMPA, J. L., FERRICK, D., HUM, B., ISCOVE, N., OHASHI, P., ROTHE, M., GOEDDEL, D. V. & MAK, T. W. 1997. Early lethality, functional NF-kappaB activation, and increased sensitivity to TNF-induced cell death in TRAF2-deficient mice. *Immunity,* 7**,** 715-25.

YONEYAMA, M., KIKUCHI, M., NATSUKAWA, T., SHINOBU, N., IMAIZUMI, T., MIYAGISHI, M., TAIRA, K., AKIRA, S. & FUJITA, T. 2004. The RNA helicase RIG-I has an essential function in double-stranded RNA-induced innate antiviral responses. *Nat Immunol,* 5**,** 730-7.

YOSHIKUBO, H., SUZUKI, N., TAKEMURA, K., HOSO, M., YASHIMA, S., IWAMURO, S., TAKAGI, Y., TABATA, M. J. & HATTORI, A. 2005. Osteoblastic activity and estrogenic response in the regenerating scale of goldfish, a good model of osteogenesis. *Life Sci,* 76**,** 2699-709.

YU, D., RAO, S., TSAI, L. M., LEE, S. K., HE, Y., SUTCLIFFE, E. L., SRIVASTAVA, M., LINTERMAN, M., ZHENG, L., SIMPSON, N., ELLYARD, J. I., PARISH, I. A., MA, C. S., LI, Q. J., PARISH, C. R., MACKAY, C. R. & VINUESA, C. G. 2009. The transcriptional repressor Bcl-6 directs T follicular helper cell lineage commitment. *Immunity,* 31**,** 457-68.

YU, M., QI, X., MORENO, J. L., FARBER, D. L. & KEEGAN, A. D. 2011. NF-kappaB signaling participates in both RANKL- and IL-4-induced macrophage fusion: receptor cross-talk leads to alterations in NF-kappaB pathways. *J Immunol,* 187**,** 1797-806.

YU, Q., GU, J. X., KOVACS, C., FREEDMAN, J., THOMAS, E. K. & OSTROWSKI, M. A. 2003. Cooperation of TNF family members CD40 ligand, receptor activator of NF-kappa B ligand, and TNF-alpha in the activation of dendritic cells and the expansion of viral specific CD8+ T cell memory responses in HIV-1-infected and HIV-1-uninfected individuals. *J Immunol,* 170**,** 1797-805.

YUN, T. J., CHAUDHARY, P. M., SHU, G. L., FRAZER, J. K., EWINGS, M. K., SCHWARTZ, S. M., PASCUAL, V., HOOD, L. E. & CLARK, E. A. 1998. OPG/FDCR-1, a TNF receptor family member, is expressed in lymphoid cells and is up-regulated by ligating CD40. *J Immunol,* 161**,** 6113-21.

YUN, T. J., TALLQUIST, M. D., AICHER, A., RAFFERTY, K. L., MARSHALL, A. J., MOON, J. J., EWINGS, M. E., MOHAUPT, M., HERRING, S. W. & CLARK, E. A. 2001. Osteoprotegerin, a crucial regulator of bone

metabolism, also regulates B cell development and function. *J Immunol,* 166**,** 1482-91.

ZAREMBER, K. A. & GODOWSKI, P. J. 2002. Tissue expression of human Toll-like receptors and differential regulation of Toll-like receptor mRNAs in leukocytes in response to microbes, their products, and cytokines. *J Immunol,* 168**,** 554-61.

ZHAI, Y., GUO, R., HSU, T. L., YU, G. L., NI, J., KWON, B. S., JIANG, G. W., LU, J., TAN, J., UGUSTUS, M., CARTER, K., ROJAS, L., ZHU, F., LINCOLN, C., ENDRESS, G., XING, L., WANG, S., OH, K. O., GENTZ, R., RUBEN, S., LIPPMAN, M. E., HSIEH, S. L. & YANG, D. 1998. LIGHT, a novel ligand for lymphotoxin beta receptor and TR2/HVEM induces apoptosis and suppresses in vivo tumor formation via gene transfer. *J Clin Invest,* 102**,** 1142-51.

ZHANG, D., ZHANG, G., HAYDEN, M. S., GREENBLATT, M. B., BUSSEY, C., FLAVELL, R. A. & GHOSH, S. 2004. A toll-like receptor that prevents infection by uropathogenic bacteria. *Science,* 303**,** 1522-6.

ZHANG, D. H., COHN, L., RAY, P., BOTTOMLY, K. & RAY, A. 1997. Transcription factor GATA-3 is differentially expressed in murine Th1 and Th2 cells and controls Th2-specific expression of the interleukin-5 gene. *J Biol Chem,* 272**,** 21597-603.

ZHANG, J., ZHU, J., BU, X., CUSHION, M., KINANE, T. B., AVRAHAM, H. & KOZIEL, H. 2005. Cdc42 and RhoB activation are required for mannose receptor-mediated phagocytosis by human alveolar macrophages. *Mol Biol Cell,* 16**,** 824-34.

ZHANG, L., LIU, R., SONG, M., HU, Y., PAN, B., CAI, J. & WANG, M. 2013. Eimeria tenella: interleukin 17 contributes to host immunopathology in the gut during experimental infection. *Exp Parasitol,* 133**,** 121-30.

ZHANG, M., WANG, L., ZHAO, X., ZHAO, K., MENG, H., ZHAO, W. & GAO, C. 2012. TRAF-interacting protein (TRIP) negatively regulates IFN-beta production and antiviral response by promoting proteasomal degradation of TANK-binding kinase 1. *J Exp Med,* 209**,** 1703-11.

ZHANG, Y. Y., SHAO, M. Y., YU, X. H., ZHAO, J. & ZHANG, G. Z. 2014. Molecular characterization of chicken-derived genotype VIId Newcastle disease virus isolates in China during 2005-2012 reveals a new length in hemagglutinin-neuraminidase. *Infect Genet Evol,* 21**,** 359-66.

ZHAO, F., LI, Y. W., PAN, H. J., WU, S. Q., SHI, C. B., LUO, X. C. & LI, A. X. 2013. Grass carp (Ctenopharyngodon idella) TRAF6 and TAK1: molecular cloning and expression analysis after Ichthyophthirius multifiliis infection. *Fish Shellfish Immunol,* 34**,** 1514-23.

ZHENG, C., KABALEESWARAN, V., WANG, Y., CHENG, G. & WU, H. 2010. Crystal structures of the TRAF2: cIAP2 and the TRAF1: TRAF2: cIAP2 complexes: affinity, specificity, and regulation. *Mol Cell,* 38**,** 101-13.

ZOTOS, D., COQUET, J. M., ZHANG, Y., LIGHT, A., D'COSTA, K., KALLIES, A., CORCORAN, L. M., GODFREY, D. I., TOELLNER, K. M., SMYTH, M. J., NUTT, S. L. & TARLINTON, D. M. 2010. IL-21 regulates germinal center B cell differentiation and proliferation through a B cell-intrinsic mechanism. *J Exp Med,* 207**,** 365-78.

ZOTTI, T., UVA, A., FERRAVANTE, A., VESSICHELLI, M., SCUDIERO, I.,

CECCARELLI, M., VITO, P. & STILO, R. 2011. TRAF7 protein promotes Lys-29-linked polyubiquitination of IkappaB kinase (IKKgamma)/NF-kappaB essential modulator (NEMO) and p65/RelA protein and represses NF-kappaB activation. *J Biol Chem,* 286**,** 22924-33.

Appendix 1

General buffers and solutions

Restriction enzyme buffers

1X NEBuffer 1:	10mM Bis-Tris-Propane-HCL
	10 mM $MgCl_2$
	1mM Dithiothreitol
	pH 7.0
Buffer H:	50 mM Tris-HCL (pH 7.5), 10 mM $MgCL_2$, 100 mM NaCl, 1 mM Dithioerythritol, pH 7.5

Qiagen molecular biology kit buffers

RNeasy Mini Kit

Buffer RTL (Lysis buffer)	contains guanidine thiocyanate
Buffer RW1	
Buffer RPE (Wash buffer)	contains ethanol

QIAquick PCR Purification Kit

Buffer PB (binding buffer)	guanidine hydrochloride and isopropanol
Buffer PE (wash buffer)	contains ethanol

QIAquick Gel Extraction Kit

Buffer QG (dissolving buffer)	contains guanidine thiocyanate
Buffer PE (Wash buffer)	contains ethanol

QIAprep Spin Mini prep Kit

Buffer P1 (dissolving buffer)	50mM Tris-Cl (pH 8.0), 10 mM EDTA and
	100 μg/ml RNase AwBuffer P2 (lysis buffer) 200 mM NaOH and 1% SDS (w/v)
Buffer N3 (neutraliser buffer)	contains guanidine hydrochloride

Buffer PB (binding buffer)	contains guanidine hydrochloride
Buffer PE (wash buffer)	contains guanidine hydrochloride and ethanol

EndoFree®Plasmind Purification Kits (Maxi)

Buffer P1	50mM Tris-Cl (pH 8.0), 10 mM EDTA and 100 μg/ml RNase A
Buffer P2	200 mM NaOH and 1% SDS (w/v)
Buffer P3	3 M potassium acetate (CH_3CO_2K), pH 5.5
Buffer ER	contains isopropanol and polyethylene glycol octylphenyl ether
Buffer QBT (equilibrium buffer)	750 nM NaCl, 50 mM MOPS, pH 7.0, 15% isopropanol (v/v) and 0.15% Triton®X-100
Buffer QC (wash Buffer)	1 nM NaCl, 50 mM MOPS, pH 7.0 and 15% isopropanol (v/v)
Buffer QN (elution buffer)	1.6 M NaCl, 50 mM MOPS, pH 7.0 and 15% isopropanol (v/v)

General Buffers

FACS Buffer	PBS, 0.5% (w/v) Bovine Serum Albumin (Sigma) and 0.05% Azide
Versene	0.25 g KCL, 1.437 g Na_2HPO_4, 0.25 g KH_2PO_4, 0.2 g EDTA, H_2O to 11, pH 7.2

ELISA Buffers:

Coating Buffer:		15 mM Sodium carbonate, 35 mM Sodium bicarbonate, 3 mM Sodium azide
Blocking Buffer:		0.2 g of casein in 1 l of PBS
Wash Buffer:		PBS, 0.05% Tween-20 (PBST)
Substrate Buffer:	Buffer A:	0.1 M Citric Acid (10.5 g Citric acid in 500 ml dH_2O)

Buffer B:	0.2 M Disodium hydrogen orthophosphate (14.2 g Na_2HPO_4 in 500 ml dH_2O)

25.7 ml of Buffer A + 24.3 ml of Buffer B + 1 o-phenylenediamine dihydrochloride tablet (OPD) (SIGMA P-8787) + 30 µl fresh H_2O_2.

Stop Solution:	2 N H_2SO_4
Non-Reducing buffer	H_2O, 0.5 M Tris-HCl, Glycerol, 10% SDS, 0.05% and Bromophenol Blue
Reducing Buffer	H_2O, 0.5M Tris-HCl, Glycerol, 10% SDS, 0.05% Bromophenol Blue and 2-mercaptoethanol

AutoMacs Pro™ Cell Separator Buffers

AutoMacs Pro™ Pro Washing Solution (1.5 litre)	Detergents, Stabiliser, pH 11.5-12.5
AutoMacs Pro™ Running Buffer (1.5 litre)	Bovine Serum Albumin, EDTA, PBS, 0.009% Azide and pH 7.2 (2 µm filtered)

Cell Culture Reagents

COS-7 cell growth media

DMEM

10% Foetal calf serum (FCS)

1% 200 mM L-glutamine

500 µl 1000X Penicillin/streptomycin

1% 100X Non-essential amino acids

Cos-7 cell transfection media

1% 200 mM L-glutamine

500 µl 1000X Penicillin/streptomycin

1% 100X Non-essential amino acids

HEK-293T growth media

DMEM

2% Foetal calf serum (FCS)

1% 200 mM L-glutamine

500 µl 1000X Penicillin/streptomycin

1% 100X Non-essential amino acids

BMDC growth media

RPMI

10% Chicken Serum (CS)

1% 200 mM L-glutamine

500 µl 1000X Penicillin/streptomycin

BMDM growth media

RPMI

2% Chicken Serum

3% FCS

1% 200 mM L-glutamine

500 µl 1000X Penicillin/streptomycin

Bone marrow-derived osteoclasts growth media

5% Chicken Serum

5% FCS

1% 200 mM L-glutamine

500 µl 1000X Penicillin/Streptomycin

Appendix 2

Primers, probes and Ensembl accession numbers

Primer name	Plasmid name	Sequence (5'-3')
T7	pGEM T-EASY/pcDNA3-HA	TAATACGACTCACTATAGG
Sp6 (reverse)	pGEM T-EASY	ATTTAGGTGACACTATAG
pKW06F	pKW06/pKW07	CAGTTCAATTACAGCTCTTAA
pKW06R	pKW06/pKW07	ACTCATCAATGTATCTTATCA

Table 1 *Primers designed for sequencing cDNA and sub-cloned cDNA into sequencing and expression plasmids.*

Primer name	Target for amplification	Sequence (5'-3')
RANKF1 RANKR1	Extracellular domain of RANK	TTGTCACTACAAAGCACTCTG ACAAACTGCATCGGACTTATC
exRKF1 (*Nho*I) exRKR2 (*Bgl*II)	Subcloning the extracellular domain of RANK for insertion into signal pKW06 vector	*GCTAGC*CAAAGCACTCTGCCGTGTG *AGATCT*ACAAACTGCATCGGACTTATCA
RANKLF1 RANKLF2	Full-length chRANKL	ATGCGGCGCGCCAGCCG TCAGTCTAAATCCCTTACTTTAAATGCCCCAAA
exRANKLF1 exRANKLF2	Extracellular domain of RANKL	TCAGTCTAAATCCCTTACTTTA TGCTTCTTGTGATGAATCCAGT
exRKLFSB (*Xho*I) exRKLRSB (*Not*I)	Subcloning the extracellular domain of chRANKL into the pV20/V22 vectors	GG*CTCGAG*TATGGACCCTAGTAGA AA*GCGGCCGC*TCAGTCTAAAT
OPGF OPGR	Full-length OPG	ATGAACAAGTTCCTGTGCTGCA TTAGACACATCTTACTTTCACTGATTTCA

OPGFSB (*Not*I) OPGRSB (*Bgl*II)	Subcloning into pKW07	*GCTAGC*ATGAACAAGTTCCT C*AGATCT*ACACATCTTACTTTC
TRAF2F TRAF2R	Full-length chTRAF2	ATGGCAGCAGCAAACTCGA TGGCCCAGCATAGGGCAG
TRAF2FSB (*Eco*RI) TRAF2RSB (*Xba*I)	Subcloning into the pcDNA3-HA vector	ATT*GAATTC*GAGCAAACTCAA AAT*TCTAGA*TTAAAGGCCCGAGGTCA A
TRAF5F TRAF5R	Full-length chTRAF5	ATGGCCTGTGACGAGCTCACT TCACAATTCCTCCAGATCAGTTAAAT CCACA
TRAF6F TRAF6R	Full-length chTRAF6	ATGAGCTTGCTACACAGT CAGCTCCATCAGTACTGCGAGCTT
TRAF7F TRAF7R	Full-length chTRAF7	ATGAGCTCAAACAAGAACGCTCGCTT TACAGTCTAGCACGTCCAGACCTT
GAPDHF GAPDHR	Full-length	GGGCACGCCATCACTATCTTCCA GCCCATCAGCAGCAGCCTTCACT

Table 2 *Primers designed to clone and subclone chRANKL, chRANK, chOPG, chTRAF2, chTRAF5, chTRAF6 and chTRAF7. Italic and underline indicate the location of the intregated restriction digestion sites for subcloning.*

Name	**Sequence (5'-3')**	**Exon boundaries**
TRAF2F TRAF2R	AAGGAATATACGAAGAAGGAATTT ATCACAAGTCAATGGAAATTTTG	Exon 3 and exon 5
TRAF5F	CAGGAACATCTTCAGCAGTGTT	Exon 1 and exon 4

TRAF5R	TTTGCCATCTGTATTAGCTGTT	
TRAF6F TRAF6R	TCGGGAAGCAGTGCAGACGC AGCACACCGCTGAGCACTTGG	Exon 1 and exon 5
TRAF7F TRAF7R	ATGAGCTCAAACAAGAACGCTC TTCCTGACGCTCAGTTTAATTGTA	Exon 1 and exon 6

Table 3 *Primers designed for RT-PCR analysis of chTRAF2, chTRAF5, chTRAF6 and chTRAF7 mRNA expression levels.*

Target	**Sequence (5'-3')**	**Standard RNA**	**(µM)**
28S	**F:**GGCGAAGCCAGAGGAAACT **R:**GACGACCGATTTGCACGTC **P:**AGGACCGCTACGGACCTCCACCA	LPS-stimulated HD11 mRNA	0.6
IL-1β	**F:**GCTCTACATGTCGTGTGTGATGAG **R:**TGTCGATGTCCCGCATGA **P:**CCACACTGCAGCTGGAGGAAGCC	ExCOS-7 IL-1β mRNA	0.4
IL-6	**F:**GCTCGCCGGCTTCGA **R:**GGTAGGTCTGAAAGGCGAACAG **P:**AGGAGAAATGCCTGACGAAGCTCTCCA	ExCOS-7 IL-6 mRNA	0.4
IL-10	**F:**CATGCTGCTGGGCCTGAA **R:** CGTCTCCTTGATCTGCTTGATG **P:** CGACGATTCGGCGCTGTCACC	ExCOS-7 IL-10 mRNA	0.4
IL-12α	**F:**TGGCCGCTGCAAACG **R:**ACCTCTTCAAGGGTGCACTCA **P:**CCAGCGTCCTCTGCTTCTGCACCTT	ExCOS-7 IL-12 p70 mRNA	0.4
RANKL	**F:**CTGGAACTCGCAAAGTGAACCT **R:**TTTCCCATCACTGAACGTCATATTT **P:**TGGCATCATAACAAAGGCCAGGCAAAC	ExCOS-7 sRANKL mRNA	0.4
RANK	**F:**GCCATGTCCC AGAGGATACT **R:**GCCAATCCCAGAGCTGAACA **P:**TGCTTCATCCACTGATGAGTGTAAATCCTGGACCA	ExCOS-7 sRANK mRNA	0.4
OPG	**F:**ACAGCCAGGCACTCCTGAGA **R:**GCTTTTGACAGACTGCTTTGGA **P:**CCCAGAGGGATTTTTCTCCAATGAAACG	ExCOS-7 OPG mRNA	0.4

Table 4 *Primers and probes designed for qRT-PCR (TaqMan®). **F**=forward primer, **R**=reverse primer and **P**=probe.*

Name	Ensembl Accession Number
ChTRAF1	ENSGALP00000002401
ChTRAF2	ENSGALT00000014665
ChTRAF4	ENSGALP00000006340
ChTRAF3	ENSGALP00000018553
ChTRAF5	ENSGALT00000016038
ChTRAF6	ENSGALT00000012888
ChTRAF7	ENSGALT00000009263
HuTRAF1	ENSP00000362994
HuTRAF2	ENST00000247668
HuTRAF3	ENSP00000454207
HuTRAF3A	ENSP00000328003
HuTRAF3B	ENSP00000332468
HuTRAF4	ENSP00000262395
HuTRAF5	ENSP00000261464
HuTRAF6	ENSP00000433623
HuTRAF7	ENSP00000318944
MTRAF1	ENSMUSP00000130759
MTRAF2	ENSMUSP00000028311
MTRAF2A	ENSMUSP00000109872
MTRAF3A	ENSMUSG00000021277
MTRAF3B	ENSMUSP00000112517
MTRAF4	ENSMUSP00000017530
MTRAF5	ENSMUSP00000082710
MTRAF6	ENSMUSP00000004949
MTRAF7	ENSMUSP00000134759
ZFTRAF1	ENSTGUP00000006737
ZFTRAF4	ENSTGUP00000006363
ZFTRAF5p	ENSTGUP00000003276
ZFTRAF6	ENSTGUP00000010462
ZFTRAF7	ENSTGUP00000006517

Table 5 *Ensembl Accession Numbers of TRAF sequences used for phylogenetic analysis.*

Appendix 3

Subcloning of chTRAF2 into pcDNA3-HA

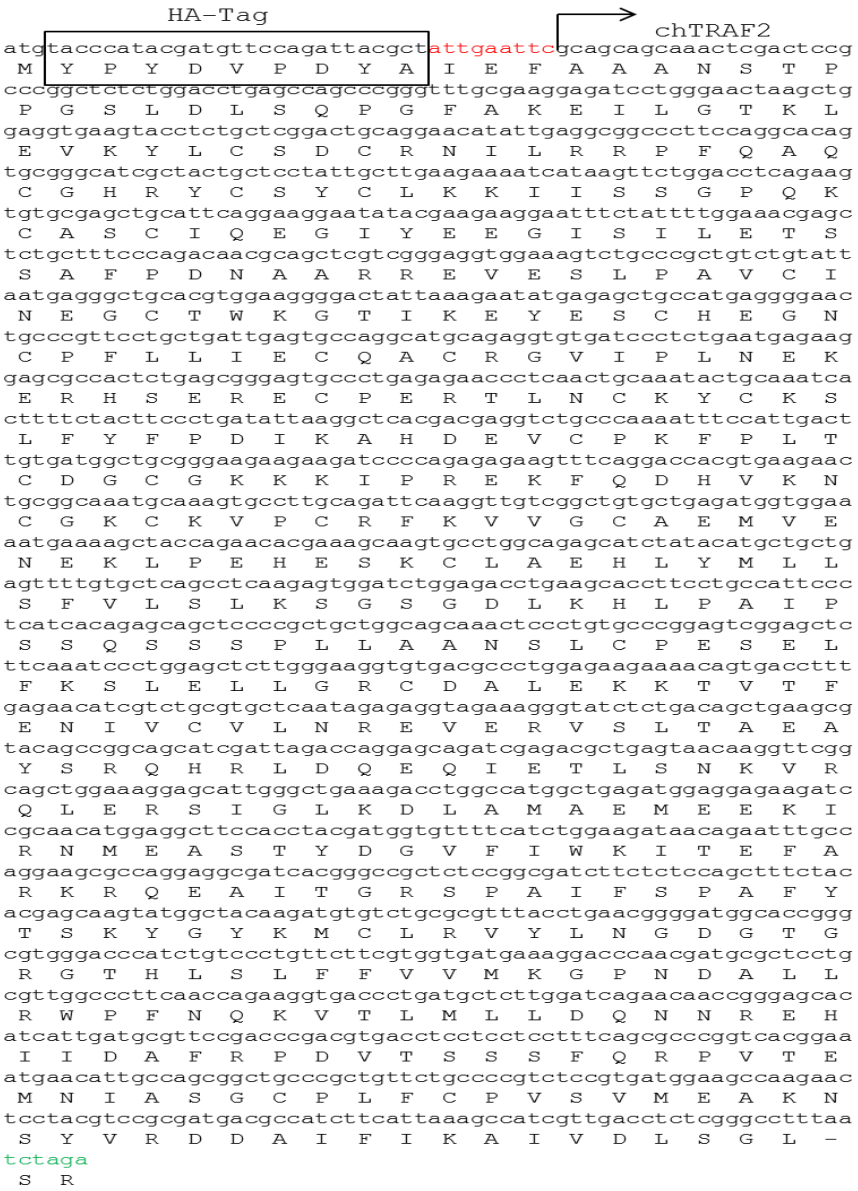

Figure 7.1 ***Subcloning of chTRAF2 cDNA into a modified pcDNA3 vector expressing an NH_2~terminal HA-tag.*** *ChTRAF2 was subcloned into the* EcoR1 *(red) and Xba*I *(green) restriction sites of pcDNA-3-HA.The box indicates the HA-tag sequence and arrow the start of the chTRAF2.*

Appendix 4

Antibodies and dilutions

Primary antibody	Information	Dilution	Secondary antibody
M2 anti-FLAG monoclonal	Mouse anti-FLAG tag (Sigma/F1804)	1:1000	Goat anti-mouse IgG-HRP conjugated (Southern Biotech/1030-05)
IgG-Fc monoclonal	Goat anti-human (Southern Biotech/2040-05)	1:5000	Mouse anti-human IgG-HRP conjugated (Southern Biotech/2040-05)
Anti-HA monoclonal	Mouse anti-HA (Covance HA.11 Clone 16B12)	1:250	Goat anti-mouse IgG-HRP conjugated (Southern Biotech/1030-05)

Table 5 *Primary and secondary antibodies used for the detection of recombinant fusion proteins.*

Primary antibody	Description	Secondary antibody	Cell numbers prior to separation	Cell numbers post-separation
CD4	Mouse anti-chicken CD4 monoclonal (IgG1)(Southern Biotech/8210-01)	Goat anti-mouse-IgG1-FITC (Southern Biotech/1070-02)	Bird 1: 3 X 10^7 Bird 2: 3 X 10^6 Bird 3: 3 X 10^6	2 X 10^5 1.4 X 10^6 1.4 X 10^6
CD8β	Mouse anti-chicken CD8β monoclonal (IgG2) (Southern Biotech/8280-01)	Goat anti-mouse-IgG2a-PE (Southern Biotech/1090-02)	Bird 1: 3 X 10^7 Bird 2: 3 X 10^6 Bird 3: 3 X 10^6	8.8 X 10^6 1.4 X 10^6 1.8 X 10^6
TCR1 (γδ)	Mouse anti-chicken monoclonal (IgG1) (Southern Biotech/8230-01)	Goat anti-mouse-IgG1-FITC (Southern Biotech/1070-02)	Bird 1: 3 X 10^7 Bird 2: 3 X10^6 Bird 3: 3 X10^6	4 X 10^6 1 X 10^6 8.4 X 10^5

TCR2 (αβ1)	Mouse anti-chicken monoclonal (IgG1) (Southern Biotech/8240-01)	Goat anti-mouse-IgG1-FITC (Southern Biotech/1070-02)	Bird 1: 3 X 10^7 Bird 2: 3 X 10^6 Bird 3: 3 X 10^6	4 X 10^6 1 X 10^6 3.4 X 10^5
TCR3 (αβ2)	Mouse anti-chicken monoclonal (IgG1) (Southern Biotech/8250-01)	Goat anti-mouse-IgG1-FITC (Southern Biotech/1070-02)	Bird 1: 3 X 10^7 Bird 2: 3 X10^6 Bird 3: 3 X10^6	4 X 10^6 1 X 10^6 3.6 X 10^5
KUL01	Mouse anti-chicken KUL01 monoclonal (Southern Biotech/8420-01)	Goat anti-mouse-IgG1-FITC (Southern Biotech/1070-02)	Bird 1: 3 X 10^7 Bird 2: 3 X10^6 Bird 3: 3 X10^6	4 X 10^6 4 X 10^6 5 X 10^6
Bu1	Mouse anti-chicken Bu-1/AV20 monoclonal (Southern Biotech/8395-01)	Goat anti-mouse-IgG1-FITC (Southern Biotech/1070-02)	Bird 1: 3 X 10^7 Bird 2: 3 X10^6 Bird 3: 3 X10^6	1.5 X 10^6 1 X 10^6 2 X 10^6

Table 6 *The Primary and secondary monoclonal antibodies used for the separation of chicken splenocyte subsets using an AutoMacs pro-separator. Cell numbers before and after separation are indicated.*

Target	Information	Dilution	Secondary
MHC Class II	Mouse anti-chicken MHC class II IgG1 (Gift from Colin Butter, IAH. UK)	1:500	Goat anti-mouse-IgG1-FITC (Southern Biotech/1070-02) at 1:2000
CD40	Mouse anti-chicken CD40/AV79 IgG2a (Serotec/MCA2836)	1:500	Goat anti-mouse-IgG2a-PE (Southern Biotech/1080-09S) at 1:2000
KUL01	Mouse anti-chicken KUL01 IgG1 (Southern Biotech/8420-01)	1:500	Goat anti-mouse-IgG1-FITC (Southern Biotech/1070-02) at 1:2000

Table 7 *Monoclonal antibodies and dilutions used for analysis of cell surface expression of activation markers on BMDC and BMDM*

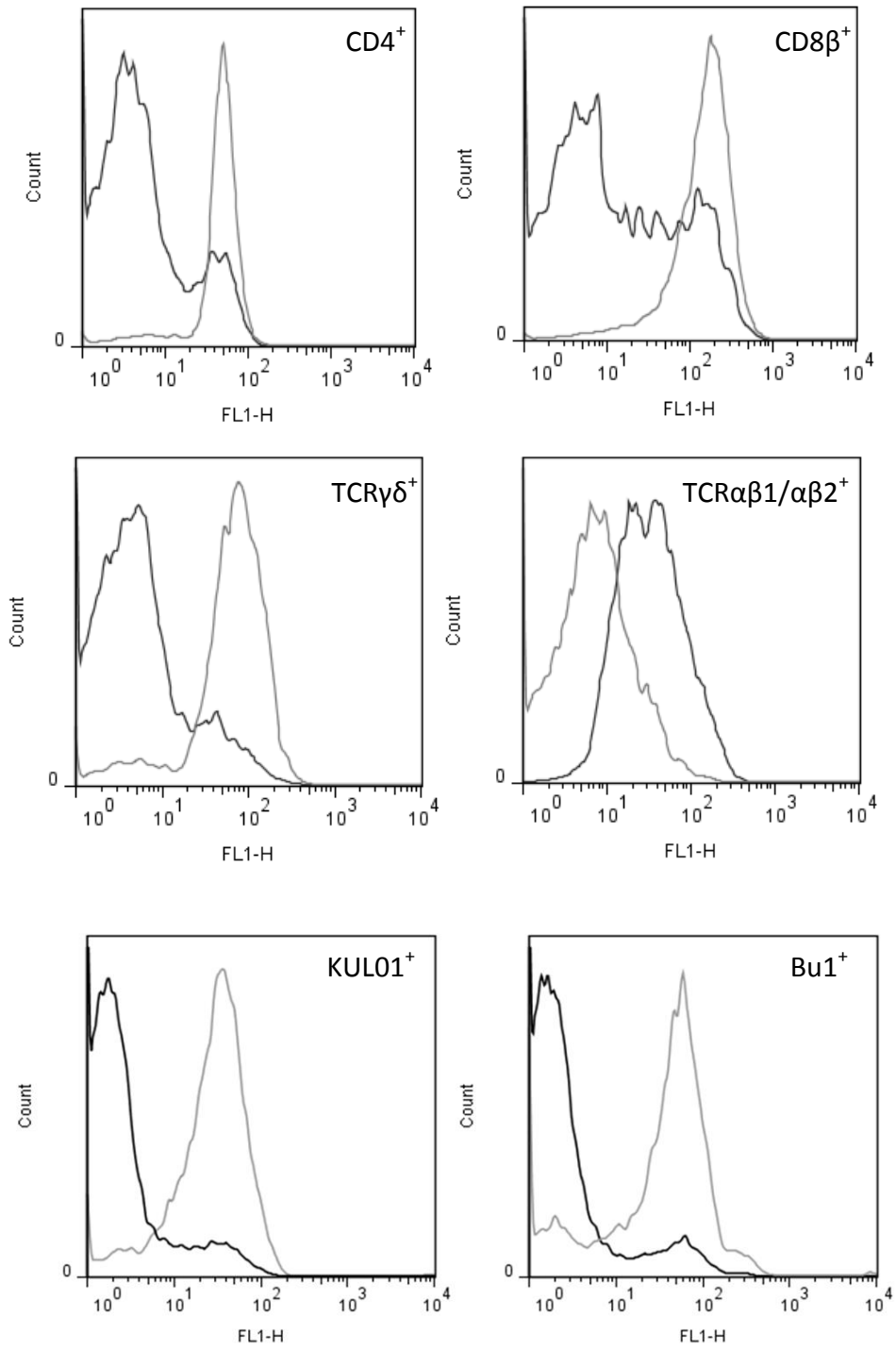

Figure 2 *FACS analysis of splenocyte subsets purified using an AutoMacs pro-seperator. Unsorted cells (black lines) and sorted cells (grey lines) for CD4, CD8β, TCRγδ, TCRαβ1/αβ2, KUL01 and Bu1 subsets. Data represent the results of one of three independent experiments with similar results.*

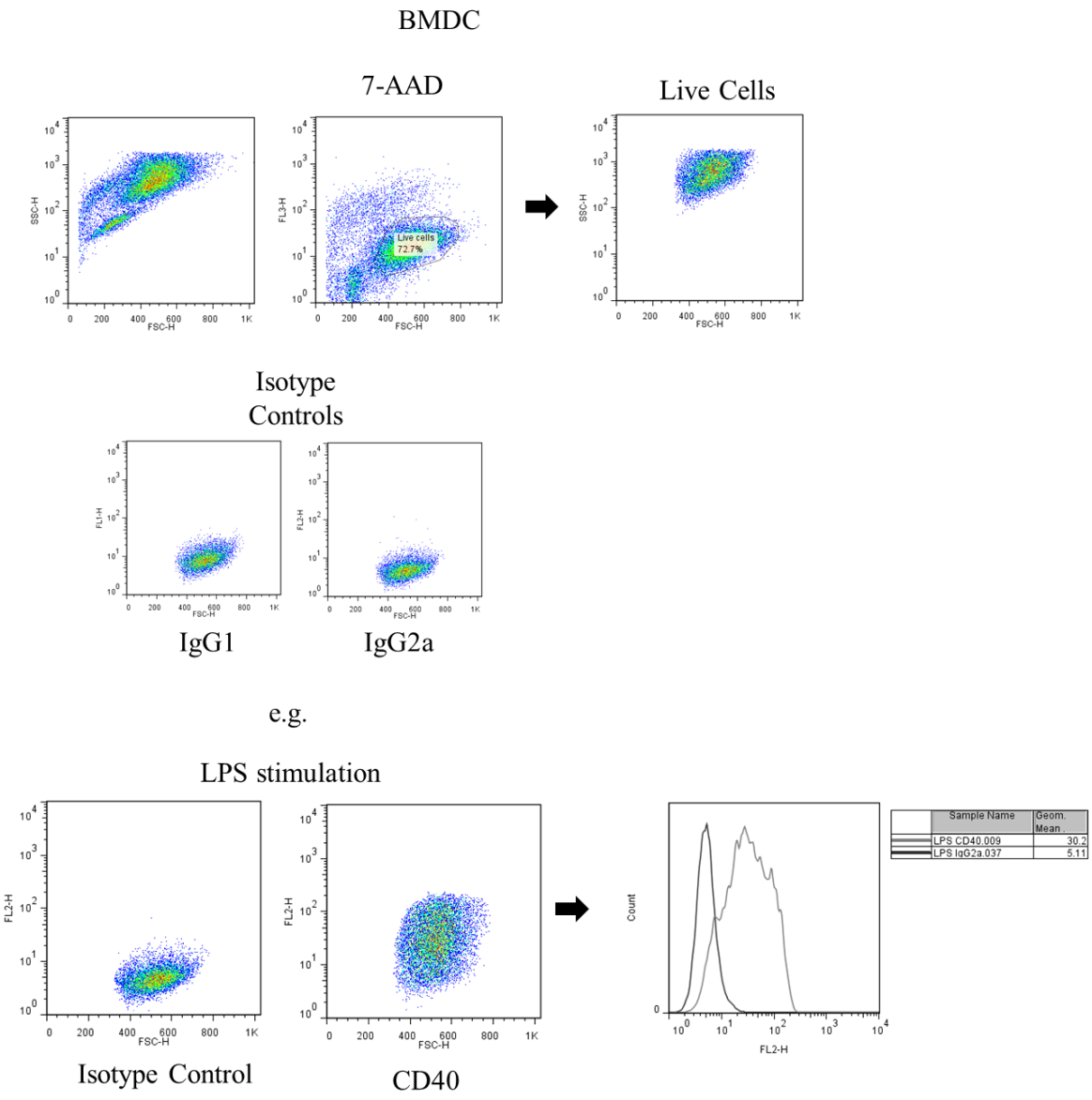

Figure 3 *FACS gating strategy. Prior to FACS analysis of BMDC or BMDM the viability dye 7-AAD was added to cells. Cells stained with 7-AAD were removed for data analysis by gating around the large FL3^{-} cell population. Cells were also analysed for non-specific binding using isotype controls. In the example used above BMDC stimulated with LPS (1 ng/ml) for 24 h were stained with mouse anti-chicken CD40 mAb and expression levels were analysed using histograms comparing isotype control to CD40 surface expression.*